Sobolev Institute of Geology and Mineralogy SB RAS (IGM SB RAS)
Trofimuk Institute of Petroleum Geology and Geophysics SB RAS (IPGG SB RAS)
Novosibirsk State University (NSU)

X INTERNATIONAL SIBERIAN EARLY CAREER GEOSCIENTISTS CONFERENCE

13-17 June 2022, Novosibirsk

PROCEEDINGS OF THE CONFERENCE

MINERALOGY
2022

Sobolev Institute of Geology and Mineralogy SB RAS (IGM SB RAS)
Trofimuk Institute of Petroleum Geology and Geophysics SB RAS (IPGG SB RAS)
Novosibirsk State University (NSU)

X INTERNATIONAL SIBERIAN EARLY CAREER GEOSCIENTISTS CONFERENCE

PROCEEDINGS OF THE CONFERENCE

MINERALOGY
2022

13-17 June 2022

Novosibirsk, Russia

УДК 55(061)
ББК Д 26
Т35

X International Siberian Early Career GeoScientists Conference: Proceedings of the Conference (13-17 June 2022, Novosibirsk, Russia)/ IGM SB RAS, IPPG SB RAS, NSU. – Novosibirsk: IPC NSU, 2022. - 228 p. - ISBN 978-5-4437-1337-3.

The volume contains short papers of the X International Siberian Early Career GeoScientists Conference and offer information on multidisciplinary aspects of the Earth Science: petrology, geochemistry, geochronology, mineralogy, metallogeny, geodynamics and tectonics, sedimentology, geomorphology and neotectonics, paleontology and paleoclimatology, petroleum geosciences, economic geology, geoecology, hydrogeology, geophysics, mining engineering and geoinformation systems in the Earth Science.

The Conference was supported by IGM SB RAS, IPPG SB RAS, NSU, JSC "Siberian Anthracite", JSC "Almazy Anabara", Data East, LLC, PJSC "Gazprom Neft", Laboratory of ore-forming systems IGM SB RAS and SGA Siberian Student Chapter.

УДК 55(061)
ББК Д 26

ISBN 978-5-4437-1337-3

CONTENTS

Section MINERALOGY

Section EXPERIMENTAL MINERALOGY

Section METALLOGENY, MINERAGENY AND ORE GENESIS

Section PETROLOGY

Section GEOCHEMISTRY AND GEOCHRONOLOGY

Section REGIONAL GEOLOGY AND TECTONICS

Section PALEONTOLOGY AND STRATIGRAPHY

Section GEOMORPHOLOGY AND QUATERNARY GEOLOGY

Section GEOECOLOGY, HYDROGEOLOGY, ENGINEERING GEOLOGY AND ENVIRONMENTAL MANAGEMENT

Section NEW INFORMATION AND GEO-INFORMATION TECHNOLOGIES IN GEOLOGY

Section GEOPHYSICAL RESEARCH METHODS

Section MINERALOGY

THE COMPOSITION OF LITHOSPHERIC MANTLE BENEATH THE LOW-DIAMONDIFEROUS TSNIGRI-ARKHANGELSKAYA KIMBERLITE PIPE (ARKHANGELSK DIAMONDIFEROUS PROVINCE, NW RUSSIA)

Agasheva E.V.

V.S. Sobolev Institute of Geology and Mineralogy, Novosibirsk, Russia,
shchukinalena@igm.nsc.ru

Abstract. This study shows the results of reconstruction of the composition, structure, thermal state and metasomatic enrichment of the lithospheric mantle beneath the Tsnigri-Arkhangelskaya kimberlite pipe, based on major- and trace-element composition of 450 garnet xenocrysts. It was found that the thermal state of the lithospheric mantle was 40-45 mW/m^2, maximum lithosphere depth at 170-200 km, the thickness of the "diamond window" – from 22 to 60 km, at the time of kimberlite magmatism. The low diamond grade of the pipe was not caused by the large-scale high-temperature melt metasomatism.

Key words: kimberlite, diamond, mantle metasomatism, lithospheric mantle, pyrope.

The composition of the lithospheric mantle, the substance of which is presented in kimberlite in the form of mantle xenoliths and their fragments (xenocrysts) is the key factor controlling the diamond grade of these pipes. The study of mantle samples makes it possible to evaluate the main characteristics of the lithospheric mantle, such as: 1) types of mantle rocks involved in its structure and their proportion; 2) geothermal gradient; 3) maximum lithosphere depth and the thickness of the "diamond window"; 4) types, sequence and scale of metasomatic enrichment and an assessment of the influence of these processes on the possibility of the formation and preservation of diamonds in mantle rocks up to the stage of kimberlite emplacement. Garnet is a constituent mineral of the Arkhangelsk diamondiferous province (ADP) mantle samples, including those that potentially could be the sources of diamonds (peridotite and eclogite). The existing ways of interpreting its major- [1,2] and trace-element [3] compositions, including P-T calculations [4] allows to obtain the main characteristics of the lithospheric mantle and conclude about its diamond potential. The goal of this study is to evaluate main features of the low-diamondiferous lithospheric mantle in the ADP.

Based on CaO and Cr_2O_3 contents [1, 2] garnets were divided into the following groups: lherzolite/G9 (72 %), megacrysts/G1 (7.6 %), low-chromium pyroxenite/G4 (7.4 %), deformed lherzolite/G11 (7 %), harzburgite/G10 (3.6 %), eclogite /G3 (1.1 %), wehrlite /G12 (0.9 %) and harzburgite of diamond association/G10D (0.4 %). Based on RE content and style of chondrite-normalized REE patterns, garnets were divided into the several groups, each formation was due to different style of metasomatic enrichment: 1) high-chromium G10, G10D and G9 with sinusoidal REE patterns (12 % from the total amount of peridotitic and megacryst garnets) – due to influence of C–H–O melt/fluid with high LREE/HREE ratio, probably of carbonatite composition; 2) middle to high chromium G9 with “humped” REE patterns (3 %) – due to influence of silicate melt with high LREE; 3) low to middle chromium G9 with flat REE patterns (29 %) – due to influence of high-temperature silicate melt; 3) low to middle chromium G9 with

fractionated MREE-HREE with MREE at chondritic value (19 %) – residues after partial melting with no/minimal metasomatic enrichment,- and with elevated MREE at 2-8 chondritic (23 %) – weak influence of high-temperature silicate melt. All garnets of peridotite and megacryst associations have high Ni content (50-127 ppm). The results of T_{Ni} [4] calculation show that dominant G9 and G10 garnets were equilibrated at 1100 – 1200° C (68 %) and 1200-1300° C (30 %); G11 and G1 – at 1100-1300° C (89 %). The absence of any correlations between Ni content and TiO_2, mg#, Y, Zr, Sm in garnets is evidence of high T regime within all sections of the sampled lithospheric mantle (from 60-80 to 170-200 km). The thermal state is 40-45 mW/m^2, graphite-diamond transition at T ~ 1050-1200° C (140-147 km), maximum lithosphere depth at 170-200 km, the thickness of the "diamond window" – from 22 to 60 km. The study shows that metasomatic enrichment of the lithospheric mantle beneath the Tsnigri-Arkhangelskaya pipe was similar to those beneath the high-diamondiferous Arkhangelskaya [5] and V. Grib [3] kimberlite pipes while the low diamond content of the pipe was not associated with a large-scale high-temperature melt metasomatism. However, the thickness of the "diamond window" beneath the Tsnigri-Arkhangelskaya pipe was much less compared to those beneath the high-diamondiferous ADP kimberlite pipes.

Funding: This work is supported by the Russian Science Foundation under grant 20-77-10018.

References:

1. Sobolev N.V., Lavrentyev Y.G., Pokhilenko N.P., Usova, L.V. Chrome-rich garnets from the kimberlites of Yakutia and their parageneses. Contributions to Mineralogy and Petrology. 1973. No. 40. P. 39–52.

2. Grütter H.S., Gurney J.J., Menzies A.H., Winter F. An updated classification scheme for mantle-derived garnet, for use by diamond explorers. Lithos. 2004. No. 77. P. 841–857.

3. Shchukina E.V., Agashev A.M., Pokhilenko N.P. Metasomatic origin of garnet xenocrysts from the V. Grib kimberlite pipe, Arkhangelsk region, NW Russia. Geoscience Frontiers. 2017. No. 8. P. 641–651.

4. Canil D. The Ni-in-garnet geothermometer: calibration at natural abundances. Contributions to Mineralogy and Petrology. 1999. No. 136. P. 240–246.

5. Lehtonen M., O'Brien H., Peltonen P., Kukkonen I., Ustinov V., Verzhak V. Mantle xenocrysts from the Arkhangelskaya kimberlite (Lomonosov mine, NW Russia): Constraints on the composition and thermal state of the diamondiferous lithospheric mantle. Lithos. 2009. No. 112. P. 924–933.

MODULARITY OF THE CRYSTAL STRUCTURES OF MINERALS AND SYNTHETIC COMPOUNDS WITH THE GENERAL FORMULA $A_2M_3(TO_4)_4$

Aksenov S.M.[1,2], Merlino S.[3]

[1]Laboratory of Arctic Mineralogy and Material Sciences, FRC "Kola Science Centre" RAS, Apatity, Russia, aks.crys@gmail.com
[2]Geological Institute. FRC "Kola Science Centre" RAS, Apatity, Russia
[3]Accademia Nazionale dei Lincei, Rome, Italy

Abstract. The crystal structures of natural and synthetic compounds with the general formula $A_2M_3(TO_4)_4$ displays order-disorder (OD) character and can be described using the OD groupoid family. Synthetic compounds $Na_2Mn_{3-x}Mg_x(SO_4)_4$ can be described in terms of modularity as a sequence of *A*-, S_1-, and S_2-modules:…$|AS_1AS_2AS_1AS_2|$… or (AS_1AS_2), together with MDO1 (AS_1AS_1) and MDO2 (AS_2AS_2). The crystal structure of itelmenite, $NaCaFe^{3+}{}_3(PO_4)_4$ is crystal-chemical isotypic to $Na_2Mn_{3-x}Mg_x(SO_4)_4$ and should be considered as ($A^*S_1A^*S_2$)-derivative.

Key words: modularity, polytypism, heteropolyhedral frameworks, oxysalts

Natural and synthetic compounds with the general formula $A_2M_3(TO_4)_4$ (*A* = Na, Rb, Cs, Ca; *M* = Mg, Mn, Fe^{3+}, Cu^{2+}; *T* = S^{6+}, P^{5+}) [1–7] are characterized by a wide structural diversity and their crystal structures are based on the heteropolyhedral *MT*-frameworks formed by MO_n polyhedra (*n* = 5, 6) and TO_4 tetrahedra. The negative charge of the frameworks is balanced by the extra-framework mono and/or divalent *A*-cations. Due to the same stoichiometry of the heteropolyhedral *MT*-frameworks these compounds show polymorphic and modular relationships. Compounds with the chemical formula $Na_2Mn_{3-x}Mg_x(SO_4)_4$ have recently been synthesized by the solid-state reaction route [4–6] These compounds are characterized by different orthorhombic unit-cell parameters and space groups: $Cmc2_1$, a = 14.8307, b = 9.9107, c = 8.6845 Å and *Pbca*, a ~ 29.2–29.7 Å, b ~ 9.5–9.9 Å, c ~ 8.7 Å. It was recently shown, that crystal structures of both compounds have similar building blocks stacked in different ways along the axis with the longest unit-cell parameter [6]. Building blocks (modules) related to those in $Na_2(Mg_{1-x}Mn_x)_3(SO_4)_4$ have been also found in natural sulfate itelmenite $Na_2CuMg_2(SO_4)_4$ [3] and synthetic phosphates $NaCaFe^{3+}{}_3(PO_4)_4$ [2] $Ca_2MgFe^{3+}{}_2(PO_4)_4$ [1].

The crystal structures of $Na_2Mn_{3-x}Mg_x(SO_4)_4$ polymorphs [4,6] display OD character and can be described using the same OD groupoid family, more precisely a family of OD structures built up by two kinds of non-polar layers (category IV) [7]. The layers are the following:
(i) L_{2n+1} type with the layer symmetry $pmc2_1$ [or $P(m)c2_1$ in terms of the OD notation, where braces indicate the direction of missing periodicity] is represented by the heteropolyhedral modules formed by $Mn\varphi_n$ polyhedra (*n* = 5,6) and SO_4 tetrahedra;
(ii) L_{2n} type consisting of oxygen atoms on the borders of a thin slab with the layer symmetry *pbcm* [$P(b)cm$ or $P(2/b)\ 2_1/c\ 2_1/m$].

When different sequences of operators are active in the L_{2n} type layers, multilayered polytypic structures with increased **a** occur. The simplest one is that in which the two types of operators in L_{2n} layers regularly alternate. Polytypes of compounds with formula $Na_2Mn_{3-x}Mg_x(SO_4)_4$ may related through a modular series built up with the layer *A* (corresponding to the central part of the OD layer L_{2n+1}) and the sulphate layers S_1 and S_2, present in polytypes MDO1

and MDO2, respectively, and represented in Fig. 1. The different types of alternation of *A*- and S_i-modules can form a merotypic modular series. Thus, in terms of modularity it is possible to describe this structure as a sequence of modules [7]:…|$AS_1AS_2AS_1AS_2$|… or $(AS_1AS_2)_2$.

The crystal structures of natural sulfate itelmenite $Na_2CuMg_2(SO_4)_4$ [3] and synthetic phosphates $NaCaFe^{3+}{}_3(PO_4)_4$ [2], $Ca_2MgFe^{3+}{}_2(PO_4)_4$ [1] represent a modular character with the alternation of three types modules along the **a** direction. The first polar *A**-module corresponds to the derivative of the *A*-layer in polytypes and modular (AS_1AS_2)-type structure of $Na_2Mn_{3-x}Mg_x(SO_4)_4$. Despite of the changes of the coordinational environment of *M*-cation in *A**-layer the crystal structures of itelmenite, $NaCaFe^{3+}{}_3(PO_4)_4$, and $Ca_2MgFe^{3+}{}_2(PO_4)_4$ should be considered as ($A^*S_1A^*S_2$)-derivatives of the previously described (AS_1AS_2)-type structure.

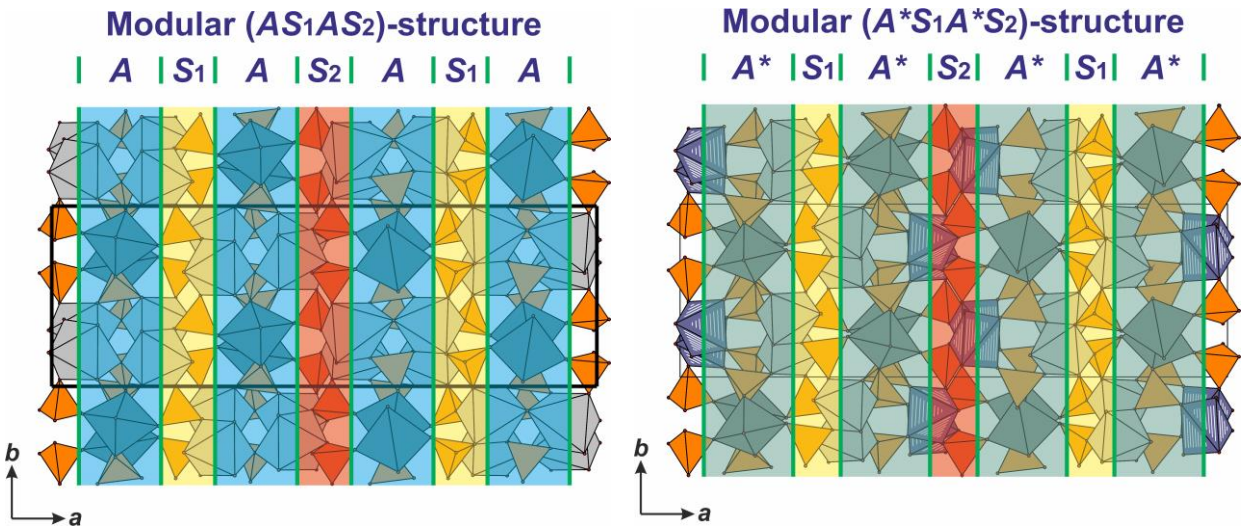

Figure 1 – The modular representation of (AS_1AS_2)-type structure of $Na_2Mn_{3-x}Mg_x(SO_4)_4$ (left) and ($A^*S_1A^*S_2$)-type derivative structures of itelmenite, $NaCaFe^{3+}{}_3(PO_4)_4$, and $Ca_2MgFe^{3+}{}_2(PO_4)_4$ (right).

Funding: This work is supported by the Russian Science Foundation under grant 20-77-10065.

References:

1. Saleck A.O., Mercier C., Follet C., Mentré O., Assani A., Saadi M., El Ammari L., Synthesis, crystal structure and magnetic behavior of a new calcium magnesium and iron orthophosphate $Ca_2MgFe_2(PO_4)_4$. Journal of Solid State Chemistry. 2020. Vol. 292. P. 121715.

2. Hidouri M., Lajmi B., Wattiaux A., Fournes L., Darriet J., Ben Amara M. Crystal structure, magnetic properties and Mössbauer spectroscopy of $NaCaFe_3(PO_4)_4$. Journal of Alloys and Compounds. 2003. Vol. 358. P. 36–41.

3. Nazarchuk E.V., Siidra O.I., Agakhanov A.A., Lukina E.A., Avdontseva E.Y., Karpov G.A. Itelmenite, $Na_2CuMg_2(SO_4)_4$, a new anhydrous sulfate mineral from the Tolbachik volcano. Mineralogical Magazine. 2018. Vol. 82. P. 1233–1241.

4. Gao J., Sha X., Liu X., Song L., Zhao P. Preparation, structure and properties of $Na_2Mn_3(SO_4)_4$: a new potential candidate with high voltage for Na-ion batteries. Journal of Material Chemistry. A. 2016. Vol. 4. P. 11870–11877.

5. Trussov I.A., Male L.L., Sanjuan M.L., Orera A., Slater P.R. Understanding the complex structural features and phase changes in $Na_2Mg_2(SO_4)_3$: A combined single crystal and variable temperature powder diffraction and Raman spectroscopy study. Journal of Solid State Chemistry. 2019. Vol. 272. P. 157–165.

6. Ben Yahia H. Crystal structure of a new polymorphic modification of $Na_2Mn_3(SO_4)_4$. Zeitschrift für Kristallographie. 2019. Vol. 234. P. 697–705.

7. Aksenov S.M., Antonov A.A., Deyneko D.V., Krivovichev S.V., Merlino S. Polymorphism, polytypism and modular aspect of compounds with the general formula $A_2M_3(TO_4)_4$ (A = Na, Rb, Cs, Ca; M = Mg, Mn, Fe^{3+} , Cu^{2+} ; T = S^{6+}, P^{5+}): Order–disorder, topological description and DFT calculations. Acta Crystallographica. B. 2022. Vol. 78. P. 61–69.

METAMORPHISM VS METASOMATISM: STABLE ISOTOPE CONSTRAINTS (CASE STUDY OF THE KOCHUMDEK CONTACT AUREOLE, EAST SIBERIA)

Deviatiiarova A.S., Sokol E.V., Kokh S.N., Reutsky V.N., Izokh O.P., Pyryaev A.N.

V.S. Sobolev Institute of Geology and Mineralogy, Novosibirsk, Russia,
devyatiyarova@igm.nsc.ru

Abstract. A database of $\delta^{18}O$ and $\delta^{13}C$ compositions was created for all types of the Kochumdek carbonate-bearing rocks, including limestone and marble, as well as for monofractions of calcite (sixty samples). The revealed $\delta^{13}C$ and $\delta^{18}O$ difference ($\Delta\ \delta^{13}C \leq 2$ ‰ and $\Delta\ \delta^{18}O \leq 4$ ‰) in limestone and marble proves the leading role of decarbonation in the C and O isotope fractionation. This composition feature also indicates very limited percolation of magmatic fluids into the sediments and, together with mineral indicators, allows detecting local permeable zones.

Key words: fluids; contact metamorphism; carbonate-bearing rocks; calcite; $\delta^{18}O$ and $\delta^{13}C$

The behavior of stable isotopes is an efficient tool for tracing the history of contact aureoles. The isotope gradients and their spatial patterns have implications for processes in zones of interactions between igneous bodies and the host sediments, as well as for the contributions of each process to the total mass balance [1]. The contributions of different sources into oxygen and carbon budgets, fluid types, and directions of fluid flow can be inferred from isotope signatures using special algorithms [1-2].

We studied oxygen and carbon isotope compositions ($\delta^{18}O$ and $\delta^{13}C$) in rocks and minerals of the Kochumdek aureole located at 62°27′54.59′′N, 91°55′42.99′′E [3]. Sixty samples of marble, marly limestone, skarn, scapolite veins, and calcite monofractions were analyzed at the V.S. Sobolev Institute of Geology and Mineralogy (IGM, Novosibirsk). The measurements were performed on a Thermo Finnigan *GasBench II* connected to a Thermo Finnigan *MAT 253* mass spectrometer, to an accuracy of 0.1 ‰ for C and 0.2 ‰ for O.

The marbles of the Kochumdek aureole have coarse granoblastic structure and closed porosity, and contain sporadic fine (< 10 μm) fluid inclusions of low density. The structure and texture features indicate limited fluid flow across the sediment-magmatic interface. In the $\delta^{18}O$ – $\delta^{13}C$ diagram (Fig. 1 A), the compositions of the protolith Early Silurian marly limestone plot a dense cluster at the bottom of the marine carbonate field according to $\delta^{13}C$. The fields of bulk marble samples, calcite from marble, and skarn partly overlap the marine carbonate field that reaches –2‰ on the $\delta^{13}C$ axis. The $\delta^{13}C$ ranges of the sedimentary protolith and the products of its thermal metamorphism are within 2 ‰. The median $\delta^{18}O$ values for limestones and marbles (+calcite and skarns) coincide but the $\delta^{18}O$ range is narrower in the sedimentary rocks (Fig. 1 A).

Metacarbonate rocks in contact aureoles commonly show trends of coupled $\delta^{18}O$ and $\delta^{13}C$ decrease, with a negative slope, starting from the limestone field [2]. The $\delta^{18}O$ and $\delta^{13}C$ decrease upon marble-to-metasomatite transition is first slow but then becomes very steep. The total shift reaches 12‰ along $\delta^{18}O$ and 17‰ along $\delta^{13}C$ (Fig. 1 B). This trend results from voluminous infiltration of magmatic, meteoric, or mixed fluids with low $\delta^{18}O$ and $\delta^{13}C$ across the contact [1].

Depleted $\delta^{18}O$ compositions (+22.0 ‰ to +17.0 ‰ SMOW) in the Kochumdek aureole rocks are restricted to few samples of vein scapolite (meionite, $Ca_4[Al_2Si_2O_8]_3CO_3$), skarn, and re-crystallized limestone (Fig. 1 A). The $\delta^{13}C$ values in fifty seven out of sixty samples are

similar, and only three samples have low $\delta^{13}C$ down to –5.3 ‰ VPDB (Fig. 1 A). This behavior of stable isotopes corresponds to very limited percolation of magma-derived fluids inward the host rocks and highlights local permeable zones in the monolith aureole rocks. The small difference between $\Delta\delta^{13}C \leq 2$ ‰ and $\Delta\delta^{18}O \leq 4$ ‰ revealed for the analyzed Kochumdek marly limestones and marbles proves that decarbonation of the sedimentary protolith was the leading process in C and O isotope fractionation during spurrite-merwinite metamorphism.

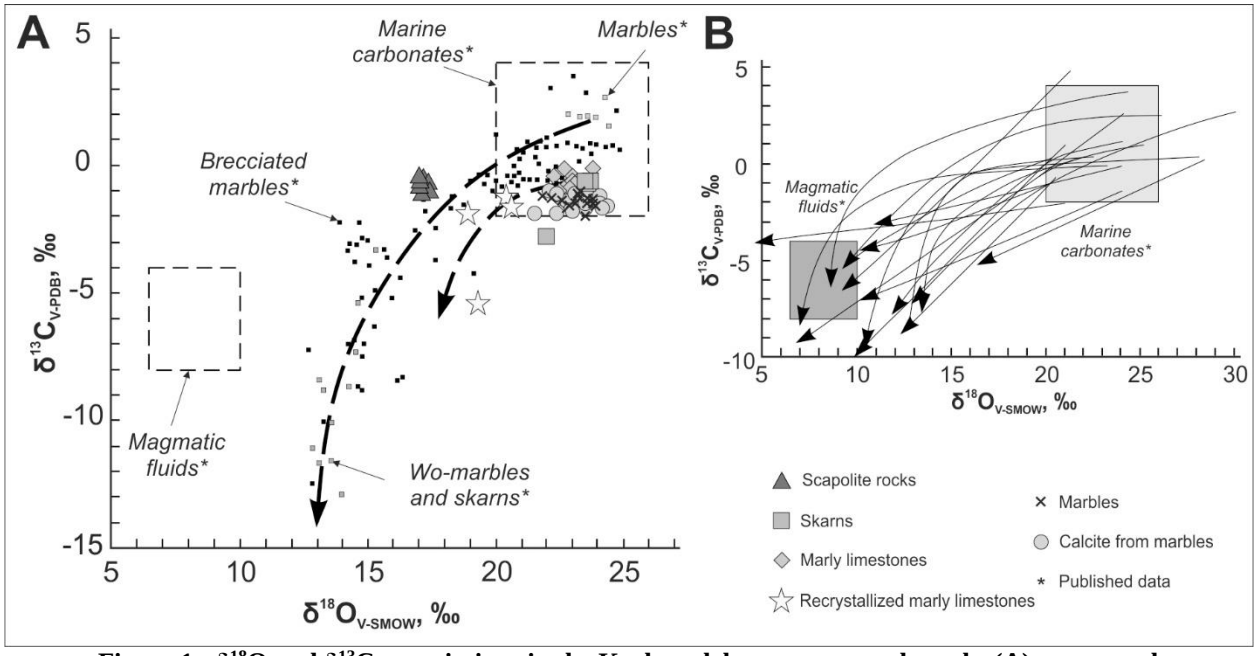

Figure 1 - $\delta^{18}O$ and $\delta^{13}C$ covariations in the Kochumdek contact aureole rocks (A), compared to metasomatized rocks from other contact aureoles according to published data (B) [1-2].

Funding. The reported study was supported by the Russian Foundation for Basic Research, Project No. 20-05-00216. The study was carried out on government assignment to IGM (Novosibirsk).

References:

1. Baumgartner L.P., Valley J.W. Stable isotope transport and contact metamorphic fluid flow. Reviews in Mineralogy and Geochemistry. 2001. Vol. 43. No. 1. P. 415–467.

2. Buick I.S., Cartwright I. Stable isotope constraints on the mechanism of fluid flow during contact metamorphism around the Marulan Batholith, NSW, Australia. Journal of Geochemical Exploration. 2000. Vol. 69. P. 291–295.

3. Sokol E.V., Polyansky O.P., Semenov A.N., Reverdatto V.V., Kokh S.N., Devyatiyarova A.S., Kolobov V.Y., Khvorov P.V., Babichev A.V. High-grade contact metamorphism in the Kochumdek River valley (Podkamennaya Tunguska basin, East Siberia): evidence for magma flow. Russian Geology and Geophysics. 2019. Vol. 60. No. 4. P. 386–399.

THE DESCRIPTION OF ARAGONITES TWINNING FROM THE DEPOSITS OF SPAIN, MOROCCO AND RUSSIA

Donskikh K.G.[1,2], Gavryushkin P.N.[1,2], Banaev M.V.[1,2]

[1]V.S. Sobolev Institute of Geology and Mineralogy, Novosibirsk, Russia, katerinoso@yandex.ru
[2]Novosibirsk State University, Novosibirsk, Russia

Abstract. Investigating the microstructure of twinned aragonite crystals from three different deposits - Morocco, Spain and Russia - we found out that only samples from Morocco and Tuva are complicated by polysynthetic twinning. Polysynthetic lamellas in the Moroccan crystal are parallel growths of aragonite, 4.5 to 31 microns thick. Spanish crystals are ordinary germination tees. Also, Spanish and Moroccan crystals have different domain boundaries - in the first case they are sharp and frequent, in the second they are even, which is due to different conditions of crystal crystallization.

Key words: aragonite, twinning, Raman spectroscopy

Aragonite is one of the polymorphic modifications of calcium carbonate. It crystallizes in the rhombobipyramidal form of the symmetry of the orthorhombic syngony – *Pmmm*.

Aragonite crystals from the deposits of Tazaut (Morocco), Molina D'Aragon (Spain) and Kuge-Dava (Tuva, Russia) were studied using the following types of analysis: X-ray diffraction (single crystal and XRD), microprobe analysis, scanning electron microscopy, EBSD analysis, RAMAN spectroscopy.

There are two types of twinning in aragonite. The first type: macro-twinning along the plane (110). The second type: micro-twinning - the presence of twin lamellas in macrodomains, no more than a fraction of a millimeter thick and having a different orientation. This type of twinning is noticeable in a microscope in transmitted light. It was found out that micro-twinning is present only in Moroccan crystals, where it can be superimposed on both twinned crystals (macro-twinning) and single crystals [1].

In the composition of the studied aragonites, two main elements can be distinguished-impurities: Na and Sr [2]. In the purple part of the Spanish crystals, Sr was detected – an average of 0.006 wt.%, while in the remaining crystals and the transparent part of the Spanish crystal, the Sr content averaged 0.002 wt.%. The highest Na content was found in the Moroccan sample – 0.0004 wt.%, in other crystals its content is on average 0.0001 wt.%. There is no regular change in the Sr content in the plane (001) (from the edge to the center) in the Spanish crystal. It can be concluded that the content of Sr and Na is not related to the color, but is related to the conditions of crystallization of aragonite.

X-ray diffraction analysis revealed the presence of well-marked diffuse scattering in samples from Morocco in two cross-sections of the reverse space. In the first case, scattering is observed in the form of arcs passing through the reflexes of the plane (001). In the second case, scattering is noticeable along the twinning axis [110]* only in sections (002), (00-2), which indicates the presence of nanoscale twinning along the plane (110). In the Tuvan sample, diffuse scattering is also observed, passing through the reflexes of the plane (001) in the form of short straight lines.

The data of the EBSD analysis at 20 microns showed the misorientation of the crystal sections along the cracks, and also confirmed the presence of stresses in the structure, expressed in a smooth change in the orientation of the stressed section by about 3-4 °. The survey of the

sample at 1 micron showed a deviation from the total flow of twin lamellas inside the area bounded by cracks by 5 °. Also, this survey allowed us to establish that some lamellas have a dimension from 4.5 to 30 microns and may, in turn, be polysynthetic twins. Most of the lamellas are indistinguishable in orientation from macrodomains, which indicates that there is no connection between diffuse scattering and disorientation of the lamellas.

Raman spectroscopy data showed that the vibrational spectra of the studied crystals do not differ from each other. Also, these spectra do not differ in the twinned and single-crystal sections. It is possible to reliably establish the presence or absence of a connection of twinning with the geometry of atoms by calculating the electron density in CO_3 triangles using DFT modeling [2].

References:

1. Richards R. P. An examination of classic twinning in aragonite. Rocks & Minerals. 2021. Vol. 96. No. 5. P. 454-459.

2. Gavryushkin P. N., Recnik A., Daneu N., Sagatov N., Belonoshko A. B., Popov Z. I., Ribic V., Litasov K. D. Temperature´ induced twinning in aragonite: transmission electron microscopy experiments and ab initio calculations. Zeitschrift für Kristallographie-Crystalline Materials. 2019. Vol. 234. No. 2. P. 79-84.

Ca-Mg-Fe OLIVINES IN PARALAVAS OF THE NYALGA COMBUSTION METAMORPHIC COMPLEX, CENTRAL MONGOLIA

Glushkova V.E.[1], *Peretyazhko I.S.*[1], *Savina E.A.*[1], *Khromova E.A.*[2]

[1]A.P. Vinogradov Institute of Geochemistry SB RAS, Irkutsk, Russia, glushkova@igc.irk.ru
[2]N.L. Dobretsov Geological Institute SB RAS, Ulan-Ude, Russia

Abstract. Ca-Mg-Fe olivines are rock-forming minerals in the paralavas of the Nyalga combustion metamorphic complex. Decomposition products of solid solution Ca-fayalite – kirschsteinite $CaFeSiO_4$ crystallize at the final stage of paralava matrix formation. The minerals of variable composition monticellite $CaMgSiO_4$ – kirschsteinite occur only in xenolith mineral assemblages of thermally modified marly limestone, and its melting resulted in paralava formation. It is established difference between monticellite from paralavas and from igneous rocks.

Key words: Ca-Mg-Fe olivine, monticellite, kirschsteinite, paralava, Nyalga combustion metamorphic complex

Mellilite-nepheline paralavas of combustion metamorphic complexes, occurring inMongolia have been formed during melting of marly limestones caused by wild coal fires [1, 2]. The Nyalga paralava matrix consists of mellilite, clinopyroxene, and plagioclase microphenocrysts and with the interstitials filled in microliths of Ca-fayalite, kirschsteinite, K-Ba feldspars, rhonite-kuratite, pyrrhotite and other minerals [3]. Thermally modified xenoliths of carbonate-silicate sedimentary rocks are also present in paralavas. The gehlenitic mellilite with the inclusions of monticellite, Ca-Mg-Fe olivines, spinel, perovskite, magnetite and pyrrhotite constitute the mineral assemblages of xenoliths of modified marly limestone (Fig. 1).

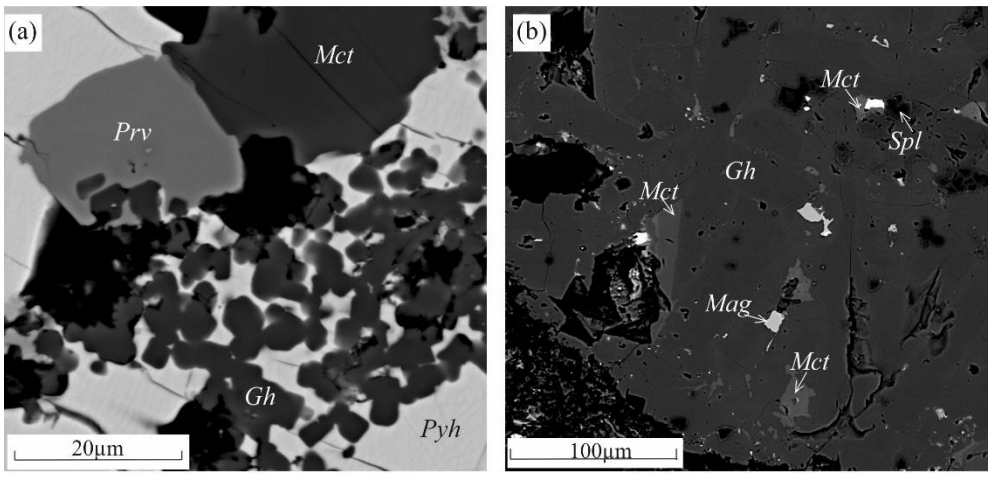

Figure 1 – Matrix fragments of thermally modified xenoliths of marly limestone in paralava samples (a) MN-1176 and (b) MN-1234-1. *Mct* = monticellite, *Gh* = gehlenite, *Mag* = magnetite, *Pyh* = pyrrhotite, *Prv* = perovskite, *Spl* = spinel.

Microliths and inclusions of Ca-Mg-Fe olivines vary widely in contents of FeO and MgO (Mg#, Mg/(Mg+Fe) from 40 to 94) in different xenoliths of marly limestone, but they do not

have zoning by composition within in a single xenolith (Table 1). Olivines also contain the impurity of Mn (up to 4 wt% MnO).

Ca-Mg-Fe olivines in mellilite-nepheline paralavas of the Nyalga combustion metamorphic complex and in products of pyrometallurgical industry [4] broadly vary in the content of kirschsteinite end-member. This distinguishes them in composition from monticellite, containing <10% of kirschsteinite end-member, in mineral assemblages of kimberlites [5], carbonatites, alkaline, ultrabasic rocks [6] and high-temperature scarn on the contact of marble and basalt traps [7].

Table 1. Major-element chemistry (wt%) and crystal chemical formulas of Ca-Mg-Fe olivines

Sample	MN-1133 (6)	MN-1180 (2)	MN-1176 (3)	MN-1179 (2)	MN-1234-1 (5)	Min	Max
SiO_2	36.66	36.51	35.32	35.58	36.28	34.08	37.55
TiO_2	0.22	bd	bd	bd	bd	bd	0.82
Al_2O_3	0.06	bd	bd	0.24	bd	bd	0.57
FeO	3.78	15.67	6.96	11.46	12.13	1.47	19.08
MnO	0.49	0.83	1.51	0.85	2.38	bd	3.42
MgO	22.56	15.71	18.81	17.07	16.40	12.14	24.13
CaO	35.57	32.68	35.83	35.62	34.28	30.96	37.19
Total	99.34	101.39	98.43	100.81	101.46	—	—
Formulas, apfu							
Si	0.987	1.005	0.980	0.980	0.996	0.969	1.013
Ti	0.005	0.000	0.000	0.000	0.000	0.010	0.016
Al	0.002	0.000	0.000	0.010	0.000	0.003	0.001
Fe	0.085	0.365	0.163	0.265	0.282	0.033	0.451
Mn	0.005	0.020	0.040	0.020	0.056	0.001	0.082
Mg	0.903	0.645	0.773	0.700	0.666	0.523	0.970
Ca	1.027	0.965	1.070	1.050	1.008	0.935	1.149
Total	3.014	3.000	3.027	3.025	3.008	—	—
Mg#	91.4	63.9	81.4	72.6	70.5	40	94

Numerals in braces denote quantity of SEM EDS analyses used to calculate average values. bd = below SEM EDS detection limit.

Funding: This workwas carried out as part of Basic Research Program 0284-2021-0006 of the Russian Academy of Sciences.

References:

1. Peretyazhko I.S., Savina E.A., Khromova E.A. Low-pressure (> 4 MPa) and high-temperature (> 1250 °C) incongruent melting of marl limestone: formation of carbonate melt and melilite–nepheline paralava in the Khamaryn–Khural–Khiid combustion metamorphic complex, East Mongolia. Contributions to Mineralogy and Petrology. 2021. Vol.176. Art. 38

2. Peretyazhko I.S., Savina E.A., Khromova E.A., Glushkova V.E. Melted Rocks (Clinkers and Paralavas) from the Khamaryn–Khural–Khiid Combustion Metamorphic Complex in Eastern Mongolia: Mineralogy, Geochemistry and Genesis. Petrology. 2020. Vol. 28. No. 5. P. 482-510.

3. Peretyazhko I.S., Savina E.A., Khromova E.A., Karmanov N.S, Ivanov A.V. Unique clinkers and paralavas from a new Nyalga combustion metamorphic complex in Central Mongolia: mineralogy, geochemistry, and genesis. Petrology. 2018. Vol. 26. No. 2. P. 181-211.

4. Warchulski R., Gawęda A., Janeczek J., Kądziołka-Gaweł M. Mineralogy and origin of coarse-grained segregations in the pyrometallurgical Zn-Pb slags from Katowice-Wełnowiec (Poland). Mineralogy and Petrology. 2016. Vol. 110. P. 681-692.

5. Abersteiner A., Kamenetsky V.S., Graham PearsonD., Kamenetsky M., Karsten G., Ehrig K., Rodemann T. Monticellite in group-I kimberlites: Implications for evolution of parental melts and post-emplacement CO_2 degassing. Chemical Geology. 2018. Vol. 478. P. 76-88.

6. D'Orazio M., Innocenti F., Tonarini S., Doglioni C. Carbonatites in a subduction system: The Pleistocene alvikites from Mt. Vulture (southern Italy). Lithos. 2007. Vol. 98. P. 313-334.

7. Sokol E.V., Polyansky O.P., Semenov A.N., Reverdatto V.V., Kokh S.N., Devyatiyarova A.S., Kolobov V.Yu., Khvorov P.V., Babichev A.V. High-grade contact metamorphism in the Kochumdek river valley (Podkamennaya Tunguska basin, East Siberia): evidence for magma flow. Russian Geology and Geophysics. 2019. Vol. 60. No. 4. P. 456-471.

SPECTROSCOPIC FEATURES OF ELECTRON IRRADIATED DIAMOND CRYSTALS FROM MIR KIMBERLITE PIPE, YAKUTIA

Komarovskikh A.Yu., Rakhmanova M.I.

Nikolaev Institute of Inorganic Chemistry, Novosibirsk, Russia, komarovskikh@niic.nsc.ru

Abstract. The effect of electron irradiation and subsequent low-temperature annealing (200-600°C) on spectroscopic features of diamond crystals from the Mir pipe have been investigated by IR, PL, and EPR techniques. One of the interesting results is observation of new characteristic photoluminescence system with a ZPL at 615 nm accompanied by phonon replicas of 41 and 90 meV in electron irradiated type IaAB diamond, while in type IIa diamond, another specific system with a ZPL at 558.5 arises.

Key words: natural diamonds, electron irradiation, annealing, photoluminescence, infrared absorption

In this work, a series of diamond crystals of different types from the Mir pipe, Yakutia has been electron irradiated (in a water cooling chamber at ~10°C, 3.5 MeV, 10^{18} electrons/cm^2) and subsequently isochronally annealed at low temperatures (200-600°C) to investigate the characteristic defects formed by photoluminescence (PL), infrared (IR), and electron paramagnetic resonance (EPR) techniques. Although much is known about the radiation-induced defects in diamond, there are still a lot of questions about the nature of centers produced and their interaction with widely present nitrogen impurity. This work is of interest also considering the specific feature of Mir pipe namely the abundance of low-nitrogen type IIa diamonds.

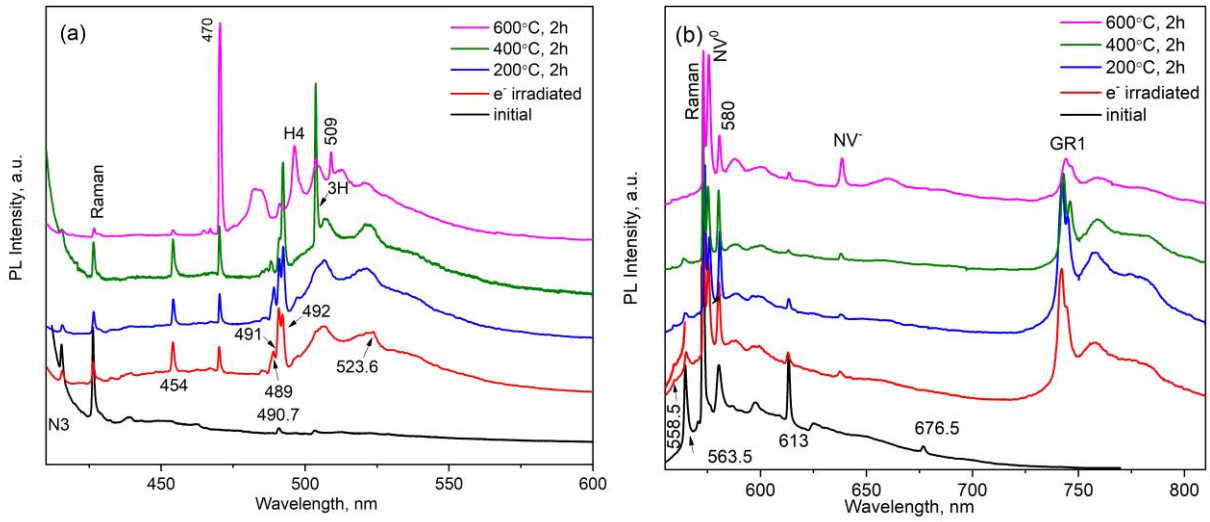

Figure 1 – PL spectra of the AO1741 diamond (a) λ_{ex}=405nm, (b) λ_{ex}=532nm. In (a), an increase of the 470 nm system (TR12) with a phonon of 75 meV is observed upon annealing at 600°C. In (b), the 558.5 nm system appears after irradiation and persists up to 600°C.

In electron irradiated diamonds of IaAB type, the new characteristic photoluminescence system with zero-phonon line (ZPL) at 615 nm accompanied by phonon replicas of 41 and 90 meV has been found. The phonons energies point out to multi-phonon interactions with a

quasilocal vibration of a vacancy and according to the obtained data, it can be proposed that the responsible nitrogen-related defect contains vacancy and possibly can be associated with some other impurity. Contrariwise, in almost nitrogen-free diamond the specific system with ZPL at 558.5 nm appears (Fig. 1). This center was described in [1] as a feature of superdeep diamonds from the São-Luis deposit. It has quasilocal vibration of 40 meV indicating the presence of a vacancy component in the defect structure. In the work [2] the crystals of different types from the Mir pipe were annealed and after HPHT treatment at 1500°C the 558.5 nm center was formed but only in the type IIa crystal. It can be suggested that at this temperature the thermal degradation of dislocations resulted in the release of vacancies involved in the corresponding defects. The absence of nitrogen seems to be of critical importance in the process of this center formation.

Regardless of the nitrogen impurity, the specific systems with ZPL at 454, 491, and 492 nm have been found in irradiated diamond crystals from the Mir pipe. To examine the defects formed, the irradiated diamond crystals have been subjected to low-temperature annealing at temperatures up to 600°C. While 454, 491, 558.5, 615 nm systems persist, annealing of the 492 nm system along with well-known 523.6, 489, and 503 nm (3H) [3] propose the interstitial-vacancy nature of the defect. As a final notion, it should be mentioned that the formation of interstitial-related defects in the diamond during electron irradiation depends on a sample temperature. Thus, an investigation of the effect of electron irradiation at different temperatures on spectroscopic properties is of interest.

Funding: This work is supported by the Russian Science Foundation under grant 20-77-00039.

References:

1. Yuryeva O.P., Rakhmanova M.I., Nadolinny V.A., Zedgenizov D.A., Shatsky V.S., Kagi H., Komarovskikh, A.Yu. The Characteristic Photoluminescence and EPR Features of Superdeep Diamonds (São-Luis, Brazil). Physics and Chemistry of Minerals. 2015. Vol. 42. P. 707–722.

2. Rakhmanova M.I., Komarovskikh A.Yu., Palyanov Y.N., Kalinin A.A., Yuryeva O.P., Nadolinny V.A. Diamonds from the Mir Pipe (Yakutia): Spectroscopic Features and Annealing Studies. Crystals. 2021. Vol. 11. No. 4. P. 366.

3. Zaitsev A.M. Optical Properties of Diamond. A Data Handbook. Berlin. Springer. 2001. 502 p.

MINERAL COMPOSITION OF SABAKTY LAKE SEDIMENTS

Kuzina D.M, Yusupova A.R., Nourgalieva N.G., Rogov A.M.

Institute of Geology and Petroleum Technologies, Kazan Federal University, Kazan, Russia,
yusupovaanast095@gmail.com

Abstract. In this study, we present lithology, mineralogy and scanning electron microscopy observations along a 294 cm sediment profile of the Lake Sabakty, with the objectives of understanding the geochemical processes and improving the paleohydrological and paleoecological information during the late Pleistocene and Holocene of the South Ural.

Key words: mineral composition, lake sediments, Holocene

Lake Sabakty (53°36'55" N; 58°39'22" E) located in the Bashkortostan republic; the length is ~2.3 km, width is ~1.0 km, average depth is 2.8 м; maximum depth is 6.0 m, the basin area is 9.0 km² [1-3]. The core No. 4 was selected for a detailed laboratory study based on the primary lithological description and the results of seismoacoustic studies [4]. The sediment was sliced at 2.0 cm thick samples. According to the radiocarbon dating, the age of the lake is ~22.5 thousand years [5].

The result of particle size analysis is presenting that the content of clay fraction in the sediment varies in the range 1.37-16.41 %, silt fraction are dominant at 33.24%-76.3%, sand - 12.02-65.39 %.

According to X-ray diffraction analysis (Fig. 1), the mineral composition is characterized by the predominance of terrigenous minerals (detrital quartz, microcline, mica, chlorite, mixed-layer clay minerals). Authigenic minerals include carbonates (calcite, dolomite), framboidal pyrite. Biogenic silica (cristobalite, tridymite) from diatom shells and stomatocysts are recorded throughout the sediment section. Scanning electron microscopy revealed the presence of framboidal pyrite, detrital and biogenic quartz in lacustrine sediments.

Fig. 1 shows, the authigenic component is inferior to the allothigenic component in content. However, in terms of variations along the section, it differs in a noticeably more differentiated behavior (especially carbonates).

The values of allothigenic component vary between 20.90%-61.14%, values of quartz ranges from 14.00% to37.94%. The quartz content curve is similar to the amplitude of the allothigenic dominant, but with contrasting behavior at some points (since part of the crystalline quartz, together with amorphous silica (cristobalite + tridymite), is involved in the composition of diatoms and stomatocysts).

The carbonate component changes from 1.79 % to 52.12 %. The precipitation of calcite-dolomite carbonates is determined by factors: Ca/Mg-ratio in water, total carbonate alkalinity, salinity, pH value, temperature and organic productivity of the reservoir [6].

The content of pyrite changes from 1.18 % to 6.94 %. The formation of framboidal pyrite is associated with the recrystallization of amorphous Fe monosulfides, which appeared in the early diagenesis. The content of biogenic quartz increases up to section from 2.55 % to 25.70 %, indicating an increase in algae activity.

The comparison of the values variations of particle size analysis and mineralogical composition made it possible to reveal the features of climatic and other environmental changes on the studied lacustrine sediments.

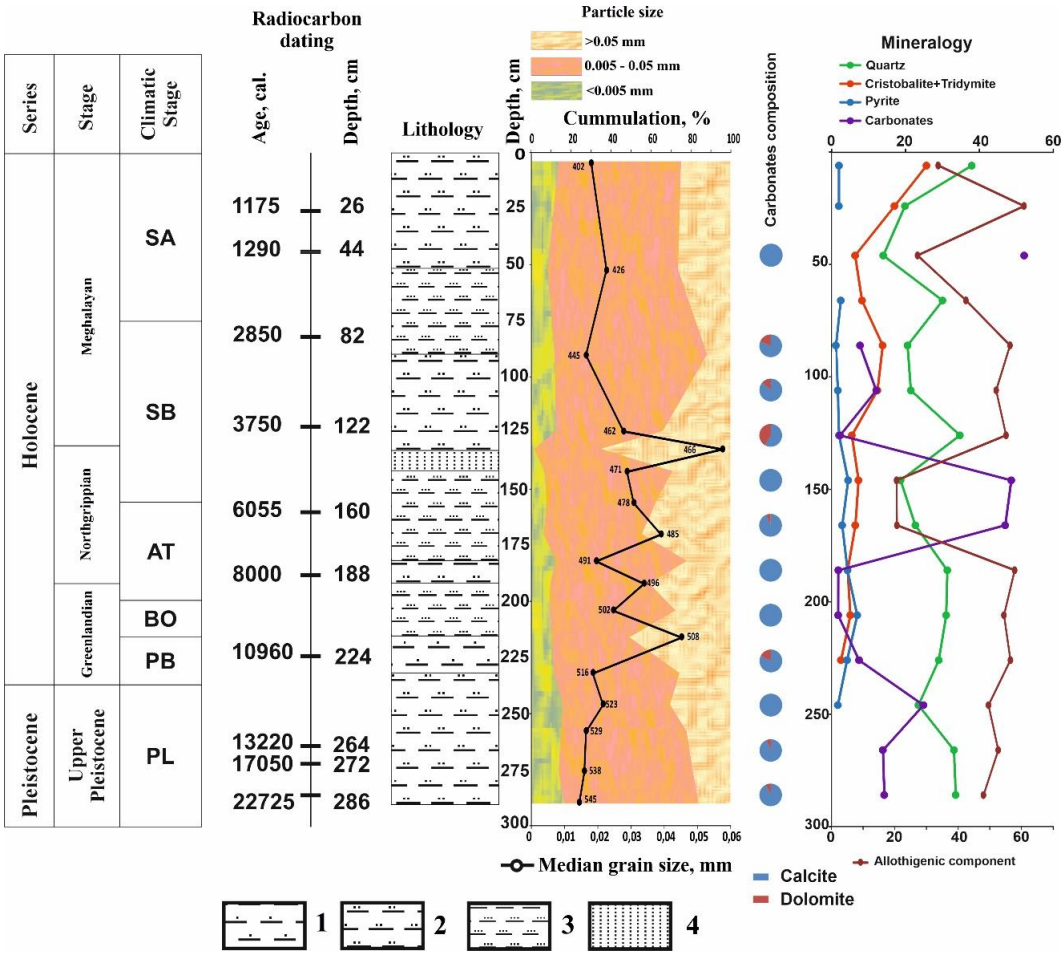

Figure 1 – Results of particle size and mineralogical analysis of Lake Sabakty sediments. Legend: 1 – clayey silt, 2 - silt, 3 – sandy silt, 4 - silty sand

Funding; This study was funded by the Russian Foundation for Basic Research, project 20-35-90058. Part of the study was funded with the subsidy allocated to the KFU in context of state assignment 671-2020-004.

References:

1. Gareev A.M. Rivers and lakes of Bashkortostan. Ufa. Kitap. 2001. 259 p.
2. Gareev A.M. Rivers, lakes and swamp complexes of the Republic of Bashkortostan. Ufa. Gilem Publ. 2012. 248 p. (In Russian).
3. Gareev A.M. Sabakty. Bashkir Encyclopedia. Ch. ed. M.A. Ilgamov. Ufa. GAUN "Bashkir Encyclopedia". 2015-2020.
4. Krylov P.S, Nurgaliev D.K, Kuzina D.M. High-resolution seismic studies of shallow Lake Sabakty (Russia). International Multidisciplinary Scientific GeoConference Surveying Geology and Mining Ecology Management, SGEM. 2019. Vol. 19. No. 4.2. P. 229-234.
5. Yusupova A.R., Nurgalieva N.G., Batalin E.A., Gareev B.I. (2021):The first results of isotope geochemistry of bottom sediments of Lake Sabakty (Southern Ural). In Proceedings of the conference of young scientists Modern problems of geochemistry. Irkutsk: Institute of Geochemistry. A.P. Vinogradova. P. 36-38.
6. Deelman J.C. Low-temperature formation of dolomite and magnesite. Open-access e-book. 2011. 512 p.

THE SEQUENCE AND MECHANISMS OF PLATINUM GROUP MINERALS CRYSTALLIZATION FROM EUTECTIC GALENA-CHALCOPYRITE ORES OF THE OKTYABR'SKOE DEPOSIT, NORIL'SK REGION, RUSSIA

Kuzmin I.A.[1], Kalugin V.M.[2]

[1]Saint Petersburg Mining University, St. Peterburg, Russia; kuzmin.kuvanechka@yandex.ru
[2]V.S. Sobolev Institute of Geology and Mineralogy, Novosibirsk, Russia; kalugin@igm.nsc.ru

Abstract. We have studied platinum group minerals (PGM) from galena-chalcopyrite ores of the Oktyabr'skoe nickel-copper deposit in order to determine the mechanism of their formation. We found 9 species of PGM in 26 multiphase PGM grains. The PGM crystallized in the following sequence: (1) taimyrite-1 + paolovite, (2) michenerite + sobolevskite + hessite, (3) maslovite + sperrylite + taimyrite-3, (4) froodite. Taimyrite-1 and paolovite crystallized from the melt. Minerals of 3, 4 and 5 stages appeared as a result of a solid solution transformation. Froodite substituted the sobolevskite as a result of late metasomatic process.

Key words: platinum group minerals, galena-chalcopyrite symplectites, solid solution, Noril'sk

Different researchers have studied platinum group minerals (PGM) located in the Norilsk ores. Various hypotheses of their crystallization were put forward, including hydrothermal-metasomatic [1]. The purpose of this study is to establish the sequence of crystallization of precious metal minerals in graphic galena-chalcopyrite ores of the Oktyabr'skoye deposit. This will help determine the mechanism of their formation. The samples were collected from the upper exocontact of the body of massive sulfide ores of the Oktyabr'skoye deposit. They are represented by galena-chalcopyrite symplectites. Presumably, they crystallized from the eutectic sulfide liquid [1]. This could cause the high concentration of PGE in these ores and the appearance of many multiphase PGM grains ranging in size from a few tens of micrometers to five millimeters. Previously, PGM from similar symplectite ores have already been studied [2, 3].

The work was carried out on a Tescan MIRA 3 LMU scanning electron microscope equipped with an Inca Energy 450+ X-Max 80 microanalysis system (Oxford Instruments Nano Analysis). Analytical studies were performed at the laboratory of X-ray spectral analysis of the Analytical Center for Multi-Elemental and Isotope Research of SB RAS at the Sobolev Institute of Geology and Mineralogy, SB RAS, Novosibirsk (Russia). We found 9 mineral species in 26 multiphase PGM grains including: sobolevskite (PdBi), michenerite (PdBiTe), altaite (PbTe), taimyrite ($(Pd,Pt,Cu)_3Sn$), paolovite (Pd_2Sn), hessite (Ag_2Te), maslovite (PtBiTe), froodite ($PdBi_2$), sperrylite ($PtAs_2$). Sobolevskite makes up the bulk of all PGM grains. It is the matrix for other minerals. Hessite, michenerite and altaite occur in sobolevskite in the form of subparallel lamellas. Partially faceted crystals of sperrylite and maslovite situated on the boundary between hessite and michenerite lamellae and sobolevskite matrix. Taimyrite occurs in three variety. Taimyrite-1 crystals intergrown with paolovite form druses and large crystals in the marginal parts of large PGM grains. Taimyrit-2 is represented by small (up to five micrometers) isometric crystals evenly distributed by the volume of multiphase grains. Taimyrit-3 forms lamellae in sobolevskite. Froodite intergrows with sobolevskite that contains taimyrite-3 lamellae. At the same time, taimyrite-3 lamellae begin in sobolevskite and cross the boundary with froodite. Taimyrite-3 lamellae are absent in froodite, except for a narrow contact zone with sobolevskite.

The above observations suggest the sequence of appearance of minerals in the multiphase PGM grains. Position of Taimyrite-1 and paolovite in the marginal parts of PGM grains and the shape of the grains confirm their crystallization from the melt before the other PGM. This contradicts the assumption of late crystallization of taimyrite. [4]. From the other hand, it explains the uniform distribution of small crystals of taimyrite-2 in the multiphase grains representing a kind of suspension. It can be assumed that taimyrite-1 and taimyrite-2 belong to the same generation. The hypothesis that taimyrite-1 and taimyrite-2 belong to the same generation is also confirmed by the identity of the composition of taimyrite-1 and taimyrite-2, differing from taimyrite-3 [5]. We can make a conclusion that hessite and michenerite crystallized either later than or simultaneously with sobilevskite as their lamellaes are presented in the later. Crystals of maslovite at the contacts between sobolevskite-michenerite and sobolevskite-hesite show that they formed later than hessite and maichnerite. This is probably due to the continued decay of solid solutions, or metacrystals formation. Taimyrite-3 lamellae found in sobolevskite apparently formed after crystallization of sobolevskite. Froodite crystallized later than taimyrite lamellae. It is often possible to see that lamellae of the taimyrite-3 cross the sobolevskite-froodite contact. It is possible that froodite formed as a result of superimposed processes after the formation of a multiphase grain. Thus, multiphase PGM grains from galena-chalcopyrite symplectites crystallized from magmatic melt in the form of complex solid solutions. Later, probably, the disintegration of these solid solutions led to the appearance of most of the investigated PGM. These minerals crystallized in the following sequence: (taimyrite-1, 2 - paolovite) - (michenerite- sobolevskite) - hessite - maslovite - sperrylite - taimyrite-3. Froodite substituted the sobolevskite in the marginal part of the multiphase PGM grains as a result of a late metasomatic process.

References:

1. Spiridonov E.M., Serova A.A., Korotaeva N.N., Zhukov N.N., Kulagov E.A., Belyakov S.N., Kulikova I.M., Sereda E.V., Tushentsova I.N. Genetic Pd, Pt, Au, Ag, and Rh mineralogy in Noril’sk sulfide ores. Geology of Ore Deposits. 2015. Vol. 57. No. 5. P. 402-432.
2. Cook N.J., Ciobanu C.L., Merkle R.K.W., Bernhardt H.J. Sobolevskite, taimyrite, and Pt_2CuFe (tulameenite?) in complex massive talnakhite ore, Noril'sk ore field, Russia. The Canadian Mineralogist. 2002. Vol. 40. P. 329-340.
3. Spiridonov E.M. Ore-magmatic systems of the Noril’sk ore field. Russian Geology and Geophysics. 2010. Vol. 51. No. 9. P. 1059-1077.
4. Barkov A.Y., Martin R.F., Poirier G., Yakovlev Y.N. The taimyrite-tatyanaite series and zoning in intermetallic compounds of Pt, Pd, Cu, and Sn from Noril'sk, Siberia, Russia. The Canadian Mineralogist. 2000. Vol. 38. P. 599-609.
5. Kuzmin I.A., Kalugin V.M. (2021): Morphological varieties of taimyrite in eutectic galena-chalcopyrite ores of the Oktyabr’skoe copper-nickel deposit, Norilsk region, Russia. New in the knowledge of ore formation processes: Collection of materials of the X Russian Youth Scientific and Practical School with International Participation. P. 164-167. Moscow: Institute of Geology of Ore Deposits, Petrography, Mineralogy and Geochemistry of the Russian Academy of Sciences (In Russian)

PECULIARITIES OF THE MINERAL COMPOSITION OF THE POBEDA-2 HYDROTHERMAL FIELD (MAR)

Lyutkevich A.D.[1]

Geological Institute, Russian Academy of Sciences, Moscow, Russia, nastya.lyutkevich@mail.ru

Abstract. The Pobeda Hydrothermal Cluster (17°07.45′-17°08.7′N MAR) was discovered in 2014-2015 during cruise No. 37 of the RV "Professor Logachev". Ore-bearing sediments were raised, the mineral composition of which was studied by a complex of methods. A detailed study of ore-bearing sediments of column 37L245g revealed zinc minerals unusual for modern oceanic sediments, represented by zinc phosphates, zincite, willemite, zinc-bearing forsterite, gahnite(?) - and most of them have been identified in this sector of the MAR for the first time.

Key words: zinc minerals, ore-bearing oceanic sediments, the hydrothermal cluster Pobeda.

In 2014-2015 the Polar Marine Geological Exploration Expedition carried out cruise No. 37 of the RV "Professor Logachev" in the near-quaternary zone of the Mid-Atlantic Ridge, during which the Pobeda hydrothermal cluster (17°07.45′-17°08.7′N MAR) was discovered. The Pobeda hydrothermal cluster consists of the Pobeda-1 and Pobeda-2 ore fields and the Pobeda-3 ore occurrence, where sulfide ores and ore-bearing sediments were raised. Sediments were sampled from a depth of 2208 m to 3106 m using a television grab (g) and a box corer (k). This paper presents the results of a study of the sediment column of stations 37L245g (Pobeda-2 ore field). The total length of the column is 50 cm.

The mineral composition was investigated by a complex of methods: scanning electron microscopy and X-ray spectral microanalysis (analyst V.O. Yapaskurt), X-ray diffractometry (analyst O.M. Dara), Raman spectroscopy (analyst V.D. Shcherbakov) and electron backscattered diffractometry (analyst P.A. Somov).

Sediments are represented by ore-bearing coccolithic foraminiferal silt with a layer of pterapod sands in the interval of 25-30 cm. Ore minerals are represented by atacamite, goethite, iron sulfates, pyrite, and marcasite. Sulfides predominate in the lower part of the column section. In intervals 14-18 cm and 35-38 cm the presence of rare minerals was detected - zincite $Zn_{0,93-1,00}O_{0,91-0,95}$, zinc phosphates with ideal formulas: tarbuttite ($Zn_2[PO_4][OH]$), paragopeitis ($Zn_3(PO_4)_2 \cdot 4H_2O$) and spencerite ($Zn_4(PO_4)_2(OH)_2 \cdot 3H_2O$). Willemite has also been identified $Zn_{1,41-1,84}Mg_{0,24-0,69}Si_{1,03-1,07}O_{3,75-3,90}$, zinc-bearing forsterite $Mg_{1,65}Zn_{0,37}SiO_{3,89}$, gahnite(?) $(Zn_{0,80-0,88}Mg_{0,21-0,38})\ Al_{1,83-1,95}O_{3,77-3,93}$.

Zinc phosphates form clusters in the pore space of coccolithic foraminiferal silt (fig. 1), framing on the outer surface of calcite shells of microorganisms, excretions on their inner surface in a fine mixture with clay minerals, and pseudomorphs along the shells. Zinc phosphates almost always contain inclusions of zincite. The zinc phosphates in the sediments of column 37L245g are characterized by high content of impurities, such as Fe, Ca, Mg, Al, Si [1].

Another rare mineral first identified in this sector of the MAR is zincite $Zn_{0,93-1,00}O_{0,91-0,95}$, in association with zinc phosphates as small (up to 20 μm) precipitates of irregular, less often isometric circular shape in pore spaces(?) of coccolithic foraminiferal sediments, as well as in crusts on the surface of calcite foraminifer shells. Zincite and zinc-bearing forsterite intergrowths are encountered (fig. 1).

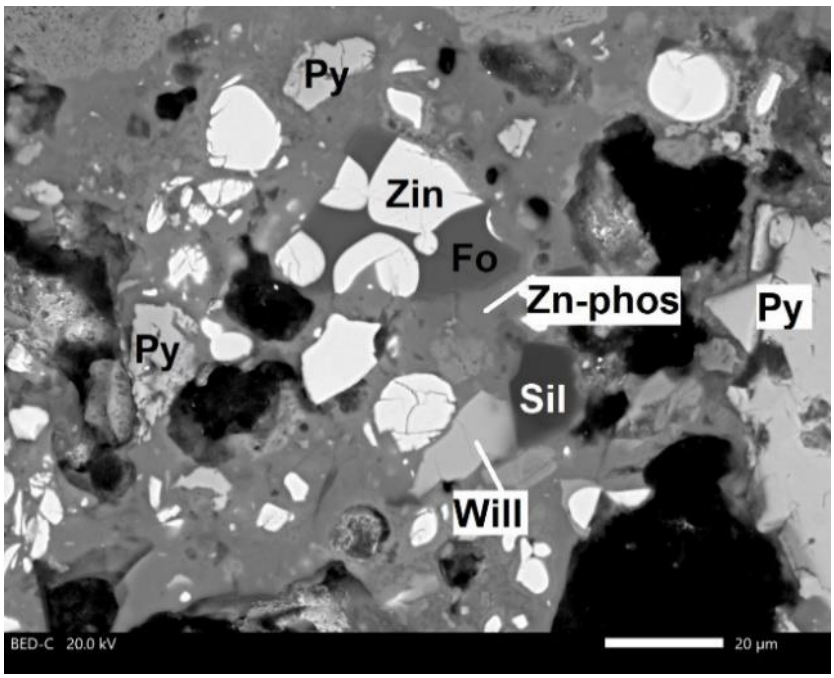

Figure 1 - Interval 35-38 cm column 37L245g. Photo in reflected electrons: a - intergrowth of zincite (Zin) and zinc-containing forsterite (Fo), willemite (Will), zinc phosphate with impurities (Zn-phos), large excretions of pyrite (Py) [2].

Zinc-containing forsterite in the horizons of column 37L245g forms intergrowths with zincite. The zinc impurity in forsterite is a rather rare phenomenon [3], and probably can be explained by the fact that the characteristic X-ray generation region during the measurement extends to other phases as well.

Willemite with the theoretical formula Zn_2SiO_4 is represented by angular isometric precipitates up to 10 μm in a matrix of zinc phosphates. Willemite is also observed as aggregates with sodium and zinc silicate. The size of such polymineral formations is up to 20 μm (fig. 1).

Ganit(?) with the formula (Zn, Mg) Al_2O_4 forms individual grains or their clusters, up to 10 μm in size, in a matrix of zinc phosphates.

The appearance of these rare minerals indicates unusual physicochemical conditions of ore formation in the column 37L245g of the Pobeda hydrothermal cluster, possibly associated with increased P content in ore-bearing solutions coming from the substrate, and requiring further research in this direction.

Funding: This work is supported by the Russian Science Foundation (GIN RAS, IO RAS № 0128-2021-0006).

References:

1. Gablina I.F., Dobretsova I.G., Popova E.A, Dara O. M., Sadchikova T. A., Gor'kova N. V., Mikheev V. V. Mineral composition and geochemical zoning of bottom sediments of the Pobeda hydrothermal node (17°07.45′N - 17°08.7′N of the Mid-Atlantic Ridge). Lithology and Mineral Resources. 2021. No. 2. p. 101-121.

2. Lyutkevich A.D., Gablina I.F., Dara O.M. et al. Mineral phases of zinc in ore-bearing sediments of the Pobeda hydrothermal cluster (17°07.45′-17°08.7′ N, MAR). Lithology and Mineral Resources - in press.

3. Vlasov E.A. Training course "Mineralogy". Moscow. Geological Faculty of the Lomonosov Moscow State University. 2010.

VIVIANITE IN BOTTOM SEDIMENTS OF LAKE ONEGO

Malov V.I.[1,2], Strakhovenko V.D.[1,2], Ovdina E.A.[1]

[1]V.S. Sobolev Institute of Geology and Mineralogy, Novosibirsk, Russia, malov@igm.nsc.ru
[2]Federal State Autonomous Educational Institution of Higher Professional Education "Novosibirsk National Research State University", Novosibirsk, Russia

Abstract. The study of the mineral composition of Lake Onego bottom sediments showed that in the section of bottom sediments there are layers, interlayers, and green nodules. These secretions are the mineral iron phosphate. The chemical composition of this mineral is in the following ranges of element content (%): Fe 26.3-30.0, Mn 3.9-6.6, P 10.9-12.6 and O 40.2-47.0. According to XRD data, this mineral is vivianite. The study of this mineral phase using Raman spectroscopy showed a similar spectrum to vivianite, but with no water peak.

Key words: vivianite, Lake Onego, bottom sediments.

Phosphorus plays an important role in the geochemistry of lakes. This is because phosphorus is the main nutrient that determines the primary bioproductivity in lakes. The formation of phosphorus minerals in bottom sediments can significantly increase the uptake of phosphorus from water. This, in turn, affects the availability of phosphorus for primary producers in water and leads to a change in the N:P stoichiometry and the trophic status of lakes [1].

The aim of the work is to search for and diagnose phosphorus minerals in the bottom sediments of Lake Onego.

The object of the study is Lake Onego. Lake Onego is located in the zone of the European North of Russia, between 60º53' and 34º55' N, 34º13' and 36º28' E. The area of the lake is ~10 thousand km^2, the length from north to south is 290 km and from east to west 82 km and is the second largest fresh water body in Europe. Cores of bottom sediments up to 3.2 m thick were taken from different regions of Lake Onego, represented by Late Pleistocene lacustrine-glacial and Holocene lacustrine sediments. The following samplers carried out sampling: Limnos stratometer, GOIN tube up to 1.5 m, heavy gravity tubes up to 3 m.

Bottom sediment samples were studied by the following methods: mineral composition was studied using by X-ray diffractometry; study of the morphology and phase composition of samples by scanning electron microscopy, equipped with an energy spectrometer; the mineral composition was studied by Raman spectroscopy. Analytical work was carried out at the Analytical Center for multi-elemental and isotope research SB RAS, Novosibirsk, Russia.

The study of bottom sediments samples showed the following: in addition to such basic minerals as quartz, feldspars, chlorite, illite, Fe and Mn hydroxides, which were previously presented in [2], the iron phosphate mineral was found in the bottom sediments of Lake Onego.

This mineral is found in bottom sediment cores below the upper oxidized layers. It is unevenly distributed along the section in the form of enriched layers up to 1.5 cm thick, visually distinguished by a clearly green color; individual layers; as well as small contractions. Individuals have an elongated morphology, often forming radially radiant aggregates, which in turn can become isolated. There are also individuals whose size reaches 200 μm (Fig. 1). The absence of this mineral in some cores indicates an uneven lateral distribution in the bottom sediments of Lake Onego.

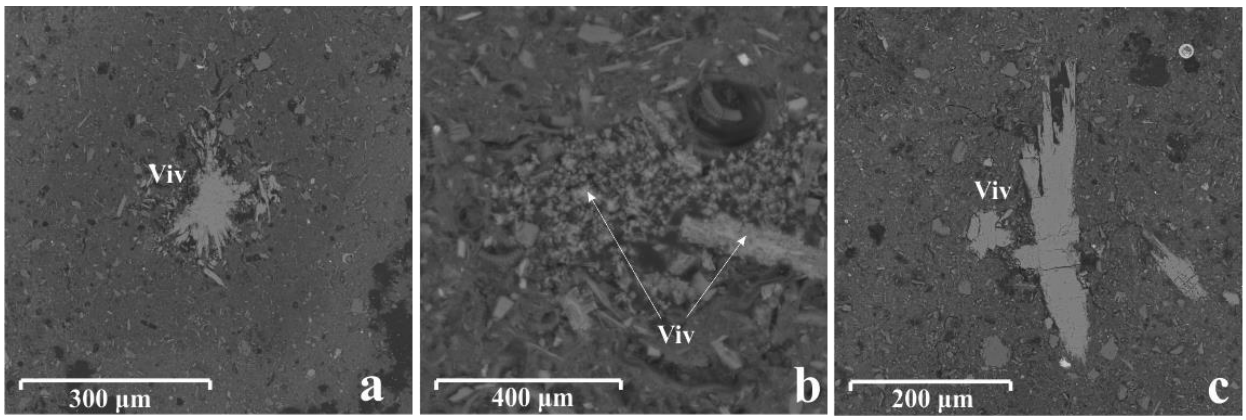

Figure 1 – Electron microscope images of vivianite - a) radially radiant aggregates of vivianite; b) segregation of radially radiant aggregates of vivianite; c) elongated vivianite individuals.

The study of bottom sediments on a scanning microscope showed that this mineral is iron phosphate. Microanalysis of the chemical composition on the SEM of this mineral made it possible to determine the composition of this mineral phase (according to 69 analyses), where the ranges of element content (%) are as follows: Fe 26.3-30.0, Mn 3.9-6.6, P 10.9-12.6 and O 40.2-47.0, giving an overall range of 86.1-92.2. A similar composition corresponds to the composition of vivianite. Vivianite regularly contains significant amounts of Mn and/or Mg, which replace Fe in the vivianite lattice [3]. According to the XRD method, this mineral is vivianite. The study of this mineral phase by Raman spectroscopy showed that although the spectral range of the Raman spectrum of this mineral phase from 200 to 1300 cm^{-1} shows a similar profile with the Raman spectroscopy characteristic of vivianite, unlike vivianite, Raman spectroscopy here shows the absence of water in the structure of this mineral phase.

Based on the data obtained, it can be concluded that the mineral limiting the amount of phosphorus in the lake system is iron phosphate, due to the conservation of phosphorus in bottom sediments in vivianite.

Funding: The work was supported financially by the Russian Foundation for Basic Research (Project No. 19-05-50014) and by the Russian Science Foundation under Research (Project No. 18-17-00176-n).

References:

1. Rothe M., Kleeberg A., Hupfer M. The occurrence, identification and environmental relevance of vivianite in waterlogged soils and aquatic sediments. Earth-Science Reviews. 2016. Vol. 158. P. 51-64.

2. Strakhovenko, V., Subetto, D., Ovdina, E., Danilenko, I., Belkina, N., Efremenko, N., Maslov, A. Mineralogical and geochemical composition of Late Holocene bottom sediments of Lake Onego. Journal of Great Lakes Research. 2020. Vol. 46. No. 3. P. 443-455.

3. Nakano S. Manganoan vivianite in the bottom sediments of Lake Biwa, Japan. Mineralogical Journal. 1992. Vol. 16. No. 2. P. 96-107.

ALLANITE IN MANTLE ECLOGITE

Mikhailenko D.S.[1,2], Stepanov A.S.[3], Aulbach S.[4], Gubanov N.V.[1], Korsakov A.V.[5], Xu Yi-G[2].

[1]Sobolev Institute of Geology and Mineralogy, Novosibirsk, Russia, mikhailenkodenis@gmail.com
[2]Key Laboratory of Isotope Geochemistry, Guangzhou Institute of Geochemistry, Chinese Academy of Science, Guangzhou, 510640, China.
[3]Collaborative Innovation Center for Exploration of Strategic Mineral Resources, School of Earth Resources, China University of Geosciences, Wuhan 430074, China.
[4]Institut für Geowissenschaften, Goethe-Universität Frankfurt, Germany.

Abstract. Rare-Earth Elements (REEs) are key geochemical tracers of crust-mantle differentiation but there are only a few direct data on REE-bearing accessory phases in the samples of mantle rocks transported to the surface by kimberlites. Here we report the first observations of allanite in three melt-, coesite- and kyanite-bearing eclogite xenoliths from Udachnaya, Siberian craton (Russia). The discovery of allanite in the Udachnaya eclogites demonstrates that REE minerals can occur in Al-rich mantle rocks, such as eclogite, and may be more common than hitherto recognized.

Key words: eclogite; allanite; partial melting; kimberlite

The subduction of oceanic lithosphere rocks into the mantle is the most important geological process that connects the various spheres of the Earth [1]. Accessory monazite and allanite typically host 75-90 % of LREE, Th and U in granites and crustal rocks that underwent HP/UHP metamorphism, and control the behaviour of these elements during metamorphism [2, 3]. Xenoliths of mantle eclogite from kimberlite represent some of the deepest rock samples of subducted oceanic crust [1]; however, while REE, Th and U are routinely measured for rock-forming minerals, data on the residence of these elements in accessory phases are limited. Isotopic and geochemical studies tend to assume that garnet is the principal host of HREE, while clinopyroxene is the principal host of LREE and MREE [1, 4], however, the residence of LREE, Th, and U in these rocks is not well constrained. Here we present the results of studying the first discovery of allanite in kimberlite-born mantle eclogites from the Udachnaya kimberlite pipe.

Extensive search of REE minerals performed on a collection of eclogite xenoliths from the Udachnaya-East pipe resulted in the discovery of three xenoliths containing REE-rich minerals. All samples have massive coarse-grained texture with the grain size of garnet and pyroxene 0.5-3.0 mm. In all three xenoliths the rock-forming minerals are represented by orange-red garnet, light-green omphacite and kyanite. The garnet is less altered than omphacite and contains inclusions of rock-forming (omphacite, kyanite) and primary accessory minerals (rutile and coesite). Primary accessory minerals include coesite, sulfides (exsolved low-temperature assemblages of pyrrhotite, pentlandite and chalcopyrite), rutile, and, in Uv-567, diamond with graphite.

Idiomorphic allanite grains (50-70 μm in size) in eclogites Uv-567 and Uv-505 occurred at the boundaries between garnet and omphacite grains surrounded by secondary minerals including diopside, plagioclase, K-feldspar, serpentine, amphibole and calcite. In sample Uv-567 allanite has variable CaO content from 13 to 15.6 wt. %, and Al_2O_3 content between 15.6 and

18.3 wt. %. Allanite grains in eclogite Uv-505 contain the highest content of Al_2O_3 and CaO (up to 20.2 and 17.8 wt. %, respectively). Allanite in all studied samples has very high concentrations of light to middle REE (19.3-25.9 wt. % ΣREE_2O_3). Overall, mineralogical, petrographic and geochemical features of the allanite indicate its secondary origin during the interaction of eclogite residing in the lithospheric mantle and a (proto-) kimberlite melt.

The prevailing view is that the depletion of the bulk composition of eclogites from kimberlite in terms of LREE content is caused by their formation from depleted MORB protoliths followed by partial melting in the subduction process, during which LREE partitioned to the melt [1,4-6]. The presence of secondary REE minerals in the mantle rocks, though rarely detected, would significantly affect such estimates. The rare occurrence of REE minerals in mantle eclogites might include several geochemical reasons. Firstly, subduction of Archean oceanic crust likely was related with partial melting of the metabasalts that has generated trondhjemitic melts and extracted LREE via allanite dissolution [2]; secondly, high temperatures favor increased solubility of REE in the rock forming minerals and melts; and thirdly, the transport of eclogites from the mantle is associated with great change of conditions and alteration, which could be unfavorable for preservations of REE silicates. Moreover, although allanite in the studied samples is most likely a product of the interaction of (proto-) kimberlite melt and eclogite, the question of LREE-hosted minerals in deeply subducted rocks remains open, and requires further studies of accessory minerals in kimberlite-borne eclogite xenoliths.

Funding: The study was supported by the Russian Science Foundation (Project 21-77-10006) and Chinese Academy of Sciences President's International Fellowship Initiative (PIFI) for Postdoctoral Researchers, grant № 2019PC0033.

References:

1. Jacob D.E. Nature and origin of eclogite xenoliths from kimberlites. Lithos. 2004. Vol. 77. No. 1-4. P. 295-316.

2. Hermann J. Allanite: thorium and light rare earth element carrier in subducted crust. Chemical Geology. 2002. Vol. 192. P. 289-306.

3. Stepanov A.S., Hermann J., Korsakov A.V., Rubatto D. Geochemistry of ultrahigh-pressure anatexis: fractionation of elements in the Kokchetav gneisses during melting at diamond-facies conditions. Contributions to Mineralogy and Petrology. 2014. Vol. 167. No. 5. P. 1002.

4. Snyder G.A., Taylor L.A., Crozaz G., Halliday A.N., Beard B.L., Sobolev V.N., Sobolev N.V. The Origins of Yakutian Eclogite Xenoliths. Journal of Petrology. 1997. Vol. 38. No. 1. P. 85-113.

5. Jerde E.A., Taylor L.A., Crozaz G., Sobolev N.V., Sobolev V.N. Diamondiferous eclogites from Yakutia, Siberia: evidence for a diversity of protoliths. Contributions to Mineralogy and Petrology. 1993. Vol. 114. No. 2. P. 189-202.

6. Agashev A.M., Pokhilenko L.N., Pokhilenko N.P., Shchukina E.V. Geochemistry of eclogite xenoliths from the Udachnaya Kimberlite Pipe: Section of ancient oceanic crust sampled. Lithos. 2018. Vol. 314. P. 187-200.

FORMATION CONDITIONS OF FE-MN CARBONATES FROM KERCH IRONSTONES: EVIDENCE FROM STABLE ISOTOPES

Nekipelova A.V., Sokol E.V., Kokh S.N.

V.S. Sobolev Institute of Geology and Mineralogy, Novosibirsk, Russia, nekipelova@igm.nsc.ru

Abstract. Oxygen and carbon isotopic compositions of Fe-Mn carbonates from the Kerch ironstones (-9.1 to -36.3 ‰ VPDB $\delta^{13}C$ and -3.2 to -8.6 ‰ VPDB $\delta^{18}O$) indicate that the minerals formed during the early diagenetic stage and that most of carbon came from degrading organic matter. The formation conditions of authigenic carbonates reconstructed from their isotopic signatures agree well with the conditions inferred previously for the Kerch ironstones.

Key words: Fe-Mn carbonate, Kerch ooidal ironstones, isotope composition

Sediments are excellent archives of past environments but the primary geochemical signals are frequently biased by post-depositional alteration. This is the case of early Pliocene (N_2^1) Kerch ironstones which were deposited in the northern shelf of the Euxine Paleosea in paleogeographic and climatic (semiarid subtropics) conditions favorable for iron accumulation. In the Early Pliocene, the territory of the present northern Black Sea was occupied by numerous shallow-water systems of bogs, freshened lagoons and limans connected through Don, Dnieper and other rivers and their tributaries. The water systems were highly bioproductive and transported lateritic weathering residue shed from the Ukrainian shield. Interaction of river and sea waters produced geochemical barriers which captured voluminous coagulated iron colloids and Fe-bearing sediments (future ironstones) [1]. The ore beds in the area consist of alternating Fe^{3+}(Mn)-(oxy)hydroxide (the so-called tobacco, brown and caviar ores) and Fe-Mn carbonate layers [2, 3]. The complex composition of the Kerch ironstones results from multiple redox changes caused by sealevel fluctuations and high-energy hydrodynamic conditions of the littoral zone [1, 2]. This study focuses on authigenic carbonates from the Kerch ironstones (Kamysh-Burun deposit) and their deposition environments inferred from isotopic signatures. The structure of the Kamysh-Burun deposit and analytical methods were reported previously: details of stratigraphy and lithology in [2, 3] and methods for analysis of stable isotopes in [4].

Carbonates mainly occur in the Kerch ooidal ironstones as 0.1-0.2 m concretions in brown ore. Sporadic allochems are buried in a matrix of mixed Fe-Mn-carbonates, which form micritic aggregates of subhedral to anhedral grains (5-10 – 50-70 μm). The minerals make up an almost continuous series from siderite to rhodochrosite: $(Fe_{0.00\text{-}0.90}Mn_{0.02\text{-}0.83}Ca_{0.06\text{-}0.33}Mg_{0.00\text{-}0.09})(CO_3)$, which are highly depleted in ^{13}C ($\delta^{13}C$ = -9.1 ÷ -36.3 ‰ VPDB) and slightly depleted in ^{18}O ($\delta^{18}O$ = -3.2 ÷ -4.7 ‰ VPDB). Rhodochrosite in caviar ores occurs locally as cement composed of 80-100 μm isometric grains or frequently as pseudomorphs after bivalve and gastropod mollusk shells. Both modes of Mn-rich carbonate belong to a solid solution series toward kutnahorite $(Mn_{0.56\text{-}0.83}Ca_{0.14\text{-}0.39}Fe_{0.00\text{-}0.08}Mg_{0.00\text{-}0.08})(CO_3)$ and have somewhat different $\delta^{13}C$ (-12.9 ÷ -19.0 ‰ VPDB) and $\delta^{18}O$ (-5.5 ÷ -8.6 ‰ VPDB) values (Fig. 1). Bivalve mollusk shells hosted by brown ores are mainly composed of aragonite and are very close to the $CaCO_3$ composition. Their $\delta^{13}C$ (-0.4 to -2.4 ‰) and $\delta^{18}O$ (-3.5 to -5.1 ‰ VPDB) values fall into the field of carbonates deposited in marine environments [5] (Fig. 1).

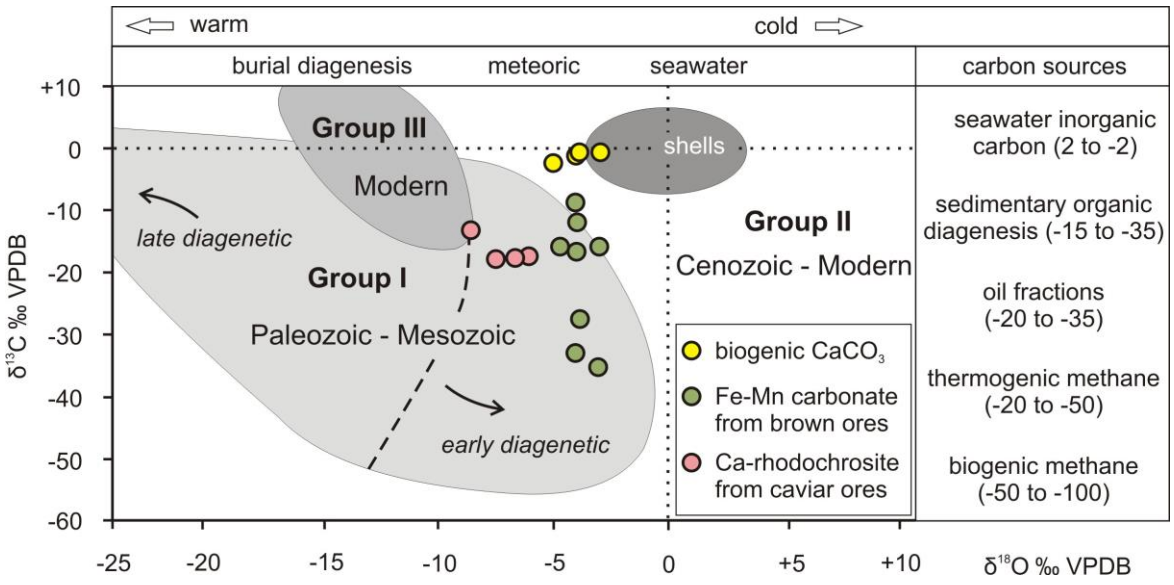

Figure 1 - Carbon isotope compositions of carbonates from the Kerch ironstones with a sketch of carbon sources and principal controls of isotopic variability, after [5].

The isotopic signatures of authigenic Fe-Mn carbonates from the Kerch ironstones indicate that they formed during early diagenesis while most of carbon was produced by oxidation of organic matter [5]. Diagenesis of Fe(Mn)-(oxy)hydroxides in oxygen-deficient environments led to gradual reduction of Fe^{+3} and $Mn^{+3(+4)}$. Since $Mn^{+3}(^{+4})$ can convert to Mn^{+2} under less reducing conditions than the Fe^{+3} change to Fe^{+2}, rhodochrosite is inferred to form in suboxic to weakly reducing environments, whereas siderite precipitation requires a higher reducing potential. Intermediate redox conditions maintained precipitation of mix Mn-Fe carbonates. Magnesium depletion typical of all authigenic carbonates from the Kerch ironstones is consistent with their formation in a highly freshened lagoon environment. The new isotopic data fit well the existing genetic model explaining the early Pliocene deposition of Fe-rich sediments.

Funding: The analytical work was supported by the Russian Science Foundation (grants 17-17-01056 and 17-17-01056P).

References:

1. Shnyukov E.F. The genesis of the Cimmerian iron ores of the Azov-Black Sea ore province. Naukova Dumka. Kiev. 1965. 194 p. (In Russian)

2. Sokol E.V., Kokh S.N., Kozmenko O.A., Nekipelova A.V., Rudmin M., Khvorov P.V., Artemyev D.A. Geochemistry and mineralogy of rare earth elements in high-phosphorus ooidal ironstones: a case study of the Kamysh-Burun deposit (Azov-Black Sea iron Province). Ore Geology Reviews. 2020. Art. 103827.

3. Nekipelova A.V. Sokol E.V., Kokh S.N., Khvorov P.V. Rare earth phosphates in the Kerch caviar ironstones. Russian Geology and Geophysics. 2021. Vol. 62. No. 10. P. 1189-1207.

4. Sokol E., Kokh S., Kozmenko O., Novikova S., Khvorov P., Nigmatulina E., Belogub E. Kirillov M. Mineralogy and geochemistry of mud volcanic ejecta: a new look at old issues (a case study from the Bulganak field, Northern Black Sea). Minerals. 2018. Vol. 8. No. 8. Art. 344.

5. Campbell K.A. Hydrocarbon seep and hydrothermal vent paleoenvironments and paleontology: Past developments and future research directions. Palaeogeography, Palaeoclimatology, Palaeoecology. 2006. Vol. 232. No. 2-4. P. 362-407.

PHLOGOPITE FROM AILLIKITES OF THE ZIMINSKY COMPLEX OF THE EAST SAYAN REGION, RUSSIA

Nugumanova Ya.N.

V.S. Sobolev Institute of Geology and Mineralogy, Novosibirsk, Russia,
nugumanovayn@igm.nsc.ru

Abstract. In this paper, we report about zonal phlogopite from the groundmass of aillikites of the Ziminsky complex of the East Sayan region. We found 5 types of phlogopite with different content of Al, Mg, Ti, Fe. Aluminous phlogopites I and II form a general trend in composition change with a gradual decrease Al, Mg, Ti, and an increase in Fe from the first to the second. Phlogopites IV and V have their own trend of composition change with a decrease in Al, Mg and an increase in Ti, Fe. We assume that the phlogopite in aillikites of the Ziminsky complex has a complex genesis and distinguish xenocrystal, metasomatic, igneous phlogopite in the groundmass of the studied rocks.

Key words: phlogopite from aillikites, zoned phlogopite, Ziminsky complex.

Phlogopite is a characteristic mineral of the groundmass of kimberlites and ultramafic lamprophyres, and belongs to the final stage of rock formation. There are two main genetic generations of phlogopite in the groundmass of rocks: phlogopite crystallized from melt and postmagmatic (metasomatic), which was formed when other minerals of the groundmass were replaced by postmagmatic solutions [1]. Phlogopite is often used to determine the absolute age of formation of kimberlites and related rocks. But this method of determining the age may not be successful if the genesis of phlogopites is not correctly deciphered and they are insufficiently studied in kimberlites and related rocks. In order to determine the possibility of using phlogopite for dating ultramafic lamprophyres, we carried out a detailed study of the composition of phlogopites from the aillikite groundmass of the Ziminsky complex (Bolshetagninskii massif).

The studied aillikites of the Bolshetagninskii massif consist of olivine phenocrysts and a completely crystallized fine-grained groundmass. Olivine is completely replaced by talc and chlorite. The groundmass is represented by spinels (chromite, magnetite), phlogopite, perovskite, apatite, calcite, dolomite, and chlorite.

Phlogopite is widespread mineral in the groundmass of the studied rocks and is represented by tabular crystals and flakes with a grain size of 20-50 μm in width. The composition of phlogopite grains is heterogeneous, they have stepped zoning (Fig. 1).

The cores of the crystals are mainly composed of Al-high phlogopites with an Al_2O_3 content of 16.31-18.01 wt.%, MgO - 19.01-19.21 wt.%, FeO - 9.07 - 9.15 wt.%, TiO_2 - 3.65-3.67 wt.%. Phlogopites II are characterized by a lower content of Al_2O_3 – 14.5-15.1 wt.%, MgO – 16.82 - 16.91 wt.%, TiO_2 up to 3.05 wt.% and higher FeO up to 15.17 wt.% relative to phlogopites I. Phlogopites III relative to the above described phlogopites are depleted in Al_2O_3 up to 13.5 wt.%, TiO_2 up to 1.62, FeO up to 10.77 wt.% and enriched with MgO to 21.04 wt.%. Phlogopites IV are characterized by a lower content of Al_2O_3 up to 12.01 wt.%, TiO2 up to 0.6 wt.%, and higher FeO and MgO. Phlogopites V are represented by tetraferriflogopites with an Al_2O_3 content of up to 10.03 wt.%, MgO up to 11.81 wt.%, FeO up to 23.58 wt.%, TiO_2 up to 3.4 wt.%. The content of Cr_2O_3 in all varieties of phlogopites is below 0.1 wt.%.

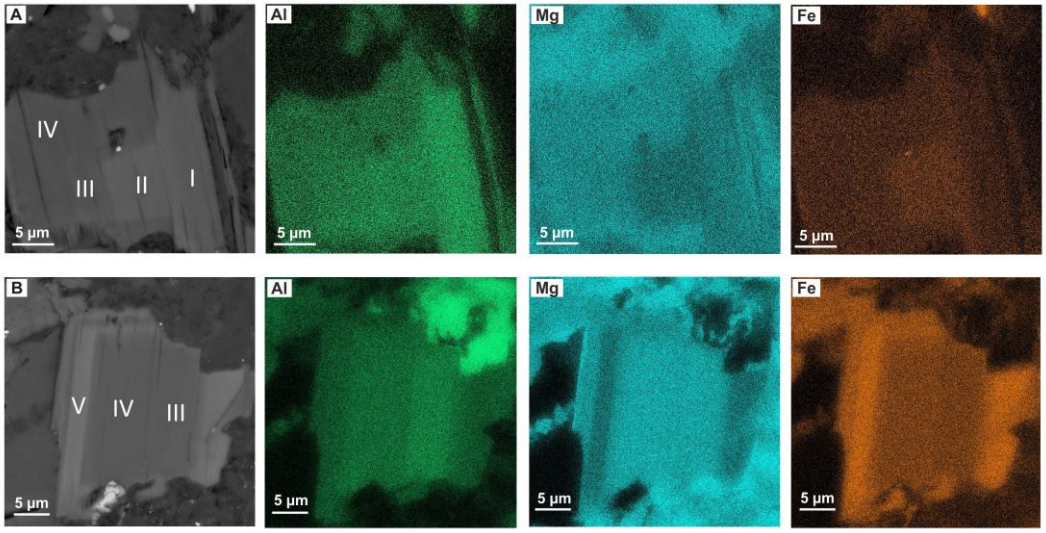

Figure 1 – BSE-images and elemental maps for phlogopites from aillikites of the Bolshetagninskii massif.

According to Mitchell, 1995, primary phlogopite from aillkitites crystallized from aillikite melt should have Al_2O_3 - 9-13 wt.%, FeO - 4-8 wt.%, TiO_2 - 1-4 wt.%. The author also notes that kimberlite-like rocks often contain high-Al phlogopites differing in Ti and Fe content from the primary groundmass phlogopites. Their origin is unclear. Mitchell, 1995 suggested that high-Al phlogopites are not from mantle xenoliths, since primary phlogopites in mantle ultramafic rocks (Al_2O_3 - 12.4-14.5 wt.% [3]) and in basalts (Al_2O_3 - 8-13 wt.% [4]) have a relatively low Al content. Kharkiv, 1989 notes that phlogopite from xenoliths of deep rocks in most cases contains an increased amount of Cr_2O_3.

We assume that phlogopite from the groundmass of aillikites of the Bolshetagninskii massif has 4 genetic generations. Phlogopites I and II are probably xenocrystals and were formed as a result of the capture of early Middle Riphean kimberlites of the Ingashinsky complex by aillikitic melt [5]. Phlogopites III are probably metasomatic, formed by the interaction of aillikitic melt and xenocrystals. Phlogopites IV crystallized directly from the aillikitic melt, which is confirmed by the study of primary melt inclusions in chromites. Crystallization of tetraferriflogopites indicates a sharp change in redox conditions at the final stages of crystallization. Its formation may be associated with the addition of groundwater to magma and/or rapid loss of carbon dioxide [2].

Thus, phlogopite crystals from the groundmass of aillikites of the Bolshetagninskii massif show a wide variation in composition, and it is rather unreliable to use them for dating these rock types.

Funding: This work is supported by the Russian Science Foundation under grant 19-17-00019.

References:

1. Kharkiv A.D., Kvasnitsa V.N., Safronov A.F., Zinchuk N.N. Typomorphism of diamond and its minerals-satellites. Kyiv. Science thought. 1989. 184 p.

2. Mitchell R.H. Kimberlites, Orangeites and Related Rocks. New York. Plenium Press. 1995. 410 p.

3. Delaney J.S., Smith J.V., Carswell D.A., Dawson J.B. Chemistry of micas from kimberlites and xenoliths. II: Primary- and secondary-textured micas from peridotite xenoliths. Geochimica and Cosmochimica Acta. 1980. Vol. 44. P. 857-872.

4. Dawson J.B., Smith J.V. The MARID (mica-amphibole-rutile-ilmenite-diopside) suite of xenoliths in kimberlite. Geochimica and Cosmochimica Acta. 1977. Vol. 41. P. 309-332.

5. Egorov K.N., Kiselev A.I., Men'Shagin Y.V., Minaeva Y.A. Lamproite and Kimberlite of the Sayany Area: Composition, Sources, and Diamond Potential. Doklady Earth Sciences. 2010. Vol. 435. No. 2. P. 1670-1675.

METHANE-DERIVED AUTHIGENIC CARBONATES OF THE LAPTEV SEA CONTINENTAL SLOPE

Ruban A.S.

National Research Tomsk Polytechnic University, Tomsk, Russia, ruban@tpu.ru

Abstract. The authigenic carbonates are mainly represented by high-magnesium calcite. The negative carbon isotope compositions of studied carbonate samples suggests that carbonate formation was a result of the anaerobic oxidation of strongly ^{13}C-depleted methane (average $\delta^{13}C$ = –43.2‰). The source of carbon is biogenic methane with minor participation with other carbon sources. High $\delta^{18}O$ values of the carbonates might be inherited from fluids enriched in ^{18}O due to dissociation gas hydrates. Authigenic pyrite inclusions in carbonate is evidence of sulfate reduction during anaerobic oxidation of methane.

Key words: carbonates, cold seep, anaerobic oxidation of methane, Laptev Sea

Methane cold seeps are a widespread phenomenon that occur on the shelves and continental slopes of inland and marginal seas around the world, including the arctic seas. The anaerobic oxidation of methane coupled (AOM) with sulfate reduction is a key biogeochemical process at seep sites [1]. As a result of AOM, an abundance of dissolved inorganic carbon arises and the alkalinity of pore water also increases. The presence of seawater cations (Ca^{2+}, Mg^{2+}) and elevate carbonate alkalinity promotes the precipitation of authigenic carbonates [2], which shows a wide range of mineralogical compositions. Authigenic carbonates from cold seeps are unique archives for studying environment conditions including biogeochemical processes associated with the migration of methane-rich fluid through the sediment column [3].

Authigenic carbonates were collected at the Laptev Sea continental slope, during the 82nd cruise of the research vessel «Akademik Mstislav Keldysh». Analytical investigations of the nine carbonate samples included optical microscopy, X-ray diffraction analysis and scanning electron microscopy with energy dispersive analysis. For calculating the equilibrium $\delta^{18}O$ values for carbonates precipitated under present-day seafloor conditions used the equation of Kim and O'Neil [4].

Studied carbonates are mainly represented by three varieties of their form: isometric crusts, spherical or elliptical nodules, and chimney-like nodules with sizes up to 10 cm in diameter. The microcrystalline carbonate matrix is mainly composed of an aggregate of Mg-calcite and clay minerals. Various authigenic pyrite aggregates occurred in paragenesis with Mg-calcite such as long pyrite bands, general framboids, and specific framboids with radial overgrowths like sunflowers in shape (Fig. 1). The associated framboidal pyrite with the studied carbonate is pointed at the high activity of microbial sulfate reduction process during anaerobic oxidation methane and at a reducing environment carbonate precipitation.

All carbonate samples had negative $\delta^{13}C$ values (from –50.6‰ to –32.4‰ V-PDB) and positive $\delta^{18}O$ values (from 4.7‰ to 5.5‰ V-PDB). The most likely carbon source is biogenic methane at the same time range of $\delta^{13}C$ values reveal a mixing of biogenic methane with carbon from other sources. The calculated value of $\delta^{18}O$ of Mg-calcite with an average content of $MgCO_3$ of 10.7 mol % in equilibrium with the bottom water is 4.0‰, that lower than measured $\delta^{18}O$ values in studied carbonates. ^{18}O enrichment in the carbonate-precipitating fluid can be

caused by processes such as dehydration of clay minerals in deeper sediments (e.g. smectite-illite transformation) or destabilization of gas hydrates.

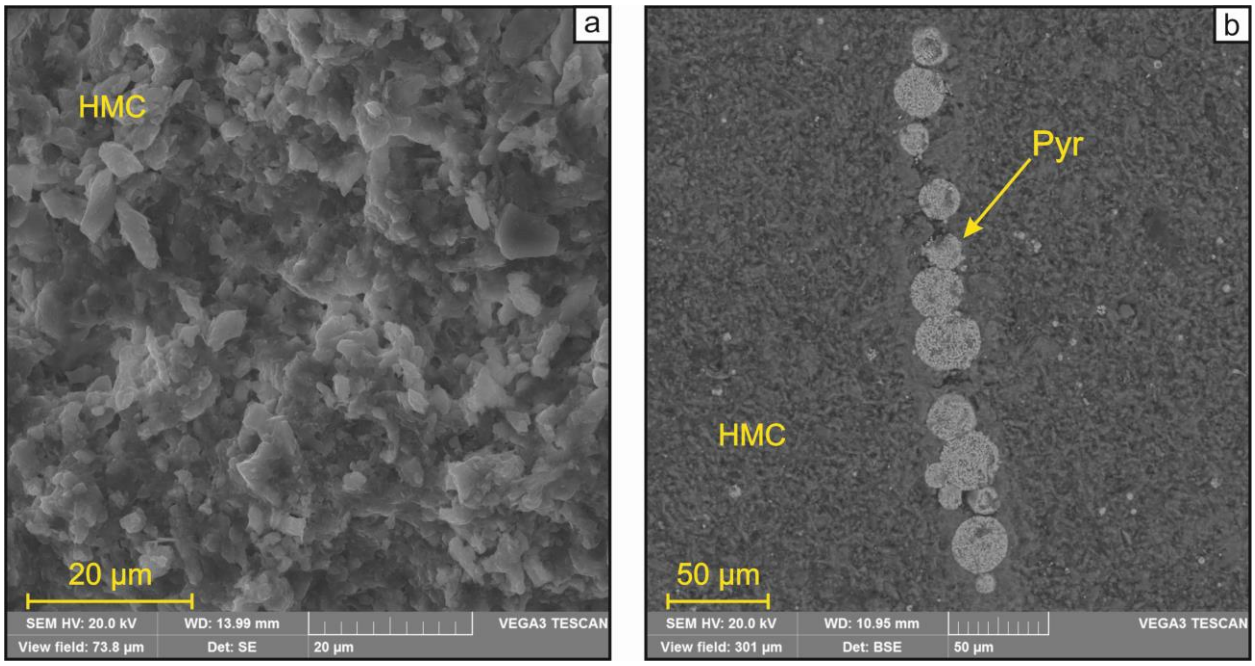

Figure 1 – SEM-images illustrating microstructure of authigenic carbonates from Laptev Sea continental slope: HMC – high magnesium calcite, Pyr – pyrite.

Funding: The research was supported by the Russian Science Foundation grants № 21-77-00033

References:

1. Boetius A., Ravenschlag K., Schubert C.J., Rickert D., Widdel F., Gleseke A., Amann R., Jørgensen B.B., Witte U., Pfannkuche O. A marine microbial consortium apparently mediating anaerobic oxidation methane. Nature. 2000. Vol. 407. P. 623–626.

2. Smith J.P., Coffin R.B. Methane flux and authigenic carbonate in shallow sediments overlying methane hydrate bearing strata in Alaminos Canyon, Gulf of Mexico. Energies. 2014. Vol. 7. P. 6118–6141.

3. Bayon G., Dupré S., Ponzevera E., Etoubleau J., Chéron S., Pierre C., Mascle J., Boetius A., De Lange G.J. Formation of carbonate chimneys in the Mediterranean Sea linked to deep-water oxygen depletion. Nature Geosciences. 2013. Vol. 6. P. 755–760.

4. Kim S.T., O'Neil, J.R. Equilibrium and nonequilibrium oxygen isotope effects in synthetic carbonates. Geochimica et Cosmochimica Acta. 1997. Vol. 61. P. 3461–3475.

CRYSTAL CHEMISTRY OF CALCIUM DICARBONATE CaC_2O_5: STRUCTURAL TREND FROM DOUBLE [CO_3] TRIANGLES THROUGH ISOLATED [CO_4] TETRAHEDRA INTO FRAMEWORK AND LAYERS

Sagatova D.N.[1,2], *Gavryushkin P.N.*[1,2]

[1]V.S. Sobolev Institute of Geology and Mineralogy, Novosibirsk, Russia,
d.sagatova1729@gmail.com
[2]Novosibirsk State University, Novosibirsk, Russia

Abstract. Based on the density functional theory and crystal structure prediction algorithms, we found a novel structure of CaC_2O_5, namely Ca-pyrocarbonate with monoclinic symmetry *Cc*, which stabilizes at 10 GPa. This structure characterized by polymerization of two [CO_3]-triangles, which form isolated [C_2O_5]-groups. With an increase in pressure sp^2-bonded carbon in the Ca-pyrocarbonate structure transformed into sp^3-hybridized state in the high pressure modifications (*I*-42*d*, *Fdd*2, *Pc*, and *C*2). All high pressure structures of CaC_2O_5 have a different type of polymerization of [CO_4] tetrahedra.

Key words: carbonate; pyrocarbonate; density functional theory; crystal structure prediction

A number of new types of carbonates, namely orthocarbonates, in the structure of which carbon atoms are in the sp^3-hybridized state, have been discovered using *ab initio* crystal structure predictions [1-3]. To date, it has been demonstrated that orthocarbonates of alkaline earth metals could be formed by the reaction of the carbonate with the oxide of corresponding metal into two different phases M_2CO_4-*Pnma* (MCO_3·MO) and M_3CO_5-*I*4/*mcm* (MCO_3·2MO), where M = Ca, Sr, and Ba at the pressures 5-20 GPa [1-2]. Subsequently, the stability of Ca_2CO_4-*Pnma*, Sr_2CO_4-*Pnma*, Sr_3CO_5-*I*4/*mcm* was confirmed by experiments [4-6]. All revealed structures of orthocarbonates contain isolated groups of [CO_4] tetrahedra and most of them have structural analogs among silicates.

In the system of CaO-CO_2, in addition to the reaction of carbonate with oxide, the reaction of carbonate with carbon dioxide was also studied. As a result, a new compound calcium dicarbonate CaC_2O_5 ($CaCO_3$·CO_2) was discovered both theoretically [3] and experimentally [7]. According to theoretical calculations, this compound is stable in the pressure range of 33–100 GPa in the following polymorphic modifications: *Pc*, *Fdd*2, and *C*2. However, a recent experimental study revealed a new structure CaC_2O_5-*I*-42*d* at pressures of 34 GPa. This disagreement between theory and experiment and the absence of a complete *P*-*T* phase diagram of CaC_2O_5 motivated us to revise this system in detail.

In the present study, based on the density functional theory and crystal structure prediction algorithms, we found a novel structure of CaC_2O_5, namely Ca-pyrocarbonate with monoclinic symmetry *Cc*, which is one of the possible agents of global carbon cycle. This structure is characterized by the isolated [C_2O_5] groups consisting of two [CO_3] triangles connected through the common oxygen atom. The thermodynamic stability field of Ca-pyrocarbonate with respect to the decomposition reaction into calcium carbonate and carbon dioxide begins at a pressure of 10 GPa (Fig. 1). As the pressure increases to 21 GPa, the structure of Ca-pyrocarbonate transforms into the recently synthesized tetragonal modification *I*-42*d*, in the structure of which carbon is in the sp^3-hybridized state and [CO_4] tetrahedra form isolated pyramidal [C_4O_{10}]

anionic groups. At 59 GPa in the temperature range 0-2500 K, CaC_2O_5-*I*-42*d* undergoes the phase transition to the CaC_2O_5-*Fdd*2, with the framework structure of [CO_4] tetrahedra. On further compression to about 80 GPa, the framework structure transforms into layered ones, *C*2 and *Pc*. In addition, we estimated the thermodynamic stability of CaC_2O_5 with respect to the minerals of Earth's mantle. We found that CaC_2O_5 can coexist with bridgmanite up to pressures of 54 GPa at 300 K, where it reacts with formation of Ca-perovskite, magnesite, and solid CO_2-V.

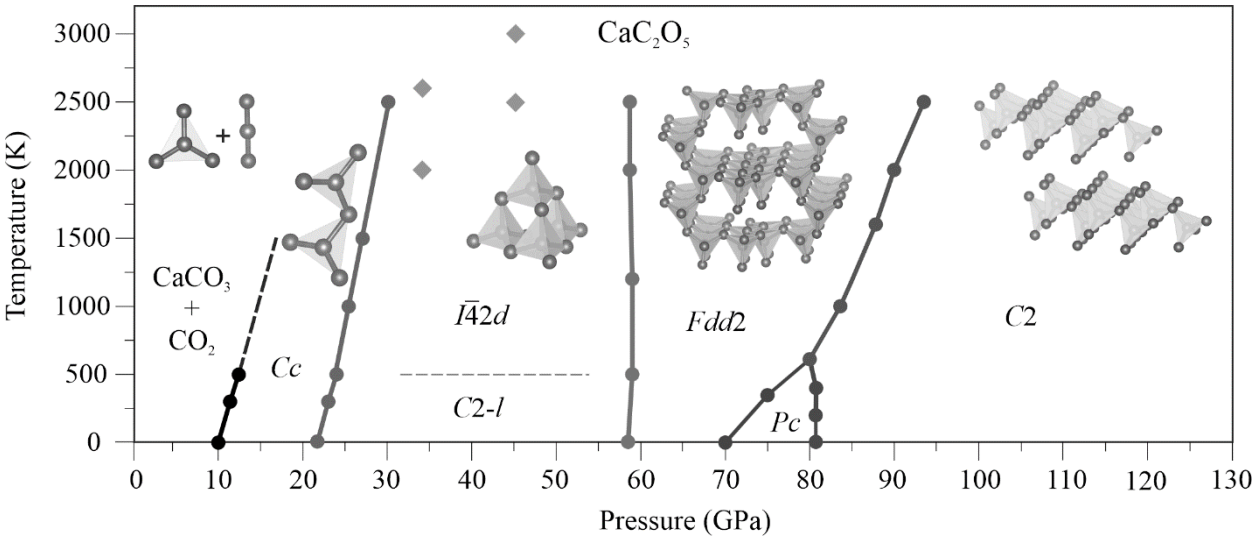

Figure 1 – *P-T* phase diagram of CaC_2O_5. Diamonds represent the synthesis conditions of CaC_2O_5-*I*-42*d* [7].

Funding: This work is supported by the Russian Science Foundation under grant 22-23-00925.

References:

1. Sagatova D., Shatskiy A., Sagatov N., Gavryushkin P.N., Litasov K.D. Calcium orthocarbonate, Ca_2CO_4-*Pnma*: A potential host for subducting carbon in the transition zone and lower mantle. Lithos. 2020. Vol. 370-371. Art. 105637.

2. Gavryushkin P.N., Sagatova D.N., Sagatov N., Litasov K.D. Orthocarbonates of Ca, Sr, and Ba—the appearance of sp^3-hybridized carbon at a low pressure of 5 GPa and dynamic stability at ambient pressure. ACS Earth and Space Chemistry. 2021. Vol. 5. P. 1948-1957.

3. Yao X., Xie C., Dong X., Oganov A.R., Zeng Q. Novel high-pressure calcium carbonates. Physical Review B. 2018. Vol. 98. Art. 014108.

4. Binck J., Laniel D., Bayarjargal L., Khandarkhaeva S., Fedotenko T., Aslandukov A., Glazyrin K., Milman V., Chariton S., Prakapenka V.B., Dubrovinskaia N., Dubrovinsky L., Winkler B. Synthesis of calcium orthocarbonate, Ca_2CO_4-*Pnma* at *P-T* conditions of Earth's transition zone and lower mantle. American Mineralogist. 2022. Vol. 107. P. 336-342.

5. Laniel D., Binck J., Winkler B., Vogel S., Fedotenko T., Chariton S., Prakapenka V., Milman V., Schnick W., Dubrovinsky L. Synthesis, crystal structure and structure–property relations of strontium orthocarbonate, Sr_2CO_4. Acta Crystallographica Section B: Structural Science, Crystal Engineering and Materials. 2021. Vol. 77. P. 131−137.

6. Spahr D., König J., Bayarjargal L., Gavryushkin P.N., Milman V., Liermann H.-P., Winkler B. $Sr_3[CO_4]O$ antiperovskite with tetrahedrally coordinated sp^3-hybridized carbon and OSr_6 octahedra. Inorganic Chemistry. 2021. Vol. 60. P. 14504.

7. König J., Spahr D., Bayarjargal L., Gavryushkin P.N., Sagatova D., Sagatov N., Milman V., Liermann H.-P., Winkler B. Novel calcium sp^3 carbonate CaC_2O_5-*I*4̄2*d* may be a carbon host in Earth's lower mantle. ACS Earth and Space Chemistry. 2022. Vol. 6. P. 73-78.

FEATURES OF THE TRACE ELEMENT COMPOSITION OF MANTLE-DERIVED CHROME SPINELS

Serebriannikov A.A., Logvinova A.M.

V.S. Sobolev Institute of Geology and Mineralogy, Novosibirsk, Russia, aos_97@ngs.ru

Abstract. Comparison of the trace element composition (Ni, Zn, Si, Ti, V, Mn) of chrome spinel inclusions in diamonds from eight kimberlite pipes of two diamondiferous regions of Siberian craton: Malo-Botuobinsky (p. Mir, International, 23rd Congress) and Daldyn-Alakitsky (p. Udachnaya, Komsomolskaya, Yubileinaya, Aikhal and Sytykanskaya) and the composition of chrome spinels from concentrates of this pipes was performed. The significant differences in the distribution of impurities were revealed not only between inclusions in diamonds and chromites from concentrates, but also within various kimberlite pipes.

Key words: kimberlite, chrome spinel, diamond, inclusion.

Chrome spinel inclusions in diamonds from kimberlites are characterized by certain chemical composition: high content of Cr_2O_3 (>62 wt.%), low Al_2O_3 (<7.5 wt.%), TiO_2 (<0.7 wt.%) and Fe_2O_3 [1, 2], which makes it possible to separate them with sufficient reliability from chrome spinels belonging to other parageneses. Chrome spinels of the diamond association are one of the main minerals associated with diamond (along with pyrope) and an important diamond-prospecting guide.

However, in the early 2000s, data began to appear that indicate the obsolescence of the typomorphic features of the composition of these chrome spinels: high chromium chrome spinels with a Cr_2O_3 content > 62 wt.%. are found in ultramafic rocks of the Polar Urals (up to 65.9 wt.%), Koryak Upland (68.4 wt.%); India (66.3 wt.%); New Caledonia (68 wt.%) [3], and in some cases the compositional fields of these chrome spinels overlapped with the compositions of chrome spinels of the diamond paragenesis. In this regard, the question arose of clarifying the typomorphic features of the composition of chrome spinels included in diamond. It was suggested that chrome spinels of the diamond association could be distinguished by the content of trace elements.

The purpose of this work is to establish differences in the composition of chrome spinels in diamonds from two territorially isolated diamond-bearing regions of the Yakutian diamond-bearing province (Malo-Botuobinsky and Daldyn-Alakitsky), and to compare their compositions with chrome spinels from concentrates of diamond-bearing kimberlites. 320 crystals of chrome spinel inclusions in diamonds were selected from 8 diamond-bearing pipes of the Yakutian diamond-bearing province: from pipes Mir, International, 23rd Congress of the CPSU, related to the Malo-Botuobinsky diamondiferous region, and from pipes Udachnaya, Komsomolskaya, Yubileinaya, Aikhal and Sytykanskaya, belonging to the Daldyno-Alakitsky region. For comparison with them, 86 crystals of chrome spinel were selected from concentrates of diamondiferous kimberlites of mantle genesis (which was established by the content of inclusions of olivine, Cr-diopside, pyrope) in them, from four kimberlite pipes of Yakutia: International, 23rd Congress of the CPSU, Udachnaya and Aikhal [4]. The concentrations in NiO, SiO_2, MnO, V_2O_3, TiO_2, and ZnO samples were determined by microprobe analysis on a JXA-8100 Jeol microanalyzer (Japan). It was preliminary established that the concentrations of

some trace elements differ significantly, for example, the concentrations of Ni and Zn in chrome spinels from diamonds and in chrome spinels from concentrates of diamondiferous kimberlites differ by 1.5 times (Fig. 1). Moreover, a difference in concentrations was also found between chromium-spinel inclusions in diamonds from different diamond-bearing regions, for example, the average content of V_2O_3 and SiO_2 in the Malo-Botuobinsky region is 0.35 and 0.07 wt.%, and for the pipes of the Daldino-Alakitsky region - 0.26 and 0.12 wt.%, respectively.

Thus, the data obtained indicate a significant difference in the concentrations of trace elements in chrome spinels from diamonds and from kimberlite pipe concentrate with the aim of their possible use to refine the existing typomorphic features of the composition of chrome spinels.

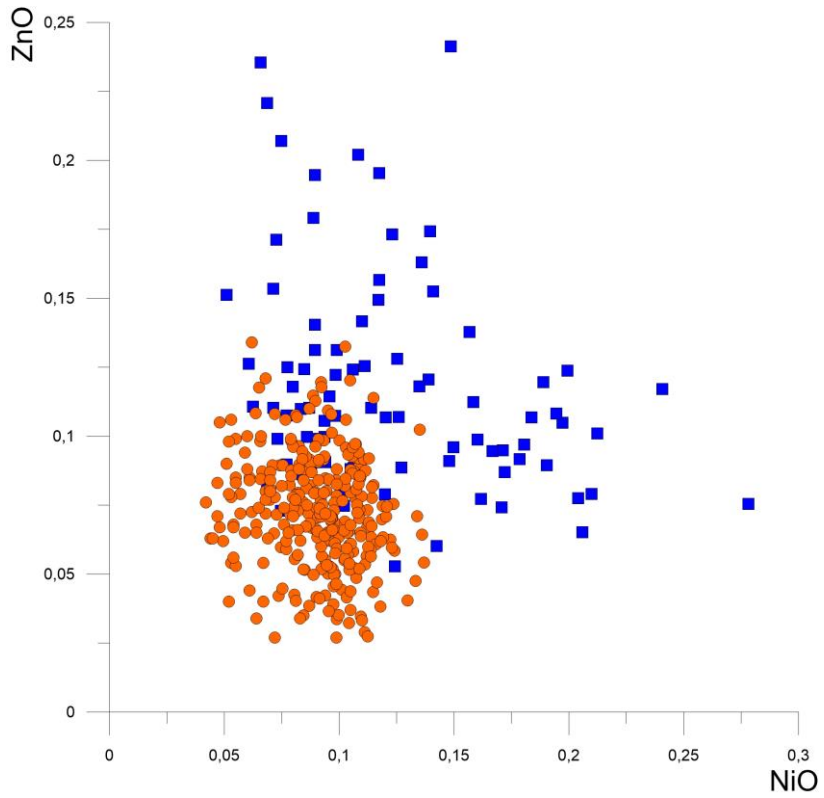

Figure 1 – Chemical composition of chrome spinels of diamond paragenesis (circles) and chrome spinels from kimberlite concentrate (squares).

Funding: The research was carried out within the framework of the state task of the IGM SB RAS and with the support of the RFBR grant (project №. 20-05-00293).

References:

1. Sobolev N.V., Pokhilenko N.P., Lavrentev Y.G., Usova L.V. Features of the composition of chrome spinels from diamonds and kimberlites of Yakutia. Geology and Geophysics. 1975. No. 11. P. 7-24.

2. Meyer H.O., Tsai H.-M. The nature and significance of mineral inclusions in natural diamond: a review. Minerals Science and Engineering. 1976. Vol. 8. No. 4. P. 242–260.

3. Ilupin I.P. High-chromium chromites from kimberlites and ultramafic rocks - similarities and differences. Ores and Metals. 2002. No. 4. P. 54-58.

4. Sobolev N.V., Logvinova A.M. Significance of Accessory Chrome Spinel in Identifying Serpentinite Paragenesis. International Geology Review. 2005. Vol. 47. P. 58-64.

MINERALOGY ASSEMBLAGE OF OLIVINE-HOSTED SECONDARY MELT INCLUSIONS FROM BULTFONTEIN PIPE (SOUTH AFRICA) AND CONSTRAINTS ON THE PRIMARY KIMBERLITE MELT COMPOSITION

Tarasov A.A.[1,2]

[1]V.S. Sobolev Institute of Geology and Mineralogy, Novosibirsk, Russia, tarasov.alexey@igm.nsc.ru
[2]Novosibirsk State University, Novosibirsk, Russia, a.tarasov2@g.nsu.ru

Abstract. Melt secondary crystallized inclusions in olivine of the sheared peridotite from the Bultfontein pipe (Kaapvaal craton, South Africa) has been studied using Raman spectroscopy and SEM-EDS. Among the daughter minerals in the inclusions were identified > 30 species. These are various carbonates, halides, sulfates, phosphates, silicates and oxides. Carbonates constitute more than 50 vol. % of the inclusions. According to various models, such inclusions are microportions of kimberlite melt which was trapped by xenolithic minerals in the lithospheric mantle. It suggests that the primitive kimberlite melt of the Bultfontein pipe was alkaline-carbonatit**ic** with a high content of volatiles.

Key words: kimberlite, melt inclusions, Bultfontein pipe

Information about the composition of primitive kimberlite melts is important for developing models of kimberlite petrogenesis and reconstruction of the diamond deposits formation processes. One approach for determining of these melts compositions is to study secondary melt inclusions in olivine from mantle xenoliths. Such inclusions, according to various models are microportions of primary kimberlitic melt that was trapped at the beginning of rise of the xenolith or shortly before [1].

Xenolith of mantle peridotite from kimberlites of the Bultfontein pipe (Kimberly field, Kaapvaal craton, Southern Africa) was studied. This xenolith is phlogopite-bearing spinel lherzolite with deformation (sheared) textures. Estimated depths of origin of the studied peridotites are 120 km. Melt inclusions were found along healed cracks within olivine grains. Visually, these inclusions consist of various crystalline phases and bubbles. Using Raman spectroscopy and scanning electron microscopy study, the following minerals were recognized in the inclusions: calcite $CaCO_3$, magnesite $MgCO_3$, dolomite $CaMg(CO_3)_2$, eitelite $Na_2Mg(CO_3)_2$, nyerereite $Na_2Ca(CO_3)_2$, gregoryite $(Na,K,Ca)_2CO_3$, natrite Na_2CO_3, K-Na-carbonate $(K,Na)_2Ca(CO_3)_2$, shortite $Na_2Ca_2(CO_3)_3$, nahcolite $NaHCO_3$, witherite $BaCO_3$, bradleyite $Na_3Mg(PO_4)(CO_3)$, northupite $Na_3Mg(CO_3)_2Cl$, burkeite $Na_6CO_3(SO_4)_2$, tychite $Na_6Mg_2(CO_3)_4(SO_4)$, glauberite $Na_2Ca(SO_4)_2$, thenardite Na_2SO_4, arcanite K_2SO_4, aphthitalite $K_3Na(SO_4)_2$, halite NaCl, sylvite KCl, apatite $Ca_5(PO_4)_3(F,Cl ,OH)$, heazlewoodite Ni_3S_2, phlogopite $KMg_3AlSi_3O_{10}(F,Cl,OH)$ and tetraferriphlogopite $KMg_3FeSi_3O_{10}(F,Cl,OH)$, richterite $Na_2Ca(Mg,Fe,Mn,Al)_5[Si_4O_{11}](OH,F)_2$, zirconolite $CaZrTi_2O_7$, magnetite $FeFe_2O_4$ and Fe-Ti-Mg spinel, rutile TiO_2, and serpentine subgroup minerals $Mg_3Si_2O_5(OH)_4$.

The mineral assemblage within melt inclusions is varied (Fig. 1). There are inclusions that predominantly consist of Na-Ca carbonates, bradleyite and aphthitalite (first type) and melt inclusions that predominantly consist of serpentine, magnetite and Ca-Mg carbonates (second type), there are also inclusions with intermediate compositions. Both type of inclusions can be found in the one healed crack, but serpentine-rich inclusions are interconnected by thin channels, while Na-Ca carbonate-rich inclusions are visually isolated. Using the analysis of BSE images,

element distribution maps and Raman maps, quantitative relationships between daughter minerals in melt inclusions were established. It was shown that more than 50% of the volume of first type inclusions filled with various carbonates, among which nyerereite, gregoryite and shortite predominate. In inclusions with an intermediate composition, the content of serpentine, calcite and dolomite decreases while Na-ca carbonates, sulfates and halides increase.

Thus, the morphological features and mineral assemblage indicate that the carbonate-rich inclusions represent trapped melt, while the mineralogy of daughter phases inside serpentine-rich inclusions has been modified by interaction with the external water fluid after inclusions formation. Therefore, the composition of the unmodified inclusions correspond a primitive melt the Bultfontein kimberlite pipe. Quantitative relationships between daughter minerals in unaltered inclusions show that this melt was alkaline carbonatitic with a high content of volatiles Cl^-, SO_4^{2-}, PO_4^{3-}.

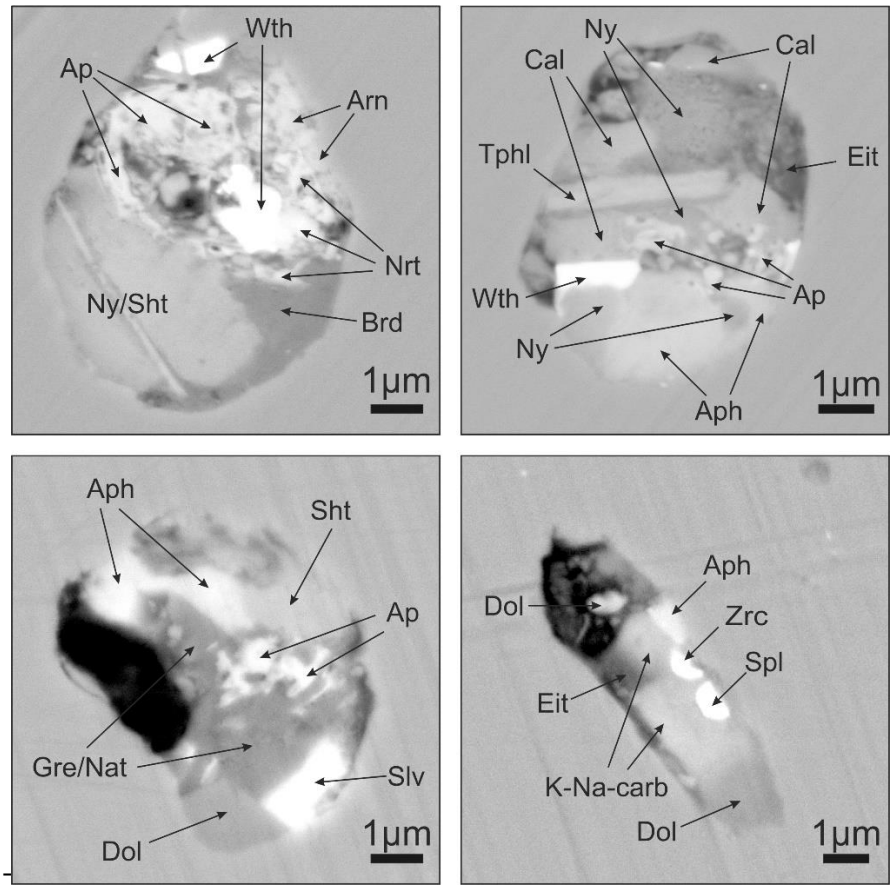

Figure 1 – **BSE images of Na-Ca carbonate rich olivine-hosted unaltered melt inclusions. Ap–apatite, Wth–witherite, Arn–arcanite, Nrt–northupite, Brd–bradleyite, Ny–nyerereite, Sht–shortite, Cal–calcite, Eit–eitelite, Aph–aphthitalite, Dol–dolomite, Slv–sylvite, Zrc–zirconolite, Gre–gregoryite, Nat–natrite, Spl– Fe-Ti-Mg spinel, Tphl–tetraferriphlogopite.**

Funding: This work is supported by the Russian Foundation for Basic Research (grant No. 20-35-70058).

References:

1. Brett R.C., Russell J.K., Andrews G.D.M., Jones T.J. The ascent of kimberlite: Insights from olivine. Earth and Planetary Science Letters. 2015. Vol. 424. P. 119-131.

Section EXPERIMENTAL MINERALOGY

P-T FIELD OF CARBONATE-ALUMOSILICATE LIQUID IMMISCIBILITY AT 3-6 GPA

Arefiev A.V.[1,2,3], *Bekhtenova A.*[1,2,3], *Shatskiy A.*[1,2,3], *Podborodnikov I.V.*[1,2,3], *Litasov K.D.*[3]

[1]V.S. Sobolev Institute of Geology and Mineralogy, Novosibirsk, Russia,
arefievanton@igm.nsc.ru
[2]Novosibirsk State University, Novosibirsk, Russia
[3]Vereshchagin Institute for High Pressure Physics, Russian Academy of Science, Troitsk, Moscow, Russia

Abstract. To evaluate the effect of pressure on the carbonate-silicate liquid immiscibility we have carried out a set of experiments at 3, 4.5, and 6 GPa in two systems: (L(S) and L(S)+L(C)) whose compositions are identical to liquids generating by partial melting of pelite at 6 GPa. The carbonate-silicate liquid immiscibility in the L(S) system stabilizes above 1150 ºC, while in the L(S)+(L(C) system it stabilizes at 1200 ºC at 3 and 4.5 GPa and 1300 ºC at 6 GPa.

Key words: liquid immiscibility, carbonates, phonolities, alkalies, high-pressure experiments

One scenario suggests that carbonatites are considered to originate from liquid immiscibility generated at upper mantle *P-T* conditions [1]. Liquid immiscibility in sodic systems is well studied [2-4], whereas liquid immiscibility in potassium bearing systems are need to be explored. Recently, it has been experimentally shown that partial melting of carbonated pelites at diamond stability field generates immiscible ultrapotassic carbonate-silicate liquids [5]. Here, we examine the stability of liquid immiscibility at a lower pressure range.

We conduct 8 experiments at 3, 4.5, and 6 GPa and 1050–1500 ºC using multianvil hydraulic DIA-type press «Discoverer-1500» at IGM SB RAS. The composition and phase relations of the recovered samples were studied using a MIRA 3 LMU scanning electron microscope (Tescan Orsay Holding) coupled with an INCA energy-dispersive X-ray microanalysis system at IGM SB RAS [6].

In the system modeling phonolitic melt (L(S)) at 3 GPa/1050 ºC and 6 GPa/1100 ºC, we observed a single carbonatite melt with crystal silicates in coexistence. As temperature and pressure increase to 4.5/6 GPa/1200 ºC, the carbonate-aluminosilicate liquid immiscibility is raised. The upper-temperature limit of stability liquid immiscibility at 6 GPa terminates between 1300 and 1400 ºC. At 1400 ºC and above, only aluminosilicate liquid is stable. In the system with carbonate and aluminosilicate melt (L(C)+L(S)) at 3 GPa/1050 ºC and 6 GPa/1100/1200 ºC liquid immiscibility was not observed, only a single carbonate melt. Increasing temperature up to 1200 ºC at 3 and 4.5 GPa (Figure 1), and up to 1300 ºC at 6 GPa stabilize two immiscible liquids which remain stable up to 1500 ºC at 6 GPa.

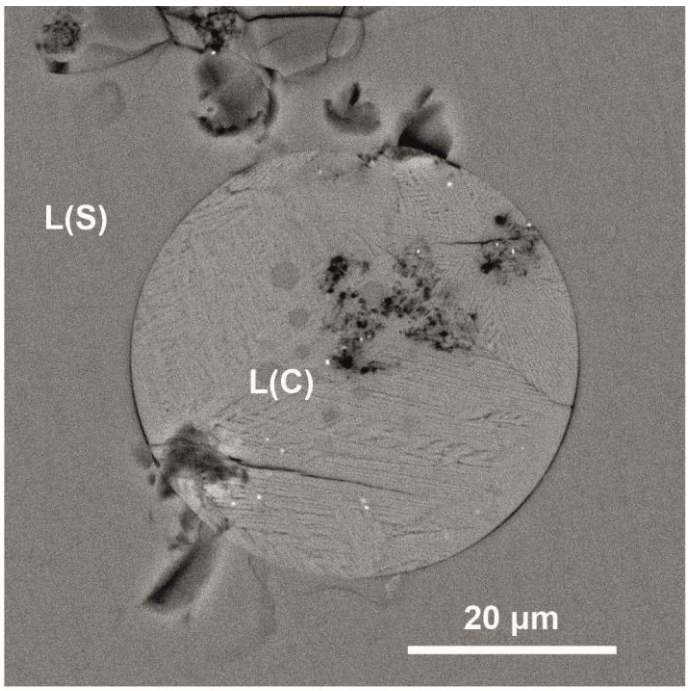

Figure 1 - BSE image of phase relations in the system L(S) observed at 4.5 GPa and 1200 ºC. L(S) – phonolitic melt, L(C) – carbonate melt.

Funding: This work is supported by the Russian Science Foundation under grant 21-77-10057.

References:

1. Jones A. P., Genge M., Carmody L. Carbonate melts and carbonatites. Reviews in Mineralogy and Geochemistry. 2013. Vol. 75. No. 1. P. 289-322.

2. Brooker R. A., Kjarsgaard B. A. Silicate-carbonate liquid immiscibility and phase relations in the system SiO_2-Na_2O-Al_2O_3-CaO-CO_2 at 0.1-2.5 GPa with applications to carbonatite genesis. Journal of Petrology. 2011. Vol. 52. No. 7-8. P. 1281-1305.

3. Van Groos A. F. K., Wyllie P. J. Experimental data bearing on the role of liquid immiscibility in the genesis of carbonatites. Nature. 1963. Vol. 199. No. 4895. P. 801-802.

4. Lee W. J., Wyllie P. J. Liquid Immiscibility in the Join NaAlSi3O8-CaCO3 to 2.5 GPa and the Origin of Calciocarbonatite Magmas. Journal of Petrology. 1996. Vol. 37. No. 5. P. 1125-1152.

5. Shatskiy A., Arefiev A. V., Podborodnikov I. V., Litasov K. D. Origin of K-rich diamond-forming immiscible melts and CO_2 fluid via partial melting of carbonated pelites at a depth of 180-200 km. Gondwana Research. 2019. Vol. 75. No. 11. P. 154-171.

6. Lavrent'ev Y. G., Karmanov N. S., Usova L. V. Electron probe microanalysis of minerals: Microanalyzer or scanning electron microscope? Russian Geology and Geophysics. 2015. Vol. 56. No. 8. P. 1154-1161.

SOLIDUS OF CARBONATED PHLOGOPITE PERIDOTITE AT 3-6.5 GPA

Bekhtenova A. [1,2,3], *Shatskiy A.* [1,2,3], *Arefiev A.V.* [1,2,3], *Podborodnikov I.V.* [1,2,3], *Litasov K.D.*[3]

[1]V.S. Sobolev Institute of Geology and Mineralogy, Novosibirsk, Russia,
bekhtenova@igm.nsc.ru
[2]Novosibirsk State University, Novosibirsk, Russia
[3]Vereshchagin Institute for High Pressure Physics, Russian Academy of Science, Troitsk, Moscow, Russia

Abstract. We present experimental results on the interaction of K-rich carbonate melts with the natural garnet lherzolite from the Udachnaya kimberlite (Russia) in the presence of water at 3.0–6.5 GPa, corresponding to depths of 100–200 km. At 4.0–6.5 GPa, the solidus of carbonated phlogopite peridotite is bracketed between 1100 and 1200 °C and controlled by the following reaction: Phl + Cpx + Mgs = Grt + Opx + Ol + hydrous K-carbonate melt. At 3 GPa, the solidus temperature decreases to about 1050 °C presumably owing to the Ca-Mg exchange reaction, Cpx + Mgs = Opx + Dol, which stabilizes dolomite reacting with phlogopite at a lower temperature than magnesite.

Key words: mantle metasomatism, peridotite-CO_2-H_2O, carbonate melt, high-pressure experiment, Earth's mantle

An analysis of the literature data on carbonates of mantle origin indicates their frequent association with phlogopite in mantle xenoliths [1] and as inclusions in diamonds from kimberlites and places [2]. However, the composition of the metasomatic agent, resulting in phlogopite formation, remains debatable. One of the most probable can be considered the hydrous K-rich carbonate composition of metasomatic agent. The studies on the stability of Phl and Mgs in the complex peridotitic systems are restricted to a pressure of 3 GPa at which the established solidi are located at 1065 °C [3]. In this work, we present experimental results on solidus and melting phase relations in the carbonated phlogopite peridotite in the range of 3.0–6.5 GPa and 850–1250 °C, corresponding to depths of 100–200 km. The results were also published in the study of Shatskiy A. et al. [4] and PhD thesis of Bekhtenova A. [5].

Experiments were run using a 1500-ton DIA-type press at IGM SB RAS. Starting materials were prepared by blending natural garnet lherzolite from the Udachnaya kimberlite pipe (Russia) with mixtures modeling hydrous K- and Na-K-carbonate melts (KH1 and NKH1, respectively). The studied systems (Lhz-KH1 and Lhz-NKH1) have $H_2O/K_2O = 2$, like that in phlogopite, and therefore correspond to carbonated phlogopite peridotite under fluid-absent conditions.

At 4-6.5 GPa, the solidus of magnesite-bearing phlogopite peridotite in the Lhz-KH1 system is controlled by the reaction: $2KMg_3AlSi_3O_{10}(OH)_2$ (Phl) + $CaMgSi_2O_6$ (Cpx) + $3MgCO_3$ (Mgs) = $Mg_3Al_2Si_3O_{12}$ (Grt) + $2Mg_2Si_2O_6$ (Opx) + Mg_2SiO_4 (Ol) + K_2CO_3 (L) + $CaMg(CO_3)_2$ (L) + $2H_2O$ (L), which takes place at temperatures between 1100 and 1200 °C (1 in Figure 1a). At 3 GPa, the solidus temperature decreases to about 1050 °C, presumably owing to the Ca-Mg exchange reaction: $CaMgSi_2O_6$ (Cpx) + $2MgCO_3$ (Mgs) = Mg_2Si_2O6 (Opx) + $CaMg(CO_3)_2$ (Dol), which stabilizes dolomite reacting with phlogopite at lower temperature than magnesite (2 in Figure 1a).

At 1200 °C and 6 GPa in the Lhz-KH1 system, K-rich hydrous carbonatite melt with Ca# 31 mol% and $CO_2/(CO_2+H_2O)$ = 61 mol% appears in equilibrium with garnet lherzolite, while at lower temperatures along cratonic geotherms (37-43 mW/m^2), the melt completely disappears to produce phlogopite and magnesite, unlike anhydrous K-carbonatite melt which remains stable under those conditions. Thus, the addition of water to the K-rich carbonate melt infiltrating SCLM should yield its partial or complete disappearance, accompanied by the formation of carbonated phlogopite metasomes.

The results in the Lhz-NKH1 system indicate that the presence of sodium expands the stability region of the K-rich hydrous carbonate melt to at least 1100 °C at 5 GPa (3 in Figure 1b), while the reaction, producing phlogopite and magnesite with the expense of garnet and orthopyroxene, continues. Unlike Na-free composition, the reaction yields only partial consumption of the melt and changes its composition toward higher Na_2O and lower H_2O contents. This may explain variations of mantle carbonatite melt composition from hydrous ultrapotassic, like microinclusions in diamonds, toward water-poor and sodium-rich, like inclusions in sheared garnet peridotites, spinel harzburgites, and kimberlite minerals.

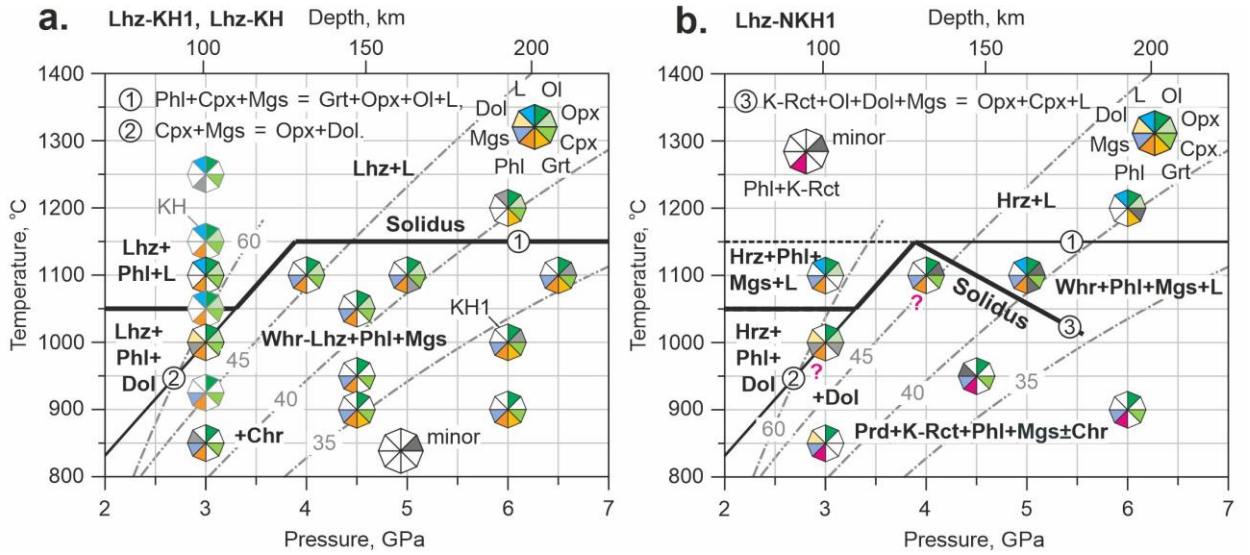

Figure 1 – *P-T* plots illustrating phase relations in the systems Lhz-KH1, Lhz-KH (a), and Lhz-NKH1(b).

Funding: This work is supported by the Russian Science Foundation under grant 21-77-10057.

References:

1. Kargin, A.V., Sazonova, L.V., Nosova, A.A., Lebedeva, N.M., Kostitsyn, Y.A., Kovalchuk, E.V., Tretyachenko, V.V., Tikhomirova, Y.S. Phlogopite in mantle xenoliths and kimberlite from the Grib pipe, Arkhangelsk province, Russia: Evidence for multi-stage mantle metasomatism and origin of phlogopite in kimberlite. Geoscience Frontiers. 2019. Vol. 10. P. 1941–1959.

2. Sobolev, N.V., Logvinova, A.M., Efimova, E.S. Syngenetic phlogopite inclusions in kimberlite-hosted diamonds: implications for role of volatiles in diamond formation. Russian Geology and Geophysics. 2009. Vol. 50. P. 1234–1248.

3. Tumiati, S., Fumagalli, P., Tiraboschi, C., Poli, S. An experimental study on COH-bearing peridotite up to 3–2 GPa and implications for crust–mantle recycling. Journal of Petrology. 2013. Vol. 54. P. 453–479.

4. Shatskiy, A., Bekhtenova, A., Arefiev, A.V., Podborodnikov, I.V., Vinogradova, Y.G., Rezvukhin, D.I., Litasov, K.D. Solidus and melting of carbonated phlogopite peridotite at 3-6.5 GPa: Implications for mantle metasomatism. Gondwana Research. 2022. Vol. 101. P. 156-174.

5. PhD thesis. Bekhtenova A. https://www.nsu.ru/upload/iblock/cef/2022%20Bekhtenova%20PhD%20Eng.pdf

SEARCH OF NEW RARE EARTH BORATES PROTOTYPED BY CARBONATE MINERALS

Kuznetsov A.B. [1], Kokh K.A.[1], Bolatov A. [2], Uralbekov B.[2], Svetlichnyi V.A. [3], Kokh A.E. [1]

[1]V.S. Sobolev Institute of Geology and Mineralogy, Novosibirsk, Russia, ku.artemy@igm.nsc.ru
[2]Al-Farabi Kazakh National University, Almaty, Kazakhstan,
[3]Tomsk State University, Tomsk, Russia

Abstract. $RSc_3(BO_3)_4$, $KCaR(BO_3)_2$ and $Li_3Ba_4Sc_3B_8O_{22}$ (R=La-Eu) rare earth borates were obtained by spontaneous crystallization from flux. Thermal, structural and some optical properties (Raman spectra and UV-vis-NIR diffuse reflectance spectra were studied. Second harmonic generation relative KH_2PO_4 was estimated for noncentrosymmetric scandium borates. These data established a correlation between structural features and physicochemical properties of the obtained crystals.

Key words: crystal growth, rare earth borate, structure, SHG, luminescence

At present, many research projects are related to the development of more environmentally friendly light sources and luminophores [1-4]. These projects have focused on borates due to their high chemical stability, thermal and radiation stability, wide transparency region and high laser threshold. In addition, borate compounds have diverse chemical compositions and crystal structures due to the ability of boron to form anionic BO_3 group. According to the anionic group theory, the compounds with isolated boron groups BO_3 exhibit strong potential for use in the range of visible (VIS) to deep ultraviolet (UV) range [5]. As a rule compounds with three coordinated boron atoms crystallize in structure similar to carbonate minerals. One of the prominent examples include $YAl_3(BO_3)_4$ (YAB) (UV cut-off - 160 nm), which crystallizes in huntite ($CaMg_3(CO_3)_4$) structure. Alkali and/or alkali earth borates with a high concentration of rare earth elements were synthesized and proposed to be efficient phosphor materials. As an example, $RNa_3(BO_3)_2$ (R= Y, La, Nd, Gd) crystallizing with buetschliite-type structure ($K_2Ca(CO_3)_2$ $R\bar{3}$ space group) have a low concentration quenching of rare earth atoms. The existence of these multication borates suggests new complex compounds by replacing part of the Na^+ by Ba^{2+}cations, as well as the REE variation. Novel rare earth borates, such as $NaBaSc(BO_3)_2$ and $NaBaY(BO_3)_2$, have been discovered in the system R_2O_3–BaO–Na_2O–B_2O_3. The consequent substitution of Na→K and of Ba→Sr results in obtaining two new compound families of $KBaR(BO_3)_2$ and $KSrR(BO_3)_2$, which crystallize in the $R\bar{3}$ and $C2/c$ space groups, respectively.

In this study, by substituting the cationic part in $KBaR(BO_3)_2$ and $YAl_3(BO_3)_4$ the new rare earth borates ($SmSc_3(BO_3)_4$, $KCaR(BO_3)_2$ and $Li_3Ba_4Sc_3B_8O_{22}$) crystalized with carbonate type structure were obtained. The crystal structure, thermal properties and the phase transformations were discussed. Also, some optical properties are presented, including the Raman spectra and UV-vis-NIR diffuse reflectance spectra (DRS) of the crystal.

Funding: GF MES RK IRN AP08855427 and state assigned project of IGM SB RAS.

References:

1. Yang Y., Jiang X., Lin Z., Wu Y., Borate-based ultraviolet and deep-ultraviolet nonlinear optical crystals, Crystals (Basel) MDPI AG, 2017.

2. Zhang W., Zhang Z., Jin W., Zhang R., Cheng M., Yang Z., Pan S., From borophosphate to fluoroborophosphate: a rational design of fluorine-induced birefringence enhancement. Science China Chemistry. 2021. Vol. 64. P. 1498–1503.

3. Verma S., Verma K., Kumar D., Chaudhary B., Som S., Sharma V., Kumar V., Swart H.C., Recent advances in rare earth doped alkali-alkaline earth borates for solid state lighting applications. Physica B: Condensed Matter. 2018. Vol. 535. P. 106–113.

4. Uralbekov B., Shevchenko V., Kuznetsov A., Kokh A., Kononova N., Bolatov A., Kokh K., Novel compounds in the $MMeR(BO_3)_2$ borate family (M = alkali metal, Me = alkaline earth metal, R = rare-earth element): Syntheses, crystal structures and luminescent properties. Journal of Luminescence. 2019. Vol. 216. Art. 116712.

5. Mutailipu M., Poeppelmeier K.R., Pan S., Borates: A Rich Source for Optical Materials. Chemical Reviews. 2021. Vol. 121. P.1130–1202.

EXPERIMENTAL MODELING OF CARBONATION AND DECARBONATION REACTIONS INVOLVING ECLOGITIC GARNET UNDER UPPER MANTLE P,T-PARAMETERS

Novoselov I.D.[1,2], *Bataleva Yu.V.*[1], *Palyanov Yu.N.*[1,2]

[1]V.S. Sobolev Institute of Geology and Mineralogy, Novosibirsk, Russia,
novoselovid@igm.nsc.ru
[2]Novosibirsk State University, Russia

Abstract. Experimental modeling of decarbonation reactions resulting in formation of eclogitic-like garnets and eclogitic garnet carbonation was carried on the BARS equipment using hematite buffered cell. Decarbonation resulting in formation of garnet occurs at 1200-1400 °C; Mg content in garnet increases with temperature increase, while Mg content in recrystallized carbonate drops. During garnet carbonation at 950-1250 °C Mg is extracted from garnet, while Mg-carbonate is formed; garnet-CO_2 interaction at 1350-1550 °C leads to decrease of Ca content in garnet and formation of Ca-carbonate.

Key words: high-pressure experiment, garnet, carbonate, mantle metasomatism, eclogite

CO_2-enriched fluid is one of the most probable mantle metasomatic agents. There are evidences of its presence in mantle such as CO_2-bearing inclusions in diamonds [1]. During the last decades experimental modeling of carbonation and decarbonation reactions was carried out, and corresponding curves in *P,T*-field were established, such as for decarbonation reactions resulting in garnets formation [2,3,4,5]. Nevertheless, carbonation of minerals with complex, close to natural stoichiometry is still unexplored. The main objective of this study is to define changes in eclogitic garnet composition during its carbonation under upper mantle *P,T*-parameters.

Experiments were carried out on the multi-anvil high-pressure equipment of "split-sphere" type (BARS) at pressure of 6.3 GPa, temperature range of 950-1550 °C, and durations of 5-100 hours. Hematite buffered container was used in all experiments in order to prevent hydrogen diffusion. For carbonation experiments natural garnet from eclogite UD-45-02 xenoliths from Udachnaya pipe [6] with composition of $(Mg_{2.01}Fe_{0.63}Ca_{0.44}Mn_{0.02})(Al_{1.87}Cr_{0.03}Ti_{0.02})[SiO_4]_3$, and silver oxalate ($CO_2$-fluid source) were used as starting materials. For decarbonation experiments mixture of natural carbonates with average composition of $Mg_{0.53}Fe_{0.29}Ca_{0.16}Mn_{0.02}CO_3$, and synthetic SiO_2 and Al_2O_3 (99.99 % purity) were used as starting materials. Temperature, duration and final phase assemblage for each experiment are summarized in Table 1.

In carbonation experiments recrystallized garnet, carbonate, coesite, and kyanite were formed. It was determined that in the temperature range of 950-1250 °C recrystallized garnet has lower magnesium content than the initial, and newly formed carbonate is significantly magnesian, while at 1350-1550 °C recrystallized garnet has lower calcium and higher magnesium content than the initial, and newly formed carbonate has high calcium content (Figure 1).

In decarbonation experiments recrystallized carbonate and corundum, as well as garnet, coesite, kyanite were formed. It was determined that at temperatures of 1200-1300 °C recrystallized garnet has relatively low magnesium content, and recrystallized carbonate is significantly magnesian, while at 1400 °C garnet has low calcium and high magnesium content, and newly formed carbonate has high calcium content (Figure 1).

Table 1. Experimental parameters and results.

Series	Starting materials	T, °C	t, hours	Final mineral phases
Carbonation (C)	Garnet, $Ag_2C_2O_4$	950	100	Grt, Carb, Ky, Coe
		1050	100	Grt, Carb, Ky, Coe
		1150	80	Grt, Carb, Ky, Coe
		1250	60	Grt, Carb, Ky, Coe
		1350	15	Grt, Carb, Ky, Coe
		1450	10	Grt, Carb, Ky, Coe
		1550	5	Grt, Carb, Ky, Coe
Decarbonation (D)	Carbonate, SiO_2, Al_2O_3	1100	40	Carb, Ky, Coe, Crn
		1200	40	Grt, Carb, Ky, Coe, Crn
		1300	20	Grt, Carb, Ky, Coe, Crn
		1400	10	Grt, Carb, Ky, Coe

Grt – garnet, Carb – carbonate, Ky – kyanite, Coe – coesite, Crn – corundum.

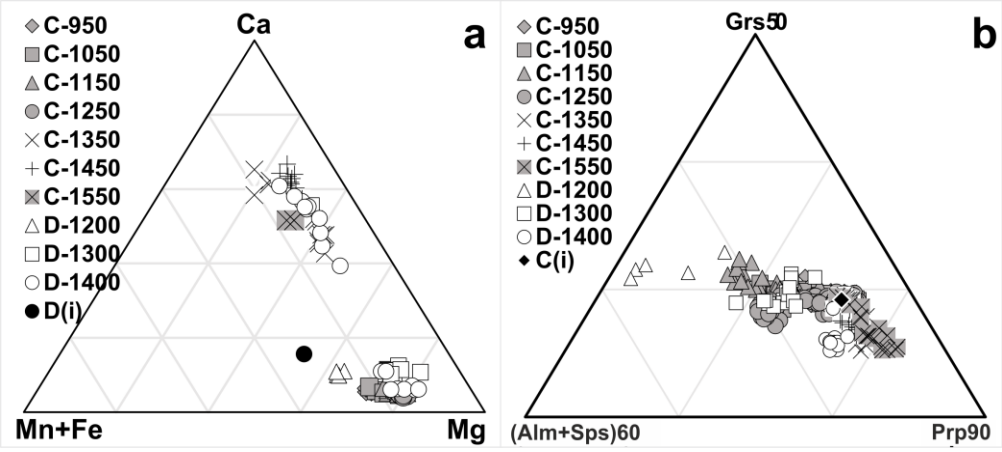

Figure 1 – Compositions of coexisting carbonates (a) and garnets (b) from experiments modeling carbonation of eclogitic garnet (D) and modeling decarbonation resulting in formation of eclogitic-like garnet (C). D(i) – composition of the initial carbonate, C(i) – composition of the initial garnet. Grs – grossular, Alm – almandine, Sps – spessartine, Prp – pyrope.

Results obtained in both experimental series are in good agreement and show that in (Mg,Fe,Ca,Mn)O-SiO_2-Al_2O_3-CO_2 system compositions of coexisting garnet and carbonate change complementarily with increasing temperature; results allow considering aforementioned changes in garnets composition as indicators of mantle CO_2-induced metasomatism.

Funding: This work is supported by the Russian Science Foundation under grant 19-17-00075

References:

1. Schrauder M., Navon O. Solid carbon dioxide in a natural diamond. Nature. 1993. Vol. 365. No. 6441. P. 42–44.

2. Bataleva Yu.V., Novoselov I.D., Kruk A.N., Furman O.V., Reutsky V.N., Palyanov Yu.N. Experimental modeling of decarbonation reactions resulting in Mg,Fe-garnets and CO_2 fluid at the mantle P-T parameters. Russian Geology and Geophysics. 2020. Vol. 61. No. 5-6. P. 650-662.

3. Bataleva Y.V, Kruk A.N., Novoselov I.D., Furman O.V., Palyanov Y.N. Decarbonation Reactions Involving Ankerite and Dolomite under upper Mantle P,T-Parameters: Experimental Modeling. Minerals. 2020. Vol. 10. No. 8. Art. 715.

4. Palyanov Y.N., Sokol A.G., Tomilenko A.A., Sobolev N.V. Conditions of diamond formation through carbonate-silicate interaction. European Journal of Mineralogy. 2005. Vol. 17. No. 2. P. 207–214.

5. Knoche R., Sweeney R.J., Luth R.W. Carbonation and decarbonation of eclogites: the role of garnet. Contributions to Mineralogy and Petrology. 1999. Vol. 135. No. 4. P. 332–339.

6. Kolesnichenko M.V., Zedgenizov D.A., Ragozin A.L., Litasov K.D., Shatsky V.S. The role of eclogites in the redistribution of water in the subcontinental mantle of the Siberian craton: results of determination of the water content in minerals from the Udachnaya pipe eclogites. Russian geology and geophysics. 2018. Vol. 59. No. 7. P. 763-779.

DEVELOPMENT OF THE QUASI-EQUILIBRIUM OXYGEN RELEASE METHOD FOR OBTAINING CONTINUOUS PHASE DIAGRAMS OF NONSTOICHIOMETRIC PEROVSKITES

Popov M.P., Popova M.A., Chizhik S.A., Nemudry A.P.

Instite of Solid State Chemistry and Mechanochemistry, Novosibirsk, Russia,
misha.popov90@gmail.com

Abstract. From continuous phase diagrams 3-δ vs log pO_2 of non-stoichiometric perovskites $SrCo_{0.8-x}Fe_{0.2}Nb_xO_{3-\delta}$, the thermodynamic parameters are determined as functions of the non-stoichiometric oxide δ. Within the framework of the free electron gas model, a calculation was carried out and it was shown that the features of the phase diagram can be associated with the density of electronic states near the Fermi level of electrons.

Key words: perovskites, phase diagram, mixed conductivity, oxygen release.

Oxides with mixed ion-electron conductivity (MIEC) are attracted the attention due to their prospective of using as membrane materials for producing pure oxygen, catalytic conversion of methane to synthesis gas, as sorbents for oxy-fuel combustion, oxygen sensors, and electrodes for solid oxides fuel cells [1-3].

Despite the practical importance of these processes, there are no universally accepted notions today about the stages that determine the course of oxygen exchange on the surface of nonstoichiometric MIEC oxides. In our opinion, this is due to the lack of a correct approach to obtaining and analyzing kinetic data necessary to form ideas about the mechanism of the reaction. As a result, there is a large scatter in the literature experimental data which prevents the development of a reliable conception of the oxygen permeability mechanism in the MIEC membranes and advance in technological aspects. Thus, understanding the factors that can ensure high oxygen permeability of perovskite oxides continues to be a challenging and actual problem. Earlier, we have developed new quasi-equilibrium oxygen release technique (QEOR) to obtain equilibrium parameters in grossly nonstoichimetric perovskites [4, 5].

The aim of this work was to carry out a comprehensive analysis of the effect of niobium concentration on oxygen nonstoichiometry and thermodynamic properties of $SrCo_{0.8}Fe_{0.2-x}Nb_xO_{3-\delta}$ (SCFNx). A feature of this system is the *T*-phase discovered for the first time in samples doped with niobium, which leads to the appearance of features in the equilibrium dependences $pO_2(\delta)$ and, consequently, in the chemical potential of the electrons. To obtain the necessary information, detailed continuous equilibrium phase diagrams 3-δ vs log pO2 were used.

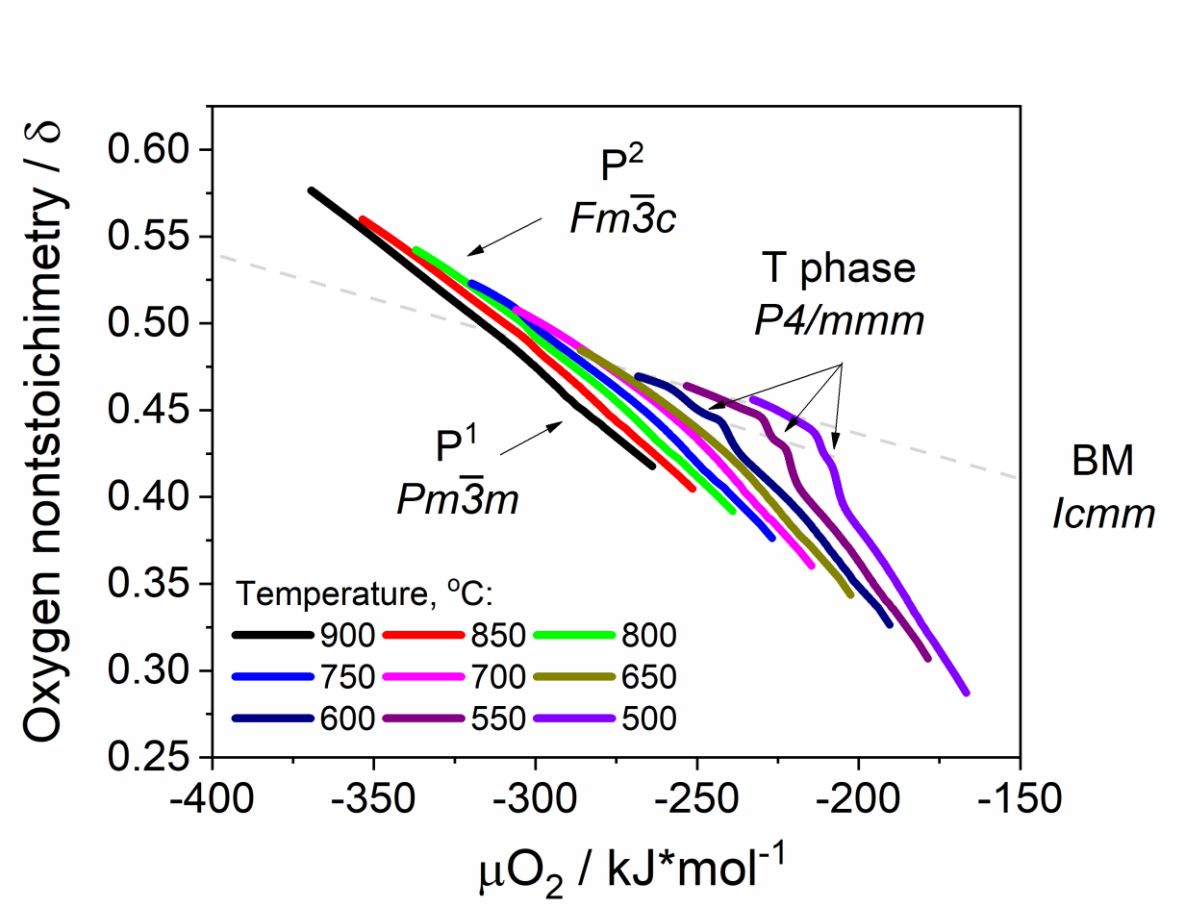

Figure 1 – SCFN5 nonstoichiometry on μO_2 dependence within temperature range 500–900°C.

Funding: The reported study was funded by Russian Science Foundation (Project № 21-79-30051).

References:

1. Tan X., Wang Z., Meng B., Meng X., Li K. Pilot-scale production of oxygen from air using perovskite hollow fibre membranes. Journal of Membrane Science. 2010. Vol. 352. P. 189-196.

2. Wang H.H., Tablet C., Schiestel T., Werth S., Caro J. Partial oxidation of methane to syngas in a perovskite hollow fiber membrane reactor. Catalysis Communications. 2006. Vol. 7. P. 907-912.

3. Rui Z., Ding J., Li Y., Lin Y.S. $SrCo_{0.8}Fe_{0.2}O_{3-\delta}$ sorbent for high-temperature production of oxygen-enriched carbon dioxide stream. Fuel. 2010. Vol. 89. P. 1429-1434.

4. Starkov I.A., Bychkov S.F., Matvienko A.A., Nemudry A.P. Oxygen release technique as a method for the determination of "δ–pO_2–T" diagrams for MIEC oxides. Physical Chemistry Chemical Physics. 2014. Vol. 16. P. 5527-5535.

5. Chizhik S.A., Bychkov S.F., Voloshin B.V., Popov M.P., Nemudry A.P. Development of the Crank's diffusion model for the case of material-gas feedback regime in gas flow reactors. Advanced methodology of oxygen partial pressure relaxation for the kinetics of oxygen exchange in nonstoichiometric oxides. Chemical Engineering Journal. 2021. Vol. 420. No. 2. Art. 127711.

DEVELOPMENT OF AN EXPRESS METHOD FOR OBTAINING CONTINUOUS PHASE DIAGRAMS OF PEROVSKITE-LIKE OXIDES

Popova M.A., Popov M.P., Nemudry A.P.

Institute of Solid State Chemistry and Mechanochemistry, Novosibirsk, Russia,
misha.popov90@gmail.com

Abstract. Continuous phase diagrams 3-δ vs log pO_2 of non-stoichiometric perovskites $SrCo_{1-x}Ta_xO_{3-\delta}$ are obtained by express quasi-equilibrium oxygen release (QEOR) technique. Work has been done to obtain reliable data in the shortest possible time frame. The coincidence of the obtained data with the literature data is shown.

Key words: perovskites, phase diagram, mixed conductivity, oxygen release.

Oxides with mixed ion-electron conductivity (MIEC) are attracted the attention due to their prospective of using as membrane materials for producing pure oxygen, catalytic conversion of methane to synthesis gas, as sorbents for oxy-fuel combustion, oxygen sensors and electrodes for solid oxides fuel cells [1-3].

Despite the practical significance of these processes, at present there is no convenient, and most importantly, fast method for studying the phase composition of these oxides. The currently existing methods make it possible to obtain only discrete points of the phase diagram. And experiments in their duration take more than a week. Thus, the creation of an express method for constructing phase diagrams continues to be an urgent task. Earlier, we have developed new quasi-equilibrium oxygen release technique (QEOR) to obtain continuous equilibrium parameters in grossly nonstoichimetric perovskites [4, 5].

The purpose of this work was to modernize the setup and method for obtaining continuous phase diagrams in a short time. Perovskite-like oxides $SrCo_{1-x}Ta_xO_{3-\delta}$ (SCTx) were chosen as samples. It is shown that one isotherm of the phase diagram can be obtained within 2 hours, which makes it possible to obtain a detailed continuous phase diagram of perovskite within a day.

Funding: The reported study was funded by Russian Science Foundation (Project № 21-79-30051).

References:

1. Tan X., Wang Z., Meng B., Meng X., Li K. Pilot-scale production of oxygen from air using perovskite hollow fibre membranes. Journal of Membrane Science. 2010. Vol. 352. P. 189-196.

2. Wang H.H., Tablet C., Schiestel T., Werth S., Caro J. Partial oxidation of methane to syngas in a perovskite hollow fiber membrane reactor. Catalysis Communications. 2006. Vol. 7. P. 907-912.

3. Rui Z., Ding J., Li Y., Lin Y.S. $SrCo_{0.8}Fe_{0.2}O_{3-\delta}$ sorbent for high-temperature production of oxygen-enriched carbon dioxide stream. Fuel. 2010. Vol. 89. P. 1429-1434.

4. Starkov I.A., Bychkov S.F., Matvienko A.A., Nemudry A.P. Oxygen release technique as a method for the determination of "δ–pO_2–T" diagrams for MIEC oxides. Physical Chemistry Chemical Physics. 2014. Vol. 16. P. 5527-5535.

5. Chizhik S.A., Bychkov S.F., Voloshin B.V., Popov M.P., Nemudry A.P. Development of the Crank's diffusion model for the case of material-gas feedback regime in gas flow reactors. Advanced methodology of oxygen partial pressure relaxation for the kinetics of oxygen exchange in nonstoichiometric oxides. Chemical Engineering Journal. 2021. Vol. 420. No. 2. Art. 127711.

HIGH-PRESSURE BEHAVIOUR OF Na-Ca BURBANKITE

Rashchenko S.[1,2], Shatskiy A.[1,2,3], Arefiev A.[1,2,3], Mikhno A.[1,2], Brazhnikova A.[1,2]

[1]Sobolev Institute of Geology and Mineralogy, Novosibirsk, Russia, rashchenko@igm.nsc.ru
[2]Novosibirsk State University, Novosibirsk, Russia
[3]Vereshchagin Institute for High Pressure Physics, Moscow, Russia

Abstract. We performed a high-pressure X-ray diffraction and Raman study of synthetic Na-Ca burbankite, $Na_2Ca_4(CO_3)_5$, up to 24 GPa using diamond anvil cell technique. The obtained data demonstrate that crystal structure of Na-Ca burbankite remains stable up to pressures of 24 GPa, corresponding to the mantle transition zone, and is characterized by bulk modulus K_0 = 68.7(9) GPa. Complementary Raman data demonstrates evident pressure-induced splitting of $(CO_3)^{2-}$ group ν_1 bands up to five components, which can be explained by deformation of $(CO_3)^{2-}$ triangle in crystallographic site with lower (C_s) symmetry.

Key words: Na-Ca burbankite, high-pressure, diamond anvil cell, X-ray diffraction, Raman spectroscopy

Burbankite, Na-Sr dominant end-member of burbankite group with formula $(Na,Ca,REE)_3(Sr,Ca,Ba,REE)_3(CO_3)_5$ (REE – rare earth element), is a rare mineral initially described in highly alkaline igneous rocks, alkaline lacustrine environments and carbonatites [1]. More recently a particular attention was given to burbankite inclusions in rare earth carbonatites, highlighting its important role as a REE source during formation of rare earth mineralization [2]. On the other hand, high-pressure experiments have revealed that Na-Ca counterpart of burbankite, $(Na_2Ca)_{\Sigma 3}Ca_3(CO_3)_5$ or $Na_2Ca_4(CO_3)_5$, can be synthesized under pressure of 6 GPa and temperatures up to 1075 ºC, corresponding to the Earth's upper mantle [3]. A possible role of Na-Ca burbankite in the transport of CO_2 and rare earth elements in the mantle can be also suggested on the basis of petrological experiments which demonstrated formation of Na-Ca carbonates with approximate stoichiometry $(Na,K)_2(Ca,Mg,Fe)_4(CO_3)_5$ in carbonated rocks subducted down to the mantle transition zone [4,5]. The recent findings of Na-Ca carbonates in inclusions in "superdeep" Juina diamonds [6] that allowed to distinguish *"deep natrocarbonatite association"* strongly support the experimental data on the existence of Na-Ca-carbonate and related melts in the mantle transition zone.

However, high-pressure behaviour of burbankite group minerals has never been studied neither by structural nor spectroscopic techniques, so their behaviour under mantle conditions and role in deep processes remain obscure. Moreover, further studies of "superdeep" Na-Ca carbonate inclusions require precise knowledge of Raman spectra of high-pressure Na-Ca carbonates and their response on high pressure, typical for inclusions originated at mantle depths. In order to address these issues we performed a high-pressure X-ray diffraction and Raman study of synthetic Na-Ca burbankite, $Na_2Ca_4(CO_3)_5$, up to 24 GPa using diamond anvil cell technique.

The obtained data (Fig. 1) demonstrate that crystal structure of Na-Ca burbankite remains stable up to pressures of 24 GPa, corresponding to the mantle transition zone, and is characterized by bulk modulus K_0 = 68.7(9) GPa. Complementary Raman data demonstrates evident pressure-induced splitting of $(CO_3)^{2-}$ group ν_1 bands up to five components, which can

be explained by deformation of $(CO_3)^{2-}$ triangle in crystallographic site with lower (C_s) symmetry.

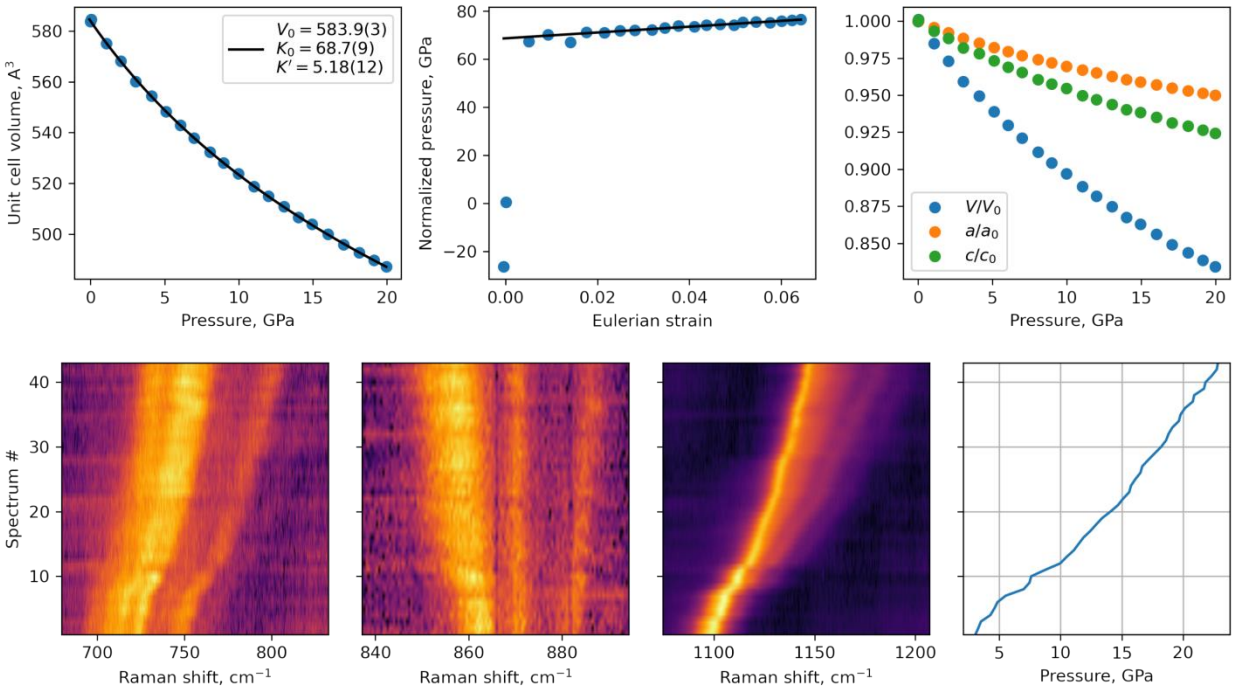

Figure 1 – X-ray diffraction (top) and Raman (bottom) data for Na-Ca burbankite at high pressure.

Funding: This work is supported by the Russian Science Foundation under grant 21-77-00016.

References:

1. Buhn B.A., Rankin H., Radtke M., Haller M., Knochel. A. Burbankite, a (Sr,REE,Na,Ca)-carbonate in fluid inclusions from carbonatite-derived fluids: identification and characterization using laser Raman spectroscopy, SEM-EDX, and synchrotron micro-XRF analysis. American Mineralogist. 1999. Vol. 84. P. 1117–1125.

2. Chakhmouradian A.R., Dahlgren S. Primary inclusions of burbankite in carbonatites from the Fen complex, Southern Norway. Mineralogy and Petrology. 2021. Vol. 115. P. 161–171.

3. Shatskiy A., Sharygin I.S., Litasov K.D., Borzdov Y.M., Palyanov Y.N., Ohtani E. New experimental data on phase relations for the system Na_2CO_3–$CaCO_3$ at 6 GPa and 900–1400 °C. American Mineralogist. 2013. Vol. 98. P. 2164–2171.

4. Grassi D., Schmidt M.W. The melting of carbonated pelites from 70 to 700 km depth. Journal of Petrology. 2011. Vol. 52. P. 765–789.

5. Thomson A.R., Walter M.J., Kohn S.C., Brooker R.A. Slab melting as a barrier to deep carbon subduction. Nature. 2016. Vol. 529. P. 76–79.

6. Kaminsky F.V. The Earth's lower mantle: composition and structure. New York. Springer. 2017. 331 p.

EXPERIMENTAL STUDY OF METHANE BEHAVIOUR AT THE HIGH-PRESSURE HIGH-TEMPERATURE CONDITIONS OF ICE GIANTS INTERIORS

Semerikova A.[1,2], Chanyshev A. D.[3,4], Glazyrin K.[4], Pakhomova A.[4], Kurnosov A.[3], Litasov K.[5], Dubrovinsky L.[3], Fedotenko T.[4], Rashchenko S.[1,2]

[1]V.S. Sobolev Institute of Geology and Mineralogy, Novosibirsk, Russia,
a.semerikova@g.nsu.ru
[2]Novosibirsk State University, Novosibirsk, Russia
[3]Bayerisches Geoinstitut, Universität Bayreuth, Bayreuth, Germany
[4]Photon Sciences, Deutsches Elektronen-Synchrotron (DESY), D-22603 Hamburg, Germany
[5]Vereshchagin Institute for High Pressure Physics RAS, Troitsk, Moscow, Russia

Abstract. Methane phase diagram is important to understand the physics of ice giants. Previous studies reported the formation of diamond from methane at pressures of 10 – 80 GPa and temperatures above 2000 K. These results may be probably affected by the presence of metallic heat absorbers. In this work the effect of absorber on the decomposition of methane was studied using platinum (as hydride-forming) and gold (as non-hydride-forming) absorbers. Diamond was formed from 50 to 95 GPa near 2000 K simultaneously with platinum hydride formation. In the case of gold, diamond formation was not observed below 95 GPa and 3700 K. So, the hypothesis of diamond precipitation in the ice giant interiors should be reconsidered.

Key words: solid methane, diamond, icy planet interiors, hydrides, LHDAC

In his famous ‘The ice layer in Uranus and Neptune – diamonds in the sky?’ paper [1], M. Ross for the first time proposed that mantles of icy giants (Neptune and Uranus) may contain significant amounts of diamonds formed during high-pressure – high-temperature decomposition of hydrocarbons (primarily methane). Such a hypothesis led to later attempts to reproduce experimentally possible diamond formation conditions typical of the deep interiors of Neptune and Uranus. All the previous works [2–4] were based on the assumption that neither metallic heater, nor metallic gasket, cannot react with methane. Herewith, to determine the real P-T conditions of CH_4 dissociation, one needs to exclude the influence of metallic heater reactivity. That is why here we compared the behavior of methane in the presence of hydride-forming (platinum) and non-hydride-forming metal (gold [5]) heat absorbers.

Several high-pressure experiments in the range of 20 – 100 GPa were performed using the laser-heated diamond anvil cell (DAC). Methane was loaded in DACs cryogenically into a hole in a rhenium gasket together with ~10 μm platinum or gold wire (Aldrich, 99.9%).

To study methane dissociation at high pressure and temperature with the presence of hydride-forming metal (platinum [6–9]), XRD mapping and Raman spectroscopy of the quenched from 2000 K samples at 50 – 95 GPa were used. A formation of “bubbles” in the heating spot was observed. The evidences of $CH_4 + Pt \rightarrow C + 4PtH$ reaction at 50 and 75 GPa and 2000 K are the growth of polycrystalline diamond in the center of the “bubble” and formation of the hcp platinum hydride. In our work [6] the same process of the diamond growth concomitant with the formation of platinum hydride at 1700 – 2400 K was observed at 60 GPa.

Raman spectra of the samples with platinum heater, quenched from ~2000 K at 50 – 95 GPa, measured near the center of the “bubble” area, showed the presence of a separate peak at

higher wavenumbers compared with the broad first-order Raman band from diamond anvil, corresponding to the diamond formed inside the sample chamber [10].

To study the methane behavior at the similar high pressure and temperature conditions without the presence of hydride-forming metal, the "Au + CH_4" samples, quenched from 2400 – 3700 K at 20 and 90 GPa, respectively, were also studied by XRD mapping and Raman spectroscopy. In contrast to the platinum-containing samples, neither diamond, nor hydride formation was observed after heating of methane with gold absorber. However, it should be mentioned, that at 20 GPa the heated spot on the gold wire was close to the rhenium gasket, so, the gasket was also heated. We observed the formation of rhenium hydride and small amount of polycrystalline diamond near to the ReH_x.

Although our results show that the $CH_4 \rightarrow C + 2H_2$ reaction does not take place up to 95 GPa we do not exclude that CH_4 at such conditions may be unstable relative to e.g. heavier hydrocarbons often observed by Raman spectroscopy after high-pressure high-temperature treatment of CH_4 [2–4,11]. However, these observations should be interpreted very carefully taking into account the strong influence of presence of hydride-forming metals on enthalpies of the following reactions: $CH_4 \rightarrow C_nH_m + H_2$ and $CH_4 + Me \rightarrow C_nH_m + MeH_x$.

To conclude, we demonstrated that in previous experimental studies a reactivity of platinum in hydrogen-containing systems was ignored leading to incorrect conclusions about possibility of $CH_4 \rightarrow C + 2H_2$ dissociation in the PT-range of 10 – 80 GPa and 2000 – 3000 K, corresponding to deep interiors of ice giants.

Funding: The reported study was funded by RFBR according to the research project #18-35-20047. The work of A.S. was partially supported by the state assignment of IGM SB RAS. We acknowledge DESY (Hamburg, Germany), a member of the Helmholtz Association HGF, for the provision of experimental facilities. The research was carried out at PETRA III, P02.2 Extreme conditions beamline.

References:

1. Ross M. The ice layer in Uranus and Neptune—diamonds in the sky? Nature. 1981. Vol. 292. No. 5822. P. 435–436.

2. Benedetti L.R. Dissociation of CH_4 at high pressures and temperatures: Diamond formation in giant planet interiors? Science. 1999. Vol. 286. No. 5437. P. 100–102.

3. Zerr A., Serghiou G., Boehler R., Ross M. Decomposition of alkanes at high pressures and temperatures. High Pressure Research. 2006. Vol. 26. No. 1. P. 23–32.

4. Hirai H., Konagai K., Kawamura T., Yamamoto Y., Yagi T. Polymerization and diamond formation from melting methane and their implications in ice layer of giant planets. Physics of the Earth and Planetary Interiors. 2009. Vol. 174. No. 1–4. P. 242–246.

5. Rahm M., Hoffmann R., Ashcroft N.W. Ternary gold hydrides: Routes to stable and potentially superconducting compounds. Journal of the American Chemical Society. 2017. Vol. 139. No. 25. P. 8740–8751.

6. Semerikova A., Chanyshev A.D., Glazyrin K., Pakhomova A., Kurnosov A., Litasov K., Dubrovinsky L., Rashchenko S. Face-centered cubic platinum hydride and phase diagram of PtH. European Journal of Inorganic Chemistry. 2020. Vol. 2020. No. 48. P. 4532–4538.

7. Scheler T., Degtyareva O., Marqués M., Guillaume C.L., Proctor J.E., Evans S., Gregoryanz E. Synthesis and properties of platinum hydride. Physical Review B. 2011. Vol. 83. No. 21. Art. 214106.

8. Matsuoka T., Hishida M., Kuno K., Hirao N., Ohishi Y., Sasaki S., Takahama K., Shimizu K. Superconductivity of platinum hydride. Physical Review B. 2019. Vol. 99. No. 14. Art. 144511.

9. Liu G., Yu Z., Li S., Wang H. The experimental compression behavior of platinum hydride to 128 GPa. Materials Letters. 2019. Vol. 249. P. 84–86.

10. Boppart H., van Straaten J., Silvera I.F. Raman spectra of diamond at high pressures. Physical Review B. 1985. Vol. 32. No. 2. P. 1423–1425.

11. Lobanov S.S., Chen P.-N., Chen X.-J., Zha C.-S., Litasov K.D., Mao H.-K., Goncharov A.F. Carbon precipitation from heavy hydrocarbon fluid in deep planetary interiors. Nature Communications. 2013. Vol. 4. No. 1. P. 1–8.

Section METALLOGENY, MINERAGENY AND ORE GENESIS

PALEOENVIRONMENTAL CONDITIONS OF CONTINENTAL IRONSTONES OF THE KOCHKOV FORMATION WITHIN THE OB-TUIM LOWLAND (WESTERN SIBERIA, RUSSIA)

Dauletova A.B.[1], Rudmin M.A.[1, 2]

[1]Division for Geology, Tomsk Polytechnic University, Tomsk, Russia, abd7@tpu.ru
[2]Laboratory of Sedimentology and Paleobiosphere Evolution, University of Tyumen, Tyumen, Russia

Abstract. The studied continental ironstone occurrence belongs to the interfluve of the Ob and Tom rivers, which is located in the eastern part of the West Siberian Plate. The Ob-Tuim lowland completely inherits the Mesozoic-Cenozoic negative structure – the Ust-Tym uplift [1]. The ironstones are localized in the sedimentary sequence of the Kireevsk ore deposit. Iron-bearing layers occur at the top of the Kochkov Formation, which is composed of Neogene and Pleistocene sediments.

Key words: ironstones, continental deposits, authigenic minerals, paleoenvironmental conditions.

Minerals of the Kireevsk deposit are divided into allothigenic (detrital or allochtonous), authigenic (*in situ* or autochtonous) and clay. The group of allothigenic minerals includes quartz, feldspar (albite, microcline), zircon, rutile, monazite, ilmenite, magnetite, hematite, titanomagnetite, pyrite and barite. Also, the minor part of the transported material is clasts of rocks. Iron-bearing rocks are characterized by the abundance of the carbonate-hydroxide assemblage, which is presented in both cement and individual, aggregated formations (Fig. 1 A, C, D). The presence of chlorite (chamosite), siderite, goethite (hydrogoethite), as well as fragments of hematite and titanomagnetite provide the relatively high iron content in the bulk rock composition. Siderite is characterized by individual nodules in the cement of sandstones and ironstones with an average size of 10-50 μm in length (Fig. 1 A, C) or crystalline cement (Fig. 1 B, F). In microconcretions of siderite (Fig. 1 A-C), there is a concentric zonation, reflected in the composition of the carbonate. The average chemical composition of siderite aggregates is as follows: 57.7-83.2 mol. % of $FeCO_3$, up to 1.8 mol. % of $MnCO_3$, up to 2 mol. % of $MgCO_3$, 0.6-1.5 mol. % of $CaCO_3$. Clay minerals are represented by ferruginous chlorite (chamosite) and illite (Fig. 1 C, I). Chlorite (chamosite) is characterized by parallel oriented short-scaled microaggregates within iron-containing and siliciclastic rocks. Less frequently, goethite (or hydrogoethite) is observed among iron-rich minerals in the form of aggregates up to 600 microns in size (Fig. 1 D). Goethite occurs a significantly smaller relative to siderite. Detrital pyrite is rarely found in the matrix of sandstone (Fig. 1 E). A distinctive feature of the studied horizon is the rare presence of zircon grains (Fig. 1 F) of relatively large sizes (up to 500 microns).

The bulk $Fe_2O_{3(total)}$ content varies from 9.7 to 15.9 % (Table 1) in iron-bearing rocks. The bulk chemical composition of siltstones is characterized by $Fe_2O_{3(total)}$ concentration of less than 4.8 %, SiO_2 between 51.0 and 69.0 %, Al_2O_3 between 11.0 and 14.0 %. Gritstones occur at the

bottom of the studied deposits. They are characterized by an increased amount of CaO (up to 15.0 %).

Two groups of trace elements can be distinguished in the studied deposit based on their distribution. The first group of metals (Zn, As, Ag, Cd, Sb) differs by increased contents. The second group (Cr, Ni, Cu, Zr, Sn, Cs, Hf, W, Tl, Pb, Th) is characterized by decreased concentrations. The proxies of P EF and Cu EF (enrichment factors) in two samples exceed above 1 in the intervals of ironstones with sandstone. The proxies of detrital input (Ti EF and Si EF) have maximum values of 1.8 and 3.2, respectively, in siltstones with siderite nodules and sandstones. The proxies of paleosalinity (Sr/Ba and Ca/(Ca+Fe)) have two similar intervals of increasing their values, which correspond to siltstones with siderite nodules, where Sr/Ba increases to 0.4. These proxies are similar to the change in the paleoclimate proxy (Sr/Cu). The Chemical Index of Alteration (CIA) increases to 81.8 in gray siltstones with clay aggregates at the top of the studied sequence. The total content of rare earth elements and yttrium (REE+Y) is characterized by relatively elevated values (up to 210.4 ppm) in gray siltstones at the top. The cerium anomaly (Ce*) ranges from 0.9 to 1.3. A weak positive europium anomaly (Eu*) is noted by the level of 1.0-1.5 in the studied section of the Kireevsk occurrence.

In conclusion, the immobilization of iron depended on the activity of microbial decomposition of detrital organic matter regularly introduced by river watercourses [3]. This factor indicates the sedimentation of siltstones with ironstone in the bottom conditions of swampy lakes. The carbonate association is characterized by the predominance of siderite, which corresponds to the conditions of the ferruginous lakes [4]. In this case, the paleoenvironmental conditions for the formation of iron-bearing layers within the Kochkov Formation consider similar to swampy paleolakes. The presence of Mg admixture in siderite of ironstones supports favorable conditions for siderite transformation [3]. In lake-marsh conditions, it was possible to modify part of siderite into goethite with the active participation of humic acids and local precipitation of brushite [2, 5]. It is assumed that one of these swampy lakes was located in the area of the Kireevsk occurrence.

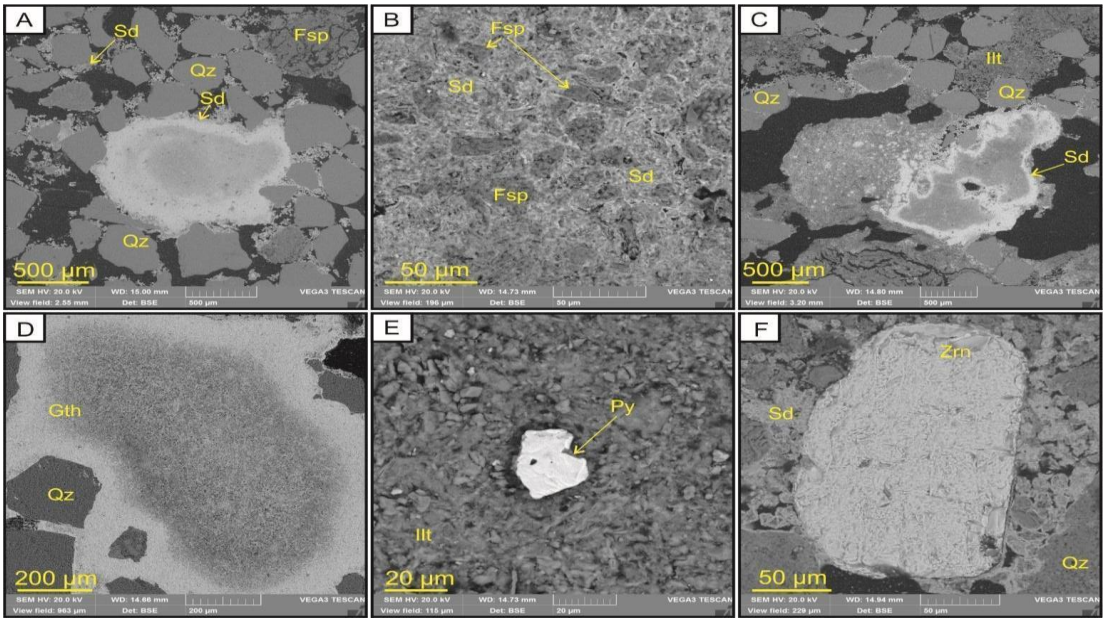

Figure 1 – SEM-images of studied rocks of the Kireevsk occurrence. (A) Siderite nodules ; (B) siderite cement; (C) aggregates of siderite in gritstone; (D) goethite aggregates; (E) detrital pyrite; (F) zircon. Gth - goethite, Ilt - illite, Py - pyrite, Qz - quartz, Sd - siderite, Zrn - zircon.

Funding: This work is supported by the Russian Science Foundation under grant № 20-77-00007.

References:

1. Arhipov S. A., Martynov V. A. Kochkovsky horizon Western Siberia and his age analogues in adjacent areas. Nobosibirsk. Nauka. 1980. 120 p.

2. Martínez-Martínez J., Benavente D., Fusi N., Cañaveras J.C. Brucite-Aragonite Precipitates as Weathering Products of Historic Non-MgO-Based Geomaterials. Minerals. 2020. Vol. 10. Art. 599.

3. Rudmin M., Ruban A., Savichev O., Mazurov A., Dauletova A., Savinova O. Authigenic and Detrital Minerals in Peat Environment of Vasyugan Swamp, Western Siberia. Minerals. 2018. Vol. 8. P. 1-13.

4. Surkov V.S. Neogean evolution of the young Ural-Siberian platform. Russian Geology and Geophysics. 2002. Vol. 43. P. 754-761.

5. Van Houten F.B., Bhattacharyya D.P. Phanerozoic Oolitic Ironstones – Geologic Record and Facies Model. Annual Review of Earth and Planetary Sciences. 1982. Vol. 10. P. 441-457.

CRYPTIC COMPOSITIONAL TRENDS OF ORES AND SILICATES AS AN EVIDENCE OF AT LEAST TWO MAGMA PULSES IN THE MAIN ORE HORIZON OF THE Ni-Cu PGE NORILSK 1 INTRUSION (MIDDLE PART)

Garcia J.A.[1,2], *Tolstykh N.D.*[1]

[1]V.S. Sobolev Institute of Geology and Mineralogy, Novosibirsk, Russia,
jonathan.andres.garcia@gmail.com
[2]Department of Geology and Geophysics, Novosibirsk State University, Novosibirsk, Russia

Abstract. Fundamental aspects on the origin and evolution of mineralized Norilsk-type intrusions remain still unknown. Geochemical and petrographic evidence on disseminated sulfide ores, platinum group minerals (PGMs) and cumulate rock-forming silicates (Ol, Pl, and Px), is presented in order to provide new insights on the evolution of the ore system and its connection with the emplacement and crystallization, from one or more magma pulses, of the ore body.

Key words: Magmatic sulfides, layered intrusion, Norilsk-Talnakh Ore Cluster, Ni-Cu PGE ores.

Using samples from the main ore horizon (MOH) of core sample PH-265, located in the middle part of the Norilsk 1 intrusion and by means of EPMA, SEM-WDS/EDS and ICP-AES, it was established that the MOH consists of at least 3 different rock types, that according to their modal composition, texture and typomorphic minerals correspond to: picritic gabbro-dolerite (g-d), taxitic texture g-d and olivine-bearing g-d. The following two main sulfide paragenesis were interpreted: Low-S association including Tro or Po(hex) +Pn(Fe)+Ccp+Cub in picritic rocks and a High-S association in taxitic and olivine-bearing g-d consisting of Po(mon-hex)+Pn(Ni) +Ccp ± Sph, with whole rock Ni/Cu ratio > 1 in the former and < 1 in the latter.

A relatively similar compositional pattern in 100% sulfide, with predominance of Ni, Pd and Pt in picritic rocks, suggest a common source of sulfide liquid for all layers with slightly different fractionation paths or to a certain degree higher interaction with fresh magma (picritic g-d). Cryptic compositional trends of base metal sulfides (BMS) evidence a thermal gradient that gradually decreases in temperature (T°C) towards the base of the ore body, as well as an increase in f(S2) in the same direction, These results have been confirmed in a previous study of us [1], in which also PGMs vertical zoning suggest at least two distinct thermal gradients: one for picritic layer and the other for taxitic-texture and olivine-bearing horizon, with higher T (Sn, Pb, As) Pd-compounds occurring to the top and lower T (Se, Te and Bi) to the bottom.

In addition, Mg# of olivines and pyroxenes greatly differ between layers, along with some trace elements like Cr_2O_3 and MnO, being picritic g-d higher in Mg# and Cr_2O_3 and lower in MnO, with the opposite trend being observed for taxitic-texture and olivine-bearing g-d. Plagioclase shows a widespread variation in An% between core (c) and rim (r) and decreasing in content *i.e.* more sodic cores towards the bottom in taxitic texture and olivine-bearing g-d, whereas in picritic g-d shows a more uniform calcic compositional trend with less variability (c-r). The investigated silicates together with sulfide ores show an abrupt compositional shift at the transitional boundary between picritic and taxitic-texture rocks, which does not correspond with a “normal” fractional crystallization evolution trend.

Ostensibly, all the previously revealed characteristics in ores and silicates suggest evolution of the ore system from two different sulfide melts, associated to two different magma pulses (Fig. 1).

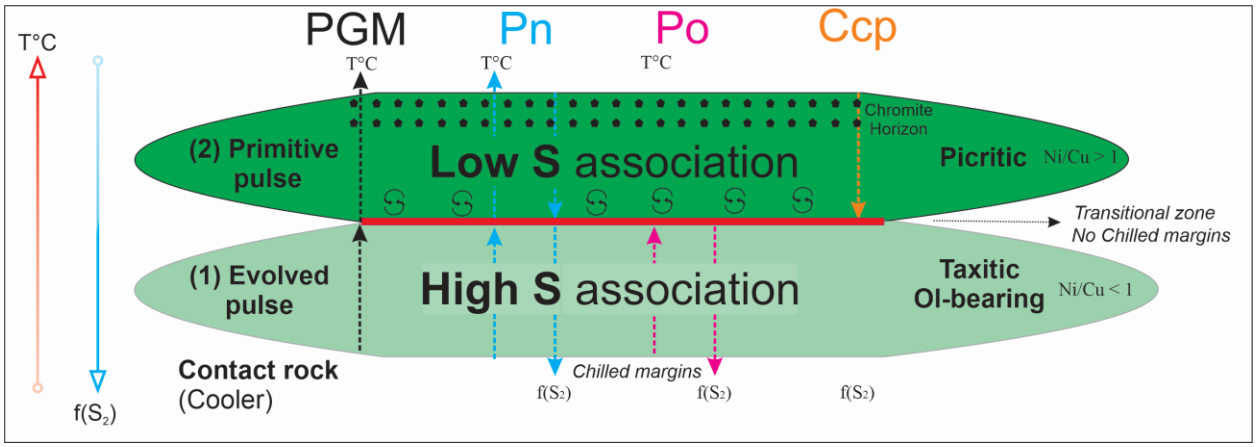

Figure 1 – Summary of the main geochemical features established in ores of the Norilsk 1 intrusion, which suggest an origin from at least two relatively different magma pulses for the MOH.

Funding: Financial support from Grant of the Ministry of Science and Higher Education of the Russian Federation No. 13.1902.21.0018 "Fundamental problems in the development of the mineral resource base of the high-tech industry and energy of Russia".

References:

1. Tolstykh N., Garcia J., Shvedov G. Distribution of sulfides and PGE minerals in the picritic and taxitic gabbro-dolerites of the Norilsk 1 intrusion. The Canadian Mineralogist. 2021. Vol. 59. No. 6. P. 1437–1451.

THE SEQUENCE OF ORE FORMATION OF THE ANOMALOUS DEPOSIT (EAST KAZAKHSTAN)

Greku E.D.

V.S. Sobolev Institute of Geology and Mineralogy, Novosibirsk, Russia, e.greku@g.nsu.ru

Abstract. The Anomalous deposit is located in the southwestern part of the West Kalba gold belt (East Kazakhstan), it belongs to the "orogenic" type. Mineralization at the Anomalous deposit is represented by two morphostructural types of ores – interspersed sulfide mineralization is manifested in carbonaceous-siliceous rocks and sulfide-quartz in monoquartz, carbonaceous-siliceous, volcanogenic, brecciated rocks. Ore formation at the deposit took place in two stages: syngenetic and hydrothermal. Visible gold is noted: in the form of inclusions, veins, free state and invisible gold in needle arsenopyrites.

Key words: West Kalba gold belt, Anomalous gold deposit, orogenic type deposit.

The purpose of this work is to restore the sequence of ore formation on the basis of studying the mineral associations of the Anomaloe gold deposit (East Kazakhstan) with the allocation of its corresponding stages. Using an optical and electronic scanning microscope, stone material from the collection of the IGM SB RAS named after V.S. Sobolev was studied.

The West Kalba gold belt of the Greater Altai is the oldest mining region. The total number of gold manifestations in the West Kalba gold belt is more than 450. Most of the ore objects during the additional exploration were transferred to the category of deposits, including large ones (Suzdal, Bakyrchik, Bolshevik, Southern Ashaly, etc.). In general, 17 ore districts and 5 large ore zones have been allocated within the West Kalba gold belt, which makes it quite reasonable to consider it the leader in the Republic of Kazakhstan. Despite the long history of its development, there are good prospects for the discovery of new ore objects and the expansion of the mineral resource base for gold. One of the most promising is the Akzhal-Boko-Ashalinsky ore region. Numerous deposits and ore occurrences of this territory are limited by deep faults of the north-western strike in the southwest Akzhal-Bokonsky, and in the northeast - Charsky.

On the territory of East Kazakhstan, gold ore deposits of the "orogenic" type [1] predominate, localized, as a rule, in carbonaceous terrigenous strata of carbon, which include the exploited deposits Bakyrchik, Bolshevik, Suzdal and many others. Within the Akzhal-Boko-Ashalinsky ore region, terrigenous carbonaceous rocks are much weaker, being replaced to a greater extent by volcanogenic-sedimentary ore-containing strata. The role of the magmatic factor is also increasing. Mineralization is represented by quartz veins of the gold-malosulfide-quartz formation and mineralized zones of the gold-sulfide formation, accompanied by the processes of near-ore change of rocks: sericitization, calcification, carbonatization, chloritization and albitization [2].

Mineralization at the Anomalous deposit is represented by two morphostructural types of ores – interspersed sulfide mineralization is manifested in carbonaceous-siliceous rocks, the so-called "black shales". The second type is represented in the form of sulfide-quartz veins, it occurs in monoquartz, carbonaceous-siliceous, volcanogenic, brecciated rocks.

During the study, it was found that ore formation at the Anomalous deposit took place in several stages. At the first, sedimentation stage, the formation of framboidal pyrite and, possibly,

needle arsenopyrite took place. The increased gold content of the latter is most likely due to later, superimposed hydrothermal processes. The processes of the hydrothermal stage were obviously accompanied by the formation of sulfides and sulfoarsenides: pyrite, pyrrhotite, arsenopyrite, glaucodote, alloclazite, gersdorfite and rutile. Even later, medium- and low-temperature processes were manifested, which caused the formation of gold, chalcopyrite, sphalerite, galena and sulfosols Cu-Pb-Sb-As (polymetallic association). Hypergenic processes at the Anomalous deposit are manifested insignificantly – secondary covellin and goethite are formed for Cu and Fe minerals.

Gold is noted in the form of inclusions in arsenopyrite, in the form of veins cutting through arsenopyrite, which indicates later processes of gold formation, it is also observed in quartz interstitials. It should be noted the high gold content of needle arsenopyrite, which is concentrated in siliceous-carbonate rocks ("black shales").

Funding: This work was performed on the state assignment of IGM SB RAS.

References:

1. Groves D.I., Goldfarb R.J., Gebre-Mariam M., Hagemann S.G., Robert F. Orogenic gold deposits – a proposed classification in the context of their crustal distribution and relationship to other gold deposit types. Ore Geology Reviews. 1998. Vol. 13. P. 7–27.

2. Kalinin Yu.A., Kovalev K.R., Serdyukov A.N., Gladkov A.S., Sukhorukov V.P., Naumov E.A., Travin A.V., Semenova D.V., Serebryakov E.V., Greku E.D. Age constraints and metallogenic prediction of gold deposits in the Akzhal-Boko-Ashalin ore zone (Altai accretion-collision system). Geodynamics & Tectonophysics. 2021. Vol. 12. No. 2. P. 392–408.

TELLURIDE MINERALIZATION IN THE PIONERSKOE GOLD-QUARTZ DEPOSIT (EASTERN SAYAN, RUSSIA)

Izvekova A.D., Damdinov B.B.

Geological Institute SB RAS, Ulan-Ude, Russian Federation, boxjer@mail.ru

Abstract. The aim of this research is to study the features of the composition and the formation conditions of Pionerskoye gold-quartz deposit (Eastern Sayan). Ore bodies, containing gold and telluride minerals present the quartz veins located in fracture zones in Archean gneisses. As a result of the study a lot of telluride minerals (altaite, petzite, cavalerite, melonite, krennerite, pilsenite, coloradoite, rucklidgeite, stützite, volynskite) have been discovered. Gold often associates with telluride minerals. Using S and Te fugacity diagram we conclude that low sulfur fugacity controlled Te mineral deposition.

Key words: gold, tellurides, fugacity

Pionerskoe gold deposit is situated in the south-east of the Eastern Sayan in the upper reaches of the Kitoy river. It is located at 8.5 km from the largest in the region Zun-Kholba gold deposit. Pionerskoe deposit is composed by Archean granite-gneisses of the basement of Tuva-Mongolian microcontinent, where carbonate and silicious-carbonate rocks of the Irkut suite of Late Neoproterozoic age overlap with tectonic discordance [1-3]. The rocks of the deposit are undergone by dynamometamorphic and metasomatic alterations. Metamorphic rocks are represented by milonites and cataclasites. Metasomatic rocks are represented by beresites and listvenites.

Ore bodies of the deposit are low-sulfide pyrite-quartz and carbonate-pyrite-quartz veinlets and veins, localized in the fractures and schistosity zones. The first generation is presented as milky low-grade quartz. The second generation is light grey quartz including ore mineralization. Chlorite, muscovite and carbonate are also present in the quartz veins. Ore minerals are dominated pyrite, with minor chalcopyrite, gold galena, sphalerite, and tellurides. It has been established that pyrite present as 2 generations. Gold and telluride mineralization is related with 2nd generation of pyrite.

Native gold fills cracks and forms inclusions in the 2nd generation quartz and the 2nd generation pyrite, because it was formed in the last stage of ore formation. High-grade gold is associated with tellurides; low-grade gold is mainly associated with sulfides.

A peculiar feature of the Pionerskoye deposit ores is a wide-spread telluride association, which are represented by a wide range of mineral species. The following minerals have been diagnosed: altaite, petzite, hessite, calaverite, melonite, krennerite, tellurobismutite, pilsenite, coloradoite, ruckledgite, volynskite, tsumoite, tetradymite. Telluride minerals are released in cracks, along grains of pyrite, and small grains in quartz 2 generation, carbonate, often in association with native gold. Most of tellurides are close to being stoichiometric.

Carbonate have been formed along with the 2nd generation quartz, which contains almost the major mass of gold and telluride mineralization. For determine the formation conditions of tellurides, fluid inclusions in carbonates with a homogenization temperature of 225-227ºC were studied.

Thus, it can be concluded that tellurides were formed at this temperature. The observed Te–Au–Ag–Pb–Bi association (calaverite, native gold, altaite, tellurobismuthite, petzite and hessite) and the absence of native Te, Bi, and Ag in this deposit allow a narrow domain in fTe_2–fS_2 to be constrained for deposition of the telluride minerals (fig.1). As there are no sulfides in the association with tellurides, and there is a common small amount of sulfide mineralization on the deposit, the area of sulfur fugacity is limited only by equilibrium lines altaite-galena and pyrite- pyrrhothite, what fits to interval fS_2 from - 17-to -11,5 and fTe_2 from -9,5 to -10,5 for 200° C.

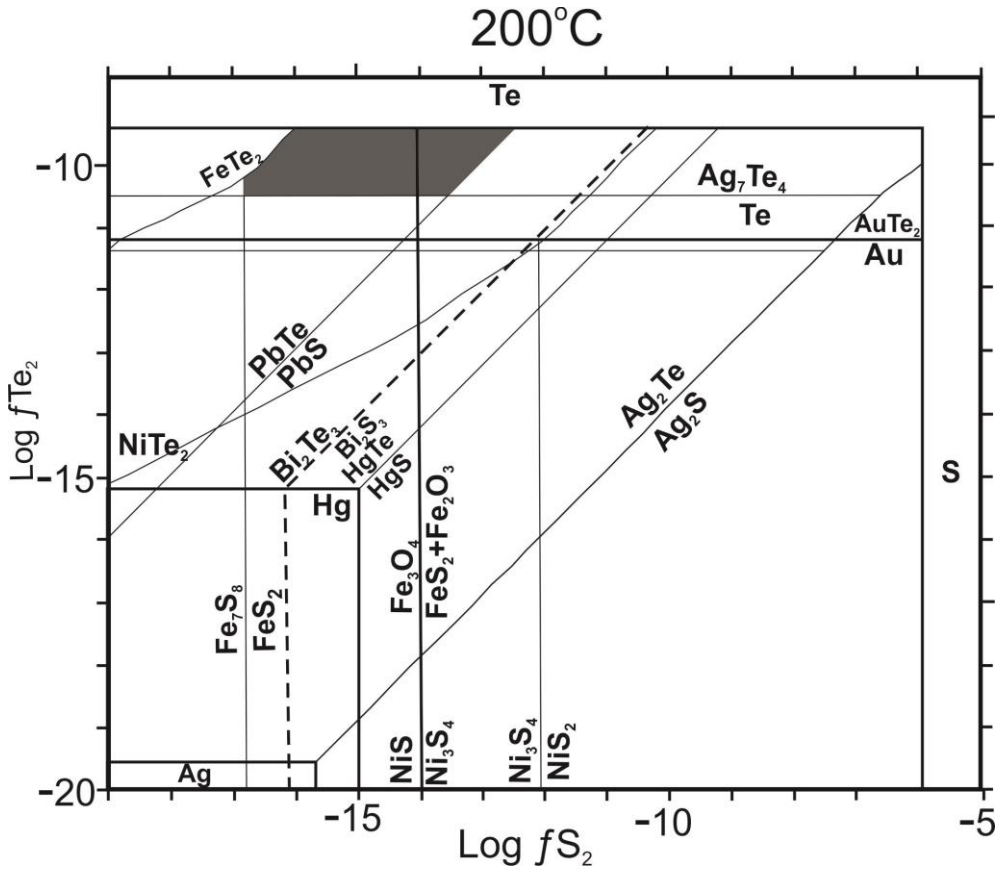

Figure 1 – The diagram of the fugacity Te и S, calculated for 200°C [4] has been plotted. Grey field shows area of fTe_2 during the forming Pionerskoe deposit.

According to the results of mineralogical and geochemical study it is possible to conclude that Pionerskoe deposit ores were reached by S and then by Te. It also means, that Pionerskoe deposit were formed at interaction between mantle matter and the Archaean fundament contains blocks of ultrabasites.

Funding: The reported study was funded by RFBR, project number 18-05-00489a

References:

1. Kuzmichev A.B. Tectonic history of the Tuva-Mongolian massif: Early Baikal, Late Baikal and Early Caledonian stages. Moscow. Publishing house Space 2000. 2004. 192 p.

2. Zhmodik S.M., Mironov A.G., Zhmodik A.S. Gold-concentrating systems of ophiolite belts (on the example of the Sayan-Baikal-Muy belt). Novosibirsk. Academic Publishing House Geo. 2008. 304 p.

3. Damdinov B.B. Mineral types of gold deposits and patterns of their location in the southeastern part of the East Sayan. Geology of ore deposits. 2019. Vol. 61. No. 2. P. 23–38.

4. Afifi A.M, Kelly W.C., Essene E.J. Phase relations among tellurides, sulfides, and oxides: I. thermochemical data and calculated equilibria. Economic Geology. 1988. Vol. 83. P. 377–394.

SECONDARY MINERALIZATION ON SULFIDES IN THE ABANDONED TAILINGS (SALAIR RIDGE, RUSSIA)

Khusainova A. Sh.

V.S. Sobolev Institute of Geology and Mineralogy, Novosibirsk, Russia, khusainova@igm.nsc.ru

Abstract. The paper presents the results of studies of redeposition and sequential deposition of secondary minerals in contrasting physical and chemical conditions of the stored wastes of barite-polymetallic ores of the Salair deposit. The formation of secondary mineralization occurs due to multiple oxidation and dissolution reactions of residual sulfides and noble metals and subsequent deposition of rims on their surfaces and in the intergranular space. The main proportion of secondary minerals are plumbojarosite, anglesite, cerussite, iron (hydr)oxides; pyromorphite and covellite occur less frequently.

Key words: abandoned sulphide tailings, secondary mineralization, supergene zone

Introduction. Secondary minerals formed on tailings play a major role in the immobilization of metals and metalloids. By forming rims over residual sulfides, they seal them from further interaction with pore solutions, which occurs in accordance with electrochemical reactions [1-3]. The aim of the work was to determine the secondary minerals formed in the conditions of lying tailings of waste processing of barite-polymetallic ores of the Salair deposit (Kemerovo region, Salair ridge).

Methods. The mineral composition of the tailings was studied in two vertical sections (along the walls of pits). Zoning was described and all visually distinguishable layers were sampled. Minerals were determined by washing the concentrate and then examining the polished section under optical and scanning microscopes (TESCAN MIRA 3LMU).

Results. The basis of the heavy fraction is barite. Among the residual ore minerals, pyrite, sphalerite, galena, chalcopyrite prevail, grains of arsenopyrite, minerals of the tetrahedrite-tennantite, vatanabeite, pierseite, and native gold groups are less common.

Secondary minerals formed under conditions of tailings oxidation occur on residual (primary) minerals in the form of monomineral and zonal formations. Among the monomineral secondary phases, iron (hydr)oxides (FeOOH), plumbojarosite ($Pb_{0.5}Fe_3(SO_4)_2(OH)_6$), anglesite ($PbSO_4$), and cerussite ($PbCO_3$) stand out in terms of chemical composition. They occur in the form of rims or grains until complete replacement.

Zonal phases are presented in the form of layers (rims) of different chemical composition, which alternately grow on top of each other. The zoning is marked mainly by galena grains. The central part is residual unoxidized galena, predominantly round or oval in shape. A rim of covellite (CuS) (from 1–2 to 20–30 μm) grows around it, which is rarely homogeneous, most often presented as a mixture with cerussite and/or anglesite. Then a layer of anglesite grows (from 1–2 to 50 μm), which occurs both in the form of thin, sintered rims and in the form of dense, granular textures. The outer zonal part of the grain is represented by cerussite (up to 10-15 microns). Cerussite has sintered and porous textures.

In addition, the zonal structure was noted on a grain of pyromorphite (Pb5(PO4)3Cl). The center part is filled with pyromorphite, rounded inclusions and edges are represented by

anglesite, the grain contour is framed by a film of plumbojarosite. Since pyromorphite was not previously described for the Salair deposit, we believe that it is newly formed in the tailings.

Conclusions. Over a period of about 100 years, the processed ores of the Talmovskiye Sands tailing dump were actively subjected to the processes of oxidation, dissolution and precipitation, which contributed to the formation of horizons of different chemical and mineralogical composition. Despite the presence of potentially neutralizing minerals such as carbonates, the abundance of sulfides, combined with the fine grain structure, controls the overall geochemical balance, resulting in strong acidity and typical acidic drainage water conditions. Evidence of active oxidation and redistribution of metals and metalloids in the tailings is the formation of secondary minerals. Newly formed mineral phases, formed under the conditions of tailings oxidation, are most often represented by rims of Fe-Pb-bearing minerals – plumbojarosite, anglesite, cerussite, and to a lesser extent are represented by iron (hydr)oxide differences, pyromorphite.

Funding: This work was performed on the state assignment of IGM SB RAS. Studies of the chemical composition of samples were conducted in the Analytical Center of Multi-elemental and Isotopes Research SB RAS (Novosibirsk).

References:

1. Bortnikova S.B., Abrosimova N.A., Devyatova A.Yu., Shevko E.P., Yurkevich N.V., Cherny N.K., Danilenko I.V., Palchik N.A. Volatility of chemical elements during the dehydration of secondary sulfates. Bulletin of the Tomsk Polytechnic University. Geo Assets Engineering. 2022. Vol. 333. No. 1. P. 121–133

2. Bortnikova S.B., Yurkevich N.V., Gaskova O.L., Volynkin S.S., Edelev A.V., Grakhova S.P., Kalnaya O.I., Khusainova A.S., Gora M.P., Khvashchevskaya A.A., Saeva O.P., Podolynnaya V.A., Kurovskaya V.V. Arsenic and metal quantities in abandoned arsenide tailings in dissolved, soluble, and volatile forms during 20 years of storage. Chemical Geology. 2021. Vol. 586. Art. 120623.

3. Swęd M., Uzarowicz Ł., Duczmal-Czernikiewicz A., Kwasowski W., Pędziwiatrc A., Siepak M., Niedzielski Pr. Forms of metal(loid)s in soils derived from historical calamine mining waste and tailings of the Olkusz Zn–Pb ore district, southern Poland: A combined pedological, geochemical and mineralogical approach. Applied Geochemistry. 2022. Vol. 139. Art. 105218.

GEOLOGICAL STRUCTURE AND QUARTZ TYPOMORPHISM OF HYDROTHERMAL VEINS OF THE KHURCHANSKAYA PERSPECTIVE AREA (MAGADAN REGION)

Krasilnikov P.A., Gareev B.I.

Kazan Federal University, Institute of Geology and Petroleum Technologies, Kazan, Russia, krasilnikovp290@gmail.com

Abstract. The conducted research allowed us to identify the features of the gold-bearing quartz veins of the perspective Khurchan district, to study the compositions of rocks and ores of quartz veins, as well as host rocks. In addition to sulfide, titanium mineralization, represented by rutile and anatase, was found in the host rocks of hydrothermal veins of the Khurchanskaya perspective area.

Key words: quartz, hydrothermal vein, mineralization, ores.

Kurchanskaya perspective area is one of the little-studied areas of the Magadan region. There are several known ore occurrences and many points of mineralization of gold. Khurchanskaya Square is located at the junction of two large metal-bearing areas: the Yano-Kolyma megasynclinorium and the Okhotsk-Chukchi volcanic belt, within the Khurchano-Orotukan metallogenic zone.

The main ore-bearing formations are the submeridional veining zones and quartz veins grouped in the north-west strike band in the southern part of the stock [1]. Ore mineralization is largely developed in granitoid intrusions and their super-intrusive zones, represented by arsenopyrite-quartz veins and stockwork zones of the gold-rare-metal formation (Stock, Khurchanskoe manifestations). The specificity of its ores is the superimposition on synaccretion gold-rare metal mineralization of late epithermal mineralization, which is associated with the Okhotsk-Chukchi volcanic belt. In mineralized crushing zones and vein-veined zones, silver-polymetallic mineralization with gold is developed (Hallucination manifestation) [2].

With the help of modern research methods, namely: SEM analysis, Raman spectroscopy, Electron paramagnetic resonance and petrographic microscope, quartz samples from hydrothermal veins were studied, as well as the host rocks of quartz veins - berezites. The morphology, compositional contrast and chemical composition of minerals were studied, and the presence of isomorphic impurities in quartz was revealed (Fig. 1). Representatives of ore mineralization were identified in quartz. The following ore minerals are represented: pyrite, arsenopyrite, molybdenum, rutile, anatase.

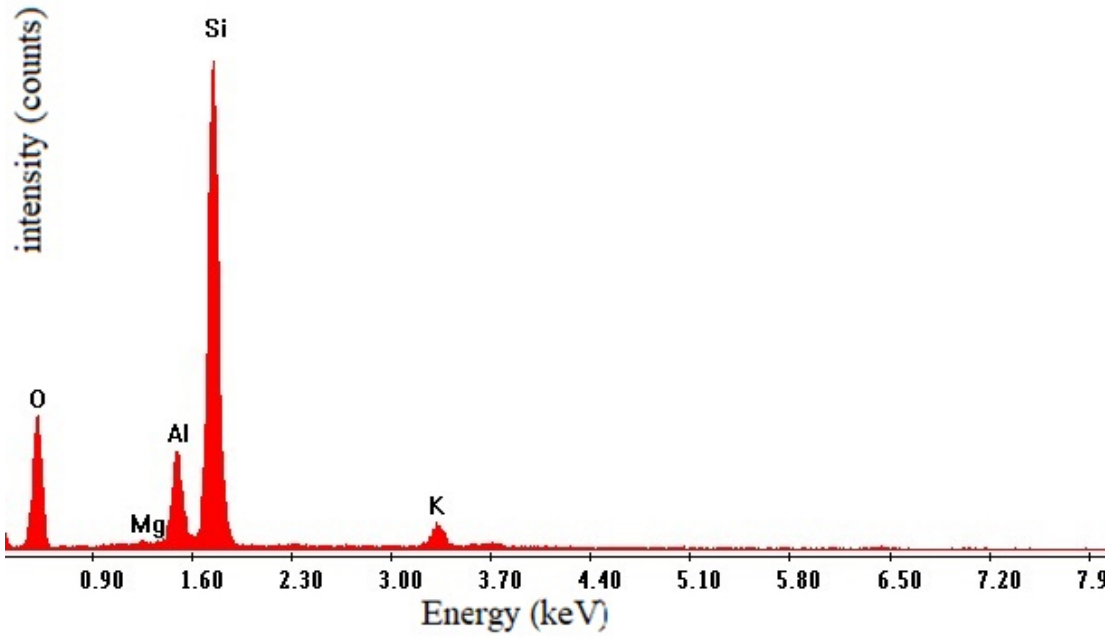

Figure 1 – EDX spectrum of quartz with isomorphic admixtures of Al, Mg and K.

The result of the presented work is to obtain new knowledge about the geological structure and quartz typomorphism of the hydrothermal veins of the Khurchanskaya perspective area. Along with the previously identified ore mineralization (pyrite, arsenopyrite, and molybdenum), titanium mineralization was found, represented by rutile and anatase of hydrothermal veins of the Khurchanskaya perspective area.

Funding: This work was carried out with the support of the Ministry of Education of the Russian Federation under Contract No. 14.Y26.31.0029 as part of the implementation of the Decree of the Government of the Russian Federation No. 220.

References:

1. Kuznetsov V.M., Goryachev N.A., Zhigalov S.V., Savva N.E. Structure and ore-bearing capacity of the Myakit-Khurchansky ore-placer node. Bulletin of the North-Eastern Scientific Center of the FEB RAS. 2011. No. 4. P. 37-51.

2. Glukhov A. N., Fomina M. I., Kozlova E. E. Golden mineralization of the stock ore field (Magadan region). Bulletin of the North-Eastern Scientific Center of the FEB RAS. 2021. No. 1. P. 13-29.

FEATURES OF THE GEOLOGICAL STRUCTURE OF THE GOLD - BEARING TARLAU PLACERS (SOUTHERN URALS)

Makhinya E.I., Mohammed A.E.I

People's friendship university of Russia, Moscow, Russia, eugenemahinya@yandex.ru

Abstract. During the geological practice in the Uchalinsky district of the Republic of Bashkortostan, a one of the placers of the Urazovsky group has been studied. This paper studies the results of the concentration samples (panning samples), and geological documentation of previous works, as the result of that the features of the geological structure of the raft, the localization of placer-forming sands, their lithological composition, and typomorphic features of gold are identified.

Keywords: gold, placer, karst, deposit, Southern Urals.

The Tarlau gold-bearing placer is located on the eastern slope of the Southern Urals, on the left side of the valley of the Tarlau River of the same name, the right tributary of the Ural River, 3 kilometers northwest of the Iltibanov reservoir. To clarify the structural and morphological features of the placer, drilling data from 1999-2001 were used, a geological map and a spatial model of the relief of the raft were constructed.

The surface of the raft is uneven with indistinct depressions observed in the longitudinal section oriented in the submeridional direction (15°) and uplifts in the side parts of the identified buried trough. The slope of the raft surface does not exceed 1.1° and is directed towards the valley of the Tarlau River. The rocks are composed of marble-like limestones, sandstones, porphyrites, serpentinites, clay weathering crusts of linear type (figure. 1 (a)). Devonian siliceous shales, quartzites, and silicified varieties of rocks were weathered to a lesser extent. In the study area there are karst forms developing along carboniferous calcareous deposits. Weathering crusts are of variable thickness. In areas with high hypsometric marks, they undergo denudation, and rarely come to the surface. Serpentinites, pebbled rocks, the presence of shale, indicate that the placer is in the zone of influence of a deep fault (the Main Ural fault) [1].

At the base of the section lies alluvium, represented by yellow-brown clays with inclusions of gravel-pebble material up to 35% and boulders up to 15%. Quartz and siliceous shales predominate in the composition of the clastic well-rounded material (figure. 1 (b)). The highest concentrations of gold are associated with the yellow-brown layer of alluvium in the placer. The maximum thickness of the deposit is 7 m [2].

Higher up the section, on yellow-brown alluvium, there is a discontinuous layer composed of reddish-brown, dense clay. In their composition, the presence of detrital material is observed, ferruginous-manganese inclusions are present. The amount of detrital material is estimated to be up to 10%. The gold content of the layer is weak, the maximum thickness of deposits is 6 m.

The upper part of the section is composed of dark brown clays, interlayers of fine-grained sand with inclusions of gravel-pebble material up to 20%. The gold content is weak and the maximum thickness of the layer is 3 m.

The most obvious finding to emerge from the study of typomorphic features of native gold in the Federal State Budgetary Institution TsNIGRI is that, a relatively flat surface of gold grains is distinguished, with large imprints of enclosing minerals giving a rough-edged appearance, with moderately, rarely intensively, corrosion (figure. 1 (c)). In general, gold is free from accretions and films, only occasionally minor fragmentary impurities and inclusions of iron and quartz hydroxides are identified. The sizes of gold particles vary from 3.5 to 0.25 mm, however gold particles with a size of 0.7-2 mm prevail (figure. 1 (d)). Goldenrods with a size of -0.5 +0.25 mm were distinguished in isolated cases. The average weight of the gold in the studied samples is 4.3 mg. The presence in the samples of only single gold pieces of 0.25-0.5mm in size and the complete absence of very fine gold (class -0.25 mm) may be due to repeated redeposition in placers and removal of very fine and fine gold. The manifestation of gold-sulfide-quartz ore-formation type is assumed to be the root source [3].

Conclusion. A comprehensive geophysical study of the buried karst for the presence of karst traps is proposed to reveal the geological and geomorphological conditions of the formation of paleochannels.

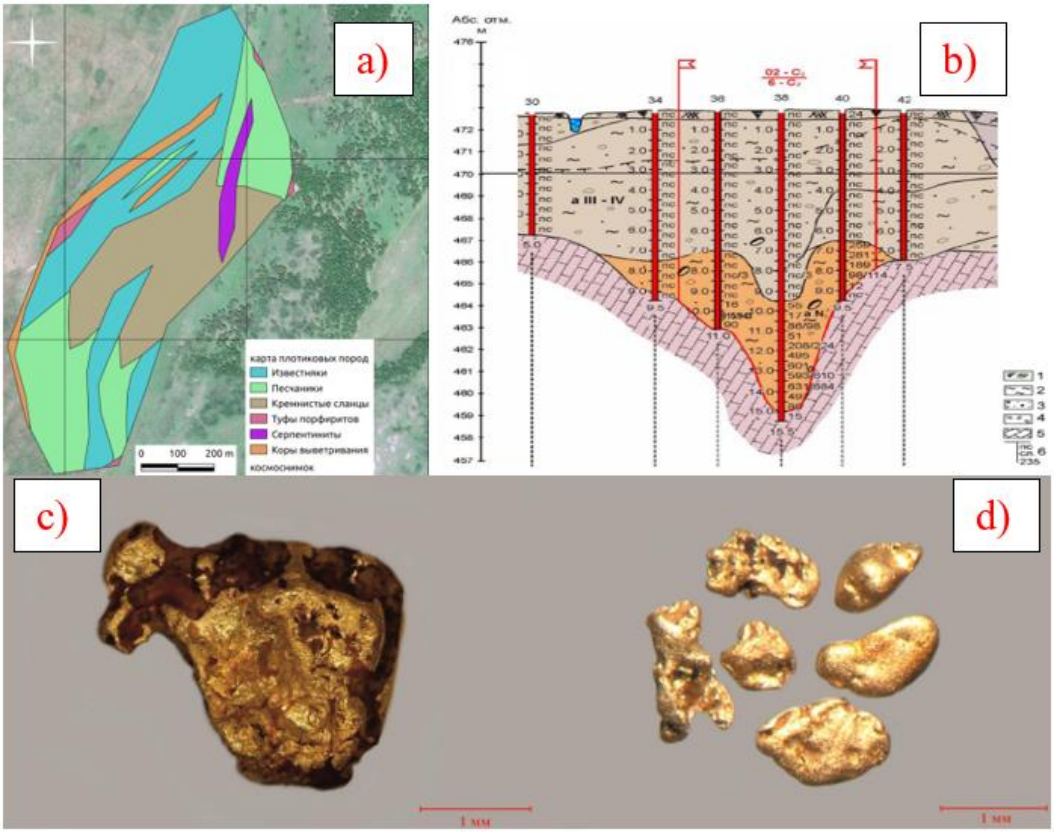

Figure. 1 – a) A map of the rocks of the raft; b) Geological sections; c) Semi-rolled gold with a rough-cellular corroded surface in fusion with iron hydroxides; d) Well-rounded crystals with a smooth surface and semi-rolled gold with inclusions of oxidized sulfides on a pitted surface.

References:

1. Map of placer gold bearing area "Birch Grove". Scale 1:25,000. 1988.
2. Sozinov V.F. Additional exploration of exploited gold placers of Kuru-Elginskaya, Afoninskaya and adjacent previously developed placers (the territory of the former mine "Birch Grove") for 1987-1992. Ufa. 2001. 360 p.
3. Shatilova L. V., Krasnov A.N., Pozdnyakova N.N. Investigation of typomorphic features of native gold from the Tarlau placer (Uchalinsky district, Republic of Bashkortostan). Moscow. FSBI TsNIGRI. 2021. P. 35-36 p.

FEATURES OF GOLD MINERALIZATION OF THE ABYZ GOLD-PYRITE DEPOSIT (CENTRAL KAZAKHSTAN)

Nikolaeva A.N.

Division for Geology, Tomsk Polytechnic University, Tomsk, Russia, ann18@tpu.ru

Abstract. The Abyz pyrite deposit is located in Central Kazakhstan in the Karaganda region and discovery in 1973. Mineralization is confined to an extended zone of observation of beresitization along volcanic-sedimentary rocks Aigyrzhal Formation of the Early Devonian [1]. Pyrite-gold-polymetallic mineralization is localized mainly in metasomatites. According to the textural and structural features at the deposit of Abyz, the interactions of two types of ores: solid and solid disseminated gold-pyrite ores.

Key words: sulfide concentrate, material composition of ores, gold morphology.

To study the material composition of ores and identify the features of gold mineralization at the deposit, furrow samples were taken from the main ore bodies, which were subjected to a detailed study. As a result of the work, it was found that, according to the textural and structural features, the ores at the deposit are represented by two types: mostly continuous and disseminated in a subordinate amount. Sulfide minerals are pyrite, chalcopyrite, galena and sphalerite. Disseminated ores are characterized by the predominance of non-metallic material over ore, 40% are composed of sulfides and 60% of non-metallic minerals. Solid ores are 95-98% composed of sulfides. Ores are characterized by a uniform, continuous addition of aggregates of minerals. This type is most widely distributed in the deposit.

During the technological study of ores, it was found that most of the gold is associated with pyrite, chalcopyrite, galena and sphalerite, which are diagnosed as part of the sulfide concentrate [2]. As a result of the scanning of ores, it was found that gold, which is usually concentrated in pyrite and to a lesser extent in chalcopyrite, is presented in a mineral form, the predominant amount of which is associated with electrum, and to a lesser extent occurs in the form of native (Table 1). The deposition of gold minerals occurred during two stages of mineral formation: gold-sulfide and gold-telluride.

AgAu electrum segregations are usually veinlet-shaped, rarely represented as isometric and irregular grains. Most often, electrum is enclosed between grains of pyrite (Fig. 1A) and chalcopyrite; also, in the process of scanning ores, cases of finding the mineral in pyrite cracks were found. The power of the discharge does not exceed 3 microns, and the length is 30 microns. Native gold Au is observed as elongated, lumpy, vein-like, interstitial segregations, clusters of irregularly shaped grains, usually intergrown with pyrite (Fig. 1B). Cases of the development of irregular gold grains, concentrating along the periphery of sulfides, were identified. Allocations in size do not exceed 3.85 microns. Petzite Ag_3AuTe_2 (Fig. 1C) with calaverite $AuTe_2$ (Fig. 1D) in the form of oval and irregular grains was found singly. To identify the supposed finely dispersed (up to 1 micron in size), scattered - the so-called "invisible" gold, mass spectral analysis was used with inductively coupled plasma of the pyrite monofraction, which revealed the presence of "nanogold" both in solid and disseminated ores.

For the first time in this deposit, such minerals as calaverite $AuTe_2$, lautite CuAsS, ilmenite $FeTiO_3$, cassiterite SnO_2, chenguodayite $Ag_9FeTe_2S_4$, raclidite $(Bi,Pb)_3Te_4$, zircon $ZrSiO_4$, monazite (La, Ce, Nd)PO_4 and turnemobite $(Ce)(Ce,La,Nd)_2Al(SiO)_2(OH)$.

Table 1. Gold mineralization in the ores of the Abyz deposit

Solid	**Disseminated**
76%	24%
Electrum AgAu	
48%	12%
Native gold Au	
12%	12%
Calaverite $AuTe_2$	
12%	-
Petzite Ag_3AuTe_2	
4%	-

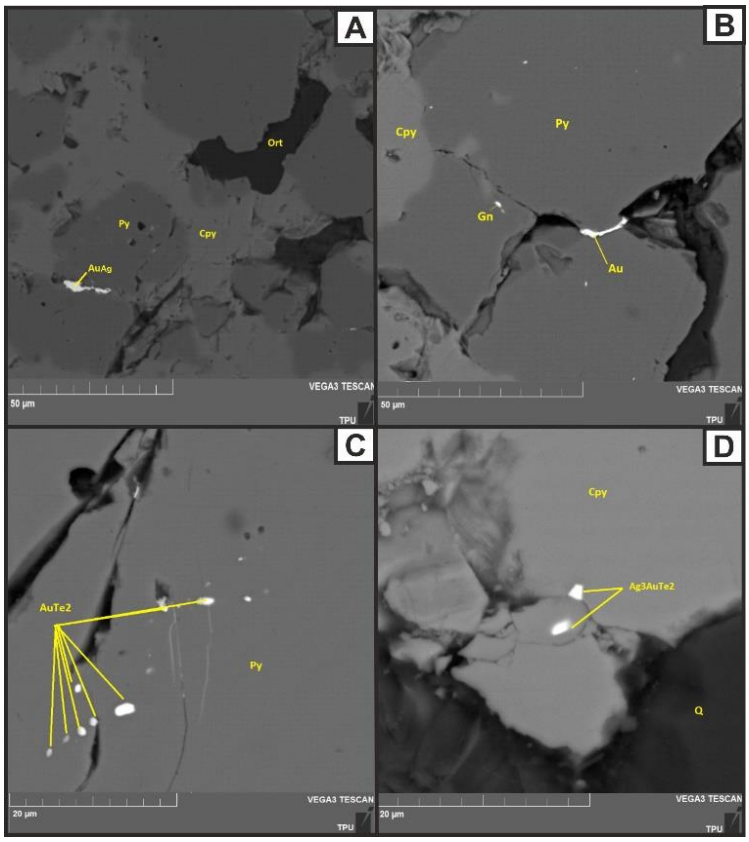

Figure 1 – SEM images of the studied ores of the Abyz deposit. (A) electrum filling cracks between pyrite and chalcopyrite; (B) incorrect extraction of gold in a crack in a pyrite grain; (C) calaverite grains in pyrite; (D) irregular petcite grains in chalcopyrite. Py - pyrite, Cpy - chalcopyrite, Gn – galena, Ort – orthoclase, AgAu – electrum, Au – gold, $AuTe_2$ – calaverite, Ag_3AuTe_2 – petzite.

Funding: This work is supported by the Russian Science Foundation under grant № 21-17-00019.

References:

1. Shcherba G.N. Geotectonics and metallogeny. Alma-Ata. Nauka. 1988. 176 p.
2. Baybatsha A.B. Models of deposits of noble metals: monograph. Almaty. KazNTU. 2016. 452 p.
3. Rodygina V.G. Beginnings of Mineragraphy. Tomsk. NTL. 2006. 175 p.

PRELIMINARY FLUID INCLUSIONS STUDIES IN THE LS EPITHERMAL KARADERE GOLD DEPOSIT (NW TURKIYE)

Oğuz B.[1], Bozkaya G.[2], Bozkaya Ö.[2]

[1]TÜMAD Mining Company, Balıkesir, Türkiye, burcin.oguz@tumad.com.tr
[2]Pamukkale University, Department of Geological Engineering, Denizli, Türkiye

Abstract. First data on the microthermometric studies of the ore forming fluids of the Karadere gold deposit are presented. The Karadere deposit can be considered an LS epithermal deposit and mineralization area consists of Triassic metamorphic basement, Oligo-Miocene Kozak granodiorite and early-middle Miocene volcanic-subvolcanic rocks. Gold mineralization was hosted by sugary, bladed, recrystallized and brecciated quartz veins. Homogenization temperature of fluid inclusions indicates two distinct fluid pulses, one at high temperature (300^{o}C) commensurate with epithermal mineralization and boiling/near boiling conditions and the second approximately 180^{o}C lower. Salinity in both instances was from 7–0.3 wt. % NaCl. The range of temperatures within individual samples is consistent with variations from near lithostatic to hydrostatic pressure during vein and fracture opening.

Key words: Fluid Inclusion, LS Epithermal Gold, Karadere, Türkiye

The Turkish segment of the Tethyan Eurasian Metallogenic Belt, which extends from Western Europe through Anatolia to Iran, is currently being intensively prospected and contains a number of active mines. The epithermal deposits in the Biga Peninsula have the same geological characteristics as other deposits of this style around the globe. A number of epithermal Au-Ag (high and low sulfidation/HS-LS), porphyry Au-Cu-Mo and base metal skarn deposits and mineralization are associated with tectonic activities in the Tertiary calc-alkaline magmatism in Western Anatolia. The Karadere deposit, is a typical example of the tectonically controlled mineralizations in the Biga Peninsula, is located 14 km SW of Burhaniye (Balıkesir). The deposit is one of a number of spatially close mineralized locations such as Küçükdere, Ovacık, Çukuralan deposit which shares many features, not only within this area, but with similar styles of mineralization in the Biga Peninsula and Western Turkey. Previous studies [1, 2]focused on the the kinematic characteristics of vein hosting faults, vein geometries and distributions in Karadere gold deposit, but there is no data on ore forming solutions or source of fluids. Our study focuses on determining to characteristics of ore formig fluids and source of them.

The mineralization area consists of Triassic metamorphic basement, Oligo-Miocene Kozak granodiorite and early-middle Miocene volcanic-subvolcanic rocks. Gold and silver mineralization are hosted by quartz veins confined to high to moderate angle normal faults traversing the andesitic domes, and overlying agglomerate-volcanic breccia in the early-middle Miocene volcanic, subvolcanic rocks. The mineralized veins are composed of sugary quartz and occasional bladed to brecciated textures and higher gold mineralization should be spatially associated with veinlets with sugary and ghost bladed quartz crytals [1]. Hydrothermal alterations are observed associated with mineralization in the volcanic-volcanoclastic rocks manifested as silicification and argillic.

Microthermometric measurements of fluid inclusions in quartz were obtained using a Linkam heating-freezing stage (THMS600) mounted on an Olympus microscope in Pamukkale University. Early quartz shows textures that are consistent with many epithermal deposits [2]. The crystals are euhedral, with several phases of euhedral overgrowths and L-V and V-L inclusions aligned at 90^{o} to the crystal face. There are also variable L/V ratios commonly observed in individual fluid inclusion arrays. Based on microthermometric data of fluid inclusions, the hydrothermal fluid is interpreted to have evolved during at least two stages: 1) an early fluid, trapped in sugary quartz, with moderate ~7 eq. wt% NaCl salinity, and temperature is about 300 ^{o}C; and 2) late-stage fluid trapped in recrystallized quartz with low ~0.3 eq. wt% NaCl salinity, and temperature is 180^{o}C.

The presence of bladed texture and of co-existing liquid-rich and vapor-rich inclusions in the ore-stage indicates a boiling event in the Karadere gold mineralization [3-5]. In order to improve the understanding of characteristic of ore-forming processes and nature of the fluids, stable and radiogenic isotope studies are planned to be carried out.

Funding: This work is supported by the Pamukkale University Scientific and Research Center under grant 2021FEBE069.

References:

1. Çam M. The geological characteristic, fluid pathways, and structural controls of Karadere low sulfidation epithermal gold deposit (Burhaniye, Balıkesir, Turkey). Muğla Sıtkı Koçman University. M.Sc Thesis. 2017. 151 p.
2. Gürler Z. Karadere low sulphıiatıon gold deposıi (Ivrindi, Balıkesir): an example for detachment-fault-related epithermal gold deposits in Western Turkey. Balıkesir University. M.Sc Thesis. 2019.
3. Bodnar R.J., Reynolds T.J., Kuehn C.A. Fluid-inclusion systematics in epithermal systems. Economic Geology. 1985. Vol. 2. P. 73-97.
4. Hedenquist J.W. Boiling and dilution in the shallow portion of the Waiotapu geothermal system, New Zealand. Geochim Cosmochim Acta. 1991. Vol. 55. P. 2753–2765.
5. Hedenquist J.W., Simmons S.F., Giggenbach W.F., Eldridge C.S. White Island, New Zealand, volcanic-hydrothermal system represents the geochemical environment of high-sulphidation Cu and Au deposition. Geology. 2013. Vol. 21. P. 731–734.
6. Drummond S.E., Ohmoto H. Chemical evolution and mineral deposition in boiling hydrothermal systems. Economic Geology. 1985. Vol. 80. P. 126–147.

FORMATION OF SIDERITE IN MARINE OOIDAL IRONSTONES ON EXAMPLE OF BAKCHAR DEPOSIT (WESTERN SIBERIA)

Rudmin M.A.[1,2], Kalinina N.A.[1], Maximov P.N.[1]

[1]Division for Geology, Tomsk Polytechnic University, Tomsk, Russia, rudminma@tpu.ru
[2]Laboratory of Sedimentology and Paleobiosphere Evolution, University of Tyumen, Tyumen, Russia

Abstract. This work is devoted to a detailed study of the siderite and clay minerals of ooidal ironstones of the Bakchar deposit (Western Siberia) to assess the mineral formation processes. Siderite is divided into two varieties that differ in morphology, chemical and isotopic composition, fluid inclusions due to different carbon sources and formation conditions. The authigenic mineral associations of ooidal ironstones cement in a thin interval mark the change of geochemical zones from methanic zone through sulfide (sulfate-methane transition zone) to ferruginous (iron reduction zone).

Key words: siderite, ooidal ironstones, stable isotopes, fluid inclusions, carbon source.

Siderite is a carbonate mineral that has been distributed from Precambrian deposits to modern sediments. In Phanerozoic ooidal ironstones, siderite is the main part of cement [1-3] in association with a clay matrix. The genesis of siderite during the accumulation of deposits of ooidal iron ores is a poorly studied problem regarding the sources of carbon and metals, the processes of mobilization and transportation, as well as the conditions and kinetics of their concentration. The purpose of this work is to study the origin and evolution of siderite as the main mineral of the cement of ooidal ironstones to assess the criteria for processes of the ore deposit formation on the example of the Cretaceous-Paleogene Bakchar deposit in Western Siberia (Russia).

The Bakchar deposit consists of the Upper Cretaceous (Kuznetsovo, Ipatovo, Slavgorod, Gan'kino) and Paleogene (Lyulinvor) Formations, with three main ore horizons separated by siliciclastic intervals. The ore horizons comprise ooidal and peloidal ironstones, glauconitolites, glauconitic sandstones and siltstones, while the intervening siliciclastic intervals are composed of claystones, siltstones, sandstones and gritstones [4]. Ironstones occur at three stratigraphic levels, viz. Bakchar, Kolpashevo and Narym from top to bottom. Ironstones in the Bakchar deposit consist mainly of iron-rich ooids include both authigenic and detrital minerals [5]. Authigenic minerals are hydrogoethite, berthierine, illite, chamosite, glauconite, siderite, pyrite, greigite, pyrrhotite, barite, authigenic monazite, with rare wurtzite, galena, cerussite and acanthite.

Siderite is the main minerals cementing iron-rich ooids and the terrigenous fraction in ironstones of the Bakchar deposit. Siderite is classified into two varieties. The first variety of siderite is veinlet (jet) or massive (most of the cementing material) with a low proportion of impurities in chemical composition (up to 5.6% of MnO + MgO + CaO), which contains primary fluid inclusions (FI) with sizes of 2–6 μm in diameter. The bimodal nature of the homogenization temperatures of FI (170–210°C and 210–300°C) of the first variety of siderite indicates a portion-wise inflow of solutions into the pore sediments. The second variety of siderite is concretions (or accumulations of individual aggregates) or impregnations with a high proportion

of impurities in chemical composition (up to 23.5% of MnO + MgO + CaO) with rare secondary FI with a size of from 0.5 to 2 μm in diameter. The distinctive in situ associations of cement minerals in ooidal ironstones of the Bakchar deposit correspond to the change in thin layers of chemical zones from methane through sulfide (sulphate-methane transition zone) to ferruginous (iron reduction zone). These zones are marked by the following mineral associations of cement (from bottom to top): illite + smectite (nontronite) + the second variety of siderite (impregnated) + wurtzite, illite + smectite (nontronite) + kaolinite + the first variety of siderite (vein or massive) + pyrrhotite + greigite, illite + kaolinite + framboidal pyrite, illite + kaolinite + hydrogoethite. Similar mineral-chemical zones are described in environments with recorded upward methane and carbon dioxide diffusion through the seabed sediments [6]. So, these layers in the Bakchar deposit have a total thickness of 2 to 6 meters. The layers with contrasting vertical zonation of authigenic minerals indicate the proximal zone of ore-forming processes. These processes were linked with areas and periods of intense inflow of metal-bearing fluids. In the sequence of the Bakchar deposit, the proximal zone with variations of siderite, rare authigenic minerals, and phyllosilicates among ironstones has a local character with linear, steeply dipping outlines in the section. It is assumed that these were the main areas of diffusion of metal-saturated fluids. Similar morphologies of carbonate structures are characteristic of methane seeps sediments [7].

As a rule, the bottom of these layers includes the first variety of siderite in cement with fluid inclusions and isotopically light inorganic carbon ($\delta^{13}C$ on average from -35.0 to -39.5 ‰). The isotope budget of inorganic carbon largely corresponds to thermogenic methane [8]. Such layers in the deposit are interpreted as periods and zones of fluid exhalation. Siderite of the ironstone cement includes FI with a relatively high homogenization temperature (170–320 °C). The gas-phase of these FI is represented by H_2S and CH_4 (Raman peaks 2678–2688 cm^{-1} and 2926–2960 cm^{-1}, respectively), which confirms the functioning of the upward fluid flow at the time of the ironstone formation.

Funding: This work is supported by the Russian Science Foundation under grant 21-17-00019.

References:

1. Mücke A. Chamosite, siderite and the environmental conditions of their formation in chamosite-type Phanerozoic ooidal ironstones. Ore Geology Reviews. 2006. Vol. 28. No. 2. P. 235–249.

2. Rudmin M., Roberts A.P., Horng C.-S., Mazurov A., Savinova O., Ruban A., Kashapov R., Veklich M. Ferrimagnetic Iron Sulfide Formation and Methane Venting Across the Paleocene-Eocene Thermal Maximum in Shallow Marine Sediments, Ancient West Siberian Sea. Geochemistry, Geophysics, Geosystems. 2018. Vol. 19. No. 1. P. 21–42.

3. Taylor K.G., Simo J.T., Yocum D., Leckie D. Stratigraphic significance of ooidal ironstones from the Cretaceous Western Interior Seaway: The Peace River Formation, Alberta, Canada, and the Castlegate Sandstone, Utah, U.S.A. Journal of Sedimentary Research. 2002. Vol. 72. No. 2. P. 316–327.

4. Belous N.C., Nikolaeva I.V., Kazansky Y.P., Berdnikov A.P., Klyarovskiy V.M., Kuznetsov V.P., Babin A.A. The Western-Siberian iron ore basin. Novosibirsk. Siberian Branch of the Academy of Sciences of the USSR. 1964. 448 p.

5. Rudmin M., Mazurov A., Banerjee S. Origin of ooidal ironstones in relation to warming events: Cretaceous-Eocene Bakchar deposit, south-east Western Siberia. Marine and Petroleum Geology. 2019. Vol. 100. P. 309–325.

6. Xu T., Bei K., Tian H., Cao Y. Laboratory experiment and numerical simulation on authigenic mineral formation induced by seabed methane seeps. Marine and Petroleum Geology. 2017. Vol. 88. No. P. 950–960.

7. Lu Y., Yang X., Lin Z., Sun X., Yang Y., Peckmann J. Reducing microenvironments promote incorporation of magnesium ions into authigenic carbonate forming at methane seeps: Constraints for dolomite formation. Sedimentology. 2021. Vol. 68. No. 7. P. 2945–2964.

8. Whiticar M.J. Carbon and hydrogen isotope systematics of bacterial formation and oxidation of methane. Chemical Geology. 1999. Vol. 161. No. 1–3. P. 291–314.

THE BLAGODATNOYE GOLD DEPOSIT (YENISEI RIDGE, RUSSIA): PTX PARAMETERS OF ORE-BEARING FLUIDS

Shaparenko E.O., Khomenko M.O.

Sobolev Institute of Geology and Mineralogy, Novosibirsk, Russia, shaparenkoe@gmail.com

Abstract. The Blagodatnoye deposit with 340 t reserves is one of the largest gold deposits in Russia. The aim of the study was to reveal temperature, pressure and composition of the fluids that formed quartz vein zones. Fluid inclusions in quartz arsenopyrite, pyrite, pyrrhotite and calcite were analyzed by microthermometry, Raman spectroscopy, gas chromatography-mass spectrometry. A comprehensive study revealed that the Blagodatnoye deposit was formed between 120 and 350 ºC and at 0.2–2.6 kbar, and from fluids with salinities ranging from 0.5 to 30 wt.% (NaCl–eq.). Volatiles in the fluid consist of H_2O, CO_2, N_2, and a wide range of hydrocarbons, N-, S- and halogenated compounds.

Key words: ore-bearing fluids; gold deposits; fluid inclusions; gas chromatography-mass spectrometry

The Krasnoyarsk Territory is the riches area with orogenic gold deposits in Russia. There are dozens of gold mines with variable reserves. The Blagodatnoye gold deposit is situated within the Yenashim ore field in the Severo–Yeniseisky district of the Yenisei Ridge. Gold reserves of the deposit are estimated at 340 tons averaging 1.3 g/t in ore, according to the data of "Polyus Gold" company [1]. Ore bodies comprise quartz veins with sulfides and native gold hosted by schists of Corda formation. The ore–bearing zones are divided into the Northern and Southern parts by submeridional upthrow. In the Northern part, ore body No.1 was identified, and in the Southern part, ore bodies No.2 and No.3, which merge with each other at a depth of 120 m. The central part of the ore bodies consists mainly quartz–vein formations of nodular and bead–like forms, which are outlined along the periphery by sulfidized sericite metasomatites with quartz–carbonate veinlets. The main ore minerals of the ore stage are arsenopyrite, pyrite and pyrrhotite, in intergrowth with which native gold occurs.

The aim of the study was to reveal temperature, pressure and composition of the fluids that formed quartz vein zones with varying gold content. Fluid inclusions in quartz were analyzed by microthermometry and Raman spectroscopy. Samples of quartz, arsenopyrite, pyrite, pyrrhotite and calcite were studied by gas chromatography-mass spectrometry (GC-MS) in order to find out bulk composition of volatiles in the ore-bearing fluid.

Individual fluid inclusions were studied in quartz and calcite [2]. Four types of fluid inclusions were found in quartz:

Type A — two-phase aqueous liquid-vapor (L_{H2O} + V).

Type B — two-phase to three phase aqueous–carbonic inclusions (L_{H2O} + $L_{CO2±CH4±N2}$, L_{H2O} + $V_{CO2±CH4±N2}$).

Type C — apparently single–phase liquid (or vapor) carbon dioxide–hydrocarbon ($L_{CO2±CH4±N2}$, $V_{CO2±CH4±N2}$, $L_{CH4±N2}$, $V_{CH4±N2±CO2}$).

Type D — three phase high-salinity inclusions (L_{H2O} + V + S).

According to microthermometric data, at the early barren stage, the temperature ranged between 180-300 °C, pressure was 0.2–1.6 kbar. The aqueous phase consists of a mixture of

chlorides Na and Mg with the salinity of 6–15 wt.%, NaCl eq. The prolific gold-rich stage has the following parameters: 220–350 ºC, 1.8–2.6 kbar and 8–16.5 wt. %, NaCl eq.

Raman spectroscopy showed that individual inclusions in quartz (two-phase vapor-liquid, single phase vapor or liquid) contain three major components: CO_2, CH_4 and N_2 (Figure 1a). According to GC-MS, apart from H_2O, CO_2 and N_2, there are oxygen-free aliphatic and cyclic hydrocarbons, oxygenated hydrocarbons, nitrogenated, sulfonated and halogenated compounds in mineral-forming fluids (Figure 1b,c) [2]. The data obtained proves that diverse organic compounds could take part in the processes of gold transport and precipitation [3].

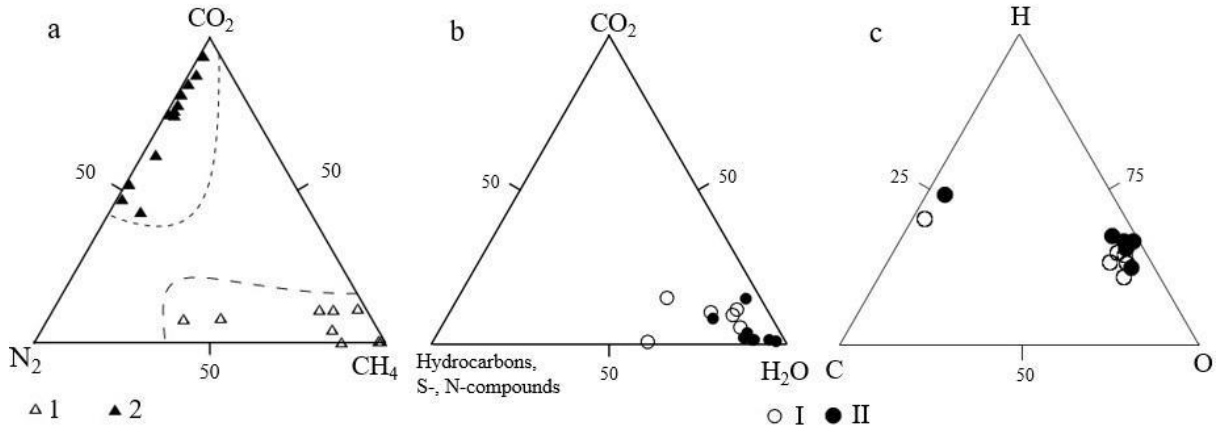

Figure 1. Composition of volatiles from fluid inclusions in minerals of Blagodatnoye gold deposit quartz veins: a – Raman spectroscopy data. Types of fluid inclusions in quartz: 1 – type B, $L_{H2O}+L(V)_{CO2±CH4±N2}$; 2 – type C , $L(V)_{CO2±CH4±N2}$. b, c – from gas chromatography-mass spectrometry data. Mineral associations: I – gold-bearing, II – barren.

To sum up, the Blagodatnoye gold deposit was formed by three types of fluid: water–carbon dioxide, carbon dioxide–hydrocarbon and high salinity fluids. The conditions of ore formation were: temperature – between 120 and 350 ºC, pressure 0.2–2.6 kbar, salinities range was from 0.5 to 30 wt.% (NaCl–eq.). The major components in volatiles were H_2O, CO_2, CH_4, N_2. A wide range of hydrocarbons, N-, S- and halogenated compounds also took part in the ore formation.

References:

1. Ore Reserve estimates as at 31 December 2020 https://polyus.com/en/operations/reserves_and_resources/?from=ru accessed on 11th of April.
2. Shaparenko E., Gibsher N., Tomilenko A., Sazonov A., Bul'bak T., Ryabukha M., Khomenko M., Silyanov S., Nekrasova N., Petrova M. Ore–Bearing Fluids of the Blagodatnoye Gold Deposit (Yenisei Ridge, Russia): Results of Fluid Inclusion and Isotopic Analyses. Minerals. 2021. Vol. 11. P. 1090.
3. Migdisov A.A., Guo X., Xu H., Williams-Jones A.E., Sun C.J., Vasyukova O., Sugiyama I., Fuchs S., Pearce K., Roback R. Hydrocarbons as ore fluids. Geochemical Perspectives Letters. 2017. Vol. 5. P. 47-52.

GEOLOGY, MINERALIZATION AND FLUID INCLUSION MICROTHERMOMETRY OF THE NAJNEH GOLD DEPOSIT, WEST OF SAQQEZ, NW IRAN

Ghasemi H., Simmonds V., Hosseinzadeh M.R.

Geosciences Department, University of Tabriz, Tabriz, Iran, simmonds_vartan@yahoo.co.uk

Abstract. The Najneh gold deposit in NW Iran is one of the orogenic gold deposits within the Sanandaj–Sirjan metamorphic belt, hosted by green-schist facies rocks of Precambrian age, occurring as gold-bearing quartz-sulfide veins. Microthermometry on 2-phase aqueous fluid inclusion reveals salinity range of 3–18 wt% $NaCl_{eq.}$ and T_H range of 120–340°C. Moreover, dilution and mixing by surface fluids and boiling is also conceivable from these data. The latter is also evident from coexistence of abundant vapor inclusions. Most of the analyzed fluid inclusions show metamorphic source, though some plot in the meteoric field, indicating the mixing of these two types of fluids.

Key words: Orogenic gold, Najneh, Sanandaj–Sirjan, Fluid inclusion.

The Najneh gold deposit is located 55 km west of the Saqqez town in northwest Iran. This area is situated on the northwestern margin of the Sanandaj–Sirjan metamorphic belt of Iran, which experienced various events of regional metamorphism, as well as opening and closure of Neo-Tethys Ocean during late Paleozoic to Paleogene. All these led to the formation of shear zones and regional uplift [1] and a favorable environment for occurrence of orogenic gold mineralization.

The area is mainly covered by metamorphic rocks attributed to Precambrian, chiefly including mica-schist, phyllite and slate illustrating green schist facies, along with lesser metarhyolite, metamorphosed acidic tuff and ignimbrite and gneiss. The green-schist facies covers the large part of the area, with a NW–SE trend parallel to the main thrust fault of the area. Magmatic activities evident in the area include several small granitic intrusive bodies, emplaced within the Precambrian metamorphic rocks, which are attributed to Jurassic period. Another small granitic–granodioritic intrusion has affected the Lower Cretaceous flysch-type rocks. However, the oldest intrusive body is the Doran granite of Infracambrian age, which intruded the Precambrian metamorphic units.

According to field investigations, the gold-bearing quartz–sulfide veins–veinlets are hosted by green-schist facies rocks, which is typical characteristic of orogenic gold deposits [2, 3]. Hydrothermal alteration is evident around the quartz veins, characterized by silicic, argillic, chloritic and carbonate alteration zones. Based on geochemical analysis results of 160 samples from these veins, the gold grade ranges from 30 to 200 ppb with a mean of 70 ppb.

In order to determine the physic–chemical characteristics and the evolutional trend of ore-bearing fluid, 4 doubly polished sections were prepared from gold-bearing quartz–sulfide veins and subjected to petrographic and microthermometric studies. Fluid inclusions within these quartz veins range in size from 2 to 20 μm and show various shapes, though the round, irregular, negative crystal and elongated shapes are more common, in order of abundance. Based on phase content at room temperatures, 3 types of fluid inclusions were recognized: liquid-rich 2-phase, vapor-rich 2-phase and monophase vapor. Microthermometry analysis was performed on large primary 2-phase fluid inclusions. During the freezing run, the last melting point for ice was

between –16 and 0°C and the calculated salinity ranges from 3 to 18 wt% NaCl eq., mainly clustering between 9 and 15 wt% $NaCl_{eq.}$. Meanwhile, the overall homogenization temperature (T_H) is about 120–340°C (Fig. 1).

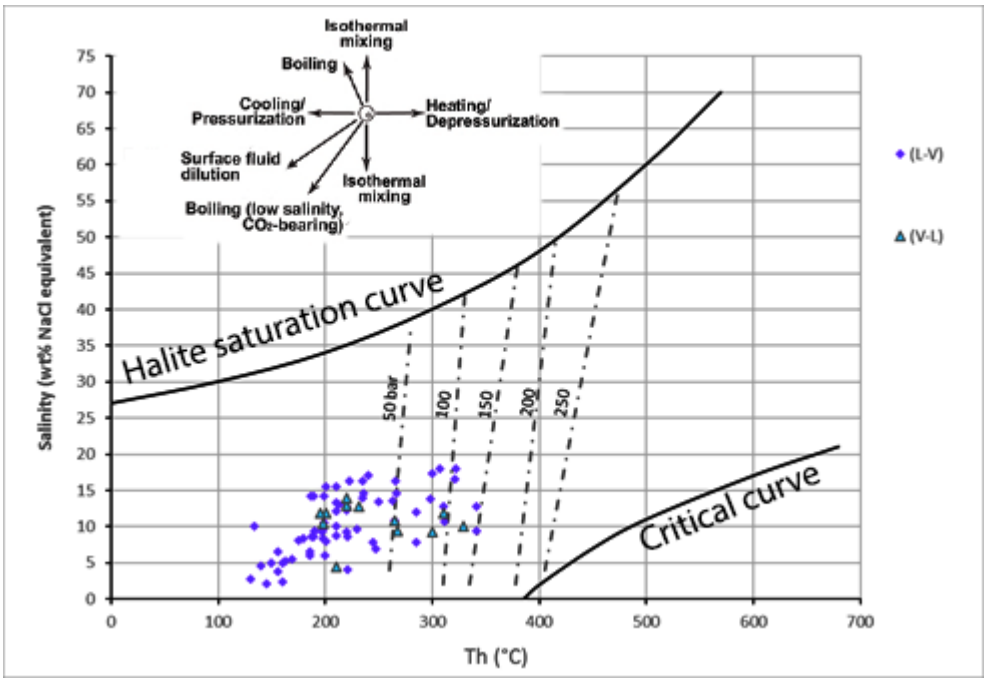

Figure 1– T_H vs. salinity diagram and the plotted data points of the Najneh gold-bearing quartz veins.

Based on T_H vs. salinity diagram, all the data points plot below the halite saturation curve, indicating entrapment from a NaCl-undersaturated fluid (Fig. 1). The minimum vapor pressure at the time of entrapment for most of the fluid inclusions is below 50 bars, though some others show values up to 150 bars. Data points trend indicates dilution and mixing with low-salinity and low-temperature surface fluids, and boiling of a low-salinity, CO_2-bearing fluid [4] (Fig.1). In this regard, most of the data points of fluid inclusions show metamorphic origin, though some plot in the meteoric field, confirming the mixing of these two types of fluids. Occurrence of boiling is also conceivable from coexistence of L-rich and V-rich 2-phase inclusions (with low to moderate salinities), which homogenize in similar range [4, 5], as well as the presence of abundant monophase vapor inclusions. Presence of cross-cutting veins and veinlets in the study area also confirms the occurrence of boiling.

Funding: this work is supported by the University of Tabriz.

References:

1. Mohajjel M., Fergusson C.L., Sahandi M.R. Cretaceous–Tertiary convergence and continental collision, Sanandaj-Sirjan zone, western Iran. Journal of Asian Earth Sciences. 2003. Vol. 21. P. 397–412.

2. Goldfarb R.J., Groves D.I., Gardoll S. Orogenic gold and geologic time: A global synthesis. Ore Geology Reviews. 2001. Vol. 18. P. 1–75.

3. Goldfarb RJ, Baker T, Dube B, Groves DI, Hart CJr, Gosselin P. Distribution, character and genesis of gold deposits in metamorphic terranes. Economic Geology. 2005. Vol. 100. P. 407–450.

4. Wilkinson JJ. Fluid inclusions in hydrothermal ore deposits. Lithos. 2001. Vol. 55. P. 229–272.

5. Van den Kerkhof A., Hein U. Fluid inclusion petrography. Lithos. 2001. Vol. 55. P. 27–47.

FLUID INCLUSION AND STABLE ISOTOPE CONSTRAINTS ON THE ORE FLUIDS IN THE BLACK-SHALE HOSTED MANGANESE DEPOSIT: ULUKENT-DENIZLI, SW TURKEY

Tenlik T.G., Bozkaya G., Bozkaya Ö.

Pamukkale University Department of Geological Engineering, Denizli, Turkiye,
tugcegogus@gmail.com

Abstract. First data on the microthermometric studies of the ore forming fluids of the Ulukent manganese deposit are presented. The Ulukent deposit is typical example of black shale – hosted manganese carbonate–silicate deposits on the Taurus belt in the southern Turkiye. The ore zone is generally in the form of carbonates (rhodochrosite) between the plated limestones forming the upper levels of the cherty limestones and the black clayey limestones. Carbonate ore and primary oxide ore were partially or completely oxidized by atmospheric effects and transformed into secondary oxide manganese minerals piroluzite and psilomelane at the surface and near the surface. Fluid inclusion and stable isotope data indicate that the manganese carbonates are formed at relatively low temperatures, probably during hydrogenetic and early diagenesis.

Key words: Fluid Inclusion, Manganese, Tavas-Denizli, Türkiye.

Manganese deposits in Turkey are generally divided into four main types; (1. Black shale – hosted deposits, 2. Radiolarian chert – hosted deposits, 3. Oligocene – hosted deposits, 4. Volcanic arc – hosted and/or vein -type deposits) according to host rocks, geological-tectonic settings and formation processes [1], [2]. Black shale-hosted Mn deposits are the most important in Turkey and Tavas-Ulukent manganese deposit, which has the biggest reserve (4.000.000 ton visible+probable, 55.000 ton possible reserve), is the typical example of the manganese carbonates occurs in SW Turkey [3]. The Ulukent deposit is located 2 km south of Ulukent town. This study deals with the geological-mineralogical composition and microthermometric characteristics of the fluid inclusions that occurred in the quartz and calcite crystals of manganese occurred within the area. Mineralizations in the study area are generally observed as carbonated minerals between the upper Liassic-Lower Cretaceous aged limestone and limestones rich in organic matter, pyrite-containing, foliated black colored clay carbonates. The ore zone is situated between two shale units in the thick bedded passive margin carbonates. Black bituminous shale at the base, includes coarse and cataclastic pyrites up to 15 mm in size. This black shale horizon also includes chalcedony – quartz veinlets. Gray colored shale does not include and large pyrites and silicification. The ore section begins with pisolitic – bauxitic low grade ore (detrital phase) at the bottom gradually passing to the carbonate – silicate ore and lastly oxidized ore. The brownish – pinkish bauxitic ore represents a sudden terrigenous input from the land into the sea associated with tectonic activity. [1]. Hausmannite, psilomelane, pyrolusite, braunite, and rhodochrosite can be seen as ore minerals, and calcite and quartz are gangue minerals.

Fluid inclusion studies were carried out on the polished thin sections prepared from the representative samples of ore veins. Calcite crystals contain a large number of fluid inclusions with various sizes, while quartz crystals are poor in fluid inclusions, and they are smaller in size. According to fluid inclusion studies, the ore-forming fluid contains NaCl, $CaCl_2$, and $MgCl_2$

types of salts, and homogenization temperatures were measured between 115-200º C. Last ice melting temperatures are determined between -1,6 and -14 ºC, and indicate the salinity (NaCl % equivalents) of the fluids change from 2,7 to 18 %.

Microthermometric data suggest that manganese mineralization from circulating meteoric waters, but combination of hot saline fluid with cool near-neutral fluids is possible. The carbon and oxygen isotopic compositions indicate that the carbon in the primary ore was derived from the bacterial decomposition of organic matter in the diagenetic zone is related to CO_2 and CO and the manganese carbonates are formed at relatively low temperatures, probably during hydrogenetic and early diagenesis.

Funding: This work is supported by the Pamukkale University Scientific and Research Center under grant 2020FEBE015.

References:

1. Öztürk H. Manganese mineralizations in Turkey: processes of formation and types. Geological Engineering. 1993. Vol. 43. P. 24–33.

2. Öztürk H., Hein J.R. Mineralogy and stable isotopes of black shale – hosted manganese ores, Southwestern Taurides. Economic Geology. 1997. Vol. 92. P. 733–744.

3. MTA. Türkiye manganez yatakları. Manganese ore deposits of Turkey. General Directorate of Mineral Research and Exploration. 1972. No. 120. 38 p. (In Turkish)

ISOTOPE-GEOCHEMICAL MODEL OF FORMATION OF THE NIKOLAIVSKOE Pb-Zn SKARN DEPOSIT (SIKHOTE-ALIN)

Tikhomirov D.V.

Far East Geological Institute, Vladivostok, Russia, tihomirov.dmitriy@bk.ru

Abstract. Pb-Zn metallogeny of the southern Sikhote-Alin is the result of Mz recycling of continental crust of the Sino-Korean Craton at East Asian margin during a change in geodynamic regime between the Eurasian and Pacific tectonic plates. Isotopic data have shown that mineralization is linked to volcanic structures of central type of the Dalnegorsk volcano-plutonic complex. The formation of metalliferous intrusions highly contaminated with the upper crust material occurred in conditions of active mantle-crust interaction. The process was realized in a narrow time interval of 60±2 million years in the Paleogene, when *transition* from *subduction*-related *regime to* a regime of transform continental margins was generated.

Key words: Pb-Zn skarns, Sm-Nd-Pb isotopy, U-Pb dating, Sikhote-Alin.

The aim of research was to create a prognostic model of formation of Pb-Zn skarn deposits of Dalnegorsk type.

For this purpose the generalization of knowledge on deposits of the southern Sikhote-Alin region was carried out and a standard deposit Nilolaevskoe was studied in detail by the up-to-date methods of isotope geochemistry.

Sn-Pb-Zn deposits in the southern Sikhote-Alin metallogenic province, including the Dalnegorsk skarns, have been studied for more than half a century. However, only a complex of the Sm-Nd-Pb and U-Pb isotopic data obtained helped to form the basis for creation of a regional model describing the stage-by-stage evolution of the territory with the final formation of the Pb-Zn skarn deposits of Dalnegorsk type.

The model is presented as a change of interrelated events ensuring accumulation and subsequent concentration of the ore substance. It involves three stages:

1. the formation of a regional geochemically specialized rock reservoir;
2. the fluid-magmatic processing of the geochemical reservoir: formation of magma reservoir and emergence of the ore-bearing magmatic associations;
3. the formation of local ore-magmatic systems with characteristic structural heterogeneities and geochemical barriers at which ore formation processes are implemented.

A regional Sn-Pb-Zn ore geochemical reservoir is represented as a segment of the newly formed Mesozoic continental crust of the Sikhote-Alin, which combined the Taukha terrane of the Early Cretaceous accretion prism and the Zhuravlevka terrane of the Early Cretaceous turbidite basin [1]. The terranes' lithology was dominated by arkosic rocks formed mainly of the material of the eroded granite-metamorphic complex of the Sino-Korean Early Proterozoic boron-polymetallic metallogenic province [2]. As a result, the terrigenous rocks are abnormally enriched, according to [3], in ore elements, including lead (31-158 ppm) and zinc (52-194 ppm).

The arkosic rocks inherit Sm-Nd and Pb isotopic characteristics of the Sino-Korean granite-metamorphic complexes, with the dominant εNd values about -15.0, and the lead isotope ratios varying in intervals of $^{206}Pb/^{204}Pb$ 18.2899 – 18.6803, $^{207}Pb/^{204}Pb$ 15.6219 - 15.6614, and $^{208}Pb/^{204}Pb$ 38.8126 - 39.1703 [1].

Fluid-magmatic processing *reworking* **of the geochemical reservoir** occurred in the Turonian-early Paleocene during subduction of PaleoPacific plate. In the middle Paleocene, prior to the Thanetian-early Eocene subalkaline volcanism under transform continental margins [4], there was a narrow interval of 60±2 million years in which centers of Dalnegorsk volcano-plutonic associations characterized by a contrast antidromic evolution of magmatism appeared locally. The U-Pb zircon dating of rocks of these centers evidences a coeval manifestation of basitic (quartz diorite - 59.5±1.1 Ma; andesibasalt - 62.0±1.9 Ma) and granitic (60.45±0.65 Ma) magmatism [5]. Based on the εNd values of the magmatites in the range of -2.9 to -6.7, the ratio of the upper crust and mantle component in the melt is estimated as 50:50. Lead isotope composition of feldspar from the intrusive bodies of the ore-bearing association ($^{206}Pb/^{204}Pb$ 18.3862 - 18.4891, $^{207}Pb/^{204}Pb$ 15.6151 - 15.6296, $^{208}Pb/^{204}Pb$ 38.6614 - 38.7378) is close to the isotopic characteristics of rocks of the upper crust geochemical reservoir, differing in less radiogeneity of lead, probably due to involvement of the mantle component. The same type of isotopic composition of lead in galena and lead in feldspar from the ore-bearing skarns and intrusive rocks of the Dalnegorsk complex shows a relationship between ore formation and diorite-granodiorite-granite intrusions.

The localization of Pb-Zn skarn deposits is correlated with the middle Paleocene volcanic edifices controlled by NE-trending strike-slip faults and feathering normal faults of near NS and NE orientation. The structure of the Nikolaevskoe deposit is determined by its confinement to the Nikolaevsky volcano-tectonic depression, where Turonian-Campanian volcanics contain the fragments of olistostromes of the Taukha accretionary prism presented as limestone blocks. Morphologically, the ore bodies are blanket-like zones of hedenbergite skarns with sulfides, formed at the contact of limestones and surrounding volcanics.

There are also submeridional vein-type bodies with hydrothermally altered intra-ore andesite-basaltic dykes. The U-Pb dating of zircons from the dykes yielded has determined the middle Paleocene age of the skarn (59.0±0.4 Ma). The isotopic composition of galena lead of the Nikolaevskoe deposit (at average values: $^{206}Pb/^{204}Pb$ 18.3700, $^{207}Pb/^{204}Pb$ 15.6220, $^{208}Pb/^{204}Pb$ 38.6613) corresponds to the composition of feldspar lead of vent quartz diorite of the same name ore-bearing volcanic-tectonic depression of Paleocene age.

References:

1. Chugaev A.V., Chernyshov I.V., Ratkin V.V., Gonevchuk V.G., Eliseeva O. A. Contribution of crustal and mantle sources to genesis of Sn, B and Pb-Zn deposits in South Sikhote-Aline subprovince (Russian Far East): Evidence from high-precision MC-ICP-MS lead isotope study. Ore Geology Reviews. 2020. Vol. 125. P. 1-16.

2. Ratkin V.V., Karas O.A., Golozubov V.V. The nature of the boron mineralization in the Taukha metallogenic zone of the Sikhote-Alin and the sources of boron in the formation of the Dalnegorsk deposit. Pacific Geology. 2016. Vol. 35. No. 5. P. 101-115.

3. State geological map of the Russian Federation. Scale 1: 200,000. Sheet L-53-XXXIV, XXXV. 2006.

4. Grebennikov, A.V., Khanchuk, A.I., Gonevchuk, V.G., Kovalenko, S.V. Cretaceous and Paleogene granitoid suites of the Sikhote-Alin area (Far East Russia): geochemistry and tectonic implications. Lithos. 2016. Vol. 261. P. 250–261.

5. VSEGEI Atlas of Geochronological Data. https://vsegei.ru/ru/info/geochron_atlas.

Section PETROLOGY

DECIPHERING THE MULTI-STAGE EVOLUTION OF MANTLE XENOLITHS FROM HEARD ISLAND, SOUTHERN INDIAN OCEAN

Abersteiner A.[1], Beier C.[1], Genske F.[2], Kamenetsky V.S.[3]

[1]Department of Geosciences and Geography, University of Helsinki, Helsinki, Finland, adam.abersteiner@helsinki.fi
[2]Institut für Mineralogie, Westfälische-Wilhelms-Universität Münster, Münster, Germany
[3]School of Natural Sciences, University of Tasmania, Hobart, Australia

Abstract. Heard Island is an intraplate volcanic island located within the submarine Kerguelen Plateau (southern Indian Ocean) that has been volcanically active since the Miocene through to present day. We present the first geochemical and radiogenic isotope characterisation of petrographically fresh spinel-bearing harzburgite xenoliths from Heard Island. This study explores the multistage evolution of xenoliths from Heard Island, ranging from their formation in the mantle through to their modification due to melt-rock interaction.

Key words: Heard Island, Kerguelen, Xenolith, OIB, Intraplate

The Kerguelen Plateau is one of the largest submarine large igneous provinces (LIP) on Earth and is located in the southern Indian Ocean [1]. The Kerguelen Islands represent the largest subaerial exposure of the Kerguelen LIP and is comprised largely of tholeiitic to alkaline basalts that host compositionally diverse mantle-derived xenoliths consisting of protogranular and pokilitic harzburgites, along with lherzolites, dunites and other rare types of ultramafic xenoliths [2, 3, 4]. Many of these xenoliths have been interpreted to preserve a record of extensive partial melting and metasomatism of the underlying mantle, likely in relation to the Kerguelen Plume. In contrast, there are no detailed studies of mantle-derived xenoliths from the Heard Island, which is situated approximately 500km to the southeast of the Kerguelen Islands. Heard Island is a large volcanic edifice that has been active throughout the Mesozoic through to present day [5], and therefore presents an opportunity to examine the composition, evolution and spatial variability of the mantle underlying the Kerguelen Plateau. This study presents the first petrographic, geochemical and radiogenic (i.e. Sr-Nd-Pb) isotopic study on fresh spinel-bearing harzburgite xenoliths and their host basalts from Heard Island.

The studied samples were derived from subaerial exposures of olivine- and clinopyroxene-phyric alkali (basanite) basalts from Heard Island. These rocks contain abundant (~30 – 40 vol.%) irregularly-shaped peridotite xenoliths that range in size from 1cm and up to 8cm in size. The xenoliths are well-preserved and exhibit protogranular textures and are comprised dominantly by coarse-grain (between 1 – 5mm in size) olivine (~60 – 85 vol.%) and orthopyroxene (~10 – 20 vol.%), along with subordinate clinopyroxene (~1 – 3 vol.%) and Cr-spinel (~1 vol.%), and are therefore classified as spinel-bearing harzburgite. The xenoliths are marked by different types of reaction zones, including: i) the partial-to-complete replacement of orthopyroxene by rims (or embayments) of fine-grained assemblages of clinopyroxene (Cpx-I)

and olivine (Ol-I; Fig. 1), which are compositionally distinct from the xenolith and host basalt groundmass. ii) Symplectite intergrowths between clinopyroxene and Cr-spinel (Fig. 1).

Preliminary whole-rock isotope data indicates the host basalts conforms to a relatively enriched EM-type source, whereas the xenoliths are more depleted, indicating a more depleted PREMA-type source.

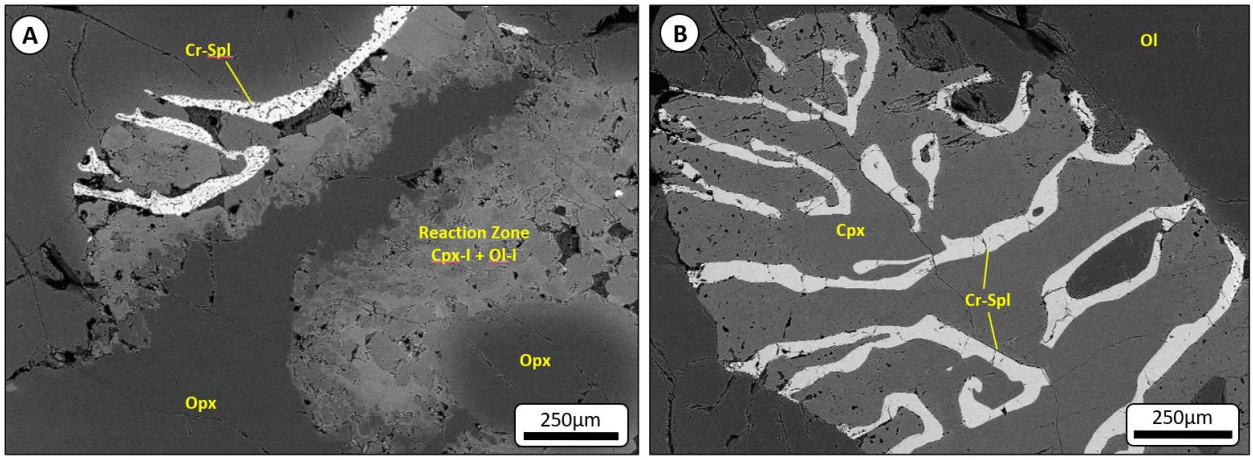

Figure 1 - Back-scattered electron images of (A) Transmitted light image of reaction zone around xenolith orthopyroxene, where it is replaced by olivine (Ol-I) and clinopyroxene (Cpx-I). (B) Back-scattered electron image of clinopyroxene and Cr-spinel (Cr-Spl) symplectites.

We present a preliminary model for the main stages of xenolith evolution: 1) partial melting of peridotitic mantle to form refractory harzburgites, likely within the garnet stability field as evident from II followed by upwelling to <80 km. 2) Breakdown of garnet to form clinopyroxene and Cr-spinel symplectites, possibly due to decompression or melt-rock interaction. 3) Melt-rock reactions involving the breakdown of orthopyroxene in xenoliths to form secondary assemblages of clinopyroxene (Cpx-I), olivine (Ol-I) and minor Cr-spinel (i.e. ‘wehrlitisation’ or refertilisation of refractory harzburgite xenoliths).

Funding: This study is supported by the University of Helsinki GeoHel and Hellabs.

References:

1. Charvis P., Operto S. Structure of the Cretaceous Kerguelen Volcanic Province (southern Indian Ocean) from wide-angle seismic data. Journal of Geodynamics. 1999. Vol. 28. P. 51–71.

2. Grégoire M., Lorand J-P., Cottin J-Y., Giret A., Mattielli N., Weis D. Xenoliths evidence for a refractory oceanic mantle percolated by basaltic melts beneath the Kerguelen archipelago. European Journal of Mineralogy 1997. Vol. 9. P. 1085–1100.

3. Moine B.N., Grégoire M., O'Reilly S.Y., Delpech G., Sheppard S.M.F., Lorand J.P., Renac C., Giret A., Cottin J.Y. Carbonatite melt in oceanic upper mantle beneath the Kerguelen Archipelago. Lithos. 2004. Vol. 75. P. 239–252.

4. Wasilewski B., Doucet L.S., Moine B., Beunon H., Delpech G., Mattielli N., Debaille V., Delacour A., Grégoire M., Guillaume D., Cottin J-Y. Ultra-refractory mantle within oceanic plateau: Petrology of the spinel harzburgites from Lac Michèle, Kerguelen Archipelago. Lithos. 2017. Vol. 272-273. P. 336-349.

5. Fox J.M., McPhie J., Carey R.J., Jourdan F., Miggins D.P. Construction of an intraplate island volcano: The volcanic history of Heard Island. Bulletin of Volcanology 2021. Vol. 83. No.5. P. 1 – 21.

PETROGRAPHIC FEATURES OF EARLY CRETACEOUS GRANITES OF THE GABASS RISE (SEA OF JAPAN)

Iakimov T.S.

V.I. Il'ichev Pacific Oceanological Institute Far Eastern Branch Russian Academy of Sciences, Vladivostok, Russia, yakimov-timur@mail.ru

Abstract. Petrographic research of granites of the Early Cretaceous complex of the Gabass Rise were carried out, mineralogical-structural and tectonic features were established. As a result of the analysis of the factual material, the morphological types of zircons have been determined, which help to investigate the staging of granitoid magmatism. Dislocation of the magmogenesis chamber of leucocratic granites is expressed by two facts: plastic deformation occurred at the stage of crystallization of plagioclases and the presence of isolated clusters of quartz with poikilitic feldspars.

Key words: Gabass Rise, petrography, granitoids, Sea of Japan.

From the 1970s to the 1980s, numerous dredging stations in the Sea of Japan sampled outcrops of rocks on the slopes of seamounts and rises, thanks to which a geological map of the sea of the same name was drawn [1]. The granitoids of the Gabas Rise are regarded as Early Cretaceous complex, 100 - 110 million years old [2].

Gabass Rise in the Central Deep-water Basin of the Sea of Japan was described during the 28th and 29th cruises of the "Pervenets" in 1977. The Gabass Rise is located in the south-western part of the basin on a block elevated by 500-600 m relative to the basement and is a volcanic ridge stretched sub-meridionally. Elevation is composed mainly of olivine-plagioclase, plagioclase basalts, ferrobasalts, trachyandesites and granitoids composing its basement [3].

Collection of samples of Gabass granitoids upland is represented by leucocratic granites.

Macroscopically leucocratic granites are light pink rocks with an irregularly grained texture. Under the microscope reveals allotriomorphic. porphyritic structure, parts of granulite (Fig. 1).

Composition: quartz, 40-45%; orthoclase, 25-30%; plagioclase, 15-20%; biotite, 2-3%.

Quartz is observed as clusters of rounded grains up to 8 mm in size, often with wavy extinction, forming a granulite structure in sections, which probably indicates outstripping crystallization of feldspars. This fact is confirmed by the presence of feldspar inclusions (Fig. 1). Secondary quartz (0.02-0.08 mm) with its characteristic zonal extinction is observed.

Orthoclase is found as isomorphic grains up to 10 mm in size, less frequently tabular grains up to 1 mm in size. Isomorphic orthoclase is pelitized with pertitic decay, tabular is unchanged. Some crystals have smooth transitions with albite, forming an isomorphic series.

Plagioclase № 5-15 forms twinned tabular grains up to 5 mm. More often weakly seritized, except for zonal crystals, where strong seritization results in small flakes of muscovite up to 0.2 mm in size. At the boundaries with orthoclase, myrmekite up to 0.6 mm in size is observed. Plagioclase is plastically deformed at the crystallization stage (Fig. 1).

Biotite is subordinate and has two morphotypes: flakes up to 2 mm as inclusions in plagioclase, in cracks (0.02 - 0.06 mm) more often between quartz grains, less often between plagioclase and quartz.

The accessory minerals are represented by zircon and apatite. Apatite is typical and is transparent elongated grains up to 0.1 mm. Zircon is in the form of idiomorphic grains (0.01-0.07 mm in size). Rarely, crystals of more or less isometric shape are found.

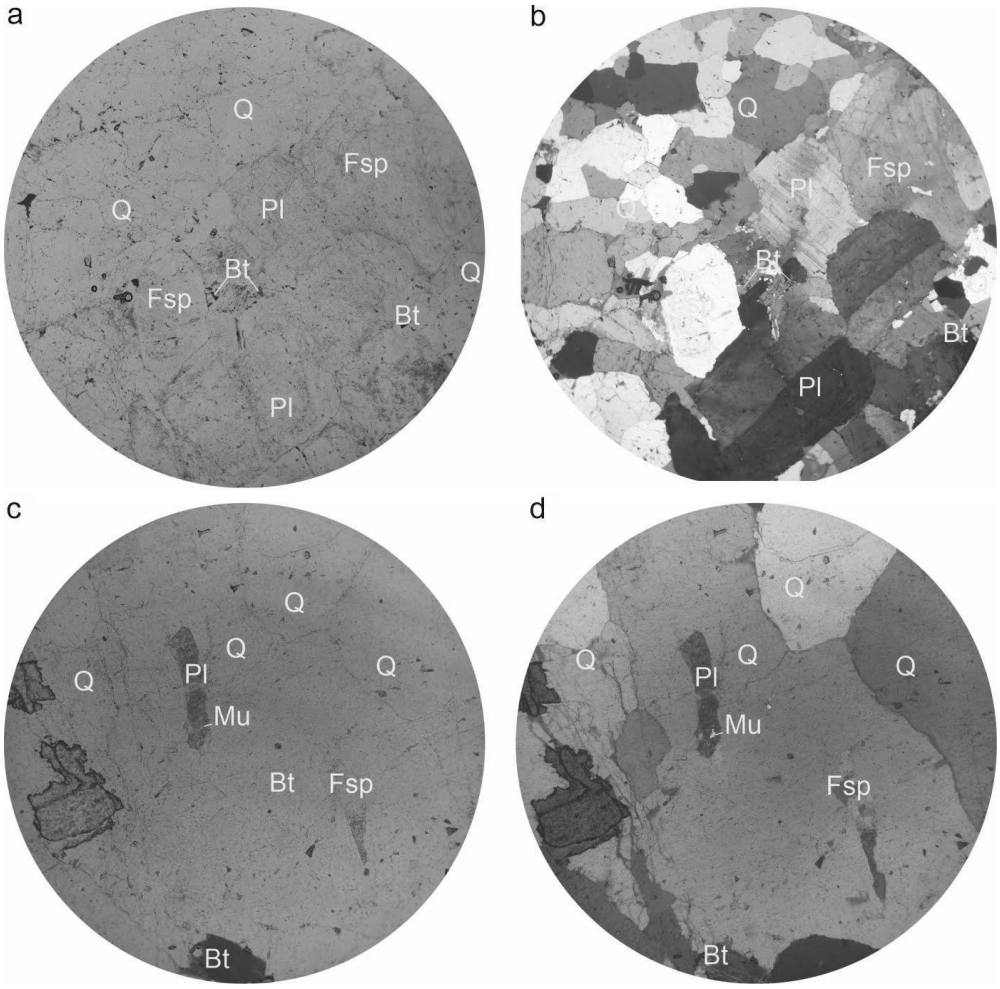

Figure 1 – A slit of the leucogranite in straight (a) and crossed (b) nicoles. Magnification 4-fold. Feldspar inclusions in quartz in straight (c) and crossed (d) nicoles. Magnification 10-fold. Q-quartz; Fsp-feldspar; Pl-plagioclase; Bt-biotite; Mu-muscovite.

Thus, because of the petrographic studies, the Gabass Rise is characterized as follows:

- plastic deformations of plagioclase at the crystallization stage;
- intense manifestation of sodium metasomatism (pertitization);
- absence of variability in structural-textural features;
- quartz crystallized earlier than feldspars.

It follows that the dislocation of the magmogenesis chamber of leucocratic granites is expressed by two facts: plastic deformation occurred at the stage of crystallization of plagioclase and the presence of isolated clusters of quartz with feldspar poikilitic.

References:

1. Geological Map of the Bottom of the Sea of Japan, Ed. By I. I. Bersenev and L. I. Krasnyi. Ministr. Geol. SSSR, Leningrad. 1988.
2. Lelikov E.P., Malyarenko A.N. Granitoid Magmatism of the Pacific Marginal Seas. Vladivostok. Dal'nauka. 1994. 265 p. (In Russian)
3. Lelikov E.P., Emelyanova T.A., Pugachev A.A. Volcanism and Tectonics of the Central Deep Basin, Sea of Japan. Oceanology. 2018. Vol. 58. No. 1. P. 116-132.

MAFIC MINERALS OF THE MEDVEDEV MASSIF (SOUTH YAKUTIA)

Ivanov M.S., Ivanov A.I., Loskutov E.E., Zhuravlev A.I.

Diamond and Precious Metal Geology Institute, Yakutsk, Russia, ivanov.michil@bk.ru

Abstract. Mafic rock-forming minerals (pyroxenes and amphiboles) of the three-phase Medvedev massif (porphyry syenite, pyroxene-amphibole syenites, monzonites) were studied by X-ray spectral analysis. Pyroxenes are represented by diopside and augite, which were formed in a wide range of pressures and temperatures. Amphiboles of the massif are represented by hastingsite in syenite porphyries, magnesiohastingsite and ferropargasite in pyroxene-amphibole syenites and monzonites of the massif. Differences in compositions and almost identical indicators of temperatures and pressures reflect a change in the conditions of their crystallization.

Key words: mafic minerals, pyroxene, amphibole, X-ray spectral analysis

The Medvedev massif is located in the Nimnyr terrane in the central part of the Aldan Shield and cuts through Precambrian schists and granites [1]. In the process of field and petrographic studies, we found that the massif is composed of rocks of three phases with clear contacts between them: phase 1 - porphyry syenite; 2nd phase – pyroxene-amphibole syenites; 3 phase - monzonites [2]. To establish the conditions for the crystallization of igneous rocks, data on the chemical composition of rock-forming minerals are widely used [3, 4, 5]. For the studied massif, pyroxenes and amphiboles are the most informative in this respect.

By chemical composition, the pyroxenes of all considered rocks belong to the Ca-Mg-Fe group of monoclinic pyroxenes and are represented by two mineral species: the predominant diopside and the less common augite [6]. Based on the geobarometer [7] and geothermometer [8], the P–T conditions for their crystallization were determined. For pyroxenes of the rocks of the first phase, they were 0.63–0.98 GPa and 828–1079°C; for the second, 0.36–0.83 GPa and 847–937°C; 814–928°C.

In X-ray spectral analysis of amphiboles, the contents of H2O and halogens were not determined. Based on the recommendations of [9], the recalculation of chemical analyzes for the standard formula of amphiboles was carried out on 23 (O) with the expected 2 (OH, F, Cl). According to calculations [9, 10], the amphiboles of the massif under consideration belong to the Ca-group, which is characterized by the following parameters: $(Ca+Na)_B>1.50$, $Na_B<0.50$ and $Ca_B\geq1.50$. According to the content of alkalis [9], to a greater extent, they belong to subalkaline varieties ($(Na + K)_A \geq 0.5$) and are represented by hastingsite in the rocks of the first phase, mainly magnesiohastingsite in the rocks of the second, and ferropargasite in the third. Amphiboles of syenite porphyries crystallized in a highly oxidized medium at high oxygen fugacity (log fO_2 from -6.36 to -10.95), amphiboles of pyroxene-amphibole syenites and monzonites crystallized in a less oxidized medium at lower oxygen fugacity (log fO_2 from -8 .36 to -12.71). According to calculations based on the geobarometer [11] and geothermometer [12], the crystallization of amphiboles took place in a wide P–T range, close for all rocks: P = 0.52–1.08 GPa, T = 915–1027°C.

Conclusions. The pyroxenes of the rocks of the Medvedev massif are represented by two mineral species: the predominant diopside and the less common augite. Based on the results of determining the physicochemical conditions that existed at the time of pyroxene crystallization,

we can conclude that it took place at various depth levels at temperatures of 828–1079 ° C and pressures up to 0.98 GPa for rocks of the first phase, and at temperatures of 814– 928°C, pressures 0.18–0.36 GPa for rocks of the late, third phase.

Amphiboles belong to calcium varieties and are represented by hastingsite in the rocks of the first phase, magnesiohastingsite and ferropargasite in the rocks of the second and third phases. The conditions of crystallization for amphiboles from rocks of the massif were determined: 915–1027°C 0.52–1.08 GPa. The temperatures of crystallization of amphiboles for all rocks with a significant variation in pressures remain close, which most likely indicates their restite genesis.

Acknowledgements: Work is done on state assignment of DPMGI SB RAS, as well as within the framework of the work under the contract with JSC "Gold of Seligdar".

References:

1. Parfenov L.M. et al. Tectonics, geodynamics and metallogeny of the territory of the Republic of Sakha (Yakutia). Moscow. Nauka/Interperiodica. 2001. 571 p.

2. Ivanov A., Ivanov M., Zhuravlev A. Chemical Composition of the Mesozoic Alkaline Rocks of the Medvedev Massif (South Yakutia, Aldan-Stanovoy Shield, Leglier Ore Cluster), in IOP Conf. Ser.: Earth Environ. Sci. 2020.

3. Wones D.R., Eugster H.P. Stability of biotite: experiment, theory and application. American Mineralogy. 1985. No. 9. P. 1228–1272.

4. Marakushev A.A., Tatarin I.A. On the mineralogical criteria for the alkalinity of granitoids. Proceedings of the Academy of Sciences of the USSR. Geologic series. 1965. No. 3. P. 20–37.

5. Korenbaum S.A. Typomorphism of micas of igneous rocks. Moscow. Nauka. 1987. 144 p.

6. Yavuz F. PYROX: A computer program for the IMA pyroxene classification and calculation scheme. Computers & Geosciences. 2001. No. 27. P. 97–107.

7. Nimis P. Clinopyroxene geobarometry of magmatic rocks. Part 2. Structural geobarometers for basic to acid, tholeiitic and mildly alkaline magmatic systems. Contributions to Mineralogy and Petrolgy. 1999. Vol. 135. P. 62–74.

8. Putirka K.D. Thermometers and Barometers for volcanic systems. Reviews in Mineralogy and Petrology. 2008. No. 69. P. 61–142.

9. Leake B.E. Nomenclature of amphiboles: report of the subcommittee on amphiboles of the international mineralogical association, commissionon new minerals and mineral names. The Canadian Mineralogist. 1997. P. 219–246.

10. Yavuz F. A program to classify microprobe and wet chemical amphibole analyses according to the IMA (1997) nomenclature scheme. Istambul, 1990.

11. Hollister L.S., Grissom G.C., Peters E.K., Stowell H.H., Sisson V.B. Confirmation of the empirical correlation of Al in hornblende with pressure of solidification of calc-alkaline plutons. American Mineralogy. 1987. Vol. 72. P. 231–239.

12. Otten M.T. The origin of brown hornblende in the Artfjallet gabbro and dolerites. Contribution to Mineralogy and Petrology. 1984. Vol. 86. P. 189–199.

GRANITIC MAGMATISM IN EASTERN KAZAKHSTAN: STAGES, SCALE, SOURCES

Kotler P.D.[1,2,3], Khromykh S.V.[1,2], Semenova D.V.[1,3], Kulikova A.V.[1,3], Saetgaleeva Ya.Ya.[3]

[1]V.S. Sobolev Institute of Geology and Mineralogy, Novosibirsk, Russia, pkotler@yandex.ru
[2]Novosibirsk State University, Novosibirsk, Russia
[3]Kazan Federal University, Kazan, Russia

Abstract. This paper presents the results of long-term studies of granitoid magmatism of the Ob-Zaisan folded system. Five stages of granite formation have been identified: Devonian, Early Carboniferous, Late Carboniferous, Early Permian, Triassic. Obtained data indicate that within the considered tectonic zones, a multi-stage remelting of various protoliths took place, which could lead to the formation of both granitoids of different ages of similar composition, and subsynchronous granitoids that differ significantly in composition.

Key words: granites, CAOB, petrogenesis, granite sources

The polygon of the conducted research is a part of the Ob-Zaisan folded system, which in recent years has been designated as the Altai accretion-collision system of Hercynides. It was formed in the Late Paleozoic (Carboniferous – Permian) during the collision of the Siberian and Kazakh paleocontinents and the closure of the Ob-Zaisan Paleoceanic basin [1, 2]. As a result of accretion-collision processes, several different types of terranes (structural-formation zones) of different geodynamic nature were combined in a relatively small area (from east to west): 1) The Kalba-Narym zone, which was formed in the Devonian as a sedimentary basin in the passive margin regime, after the ending of subduction under the margin of the Siberian continent (Rudny Altai) and is filled with thick strata of terrigenous sediments. 2) the Char zone, which is a relic of the Ob-Zaisan ocean basin with juvenile crust overlain by thin sedimentary strata; The text of the conference paper should be in English. 3) The Zharma-Saur zone, composed of Middle and Late Paleozoic volcanogenic-sedimentary complexes formed on the Kazakhstan active margin during subduction of the oceanic lithosphere of the Ob-Zaisan Ocean.

At the moment, the following stages of endogenous activity are distinguished within the studied territory [3]: 1) Devonian, associated with the subduction of the oceanic crust under the Caledonian Chingiz-Tarbagatai complexes; this stage includes felsic volcanic rocks of the Mashanskaya Formation and granitoids of the Aldzhan Complex localized in the western part of the Zharma-Saur zone. 2) Early Carboniferous, associated with the slab break-off under the the Kazakh continental margin, as a result of which gabbro-granite massifs of the Saur series were formed, plagiogranitoids of the Bugaz complex in the southern part of the Zharma-Saur zone, as well as a number of small plagiogranite massifs in the Char zone. 3) Middle-Late Carboniferous reflecting collapse of an orogenic structure, on which a number of volcanoplutonic structures were formed throughout the region and several relatively small arrays of M- and I-type granitoids in the Kalba-Narym zone. 4) Early Permian, the most large-scale stage, associated with the activity of the Tarim plume, at the beginning of this stage, the formation of the main volumes of Kalba and Zharma batholiths composed of granitoids of I- and S-types took place, and at the end of the stage, the formation of large intrusives of A1- and A2-types took place. 5) Early Triassic, associated with the activity of the Siberian plume; atThe text should be typed in

normal direct font and justified. At the moment, it is known that A-type granitoids of the Delbegetei massif and rocks of the Semeytau volcano-plutonic structure belong to this stage.

Conducted studies have shown that granitoids of all geochemical types are common in the investigated area - M-type plagiogranites, large S-I-type batholith intrusions, A2-type monzonite-syenite-leucogranite intrusions, and small massifs of A1-type leucogranites. In this case, often only rare-element and isotope-geochemical compositions allow us to reliably separate granites into complexes and phases.

Thus, obtained data indicate that within the considered tectonic zones, a multi-stage remelting of various protoliths took place, which could lead to the formation of both granitoids of different ages of similar composition, and subsynchronous granitoids that differ significantly in composition. A comparison of magmatism, which is currently interpreted as the result of the influence of two different plumes (the Tarim plume in the Early Permian and the Siberian plume in the Early Triassic), should be considered as a separate actual task for the future research. To clarify the scale and duration of various stages of endogenous activity, it is necessary to carry out large-scale U-Pb isotope dating of intrusive massifs and volcanic structures, in combination with isotope-geochemical studies.

Funding: The work was carried out on a government assignment to the V.S. Sobolev Institute of Geology and Mineralogy SB RAS (Novosibirsk) and was financially supported by Grant of the President of the Russian Federation MK-1870.2022.1.5, Russian Science Foundation, Project 21–17-00175; Ministry of Science and High Education of the Russian Federation, Contract No. 14.Y26.31.0029, Resolution No.220 of the Government of the Russian Federation.

References:

1. Vladimirov A.G., Kruk N.N., Rudnev S.N., Khromyk S.V. Geodynamics and granitoid magmatism of collision orogens. Russian Geology and Geophysics. 2003. Vol. 4. No. 12. P. 1321–1338.

2. Khromykh S.V. Basic and Associated Granitoid Magmatism and Geodynamic Evolution of the Altai Accretion–Collision System (Eastern Kazakhstan). Russian Geology and Geophysics. 2022. Vol. 63. No. 3. P. 279–299.

3. Kotler P.D., Khromykh S.V., Kruk N.N., Sun M., Li P., Khubanov V.B., Semenova D.V., Vladimirov A.G. Granitoids of the Kalba batholith, Eastern Kazakhstan: U–Pb zircon age, petrogenesis and tectonic implications. Lithos. 2021. Vol. 388–389. Art. 106056.

METAMORPHIC EVOLUTION OF THE ARCHEAN TOKMOVO MEGABLOCK AND OF SURROUNDING PALEOPROTEROZOIC OROGENIC BELTS (VOLGO-URALIA SEGMENT, EAST EUROPEAN CRATON)

Pilitsyna T.A.[1,2], Samsonov A.V.[2] , Erofeeva K.G.[2]

[1]FSBI "Institute of Mineralogy, Geochemistry and Crystal Chemistry of Rare Elements (IMGRE)", Moscow, allafia@yandex.ru
[2]Institute of Geology of Ore Deposits, Petrography, Mineralogy and Geochemistry, Russian Academy of Sciences (IGEM RAS), Moscow

Abstract. The plagiogneisses of the Tokmovo block, predominant in volume, were formed after tonalite–trondhjemite–granodiorite (TTG) intrusions with an age of 2.72–2.86 Ga. The metamorphism of the block is estimated in the interval from 2.7 to 2.6 Ga, culminating when a new portion of granitoids intruded 2.62 Ga ago. Microstructural analysis, PT parameters, as well as geochemical features of zircon indicate one-stage and duration of metamorphism of rocks of the Tokmovo block due to granulite and amphibolite facies. In the rocks framing the block a shorter HT/LP-type metamorphism, typical of collisional orogens, has been established.

Key words: metamorphic evolution, Early Precambrian, Volga-Uralia, granulite facies, TTG-gneisses.

The Early Precambrian Volga-Uralia crustal segment represents the eastern part of the East European Craton. It is completely buried beneath a thick sedimentary cover and data on its structure and composition are based on geophysics and deep wells core research [1]. GGT nature of Tokmovo block is supported by study of the core samples, which comprise three main types of rocks: predominated Bt-Opx plagiogneisses (formed 2.72-2.86 Ga – U-Pb zircone dating), tonalites with zicones depleted in heavy REE (2.62 Ga) and metabasites, which metamorphic event (due to zircons' rims) in the range age from 2.72 to 2.63 Ga is an object of this research.

A one stage metamorphic evolution has been recorded in these rocks. Maximum values of the metamorphic thermodynamic parameters were identified in the Grt-Opx-Cpx-Hbl granofels within the cores of garnets and orthopyroxenes and correspond to middle-pressure granulite facies metamorphism (9-11 kb, 720-810 ^{o}C). Lowest values correspond to the amphibolite facies (5-7 kb, 680 ^{o}C). The uniformity of garnets, absence of inclusions and oscillatory zoning, a strong decrease in pressure against gradual decrease in temperature indicate one-stage metamorphism and that it was carried out according to the "Aldan" type – an uplift with cooling along the steep Archean geotherm.

The Osnitsk-Mikashevichi Moscow orogenic belt (OMMB) rocks (TTG-gneisses, metarhyolites and metagabbronorites), framing the Tokmovo block from the north, have U-Pb age of 1.97–2.02 Ga [2], and P-T grades of metamorphism of Px-Hbl-schist and fine-medium-grained Cpx-Hbl-plagiogneiss correspond to the amphibolite facies (5-7 kb, 750-770^{o}C,). In the outline part of the Vyatka belt, framing the block from the east, supracrustal rocks (2.08–2.10 Ga) are developed, for them metamorphism corresponds to the amphibolite facies (6.3–8.3 kb, 600–700°C for peak, 4.8-5.5 kb, 590 -640°C for regressive stages). Within the Volga-Don orogenic belt from the south of the block, metasedimentary rocks metamorphism conditions correspond to a high-temperature amphibolite facies with parameters 7–8 kb, 740–750 °C.

The Tokmovo megablock represents a fragment of the Archean crust, which has preserved the Archean metamorphic history, whereas the Paleoproterozoic belts framing it experienced HT/LP-type metamorphism, which is typical of collisional orogens [3].

*PT counted by Perple_X 6.8.8, classical tools, Ti-in-Zircone thermometry.

References:

1. Bogdanova S.V., Gorbatschev R., Garetsky R.G. EUROPE. East European Craton. Reference Module in Earth Systems and Environmental Sciences. 2016. P. 1–18.

2. Samsonov A.V., Bogdanova S.V., Postnikov A.V., et al. (2018): Paleoproterozoic OMMB: new geochronology and petrology data for the Russian segment and tectonic implication. in the 33nd NGWM, Denmark.

3. Millonig L., Zeh A., Gerdes A., Klemd R., Barton J.M. Decompressional Heating of the Mahalapye Complex (Limpopo Belt, Botswana): a Response to Palaeoproterozoic Magmatic Underplating. Journal of Petrology. 2010. Vol. 51. No. 3. P. 703–729.

Section GEOCHEMISTRY AND GEOCHRONOLOGY

THERMAL EVOLUTION OF THE SIBERIAN TRAPS LARGE IGNEOUS PROVINCE BASED ON RESULTS OF APATITE FISSION-TRACK ANALYSIS AND OTHER GEOCHRONOLOGICAL DATA FROM INTRUSIVE COMPLEXES

Bagdasaryan T.E.[1,2], Veselovskiy R.V. [1,2], Latyshev A.V. [1,2], Thomson S.N.[3], Zaitsev V.A.[4], Marfin A.E.[5]

[1] Lomonosov Moscow State University, Moscow, Russia, tanya.bagdasaryan@yandex.ru
[2] Schmidt Institute of Physics of the Earth, Moscow, Russia
[3] University of Arizona, Tucson, USA
[4] Vernadsky Institute of Geochemistry and Analytical Chemistry of RAS, Moscow, Russia
[5] Institute of Earth's Crust SB RAS, Irkutsk, Russia

Abstract. We present results of apatite fission-track (AFT) and other geochronological data (apatite U-Pb (LA-MC-ICPMS) and Rb-Sr dating) from several intrusions located within the Siberian Traps Large Igneous Province. The obtained AFT ages are distributed between ca. 207 and ca. 173 Ma. We interpret the AFT ages as a consequence of sedimentary burial of the studied magmatic complexes to below the closure temperature of the AFT system, which took place after the formation of intrusions ca. 252-250 Ma. Later cooling as a result of exhumation of the studied rocks to near surface temperatures and decreasing of thermal flow then took place in the Late Triassic-Early Jurassic.

Key words: thermochronology; apatite fission-track analysis; Siberian Traps Large Igneous Province; tectonic-thermal evolution

A large-scale magmatic event occurred within the Siberian platform at the Paleozoic-Mesozoic boundary, resulting the formation of the Permo-Triassic Siberian Traps Large Igneous Province (LIP). According to U-Pb zircon dating results, the main phase of intrusive magmatism occurred in the time interval of 252-250 Ma [1, 2, 3]. However, a significant number of Ar/Ar plagioclase, phlogopite, biotite, amphibole ages [4] and few U-Pb zircon ages [3, 5, 6] fall in the interval of ~240-230 Ma. This is related to the post-Paleozoic thermal evolution of the Siberian platform and the Siberian Traps intrusions in particular and may indicate the existence of younger magmatic events within the Siberian Traps LIP or a long cooling of rocks lasted for 10 Myr, taking into account the different closing temperatures of the isotope systems.

To reveal the post-magmatic cooling history of the Siberian Traps LIP we use low-temperature thermochronology, such as apatite fission-track (AFT) analysis, which allows estimation of the time elapsed since the last cooling of rocks below 110°C (the temperature of full annealing of fission tracks in apatite) and also to trace thermal history in the range of 110-60°C (the partial annealing zone of tracks in apatite).

Apatite fission-track analysis was performed on rocks from intrusions of the Permo-Triassic Siberian Traps located in different regions of the Siberian platform: (1) alkaline-ultramafic ring plutons of Odikhincha, Yessey and Magan, (2) intrusions of Norilsk-1 and Kontay, (3) Padunsky sill and (4) Kotuy dike. The studied intrusions were emplaced close to the

age of the voluminous phase of the Siberian Traps LIP based on the new apatite U-Pb and Rb-Sr ages, as well as ages as thermochronometer data, using the following isotope system closing temperatures.

The most likely tectonic-thermal scenario to explain the younger AFT ages, is that after the emplacement at the near-surface depths at about 250 Ma, the considered intrusive bodies were then buried below the 110°C isotherm due to significant volcano-sedimentary cover accumulation. This process could occur simultaneously with the increased heat flow at the Triassic-Jurassic boundary relative to the present-day, which was noted in [7]. As a result, the rocks were heated above the temperature of full annealing of fission tracks in apatite.

Funding: The research was carried out with the support of the Russian government (assignment to the Vernadsky Institute of Geochemistry and Analytical chemistry RAS 0137-2019-0014), RFBR (grants 20-35-90066, 18-35-20058, 18-05-00590 and 18-05-70094), Research Equipment Sharing Center of IPE RAS "Petrophysics, geomechanics and paleomagnetism", and the Program of development of Lomonosov Moscow State University.

References:

1. Paderin, P.G., Demenuk, A.F., Nazarov, D.V., Chekanov, V.I., et al., 2016. Explanatory Note of State Geological Map of the Russian Federation. (Third Generation). Scale 1:1,000,000 Norilskaya Series. Sheet R-45. St. Petersburg: VSEGEI. 2016. 320 p.

2. Burgess S.D., Bowring S.A. High-precision geochronology confirms voluminous magmatism before, during, and after Earth's most severe extinction. Science Advances. 2015. Vol. 1. No. 7. P. 1-14.

3. Kamo S.L., Czamanske G.K., Amelin Yu., Fedorenko V.A., Davis D.W., Trofimov V.R. Rapid eruption of Siberian flood volcanic rocks and evidence for coincidence with the Permian-Triassic boundary and mass extinction at 251 Ma. Earth and Planetary Science Letters. 2003. Vol. 214. P. 75-92.

4. Ivanov A.V., He H., Yan L., Ryabov V.V., Shevko A.Y., Palesskii S.V., Nikolaeva I.V. Siberian Traps large igneous province: evidence for two flood basalt pulses around the Permo-Triassic boundary and in the Middle Triassic, and contemporaneous granitic magmatism. Earth-Science Reviews. 2013. Vol. 122. P. 58–76.

5. Gusev N.I., Sergeeva L.Y., Stroev T.S., Savelyev S.O., Sharipov A.G., Larionov A.N., Skublov S.G. U-Pb age, geochemistry and Lu-Hf systematics of zircon from intrusive traps of the western part of the Tunguska syneclise of the Siberian platform. Regional geology and metallogeny. 2019. Vol. 79. P. 49-67.

6. Sereda E., Belyatsky B., Krivolutskaya, N. Geochemistry and Geochronology of Southern Norilsk Intrusions, SW Siberian Traps. Minerals. 2020. Vol. 10. No. 2. Art. 165.

7. Rosen O.M., Soloviev A.V., Zhuravlev D.Z. Thermal evolution of the northeastern Siberian platform in the light of apatite fission-track dating of the deep drill core. Izv. Phys. Solid Earth. 2009. Vol. 45. P. 914–931.

IGNEOUS ROCKS OF THE TEKTURMAS ACCRETIONARY COMPLEX, CENTRAL KAZAKHSTAN: GEOLOGICAL POSITION, GEOCHEMICAL CHARACTERISTICS, AND GEODYNAMIC SETTINGS OF FORMATION

Gurova A. V.[1,2], Safonova I. Y.[1,2], Perfilova A. A.[1,2], Savinsky I. A.[1], Kotler P. D.[1,2]

[1] Novosibirsk State University, Novosibirsk, Russia, sushka386@gmail.com
[2] Sobolev Institute of Geology and Mineralogy SB RAS, Novosibirsk, Russia

Abstract. This paper presents results of the study of igneous rocks of the Tekturmas accretionary complex of Central Kazakhstan. We discuss the geological position, the petrographic and chemical composition of the rocks, and the geodynamic settings of their formation.

Key words: Central Asian Orogenic Belt, basalts, geochemistry, Paleoasian Ocean, Late Cambrian-Ordovician.

The Tekturmas zone of central Kazakhstan, which includes the Tekturmas accretionary complex (TAC) and the adjacent ophiolite belt, is located in the western Central Asian Orogenic Belt. It consists of three structural-formational segments: Tekturmas, Bazarbai, and Nura. The Tekturmas segment consists of serpentinite melange at the base and deposits of the Karamurun, Tekturmas, and Sarytau formations. The *Karamurun Fm.* ($Є_1$-O_2kr) is a mélange consisting of mafic rocks represented by deformed pillow lavas, basaltic lava breccias containing chert and chert shale olistoliths. The middle Ordovician age of the Karamurun Fm. was constrained by conodonts. Middle Darriwilian conodonts were found in chert interbeds in basalt [6]. The *Tekturmas Fm.* (O_{2-3}tk) includes predominantly red and chocolate ribbon cherts with thin layers of gray siliceous siltstones, siliceous mudstones, and shales. The age of the Tekturmas Fm. was constrained by conodonts of three complexes: middle Darriwilian (middle Ordovician), late Darriwilian (middle Ordovician), and early Sandbian (upper Ordovician) [5]. To the north of the Tekturmas segment is the Bazarbai segment, which includes rocks of the Kuzek and Bazarbai formations. The *Kuzek Fm.* (O_2kz) is composed of massive and amygdaloidal pillowed basalts with interbeds of siliceous siltstones and lenses of lava breccias and mafic tuffs. The *Bazarbai Fm.* (O_3bz) consists of ribbon chert interbedded with tuffs, siliceous mudstones, ash-dominated siliceous tuffs, basaltic and andesitic tuffs, polymictic and volcanomictic sandstones (graywacke) [2]. The Bazarbai segment consists of igneous rocks of ophiolite association: layered gabbro, sheeted dike complex, pillow-basalt, and granitoids. The pillow lavas associated with siliceous siltstones belong to the *Kuzek Fm.* Siliceous siltstones contain Upper Darriville (Middle Ordovician) and Lower Sandbian (Upper Ordovician) conodonts, and the U-Pb zircon age of a plagiogranite from serpentinite mélange is 489 ± 8 Ma [3].

The volcanic and subvolcanic rocks of the Karamurun and Kuzek formations are represented by basalts and basaltic andesites. The samples plot in the fields of basalt, trachybasalt, basaltic trachyandesite, and basaltic andesite in TAS classification diagram. Several points plot in the basanite, phonotephrite, trachyandesite, and andesite fields. In the SiO_2 - Nb/Y classification diagram, most of the samples are subalkaline basalts. In the SiO_2 - FeO*/MgO diagram, the samples belong to the tholeiite and calc-alkaline series. According to the classification of [4], most of the samples plot are high-Fe tholeiites, tholeiite basalts, and

tholeiite andesites. There are three groups of volcanic rocks: high-Ti (TiO_2 > 1.9 wt %), medium-Ti (TiO_2 = 0.9–1.8 wt %), and low-Ti (TiO_2 <0.9 wt %).

The chondrite-normalized rare-earth element (REE) patterns of the low-Ti samples are typically light REE (LREE)-enriched (La/Yb_N = 1.7-2.2), and are characterized by moderately differentiated heavy REE (HREE; (Gd/Yb_N = 1.2-1.3) and high Zr/Nb ratios (20-36). Their primitive mantle-normalized multi-component spectra show negative Nb anomalies (Nb/Th_N = 0.2-0.4, Nb/La_N = 0.2-0.4), which are typical of suprasubduction igneous rocks [7,8]. The REE patterns of medium-Ti samples are nearly flat and show no notable HREE differentiation (La/Yb_N = 0.3-0.7, Gd/Yb_N = 1); their Zr/Nb ratios are much lower (10-22) than those in the low-Ti samples. The multi-component spectra for the medium-Ti samples are characterized by positive Nb anomalies relative to Th (Nb/Th_N=3.6-2.1), but not to La (Nb/La_N=1-1.7), what is more typical of ocean ridge basalts (N-MORB) [9]. The high-Ti samples are REE-enriched alkali andesites. Their REE patterns are LREE-enriched and show HREE differentiation (La/Yb_N = 6.8-10.9, Gd/Yb_N = 1.6-2.3) and have low Zr/Nb ratios (5.7-5.9). The multi-component spectra of the high-Ti samples show negative Ti and positive Nb anomalies (Ti/Ti*= 0.2-0.3; Nb/Th_N = 1.3-1.4, Nb/La_N = 1.4-1.3). All these features are typical of oceanic islands basalts (OIB), except for the Ti anomaly. Those specific andesites can form in an intraplate oceanic setting, like OIB, for example, on the Tristan da Cunha islands. [1,9,10]. In general, the geological data and geochemical characteristics of the igneous rocks of the TAC suggest their formation in a mid-ocean ridge (mid-Ti basalts), oceanic island/seamount (high-Ti basalts and andesites), and in a suprasubduction settings (low-Ti basalts).

Funding: This work is supported by the Russian Science Foundation (projects No. 21-77-20022) and the state assignment of the Ministry of Science and Education of the Russian Federation (projects No. 0330-2019-0003 regional geology and petrography).

References:

1. An A., Hi C. S., Yu Y., Lee D. Petrogenesis of Late Cenozoic basaltic rocks from southern Vietnam. Lithos. 2016. Vol. 272-273. P. 192-204.

2. Antonyuk R.M. Oceanic crust of the eugeosynclinal region of the east of Central Kazakhstan. Tectonics of the Ural-Mongolian folded belt. Moscow. 1974.

3. Degtyarev K.E., Tolmacheva T.Yu., Tretyakov A.A., Kotov A.B., Yakubchuk A.S., Salnikova E.B., Van K.L. Polychronous formation of the ophiolite association in the Tekturmas zone of Central Kazakhstan inferred from geochronological and biostratigraphic data. Doklady Earth Sciences. 2017. Vol. 472. P. 26–30.

4. Jensen L.S. A new cation plot for classifying subalkalic volcanic rocks. Toronto. Ontario Division Mines Miscellaneous. MP 66. 1976. 22 p.

5. Kurkovskaya L.A. Complex of conodonts from siliceous and volcanogenic deposits of the Ordovician of Central Kazakhstan. In: Geology of early geosynclinal complexes of Central Kazakhstan. Moscow. Moscow State University Publishing House. 1985. 164-177 pp.

6. Novikova M.Z., German L.L., Kuznetsov I.E., Yakubchuk A.S. Magmatism and ore potential of Kazakhstan. In: Ophiolites of the Tekturmas zone. Alma-Ata. Gylym. 1991. 92-102pp.

7. Pearce J.A. Trace Element Characteristics of Lavas from Destructive Plate Boundaries. In: Thorpe R.S., Ed., Andesites. Hoboken. Wiley. 1982. 528-548 pp.

8. Safonova I., Kotlyarov A. Krivonogov S., W. Xiao W. Intra-oceanic arcs of the Paleo-Asian Ocean. Gondwana Research. 2017. Vol. 50. P. 167-194.

9. Sun S., McDonough W.F. Chemical and isotopic systematics of oceanic basalts: implications for mantle composition and processes. Magmatism in the Ocean Basins. Geological Society of London, Special Publication. 1989. Vol. 42. P. 313–345.

10. Weit A., Trumbull R. B., Keiding J. K., Geissler W. H., Gibson S. A., Veksler I. V. The magmatic system beneath the Tristan da Cunha Island: Insights from thermobarometry, melting models and geophysics. Tectonophysics. 2017. Vol. 716. P. 64-76.

RADIOGEOCHEMICAL FEATURES OF THE ALTAI-SAYAN FOLDED REGION LAMPROPHYRES

Kenesbayev B.K.

Tomsk Polytechnic University, Tomsk, Russia, bkk2@tpu.ru

Abstract. The work is devoted to the study of lamprophyres of the Altai-Sayan region. According to X-ray phase analysis, these rocks have a complex mineral composition. According to the TAS diagram, the petrochemical composition varies from alkaline picrites to trachytes. As the INAA shows, the studied samples are significantly enriched with thorium and uranium. Combining the method of electron microscopy and fission radiography (f-radiography), the occurrence forms of thorium and uranium were studied, therefore concentrating minerals were identified.

Key words: lamprophyre, uranium, thorium, f-radiography.

The term "Lamprophyre" (Greek lampros = shining) was proposed by Gumbel in 1874 to describe some mica dikes in NE Bavaria. Lamprophyres are a complex group of rocks that are mineralogically similar to some kimberlites and lamproites [11]. In the International Union of Geological Sciences (IUGS) classification of igneous rocks, lamprophyres are a special group of rocks that cannot be chemically separated from other igneous rocks. It is highly porphyritic, with feldspars and/or feldspathoids, if present, confined to the groundmass, with biotite/phlogopite and/or amphibole and sometimes clinoperoxene as the main minerals. They usually occur as dikes or small intrusions and often show signs of hydrothermal alteration [9].

The work is based on the study areas: Gorny Altai is the lamprophyres of the Aktash, Yustyd and Tarkhatinsky areas, the so-called Chui complex, as well as the South Minusinsk depression, represented by the Erbinsky neck. There are many studies and descriptions made by predecessors on these rocks. Lamprophyres are represented by minettes, camptonites, vogesites, monchikites and kersantites [1,3,4,7,8]. In addition to author's own data, for comparison, author use data on lamprophyres from the German Ore Mountains [10].

The absolute age of the lamprophyres of the Chuya complex was determined by Vasyukova E.A. using Ar-Ar and U-Pb geochronological methods. She specified and expanded the boundaries of the time of manifestation of the complex and identified two stages of formation: 251-242 and 236-234 Ma. The age of the Erbinsky neck was also determined by the precursors - 250 Ma.

The mineral composition of the studied rocks was determined by the XRD analysis. The ancaratrites of the Erbinsky neck (%): pyroxene group up to 50, two generations of phlogopite up to 14, feldspathoids 11, pectolite 8, forsterite (olivine) 6, apatite, calcite, pyrite, magnetite, garnet 1-5. The mineral composition of minettes of the Chuya complex (%): potassium feldspar 42-64, plagioclase 0.2-0.7, clinopyroxene 7-20, biotite/phlogopite 9-18.8, pseudomorphs after olivine 1-6, apatite up to 4, 3, accessory minerals (ilmenite, titanomagnetite, sphene, rutile, brookite, zircon, etc.) up to 6.6. Kersantites consist of (%): plagioclase 40-68, clinopyroxene 14-25, biotite/phlogopite 7-30, accessory (apatite, titanomagnetite, sphene) 1.5-4.5.

The petrochemical composition of the considered rocks ranges from alkaline picrites to trachytes (SiO_2 36-60%) [2]. The rocks have a rather high total content of alkalis - the composition points are located along the conditional boundary between moderately alkaline and alkaline rocks. They lie in the same area with Erzgebirge mica minettes (LD2a) and are close to the kensantite/minetta mica porphyritic transitional type (LD2c) [10]. According to the type of

alkalinity, the ancaratrites of the Erbinsky neck are of the potassium-sodium type, and the lamprophyres of the Chuya complex are of the potassium type. The rocks of the Erbinsky neck differ from the lamprophyres of Gorny Altai and Germany in lower SiO_2 contents.

The main feature of the studied lamprophyres is the increased content of U and Th. In terms of uranium content, the rocks of the Erbinsky neck and Chuya complex are comparable with lamprophyres of the Ore Mountains of Germany (Table 1). Among all the studied rocks, the lamprophyres of Gorny Altai stand out for their high thorium content, reaching over 100 g/t in some samples. Data on the contents of elements in the rocks were obtained using INAA. It should also be noted that, in terms of the level of accumulation of uranium and thorium, the rocks of the Erbinsky neck correspond to the alkaline syenites of the Yenisei Ridge [5]. And the rocks of Gorny Altai are close to potassium alkaline-ultrabasic dike rocks of the Tomtor massif [6].

Table 1. Contents of uranium and thorium in lamprophyres

Area	U, ppm	Th, ppm	Th/U
Erbinsky neck	7.3 (2.8 – 10.9)	21.5 (10.6 – 41.9)	3 (1.6 – 6)
Gorny Altai	9.3 (4.2 – 16.1)	61.8 (18 – 136)	6.6 (3 – 17)
LD2a (Mica minettes, Erzgebirge)	8.6 (1.6 – 14.6)	50.7 (8.9 – 94.3)	5.7 (4.1 – 6.5)
LD2c (Mica porphyritic transition type kensantite/minetta)	7.9 (3.5 – 14.5)	31.9 (13.1 – 58.1)	4.1 (1.5 – 5.3)

The study of the f-radiography of thin sections showed that the samples of Gorny Altai are characterized by a uniform distribution of tracks over the entire thin section. Sometimes there are denser accumulations of tracks that indicate uranium-bearing minerals. Several “hedgehogs” were also found, in which it is impossible to count the number of tracks, the author suggests that these are uranium’s own nanominerals. It should be noted that no tracks were seen in phlogopite (biotite). The Erbinsky neck is characterized by a more uniform distribution of tracks in the unaltered part of the thin section. In the altered one, there are tracks of increased density, which, as in Gorny Altai, indicates the presence of uranium-containing minerals. Using the scanning electron microscopy in the Erbinsky neck were found galena, (presumably) pyrochlore with thorium (0.8 - 13.2%) and uranium (0.7 - 10.6%). Zircon with thorium (1.1 - 12.6%) and uranium (0.9-1.4), lead oxide was found in samples of lamprophyres from Gorny Altai.

The appearance of lamprophyres with such geochemical features in different regions of the world indicates the identity of their formation in geological processes, the formation of these rocks at the final stages of the geotectonic development of a mountain-folded area and the features of metallogeny.

References:

1. Vasyukova E.A. Petrology and fluid regime of formation of lamprophyres of the Chuya complex (Southeastern Altai - Northwestern Mongolia). Publishing House of the Siberian Branch of the Russian Academy of Sciences. Novosibirsk. 2017. 158 p.

2. Kenesbaev B.K., Vasyukova E.A. (2018): On the issue of high concentrations of uranium and thorium in lamprophyres of the Altai-Sayan region, in the book: New in the knowledge of ore formation processes Collection of materials. Moscow. P. 179-181.

3. Kovalev V.P., Melgunov S.V., Nozhkin A.D., Mitropolsky A.S. Uranium and thorium in igneous and metamorphic petrogenesis. Novosibirsk. Nauka. 1983. 184 p.

4. Melgunov S.V. Radiogeochemistry and genesis of mica lamprophyres. Geology and radiochemistry of Central Siberia. Novosibirsk. Nauka. Sib. Department. 1985. P. 141-157.

5. Nozhkin A.D., Krendelev F.P., Mironov A.G., Bobrov V.A., Radioactive elements in granitoids and syenites of the Yenisei Ridge. Radioactive elements in rocks, part 1. Novosibirsk. 1972. P. 142-143.

6. Panina L.I., Rosokova E.Yu., Isakova A.T., Tolstov A.V., Elements-impurities in alkaline lamprophyres, clinopyroxenes and amphiboles of the Tomtor massif and the ore content of the melts that formed them. Geochemistry. 2018. No. 7. P. 641-660.

7. Rikhvanov L.P., Ershov V.V., Sarnaev S.I., Geochemical features of alkaline mafic and ultramafic rocks of the Minusinsk trough. Geochemical associations of rare and radioactive elements in ore and igneous complexes. Novosibirsk. Nauka. 1991. P. 97-109.

8. Obolenskaya R.V. Chuya complex of alkaline basaltoids of Gorny Altai. Novosibirsk. Nauka.1971.141 p.

9. Le Maitre, R.W., Streckeisen, A., Zanettin, B., et al. Igneous rocks - a classification and glossary of terms. Cambridge University Press, 2nd edition. Cambridge.2002. 236 p.

10. Thomas Seifert, Metallogeny and petrogenesis of lamprophyres in the Mid-European Variscides. IOS Press. 2008. 305 p.

11.Woolley, A.R., Bergman, S., Edgar, A.D., Le Bas, et al. Classification of lamprophyres, lamproites, kimberlites, and the kalsilitic, melilitic, and leucitic rocks. The Canadian Mineralogist. 1996. Vol. 34. P 175-186.

VOLCANOGENIC MATERIAL IN HIGH-CARBON SEDIMENTS OF THE BAZHENOV FORMATION OF THE WEST SIBERIAN SEDIMENTARY BASIN

Kondrashova E.S.

Research and Design institute of oil and gas, Tomsk, Russia, deevael@yandex.ru

Abstract. In the process of studying the deposits of the Bazhenov formation in the southeastern part of the West Siberian sedimentary basin were identified specific formations - layers with a bright luminescence in ultraviolet light. The mineralogical and geochemical features of the horizons indicate the volcanic nature of their formation. The identified layers can be used as marker horizons for solving problems of lithostratigraphic correlation due to their regional distribution, as well as for clarifying the regional patterns of their formation.

Key words: Western Siberia, the Bazhenov Formation, mineralogy, petrography, volcanogenic material.

The study of the core of the Bazhenov formation in the central and southeastern parts of the West Siberian sedimentary basin in ultraviolet light (UV) revealed the presence of single thin layers with anomalous luminescence (yellow, orange-yellow) (Fig. 1) [1, 2]. The layers have different glow intensity (from weak to strong), but at the same time they are clearly distinguished from the background of "ordinary" rocks of the suite. The identified layers are divided into two groups according to external features: group I - single interlayers with a thickness of 0.3 to 1 cm, group II - adjacent layers (thin millimeter series) with an average total thickness of 6 to 45 cm.

The paper presents conclusions based on the results of studies of the material (mineral) and elemental composition of the identified layers by the following methods: X-ray diffraction, petrographic analysis, inductively coupled plasma and ultraviolet spectrometry.

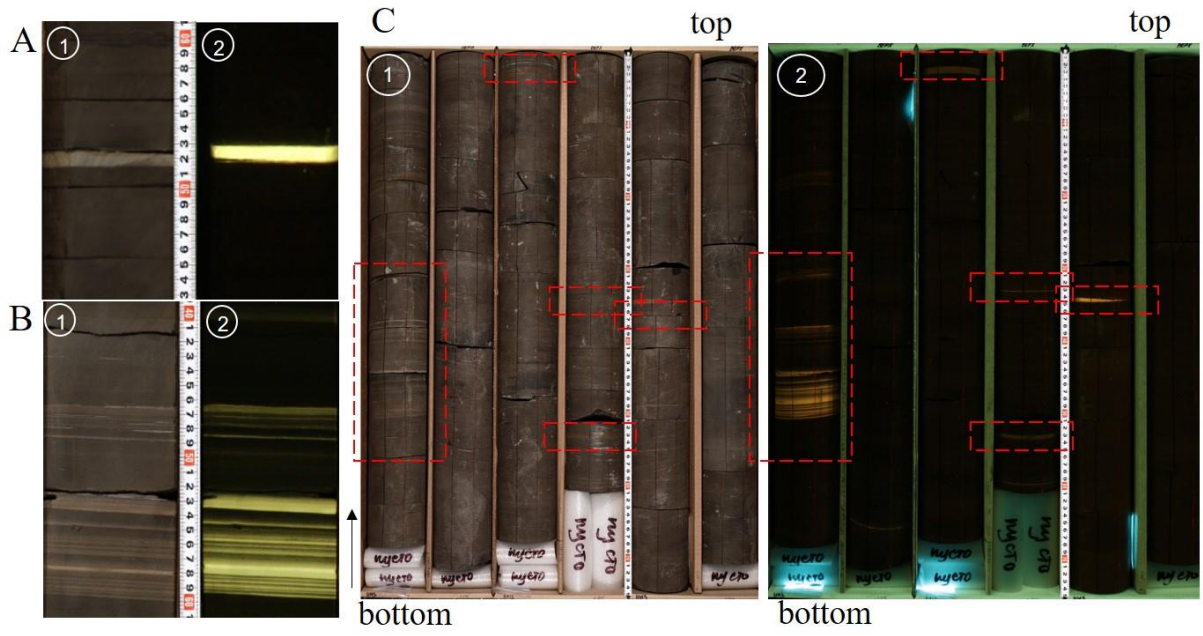

Figure 1 – Luminescence layers in the Bazhenov formation deposits. A –layers of group I, B –layers of group II, C – distribution of luminescence layers in the borehole section. Photo of the core in daylight (1) and UV light (2).

Based on the results of the mineralogical and petrographic studies, was carried out the typification of the studied layers. The layers of the I group are assigned to the ***clay type.*** Layers

of II group are characterized by the same type of mineral composition - the predominant component is quartz - and are assigned to the ***siliceous type*** [2].

The revealed features of the structure, structural and textural features, as well as mineralogical and geochemical features, made it possible to determine the nature of the studied horizons as volcanogenic-pyroclastic [1–4]. It is assumed that the layers under study were formed as a result of dia- and catagenetic transformation of the volcaniclastic material of tuff sediments in a stagnant sea with a high content of organic matter and its subsequent suppression. Luminescence layers of clay and siliceous types differ in the content of trace elements and, in general, differ significantly from each other in terms of the features of the chemical composition. Differences in the accumulation of certain elements in the studied layers and host rocks can be caused by a sharp change in the conditions of sedimentation in interstitial waters. Such conditions can be caused by the synchronous influx of volcanogenic pyroclastic (ash) material into the sediment together with sediments of normal marine sedimentation. Separately, it should be noted the nature of the distribution of the group of lithophilic rare metals, especially thorium. For clay layers was noted an abnormally high content of thorium (8-11 times higher than the content in the host rocks). The most probable source of thorium influx into the deposits of the suite is volcanogenic (ash) material. The presence of volcanic material is also evidenced by the low content of organic matter (C_{org}) in the rocks [3, 4]. According to the complex of features, the rocks of the clay type are assigned to the ***clay tuffites***, and the horizons of the siliceous composition, to the ***tuffosilicites*** [4].

The identified types of layers have different mineral and trace element compositions, correspond to several episodes of ash accumulation, and are regularly distributed over the section: altered volcanic clay type layers are confined to the middle part of the sections, and siliceous type layers to the bottom part.

The luminescence of the studied layers is associated with organic matter (residual polycyclic hydrocarbons) that has undergone transformation under the influence of volcanogenic material.

The study of volcanogenic layers made it possible to obtain new mineralogical and geochemical data on the manifestation of volcanism in the rocks of the Bazhenov Formation over a vast territory (more than 200 thousand km^2), as well as to assess the possibility of using them as reference horizons to refine paleogeographic reconstructions of the formation and solve problems of lithostratigraphic correlation due to their areal regional distribution.

Funding: The reported study was funded by RFBR, project number 19-35-90008.

References:

1. Shaldybin M.V., Krupskaja V.V., Glotov A.V., Dorzhieva O.V., Goncharov I.V., Samojlenko V.V., Deeva E.S., Lopushnjak Ju.M., Bether O.V., Zakusin S.V. Petrography and clay mineralogy of anomaly luminescent layers in Bazhenov suite of Western Siberia sedimentary basin. Oil-industry. 2018. No. 2. P. 36–40.

2. Shaldybin M.V., Wilson M.J., Wilson L., Lopushnyak Yu.M., Brydson R., Krupskaya V.V., Kondrashova (Deeva) E.S., Glotov A.V., Goncharov I.V., Samoilenko V.V., Arbuzov S.I., Bether O.V., Browen L., White D., Dorofeeva N.V. The nature, origin and significance of luminescent layers in the Bazhenov Shale Formation of West Siberia, Russia. Marine and Petroleum Geology. 2019. Vol. 100. P. 358–375.

3. Kondrashova E.S. Mineralogy, geochemistry and the nature of the luminescent interlayers of the Bazhenov Formation of the West Siberian sedimentary basin. Bulletin of the Tomsk Polytechnic University. Geo Assets Engineering. 2020. Vol. 331. No. 8. P. 123–135.

4. Kondrashova E.S. Volcanogenic layers in Bazhenov formation of the Western Siberian sedimentary basin. Bulletin of the Tomsk Polytechnic University. Geo Assets Engineering. 2021. Vol. 332. No. 3. P. 62–73.

TOWARD SUCCESSFUL ABSOLUTE DATING OF EARLY PALEOLITHIC SITES

Kulakova E.P.[1,2]

[1]Schmidt Institute of Physics of the Earth RAS, Moscow, Russia, ek.kula@yandex.ru
[2]Institute of Archaeology and Ethnography SB RAS, Novosibirsk, Russia

Abstract. Absolute dating of Early Paleolithic sites is a key task in archeology and the natural sciences. We discuss the application of two main geochronological methods – magnetostratigraphy and terrestrial cosmogenic nuclides dating – in the study of stratified archaeological sites. Dating of stone artifacts by the cosmogenic method for a long time remained challenging in the history of this method, that caused by unsuitable lithology of stone tools. We have modified the protocol of chemical sample preparation and have got the first successful results on cosmogenic absolute ages of Paleolithic artifacts.

Key words: cosmogenic nuclide dating, geochronology, magnetostratigraphy.

Absolute dating of Early Paleolithic sites is a prerequisite for the study of human evolution and hominin migration routes. Basically, it is the dating of sediments hosting archaeological artifacts and cultural horizons. There are not many geochronological methods at present suitable for dating geological objects in the time range from the first hundred thousand years to 4 million years. The most widely applicable could be the paleomagnetic method (magnetostratigraphy) and terrestrial cosmogenic nuclide dating.

The paleomagnetic method provides age points corresponding to the boundaries of geomagnetic field polarity reversals. Provided that the geological record at the studied site is continuous, this method gives reliable age definitions for sediments older than 780 ka (Brunhes-Matuyama reversal). But in the presence of hiatuses, the interpretation of paleomagnetic data can be ambiguous and therefore requires additional geochronological data obtained by an independent method. That is why the combination of magnetostratigraphy and cosmogenic dating is the most successful and reliable in the establishment of chronology for Early Paleolithic sites [1].

The method of terrestrial cosmogenic nuclides dating is aimed at obtaining the age of a burial event. In recent years this approach is most often applied on the sedimentological material of stratified archaeological sites [2]. There is only a single report on dating the burial event directly from stone artifacts [3]. The ability of dating artifacts is limited by their lithology. Compared to the well-crystallized magmatic or metamorphic rocks (granites, quartz diorites, gneisses, etc., where quartz forms pure crystals) used in glaciological studies, amorphous or diagenetic silica (flint, quartzite, chert, etc.) were favored in stone tool production, because they are characterized by their firmness and ability to produce sharp thin flakes. Despite the same chemical formula of SiO_2, which suggests the same mechanism and rate of cosmogenic nuclides production, amorphous and diagenetic silica appear to be more "contaminated" with elements-impurities (Al, Fe, Ti, Ca, Mg). This makes it difficult to isolate the target cosmogenic nuclides ^{10}Be and ^{26}Al during the chemical processing, since the work of cation-anion exchange columns is disrupted due to overloading with other elements. Such chemical composition peculiarity of amorphous and diagenetic silica is associated with their smaller natural particle size [4].

All this leads to the fact that the classical technique of sample preparation becomes unsuitable and requires modification. We have developed a new protocol for chemical works, the efficiency of which is confirmed by the results of ICP-MS purity test of quartz. The procedure was successfully tested on Early Paleolithic archaeological materials (Rubas site, Dagestan, Russia; loessic Paleolithic of Southern Tajikistan, Central Asia).

Despite the fact that cosmogenic dating can give absolute burial ages, which for stratified objects practically corresponds to the age of formation of strata/age of archaeological artifacts, these data should also be considered with caution and in combination with other methods. Complication for calculating ages can be caused by the complexity of the burial/exposure history of the site, which relies on assumptions in some of its aspects.

Funding: This work is supported by the Russian Science Foundation under grant 21-18-00552.

References:

1. Shaar R., Matmon A., Horwitz L., Ebert Y., Chazan M. ASTER Team. Magnetostratigraphy and cosmogenic dating of Wonderwerk Cave: New constraints for the chronology of the South African Earlier Stone Age. Quaternary Science Reviews. 2021. Vol. 259. Art. 106907.

2. Guo Y., Sun C., Luo L., Yang L., Han F., Tu H., Lai Z., Jiang H., Bae C., Shen G., Granger D. 26Al/10Be burial dating of the Middle Pleistocene Yiyuan Hominin fossil site, Shandong province, Northern China. Scientific reports. 2019. Vol. 9. Art. 6961.

3. Wang K., Xu X., Sun X., Tu H., Zeng Q., Lu Y., Lu H., Wang S. Cosmogenic nuclide burial dating of Liuwan Paleolithic site in the Luonan Basin, Central China. Journal of Geographical Sciences. 2019. Vol. 29. No. 3 P. 406–16.

4. Braucher R., Hidy A.J., Matmon A., Bourlès D., Aumaître G., Keddadouche K. Towards successful cleaning of chert samples for improved 10Be and 26Al measurements. Nuclear Instruments and Methods in Physics Research, Section B: Beam Interactions with Materials and Atoms. 2019. Vol. 456. P. 257–63.

GEOCHEMISTRY OF MID-CRETACEOUS GRANITIC ROCKS OF THE BADZHAL TERRANE (NORTHERN SIKHOTE-ALIN)

Lebedev A.Yu., Alexandrov I.A., Ivin V.V.

Far East Geological Institute, Vladivostok, Russia, lcah@mail.ru

Abstract. Geochemistry of mid-Cretaceous granitoids of the Badzhal accretionary terrane (northern Sikhote-Alin) is studied. The rocks are magnesian, predominantly calc-alkalic metaluminous to slightly peraluminious I-type granites ranging from diorite to leucogranite, as granodiorite being the dominant type. Rocks are depleted with Ba, Nb, P, Ti and enriched with K, Pb and Li. REE distribution spectra are asymmetrical with moderate negative Eu anomaly. LREE are more fractionated, and the HREE curve shows straightening.

Key words: granitic rocks, geochemistry, Badzhal terrane, Sikhote-Alin orogenic belt

The Badzhal Jurassic accretionary terrane is located in the Khabarovsk region of the Russian Far East (fig. 1a). The terrane is a part of the Sikhote-Alin orogenic belt. Within the Badzhal terrane igneous rocks form several mid-Cretaceous plutonic and volcanic complexes of mainly intermediate to felsic composition. In this paper we present preliminary research results of geochemical characteristics of plutonic varieties building Myao-Chan and Badzhal-Dusse-Alin complexes. According to little data obtained by the previous authors, these rocks are dated at 91.5-101.0 Ma [1,2]. Granitoid magmatism is related to the mineralization of the large Badzhal-Myao-Chan Zn-Pb-W-Sn ore province.

The studied rocks (22 samples) are represented by granitoid from diorite to leucogranite (including porphyric one), as granodiorite being the dominant type. The rocks are magnesian, predominantly calc-alkalic (rare calcic or alkali-calcic) metaluminous to slightly peraluminious I-type granites (fig.1b-d). According to SiO_2 and K_2O content, most studied samples belong to high-K calc-alkaline series. In the SiO_2 – Fe_2O_3/FeO diagram most granitoids correspond to the ilmenite series, at the same time falling into composition fields of granitoids associated with different types of ore deposits (fig. 1e).

All analyzed granitoids show similar patterns of trace element distribution both in the primitive mantle-normalized spider diagrams and in the chondrite-normalized REE diagrams. The first are described by essential negative anomalies of Ba (517 ppm), Nb (8.5 ppm), P (0.13 wt.%), Ti (0.5 wt.%), and positive anomalies of K (3.4 wt.%), Pb (16 ppm) and Li (24 ppm). Numbers in parentheses are median values. The leucogranite sample is characterized by the most significant negative anomalies of almost elements, in which the rocks are depleted. Five of granodiorite samples of the Myao-Chan complex can be classified as adakites by their Y and Sr content (fig. 1f). In the Yb_N – $(La/Yb)_N$ diagram they fall into the field of uncertainty between adakites and ordinary granitic rocks.

REE distribution spectra are asymmetrical, the La/Yb_N median value is 7.2. LREE are more fractionated, and the HREE curve shows straightening. The Eu negative anomaly value varies from insignificant (0.9) to very high for a leucogranite (0.16). The median value is 0.67. The total REE 90-230 ppm and median value is 118 ppm.

Generally, the studied rocks exhibit geochemical characteristics typical for suprasubduction granitoids. Nevertheless, over the last years efforts were made to create

geochemical discrimination models for igneous rocks formed due to asthenosphere upwelling caused by slab destruction. This kind of magmatism is typical for transform continental margins [6]. A.I. Khanchuk and colleagues identified a large Albian-Cenomanian magmatic province of the Pacific Asia that formed in this setting and includes the examined mid-Cretaceous granitoids of the Badzhal terrane [7]. The figs. 1g-h show the described rocks data placed in diagrams from [6]. In the trace element diagram (fig. 1h) all dots fall into the field of rocks related to transform margins (RTM), and in the major element diagram (fig. 1g) most samples fall into the field of rocks related to convergent margins (RCM). Particularly in the latter diagram all five samples of adakite-like granitoid and leucogranite fall into the RTM field. The ambiguous interpretation of the analyzed rocks petrogenesis is likely connected to the crustal component influence. This problem requires further geochemical and isotopic signatures investigations of granitoids and host-rocks.

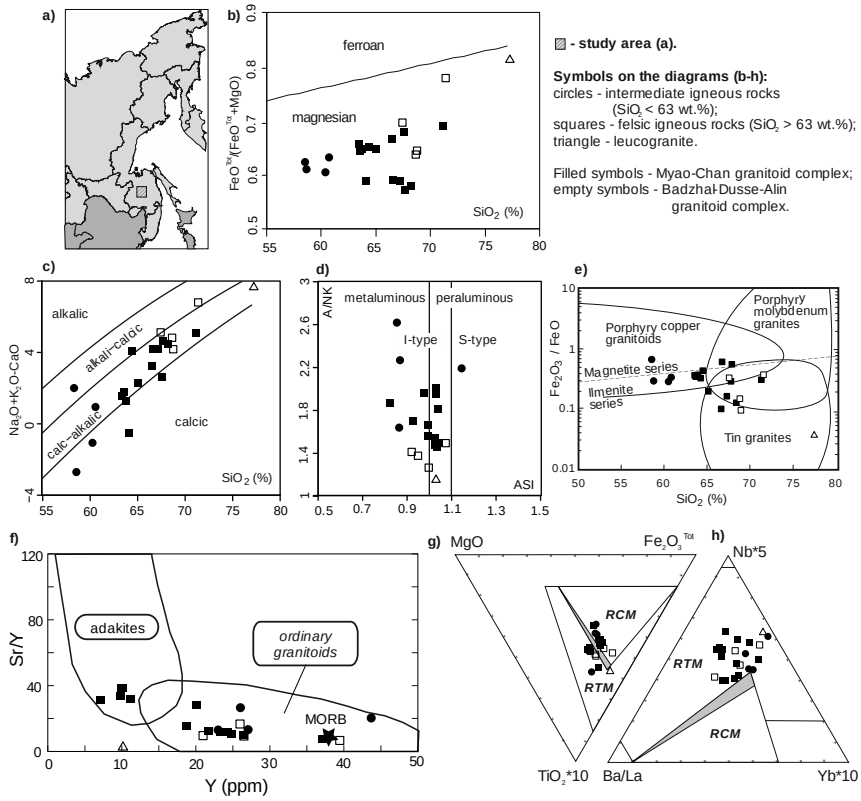

Figure 1 – Study area on an overview map (a) and geochemical diagrams for the studied rocks (b-h): b-d) after [3]; e) after [4]; f) after [5], g-h) after [6].

Funding: This work is supported by the Russian Science Foundation under grant 22-17-00198.

References:

1. State geological map of the Russian Federation. Scale 1: 1,000,000. Sheet M-53. 2009.

2. Gonevchuk G.A., Gonevchuk V.G. The heterogeneous and polychronous Chalba granite pluton in the Komsomolsk ore district in the Far East of Russia with regard to new conceptions of the geological structure of the region. Russian Journal of Pacific Geology. 2013. Vol. 7. P. 369-383.

3. Frost B.R., Barnes C.G., Collins W.J., Arculus R.J., Ellis D.J., Frost, C. D. A geochemical classification for granitic rocks. Journal of Petrology. 2001. Vol. 42. P. 2033–2048.

4. Sinclair W.D. Porphyry deposits. Mineral Deposits of Canada Special Publication. 2007. No. 5. P. 223-243.

5. Defant M.J. and Drummond M.S., Derivation of some modern arc magmas by melting of young subducted lithosphere. Nature. 1990. Vol. 347. P. 662–665.

6. Grebennikov A.V. and Khanchuk A.I. Pacific-type transform and convergent margins: igneous rocks, geochemical contrasts and discriminant diagrams. International Geology Review. 2021. Vol. 63. P. 601-629.

7. Khanchuk A.I., Grebennikov A.V., Ivanov V.V. Albian–Cenomanian Orogenic Belt and Igneous Province of Pacific Asia. Russian Journal of Pacific Geology. 2019. Vol. 13. P. 187–219.

$CACO_3$ GENETIC TYPES DISCRIMINATION IN UHP DOLOMITIC MARBLE FROM THE KOKCHETAV MASSIF: IMPLICATIONS FROM TRACE ELEMIENT COMPOSITION

Mikhno A.O. [1,2], Shatskiy A.F. [1,2,3], Korsakov A.V.[1], Berndt J.[4], Klemme S.[4], Rezvukhina O.V.[1], Rashchenko S.V.[1,2]

[1]V.S. Sobolev Institute of Geology and Mineralogy, Novosibirsk, Russia, mikhno@igm.nsc.ru
[2]Novosibirsk State University, Novosibirsk, Russia
[3]Vereshchagin Institute for High Pressure Physics, Moscow, Russia
[4]Institut für Mineralogie, Universität Münster, Corrensstraße 24, 48149 Münster, Germany

Abstract. The study of UHP dolomitic marble mineralogy was combined with the investigation of trace element distribution in garnet, pyroxene, calcite and aragonite. Two genetic types of calcite were distinguished. First calcite generation shows low LREE contents and positive Sr-anomaly and crystallized together with garnet and aragonite in presence of the carbonate melt. Aragonite coexisting with this calcite shows high LREEs and positive Sr-anomaly. Carbonate melt precipitation resulted in crystallization of second calcite generation with medium or high LREEs and negative Sr-anomaly.

Key words: calcite, dolomitic marble, UHP metamorphism, carbonate melt, trace elements

One of the most pressing questions revolves around the possibility of carbonate melting at mantle depth in the sediment part of the subducted slab. The confirmation of this melting comes from findings of former carbonatite melt inclusions associated with diamond in the UHP rocks from the Kokchetav massif [1,2].

The Kokchetav massif is the part of the Central-Asian fold belt between the former Laurasian and Gondwana continents [3,4]. It represents a 17 km wide and 80 km long megamelange zone in Northern Kazakhstan. The Kokchetav massif is divided by the Chaglinka fault zone into western Kumdy-Kol and eastern Kulet terrains, formed under UHP conditions. Previously, studies of subducted marbles from the Kumdy-Kol terrain revealed that these rocks were metamorphosed in the diamond stability field [5].

Herein we present the major and trace element composition of Ca-carbonates from aragonite-bearing UHP dolomitic marble the Kokchetav massif, northern Kazakhstan, to provide new information on the formation of different generations of Ca-carbonates including aragonite, Mg-calcite in the matrix and different types of carbonate inclusions, that were previously interpreted as mineral and melt inclusions.

Dolomitic marble consists of calcite (26 wt%), dolomite (18 wt%), garnet (11 wt%), and clinopyroxene (24 wt%) with secondary (10 wt%) and accessory sulfides (pyrrhotite + pyrite 7 wt%), and accessory aragonite, apatite, phlogopite, muscovite, allanite, amphibole, K-feldspar, plagioclase, ilmenite, rutile, zircon, titanite, and talc (each phase less than 1 wt%). K-bearing clinopyroxene was identified as the inclusion in garnet porphyroblast of dolomitic marble. Two types of Mg-calcite-bearing inclusions coexist with aragonite in one growth zone of garnet porphyroblasts. Type-A inclusions represent normal mineral inclusions, while Type-B inclusions show crown-like boundary and decrepitation features. X(Mg/Mg+Ca) in calcite from Type-A

mineral inclusions coexisting with aragonite inclusion in one garnet growth zone reaches 0.065 implying their simultaneous crystallization during a retrograde metamorphic stage at P ~ 2.3 GPa and T ~ 870 °C, where the P-T estimates were derived from the intersection of Mg-calcite isopleths with the Kokchetav massif P-T path.

Aragonite from inclusions in garnet is characterized by high LREE concentrations (La=30-50 × PM) and positive Sr anomalies. Calcite from inclusions (IC) can be divided in two groups, the first of which (low-LREE-IC) shows low LREE concentrations (La = 2-20 × PM) and positive Sr-anomalies and represents calcite that crystallized at the same time with garnet and aragonite (P ~ 2.3 GPa and T ~ 870 °C). The second group (high-LREE-IC) shows higher LREE concentrations (La = 30-50 × PM) and negative Sr-anomalies. The high-LREE-IC is interpreted as calcite crystallized from carbonate melt in the inclusion, simultaneously with H_2O-bearing silicate phases, such as amphibole, chlorite, and epidote. Calcites from Type A inclusions are low-LREE-IC, while calcites from Type B inclusions belong to both groups (low-LREE-IC and high-LREE-IC) indicating that these inclusions were enclosed by garnet as the combined inclusions consisting of calcite and carbonate melt.

Matrix calcites (MC) can also be divided into two groups (low-LREE-MC and medium-LREE-MC), resembling those of inclusion calcites based on their trace element patterns and their genesis, i.e. low-LREE-MC shows similar LREE content (La = 8-15 × PM) as the low-LREE-IC and positive Sr anomalies and represent $CaCO_3$ crystallized in equilibrium with garnet. Medium-LREE-MC, showing higher LREE (La = 10-30 × PM) and negative Sr-anomalies, probably crystallized from a carbonate melt together with zoisite, amphibole, and muscovite.

Thus, investigation of trace element composition of Ca-carbonates combined with thorough microstructural study allowed to give geochemical characterization of aragonite (and thus calcite pseudomorphs after aragonite) and to distinguish two generations of calcite. First generation represents calcite, crystallized together with garnet and aragonite in presence of the carbonate melt at T ~ 870°C and P ~ 2.3 GPa. This calcite shows low LREE contents (La = 2-20 × PM) and positive Sr anomaly. Aragonite coexisted with this calcite shows higher LREEs (La=30-50 × PM) and positive Sr anomaly. Second calcite generation together with H_2O-bearing silicates, such as zoisite, epidote, muscovite, and amphibole is the result of carbonatite melt precipitation at P = 1–1.8 GPa, T = 650-850 °C. Trace element pattern of calcite from second generation shows medium or high LREEs (La=10-50 × PM) with negative Sr-anomaly.

Funding: This work is supported by the Russian Science Foundation under grant 22-27-00667.

References:

1. Korsakov A.V., Hermann J. Silicate and carbonate melt inclusions associated with diamonds in deeply subducted carbonate rocks. Earth and Planetary Science Letters. 2006. Vol. 241. P. 104-118

2. Shatsky V., Ragozin A., Sobolev N. Some aspects of metamorphic evolution of ultrahigh-pressure calc-silicate rocks of the Kokchetav Massif. Russian Geology and Geophysics. 2006. Vol. 47. No. 1. P. 105-119.

3. Dobretsov N., Sobolev N., Shatsky V., Coleman R., Ernst W. Geotectonic evolution of diamondiferous paragneisses, Kokchetav Complex, northern Kazakhstan: The geologic enigma of ultrahigh-pressure crustal rocks within a Paleozoic foldbelt. Island Arc. 1995. Vol. 4. No. 4. P. 267-279.

4. Schertl H.-P., Sobolev N., The Kokchetav Massif, Kazakhstan: "Type locality" of diamond-bearing UHP metamorphic rocks. Journal of Asian Earth Sciences. 2013. Vol. 63. P. 5-38.

5. Ogasawara Y., Fukasawa K., Maruyama S., Coesite exsolution from supersilicic titanite in UHP marble from the Kokchetav Massif, northern Kazakhstan. American Mineralogist. 2002. Vol. 87. No. 4. P. 454-461.

GRAIN-SIZE AND GEOCHEMICAL FEATURES OF SEDIMENTS AT COLD SEEP SITES OF THE NORTHERN LAPTEV SEA

Milevsky Y.V., Ruban A.S.

National Research Tomsk Polytechnic University, Tomsk, Russia, ruban@tpu.ru

Abstract. The results of grain-size studies and geochemical of sediment cores taken from the areas of cold seepage in the Laptev Sea are presented. Sand-enriched layers are noted in the cores of cold seep sediments, which appears to be the result of fluid flushing activity. The selective enrichment of the surface layer of sediments with Mo, Ni, and Cr is probably caused by the upward migration of methane fluids, which can transport elements in dissolved form from deeper horizons.

Key words: cold seep, redox-sensitive elements, sediments, Laptev Sea

An interesting feature of the Laptev Sea shelf is the presence of methane cold seep sites [1], which are represent areas of the seafloor where methane-rich fluids in chemical non-equilibrium with seawater are transported through the sub-seafloor environment and are released at the bottom sediment-seawater boundary [2]. When the upward flow of methane interacts with the downward diffusion flow of sulfate, sulfate-controlled anaerobic oxidation occurs. This leads to a change in the redox conditions of sedimentation, which influence the behavior of redox-sensitive elements (for example, Mn, Mo, As, Sb, U, Ni, Cd, etc.) [3, 4]. In addition, seepage of methane-bearing fluid can contribute to the transformation of the lithological composition of sediments [5].

Three sediment cores up to 18 cm long taken on the outer shelf of the Laptev Sea served as factual material. Cores AMK-6027 and AMK-6948 were collected at cold seeps sites and are considered "methane" sediments. At station AMK-6053, no elevated methane contents were recorded either in sediments or in the water column. Therefore, the AMK-6053 core is considered as "background" precipitation. In this study, the chemical (including content of total organic carbon) and grain composition of sediments were studied. X-ray fluorescence and ICP-MS, laser diffraction and Rock-Eval pyrolysis were used for measuring contents of major and trace elements, grain-size fractions and TOC, respectively.

The studied samples of bottom sediments are mainly represented by clay silt, in which the content of the sand does not exceed 1.6%, and the content of the clay varies from 31.8% to 48.3%. The exception is 3 samples, represented by silt clay (core AMK-6053, horizon 10-12 cm) and mixtite (core AMK-6948, horizons 3-4 cm and 8-9 cm). The content of sand in mixtite reaches 39.9%. Probably it is likely to be the result of post-depositional sediment reworking by ascending fluids, which can change the grain size composition of sediments by flushing clay and silt and concentrating relatively immobile sand particles. The contents of TOC and Fe in sediments don't reflect the influence of anaerobic oxidation on their behavior and, probably, are controlled by the features of the spatial distribution of sedimentary material. In all studied cores, elevated Mn concentrations are noted, confined to the surface horizon of sediments. In the cold seep sites the surface layer of sediments is characterized by the enrichment of Mo, Ni, and Cr (Fig. 1). The selective enrichment of the surface layer of sediments with some redox-sensitive elements is probably caused by the upward migration of methane fluids, which can transport of

elements in dissolved form from deeper horizons. Sorption of these elements by organic matter and Fe-Mn oxyhydroxides seems to be the main mechanism controlling the deposition of Mo, Ni, and Cr.

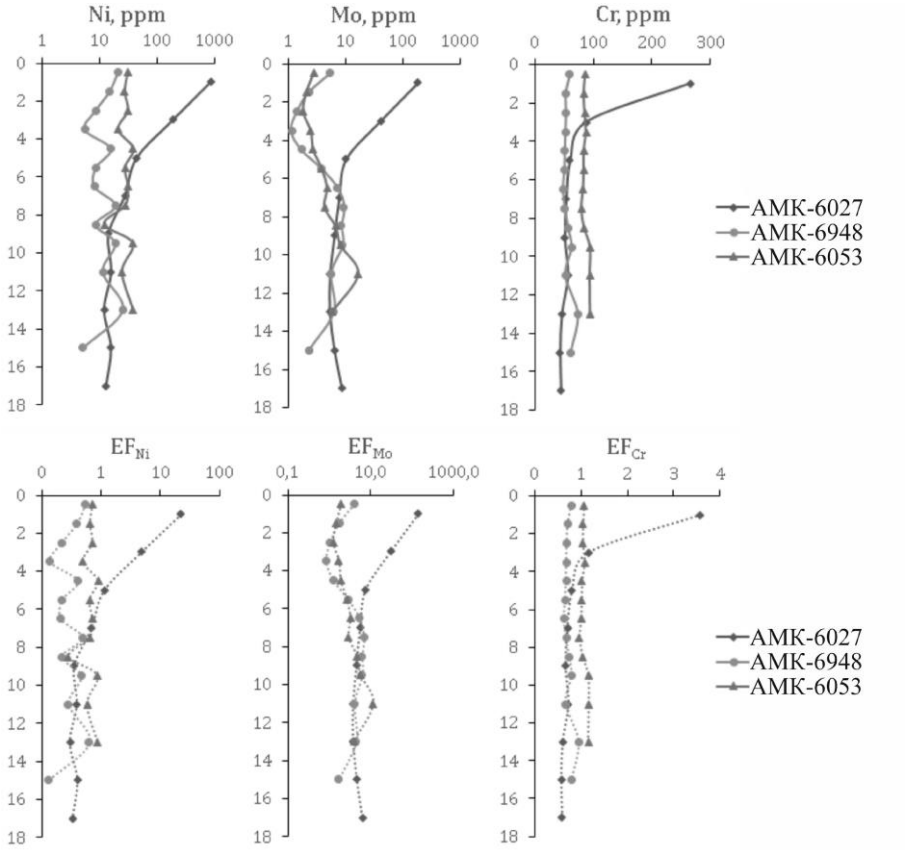

Figure 1 – Vertical distributions of concentrations (top) and enrichment factors (bottom) of Mo, Ni, and Cr in cores AMK-6027, AMK-6948 and AMK-6053.

Funding: The research was supported by the grant from the President of the Russian Federation to support young Russian scientists (project No. MK-1774.2021.1.5).

References:

1. Shakhova N., Semiletov I., Sergienko V., Lobkovsky L., Yusupov V., Salyuk A., Salomatin A., Chernykh D., Kosmach D., Panteleev G., Nicolsky D., Samarkin V., Joye S., Charkin A., Dudarev O., Meluzov A. Gustafsson O. The East Siberian Arctic Shelf: towards further assessment of permafrost-related methane fluxes and role of sea ice. Philosophical Transactions of The Royal Society A Mathematical Physical and Engineering Sciences. 2015. Vol. 373. Art. 20140451.

2. Naehr T.H., Eichhubl P., Orphan V.J., Hovland M., Paull C.K., Ussler W., Lorenson T.D., Greene H.G. Authigenic carbonate formation at hydrocarbon seeps in continental margin sediments: A comparative study. Deep-Sea Research II. 2007. Vol. 54. P. 1268–1291.

3. Scholz F., Hensen C., Noffke A., Rohde A., Liebetrau V., Wallmann K. Early diagenesis of redox-sensitive trace metals in the Peru upwelling area – response to ENSO-related oxygen fluctuations in the water column. Geochimica et Cosmochimica Acta. 2011. Vol. 75. P. 7257-7276.

4. Sato H., Hayashi K.I., Ogawa Y., Kawamura K. Geochemistry of deep sea sediments at cold seep sites in the Nankai Trough: Insights into the effect of anaerobic oxidation of methane. Marine Geology. 2012. Vol. 323–325. P. 47–55.

5. Crémière A., Lepland A., Chand S., Sahy D., Kirsimäe K., Bau M., Whitehouse M.J., Noble S.R., Martma T., Thorsnes T., Brunstad H. Fluid source and methane-related diagenetic processes recorded in cold seep carbonates from the Alvheim channel, central North Sea. Chemical Geology. 2016. Vol. 432. P. 16–33.

MINERAL COMPOSITION AND FORMATION CONDITIONS OF TURBIDITES OF THE KURAI AND TYDTUYARYK FORMATIONS (GORNY ALTAI)

Minnebaev K.R.[1], Kulikova A.V.[2], Batalin G.A.[3]

[1]Institute of Geology and Petroleum Technologies, Kazan, Russia, minnebayev17@gmail.com
[2]V.S. Sobolev Institute of Geology and Mineralogy of the Siberian Branch of the RAS, Novosibirsk, Russia
[3]Institute of Geology and Petroleum Technologies, Kazan, Russia

Abstract. The formation of turbidite deposits is associated with the development of ancient oceans. The conditions of turbidite formation recorded in sedimentary rocks are important geological information. Using this information, it is possible to create geodynamic models of the evolution of folded regions.

Key words: Turbidities, Gorny Altai, heavy minerals, U-Pb (uranium-lead) dating.

The object of the study is turbidite deposits presented in the section of tuffaceous-sedimentary rocks of the Kurai and Tydtuyaryk formations. The section is located on the right bank of the river Chuya, near the village of Chagan-Uzun. The purpose of this work is to establish the geodynamic conditions for the sedimentation of turbidites.

A turbidite is the geologic deposit of a turbidity current, which is a type of amalgamation of fluidal and sediment gravity flow responsible for distributing vast amounts of clastic sediment into the deep ocean. Sandstone samples from the turbidite sequence were used in the work.

There were made different analyzes in this work such as: description of thin rock section using polarizing microscope, determination of mineral composition using Raman spectroscopy, geochemistry analysis using inductive-couples plasma and mass spectrometry (ICP-MS), U-Pb (uranium-lead) dating of zircons.

Sandstones of the Kurai and Tydtuyaryk formations are defined as greywacke, quartz, psammite, and silty [2]. Interpretation of the results of geochemical analysis was carried out using the ratios of chemical elements Fe/Mn, Ti/Zr, Mn/Ni, Mn/Ga, Ti/Mn [3]. Composition of heavy minerals in samples corresponds to the composition of heavy minerals coming from the oceanic island arc [5] (Table 1).

As a result of the work were concluded following statements. Sandstones from the turbidite sequence of the Kurai and Tydtuyaryk formations were formed in a shallow marine forearc basin of the developing island-arc system. The collapsing massifs of the accretionary wedge and the Kuznetsk-Altai Island arc served as the main sources of clastic material [1]. It has been established that the material of the sandstones of the Tydtuyaryk formation corresponds to a young tholeiite-basalt island arc, while the material of the sandstones of the Kurai formation is characteristic of a mature calc-alkaline island arc. The age at 507 Ma of zircons from the deposits of sandstones of the Kurai formation allows us to attribute them to the middle section of the Cambrian period (Figure 1) [4]. The sandstones of the Tydtuyaryk formation will be older than this age, since they were formed by the material composition due to the destruction of a younger island arc. Thus, based on the information obtained, it can be said that the Kuznetsk-Altai Island arc is characterized by the presence of at least two stages of formation - a young tholeiite-basalt stage and a more mature calc-alkaline stage. [1].

Table 1. Mineral composition of the heavy fraction of samples Б-19-598 and Б-19-587

Sample Б-19-598			Sample Б-19-587		
Mineral	**Number of grains**	**%**	**Mineral**	**Number of grains**	**%**
Chromite	120	29.85	Chromite	7	5.74
Sphene	42	10.45	Sphene	31	25.41
Anataz	3	0.75	Anataz	1	0.82
Epidote	93	23.13	Epidote	42	34.43
Apatite	8	1.99	Apatite	1	0.82
Hornblende	7	1.74	Hornblende	1	0.82
Hematite	2	0.5	Hematite	14	11.48
Rutile	2	0.5	Biotite	3	2.46
Chlorite	7	1.74	Muscovite	1	0.82
Barite	8	1.99	Pyrite	15	12.3
Amphiboles	69	17.16	Rhodonite	6	4.92
Actinolite	38	9.45	–	–	–
Andradite	3	0.75	–	–	–
Sum	402	100	Sum	122	100

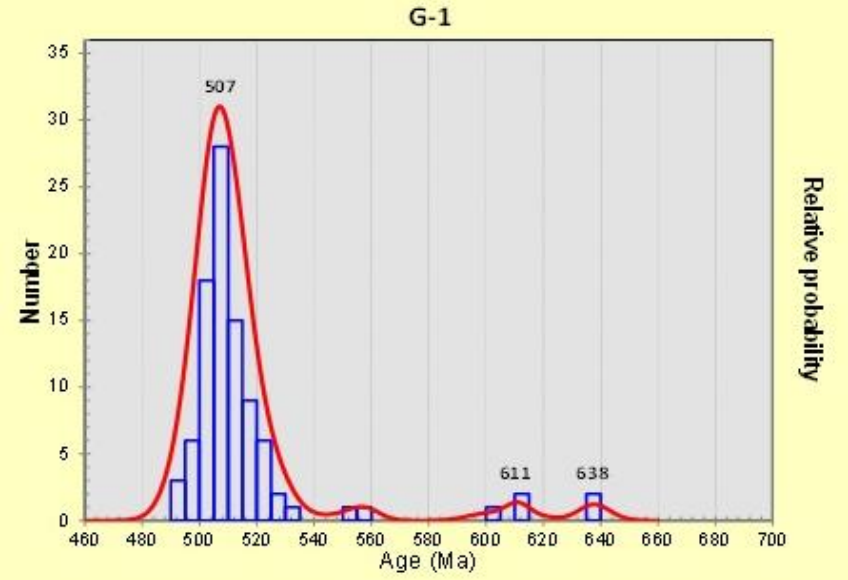

Figure 1 - Diagram of the probable age of zircons from sample G-1 [6]

Funding: The work was carried out with the support of the Ministry of Education of the Russian Federation as part of the implementation of the Decree of the Russian Federation No. 220

References:

1. Buslov M.M., Geng H., Travin A.V., Otgonbaatar D., Kulikova A.V., Chen M., Stijn G., Semakov N.N., Rubanova E.S., Abildaeva M.A., Voitishek E.E., Trofimova D.A. Tectonics and geodynamics of Gorny Altai and adjacent structures of the Altai–Sayan folded area. Russian Geology and Geophysics. 2013. Vol. 54. No. 10. P. 1250–1271.

2. Daminova A.M. Porodoobrazuyushchie mineraly (Rock-Forming Minerals). Moscow. Vysshaya Shkola. 1963. 167 p.

3. Engalychev S. Yu., Panova E.G. Geochemistry and origin of sandstones of eastern part of Main Devonian field in the north-west of Russian Plate. Litosphera. 2011. No. 5. P. 16–29.

4. Chen M., Sun M., Buslov M.M., Cai K., Zhao G., Zheng J., Rubanova E.S., Voytishek E.E. Neoproterozoic–middle Paleozoic tectono-magmatic evolution of the Gorny Altai terrane, northwest of the Central Asian Orogenic Belt: Constraints from detrital zircon U–Pb and Hf-isotope studies. Lithos. 2015. Vol. 233. P. 223-236.

5. Garzanti E., Ando S. Heavy mineral concentration in modern sands: implications for provenance interpretation. Developments in Sedimentology. 2007. Vol. 58. P. 517-545.

AN UPPER AGE CONSTRAINT FOR THE OPHIOLITE ASSOCIATION OF THE CAPE FIOLENT (WEST OF THE MOUNTAINOUS CRIMEA): RESULTS OF U-Pb ISOTOPIC DATING OF PLAGIORHYOLITES (ROCK MONAKH)

Novikova A.S.[1], Kuznetsov N.B.[1], Romanyuk T.V.[2], Strashko A.V.[1]

[1]Geological Institute of the Russian Academy of Science, Moscow, Russia
novikova2787@yandex.ru

[2]Schmidt Institute of Physics of the Earth of the Russian Academy of Sciences, Moscow, Russia

Abstract. In the western Crimean Mountains, near Cape Fiolent (Rock Monakh), a U-Pb dating of zircons from plagiorhyolites of the ophiolite association has yielded an age 168.3 ± 1.3 Ma. Together with the already published reliable geochronological data, the available ages indicate the Aalenian-Bajocian (175–168 Ma) age span of magmatic activity within the Crimean Mountains.

Key words: Mountainous Crimea, Middle Jurassic, plagiorhyolites, zircons, U–Pb isotopic dating

The results of U–Pb isotopic dating (SHRIMP-II, VSEGEI) of crystals of accessory magmatic zircon separated from the plagiorhyolites of the Rock Monakh of the Cape Fiolent area (the southern part of the Heraclea Peninsula) in the west of the Mountainous Crimea (MC) are presented. An obtained concordant age estimate of 168.3 ± 1.3 Ma corresponds to the Bajocian-Bathonian of the Middle Jurassic.

The ophiolites in the Crimea were mentioned for the first time in [1]. The igneous formations of the Cape Fiolent area are referred to as ophiolitic association in [2, 3, 4, 5, 6, 7]. They are exposed in the lower parts of the high (up to 200 m eastward of Cape Fiolent) coastal cliffs of the southern part of the Heraclea Peninsula, and also have been drilled at the Heraclea plateau [8, 9]. These are serpentinites, gabbroids, basalts, dolerites and plagiorhyolites with edaphogenic breccias and jasperoids. The included in this association plagiorhyolites are spatially and paragenetically related to the near-ore (Cape Vinogradny) and ore (Heraclea Plateau) pyrite formations [8].

There is still no consensus on the age and understanding of the geodynamic nature of the Cape Fiolent magmatic rocks, as well as other magmatic areals of the MC. Thus, heterogeneous magmatic complexes of the Cape Fiolent had been previously interpreted as a relic of a shield volcano overlapping the Upper Triassic-Lower Jurassic Tauride Series and had been correlated with Middle Jurassic (Bajocian) magmatic rocks of the Karadag (east of the MC) [10]. In [11], the area of distribution of igneous formations of the Cape Fiolent had been interpreted as a zone of mélange consisting of chaotically arranged blocks of igneous rocks. In [9], a part of magmatic rocks exposing in the coastal strip had been divided into a series of units to be formed during different stages of magmatic activity. In [2, 3, 4, 5, 6], the Cape Fiolent magmatic rocks along with the associating rocks, had been interpreted as an ophiolitic association.

A few attempts to date the magmatic rocks of the Cape Fiolent have been undertaken. Thus, U-Pb dating (SHRIMP II) of 3 zircons from the dolerite dykes has yielded an age of ca. 1771±28 Ma [9]. This value had been interpreted either as an age of the mantle melted substrate

for basic magmas, or as an age of zircon from Precambrian rocks captured during the magma movement to the surface. The K–Ar age of ca. 174 Ma has been obtained for the plagiorhyolites.

The obtained new data has allowed us to conclude the following.

1. The new U-Pb isotopic dating (168.3±1.3 Ma) of zircons from plagiorhyolites of the Rock Monakh is currently the most reliable geochronological assessment of an age of magmatic formations of the Crimea in the methodological and metrological sense.

2. The obtained age estimate constraints the upper age limit of formation of the entire ophiolitic association of the Cape Fiolent.

3. Modern high-precision and reliable isotopic dating of the MC magmatic formations challenges the reliability of most of the previously obtained K-Ar and Ar-Ar age estimates of the rocks. Thus, an Ar-Ar isotopic age of 172.8±4.5 Ma have been recently obtained for the Karadag volcanic rocks [12]. So, the earlier Ar-Ar age estimates of 151-142 Ma known for the Karadag magmatic complexes [13] were not confirmed. Currently there is no reliable geochronological data justifying a long interval of magmatic activity or the existence of various magmatic stages in MC.

4. The accumulated reliable geochronological data [12, 14], together with our new dating, indicate a narrow (Aalenian-Bajocian) interval of magmatic activity in the range of ca. 175-168 Ma within the MC. Together with other data, this makes it possible to interpret it as an indicator of the opening of an Crimean back-arc basin in the Middle Jurassic.

The research was carried in the frames of the state assignment of the GIN RAS and IPE RAS.

References:

1. Shnyukov E.F., Ryabenko V.A., Sidenko O.G., etc. The first find of Ultramafites in the Crimea. DAN of the Academy of Sciences of the Ukrainian SSR. 1979. Ser. B. No. 1. P. 18-20.

2. Demina L.I., Promyslova M.Yu., Koronovsky N.V., etc. The first discovery of serpentinites in the indigenous outcrops of the Mountainous Crimea. Bulletin of the Moscow University. Series 4. Geology. 2015. No. 5. P. 12-20.

3. Demina L.I., Promyslova M.Yu., Koronovsky N.V., etc. The first discovery of serpentinites in the coastal cliffs of the Heraclea peninsula of southwestern Crimea. DAN. 2017. Vol. 475. No. 1. P. 57-59.

4. Promyslova M.Yu., Demina L.I., Bychkov A.Yu., etc. Ophiolitic association of the Cape Fiolent area (south-western Crimea). Geotectonics. 2016. No. 1. P. 25-40.

5. Promyslova M.Yu., Demina L.I., A.I. Gushchin A.I. et al. Types of breccias of the ophiolite Association of the southwestern Crimea and their significance for the paleogeodynamics of the region. Bulletin of the Moscow University. Series 4. Geology. 2017. No. 3. P. 35-40.

6. Promyslova M.Yu., Demina L.I., Bychkov A.Yu., etc. The nature of magmatism of the Cape Fiolent area (south-western Crimea). Bulletin of the Moscow University. Ser. 4. Geology. 2014. No. 6. P. 14-22.

7. Shatalov N.N., Borisenko L.S., Pivovarov S.V., etc. Dykes of the Herakleian volcanic-tectonic structure of the Crimea. DAN of the Ukrainian SSR. 1990. No. 9. P. 19-23.

8. Shnyukov E.F., Lysenko V.I., Kutny V.A., Shnyukova E.E. Gold-silver and sulfide mineralization in rocks of the Herakleian plateau (Crimea). Geology and minerals of the world the ocean. 2008. No. 2. P. 68-86.

9. Shnyukova E.E. Magmatism of the junction zone of the Western Black Sea Basin, the Mountainous Crimea and the Scythian plate. Kiev. Naukova Dumka. 2016. 234 p.

10. Lebedinsky V.I., Soloviev I.V. Bayos volcanostructures of the Mountainous Crimea. Geological journal. 1988. No. 4. P. 85-93.

11. Yudin V.V. Magmatism of the Crimean-Black Sea region from the standpoint of actualistic geodynamics. Mineral resources of Ukraine. 2003. No. 3. P. 18-21.

12. Popov D.V., Brovchenk V.D., Nekrylov N.A. et al. Removing a mask of alteration: geochemistry and age of the Karadag volcanic sequence in SE Crimea. Lithos. 2019. Vol. 324. P. 371-384.

13. Meijers M.J.M, Vrouwe B., van Hinsbergen D.J.J. Jurassic arc volcanism on Crimea (Ukraine): Implications for the paleo-subduction zone configuration of the Black Sea region. Lithos. 2010. Vol. 119. P. 412-426.

14. Morozova E.B., Sergeev S.A., Savelyev A.D. Cretaceous and Jurassic intrusions of the Mountainous Crimea: the first data of U–Pb (SIMS SHRIMP) dating. DAN. 2017. Vol. 474. No. 1. P. 66-72.

PERM GABBROID MASSIFS OF THE KHANGAI UPLANDS WITH PGE-CU-NI MINERALIZATION (WESTERN MONGOLIA)

Shapovalova M.O., Tolstykh N.D., Shelepaev R.A.

V.S. Sobolev Institute of Geology and Mineralogy, Novosibirsk, Russia,
shapovalovam@igm.nsc.ru

Abstract. New data on the petrology, geochemistry and age of the gabbroid massifs of Khangai upland of the Central Asian Orogenic Belt are presented. All massifs were formed in the Permian age. The early and late Intrusions of the Permian polyphase massifs differ in rock-forming minerals, in the level of enrichment in incoherently elements (K, Ti, P, LREE), and in rare element composition (HFSE, LILE), that due to the change of the mantle source from depleted to enriched.

Key words: Permian age, petrology, geochemistry, gabbro, Khangai

The gabbroid massifs are located in the Khangai upland of Mongolia. The Khangai upland belongs to the Central Asian Orogenic Belt (CAOB). The objects of study are the peridotite-troctolite-gabbro massif Oortsog (2 Intrusions), the peridotite-gabbro massif Dulaan, the gabbro massif Mankhan, the gabbro-monzonite massif Yamat (3 Intrusions), and the troctolite-anorthosite-gabbro massif Nomgon. All massifs hold PGE-Cu-Ni mineralization [1,2].

On the geological maps of the Khangai upland, in earlier studies, all gabbroid intrusions are the Early Paleozoic age [1]. We have obtained the Permian age (U-Pb, ^{39}Ar-^{40}Ar). The Oortsog massif is 278.7 ± 2.5 Ma (Intrusion 1, ^{39}Ar-^{40}Ar) and 272 ± 2 Ma (Intrusion 2, U-Pb, SHRIMP-II); the Yamat massif is 255.8 ± 2.9 Ma (Intrusion 1, U-Pb, SHRIMP-II), 262.6 ± 3.1 Ma (Intrusion 2, U-Pb, SHRIMP-II), the Nomgon massif - 255±3 Ma (U-Pb, SHRIMP-II), 251.8 ± 6.3 Ma (^{39}Ar-^{40}Ar). The dating of the Nomgon massif is comparable with the obtained Sm-Nd isochron age of 256 ± 21 Ma [3]. Thus, the age of all massifs is the same for different isotope systems and corresponds to the Permian. The obtained dates of gabbroid massifs are 278–255 Ma, which indicates the formation of massifs during the formation of the Khangai batholite (269–241 Ma) [4], and as its first phase.

In the late Intrusions of polyphase massifs, primary magmatic amphibole and biotite appear with high contents of TiO_2 (Bt - 3.1-3.6 wt.%, Hbl - 3.21-4.2 wt.%). In the Intrusions 1 of massifs, the MgO content varies over a wide range: from 4 to 38 wt. % for the Oortsog massif, and from 0.5 to 8 wt. % for the Yamat massif (in the leucocratic part), with a low content of K_2O (0.03-0.14 and 0.12-0.42 wt.%, respectively). Whereas, late Intrusions (2,3) rocks containing high MgO values: 12.59-25.27 wt.% (Oortsog) and 12.54-25.17 wt.% (Yamat) are enriched in K_2O (0.20-0.87 and 0.30-0.87 wt.%, respectively). The same regularity is observed for TiO_2, P_2O_5 and Na_2O+K_2O.

The rocks of the first Intrusions of the Oortsog and Yamat massifs are characterized by a gradual increase in the Eu maximum on the REE patterns (Fig. 1. a, c), depletion of HFSE (Ta, Nb, Zr, Hf) and enrichment of LILE (Ba, K) (Fig. 1. b, d). Thus, rocks of first Intrusions have typomorphic features characteristic of mafic magmas have formed in suprasubduction zone.

The rocks of the late Intrusions of the Oortsog (2) and Yamat (2,3) massifs are obviously enriched in all rare elements, including REE, as well as high-Ti varieties of amphibole and

biotite, which suggests a more enriched mantle source for these rocks, associated, possibly, with the action of the mantle plume [5].

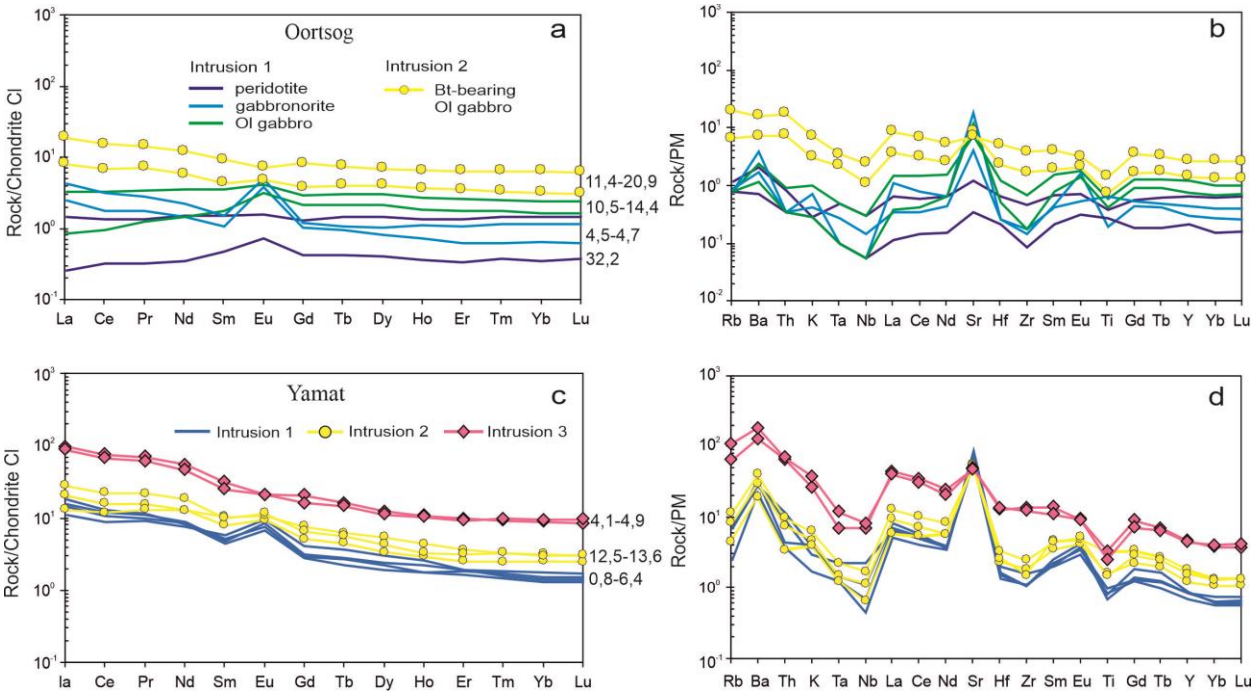

Figure 1 – Chondrite CI normalized [6] REE patterns (a, c) and primitive mantle normalized [7] trace element patterns (b, d) for the all Intrusions of the Oortsog and Yamat massifs. The numbers in the patterns (a, c) show the average contents of MgO in the rocks.

Thus, the new isotope-geochronological data indicate to the Permian age (255-278 Ma) of the gabbroid massifs of the Khangai upland: Oortsog (272-278), Yamat (256-262), Nomgon (255). The early and late Intrusions of the Permian polyphase massifs differ in rock-forming minerals (magmatic high-Ti amphibole and biotite appear in the late Intrusions), in the level of enrichment in incoherent elements (K, Ti, P, LREE), and in rare element composition (the degree of depletion of HFSE and LILE), which due to the change of the mantle source from depleted to enriched.

Funding: This work is done on state assignment of IGM SB RAS with funding from the Ministry of Science and Higher Education of the Russian Federation.

References:

1. Izokh A.E., Polyakov G.V., Krivenko A.P., Bognibov V.I., Bayarbileg L. Gabbroid formations of Western Mongolia. Novosibirsk. Nauka. 1990. 269 p.
2. Shapovalova M., Tolstykh N., Shelepaev R., Kalugin V. PGE-Cu-Ni Mineralization of Mafic-Ultramafic Massifs of the Khangai Upland, Western Mongolia. Minerals. 2020. Vol. 10. Art. 942.
3. Izokh A.E., Polyakov G.V., Gibsher A.S., Balykin P.A., Zhuravlev D.Z., Parkhomenko V.A. High-alumina layered gabbroids of the Central Asian Orogenic Belt: geochemical features, Sm–Nd isotope age, and geodynamic conditions of formation. Russian Geology and Geophysics. 1998. Vol. 39. № 11. P. 1565–1577.
4. Yarmolyuk V.V., Kozlovsky A.M., Salnikova E.B., Kozakov I.K., Kotov A.B., Lebedev V.I., Eenzhin G. Age of the Khangai batholite and problems of polychronicity of batholith formation in Central Asia. Reports of the Academy of Sciences. 2013. Vol. 452. No. 6. P. 646–652.
5. Hofmann A.W. Mantle geochemistry: the message from oceanic volcanism. Nature. 1997. Vol. 385. P. 219–229.
6. Boynton W.V. Geochemistry of the rare earth elements: meteorite studies. Rare earth element geochemistry. New York: Elsevier. 1984. P. 63–114.
7. McDonough W.F., Sun S.S., Ringwood A.E., Jagoutz E., Hofmann A.W. Potassium, Rubidium and Cesium in the Earth and Moon and the evolution of the mantle of the Earth. Geochimica et Cosmochimica Acta. 1992. Vol. 56. No. 3. P. 1001–1012.

DEVONIAN BASALTS AND DOLERITES OF THE KANIN PENINSULA AND THE TIMAN RIDGE

Shmakova A.M.[1,2], Kulikova K.V.[1]

[1] N.P. Yushkin Institute of Geology, Syktyvkar, Russia, alex.sch92@yandex.ru
[2] A.P. Karpinsky Russian Research Geological Institute (VSEGEI), St. Petersburg, Russia

Abstract. Rifting processes within the Kanino-Timan region took place in the Devonian period. As a result of these processes, the Kanino-Timansky dolerite complex was formed. At the moment, there is a lack of data on the rocks of the complex. Our research will allow us to obtain new data on the rocks of the Kanin Peninsula and compare basaltoids with similar rocks of the Timan. The rocks of the complex are tholeiitic basalts and belong to normal-alkaline and subalkaline rocks. The most REE-enriched rocks are the basaltoids of the Tsilma River region of the Middle Timan, the least enriched are the rocks of the Kanin Peninsula and Northern Timan. The ε_{Nd} value varies from +2.4 to +5.5. According to the Sm-Nd isotopy data, the assumption about the influence of the crustal component on the rock source is confirmed.

Key words: basalts, dolerites, plume, Kanin Peninsula, Timan Ridge

Devonian traps and dolerite dikes are spread within the territory of the Kanin Peninsula and the Timan Ridge. These rocks formed the Kanino-Timan dolerite complex. Its formation is associated either with the processes of rifting [1] or with the influence of the mantle plume on the formation of intrusive rocks in the Kanino-Timan region [2, 3]. The trap formation was a result of Paleozoic within-plate magmatism. At the moment, there are practically no detailed geochemical studies on the Devonian basic rocks of the Kanin Peninsula. Geochemical research will allow us to obtain new data on the rocks of the Kanin Peninsula and compare basaltoids with similar rocks of the Timan.

The rocks of the complex include blanket basalts and dolerite dikes. Basaltoids are of a dark gray color with massive, amygdaloidal texture. The structure is intersertal, porphyritic, poikiloophytic. The content of amygdale in the rocks is 10–15 %. Porphyritic phenocrysts are zoned plagioclases (labradorite-bythovnite) and zoned clinopyroxenes (augite-ferroaugite). The groundmass of the rock is composed of small microlites of zoned plagioclase (andesine-bytovnite) (size 0.05–0.2 mm) and isometric grains of zoned pyroxene (augite-ferroaugite, pigeonite) (size 0.2 mm). Ore minerals in the rock are presented by small isometric or skeletal crystals of titanomagnetite (0.05–0.15 mm). Chalcopyrite and pyrite are rare. The intergranular space consists of glass or palagonite (10–20 %).

Dolerites of the studied complex have a massive, amygdaloidal texture. The structure of the rocks is ophitic, porphyritic, poikiloophytic. Rare porphyritic phenocrysts are non-zonal elongated tablets (size 0.5–1 mm) of plagioclase (bytownite). Goundmass of the rock is composed of zoned clinopyroxenes and plagioclases. Plagioclase (andesine-bytownite) forms blades (size 0.5 – 1.5 mm). Clinopyroxene (augite-ferroaugite, pigeonite) forms xenomorphic or hypidiomorphic crystals (size 0.25 – 1.5 mm). Accessory minerals are apatite and K-feldspar. Ore minerals in dolerites are skeletal crystals of titanomagnetite with an oxidation exolution in magnetite solid-solution (size 0.5 mm, rarely 1 mm).

The basaltoids belong to normal-alkaline and subalkaline rocks, predominantly of the sodium type, less often of the potassium-sodium type. The rocks of the complex are tholeiitic basalts.

The content of rare earth elements (REE) in the rocks varies. The lowest REE concentrations are in dolerites of the central part of the Kanin Peninsula 36.50–56.80 ppm as well as in the basalts of the Northern Timan Cape Mal. Rumyanichny 28.5–61.7 ppm and in the basalts of the area of the river Sula of Northern Timan 28.53–61.70 ppm. In the South Timan, the REE content varies from 44.82 to 52.41 ppm. The REE content in the blanket basalt of the Upper Vorykva of the Middle Timan is 62.00–67.52 ppm [4]. In the rocks of the Kanin Peninsula it varies from 63.13 to 81.27 ppm. The highest values of REE content are in the basalts of the Tsilma river area in the Middle Timan 77.13–91.7 ppm.

In basalts, the values of ε_{Nd} are +2.3–+4.6 on the Kanin Peninsula, +4.9–+5.5 on the Northern Timan, +2.4–+4.1 on the Middle Timan, and on the Southern Timan +2.9. According to the $^{143}Nd/^{144}Nd$ ratio – Sm/Nd, the mantle source of the basaltoids of the complex is similar to the DUPAL anomaly, which may indicate the influence of the crustal component on this source [5].

References:

1. Parmuzin N.M., Mazurkevich K.N., Semenova L.R., Kossovaya O.L. et al. Explanatory note of State Geological Map of the Russian Federation. Scale 1:1,000,000 (third generation). Mezenskaya series. Sheet Q-39. St. Petersburg. Cartographic factory VSEGEI. 2015. 393 p.

2. Stepanenko V.I. Kanino-Timan-Pechora province of Late Devonian intraplate magmatism (position and size). Reports of the Academy of Sciences. 2016. Vol. 467. No. 5. P. 572-575.

3. Shmakova A.M., Kulikova K.V. Geochemical characteristics of the Late Devonian basaltoids of the Kanin Peninsula and the Middle Timan. Izvestiya of the Komi Scientific Center of the Ural Branch of the Russian Academy of Sciences. Earth Sciences series. 2021. Vol. 3. No. 49. P. 22-31.

4. Anferova E.A., Udoratina O.V. (2013): Basalts of the Verkhnevorykvinsky blanket (Middle Timan) "Structure, substance, history of the lithosphere of the Timan-North Ural segment. In Materials of the 22nd Scientific Conference. Geoprint: Syktyvkar.

5. Ivanov A.V. Deep-level geodynamics: boundaries of the process according to geochemic and petrologic data. Geodynamics & Tectonophysics. 2010. Vol. 1. No. 1. P. 87–102.

THE RESULTS OF U-Pb SIMS DATING OF ZIRCONS FROM HORNBLENDITES OF THE KONGOR PLUTON OF THE POLAR URALS

Sobolev I.D.[1], *Novikova A.S.*[2]

[1]Institute of Geology of Ore Deposits, Petrography, Mineralogy, and Geochemistry, Russian Academy of Sciences, Moscow, Russia, sobolev_id@mail.ru
[2]Institute of Geology, Russian Academy of Sciences, Moscow, Russia

Abstract. In the Voikar zone of the Polar Urals, among the Early-Middle Devonian island-arc monzonitoids of the Kongor complex, we studied hornblendites, which form a small tectonic block. The hornblendites contain pegmatoid lenticular segregations of diorites from which accessory zircon is separated. U-Pb (SIMS) dating yielded a Givetian – Frasnian age of zircon grains (383±2 Ma) which we consider to be the crystallization age of hornblendites.

Key words: hornblendite, zircon, U-Pb SIMS, Polar Urals, Middle Devonian

In the Voikar zone of the Polar Urals, plutonic rocks of the Late Ordovician – Devonian age are widespread related to the formation of the Polar Ural island arc and the Voikar back-arc basin [1–3, etc.]. On the left bank of the Kharamatolou river (800 m downstream from the mouth of the Makarruz river), among the Early-Middle Devonian island-arc monzonitoids of the Kongor complex [4], we have studied for the first time a tectonic block composed of hornblendites. Outcrops of these rocks stretching along the river bank for about 40 m are limited by faults from the west and east, which are expressed by grassy areas and lowering of the relief. Gornblendites from the central part of the block are melanocratic coarse-grained (5–7 mm) massive rocks consisting of hornblende partially replaced by actinolite (90–95 vol.%), plagioclase, and epidote (5–10 vol.%). Accessory minerals are represented by apatite, titanite and zircon. Near the western tectonic contact, the hornblendites acquire a weakly pronounced porphyritic texture and are dissected by a large number of thin (0.1–1 mm) albite veinlets. In the central part of the block, hornblendites contain pegmatoid lenticular areas (from 5 × 10 to 20 × 30 cm in size) composed of leucocratic giant-grained (up to 2.5 cm) hornblende diorites. The transition from hornblendites to diorites is gradual, with a decrease in the amount of mafic minerals, an increase in grain size and content of feldspars and quartz. Pegmatoid diorite varieties containe much more accessory apatite and zircon than hornblendites, which allowed us to conduct their isotope-geochronological studies.

U/Pb (SIMS) dating of individual zircons from a pegmatoid segregation composed of diorites (sample S128A/19, 66°40′24.0″N, 65°15′40.0″E) was carried out on a SHRIMP-II ion microprobe according to the method [5] adapted at the Center for Isotope Research of VSEGEI (St. Petersburg). Isotope ratios and ages corrected for measured ^{204}Pb were used for interpretation.

The studied zircons are highly fractured transparent pinkish-yellow euhedral bipyramidal-prismatic (elongation – 1.5–3) grains with a large number of additional faces. Cathodoluminescent images of grains demonstrate contrasting bright rims with oscillatory zoning and darker, weakly contrasting inner areas with sectorial zoning combined with oscillatory zoning.

Dating of 11 individual zircons (12 local analyses) yielded a $^{206}Pb/^{238}U$ age range of 387–379 Ma. Based on a coherent dating group consisting of 12 analyses, the average concordant age is 383 ± 2 Ma (2σ, MSWD = 1.9), which corresponds to the boundary of the Early and Middle Devonian (Givetian – Frasnian) and, apparently, is close to the time of formation of hornblendites.

The work was supported by the Ministry of Education and Science grant No. 075-15-2020-802. The monofraction of zircons was obtained within the framework of the state assignment of the GIN RAS (project No. FMUN-2019-0049).

References:

1. Yazeva R.G., Bochkarev V.V. Voikar volcano-plutonic belt (Polar Urals). Sverdlovsk. USC AS USSR. 1984. 160 p.

2. Remizov D.N. Island-arc system of the Polar Urals (petrology and evolution of deep zones). Ekaterinburg. Ural Branch of the Russian Academy of Sciences. 2004. 221 p.

3. Kuznetsov N.B., Romanyuk T.V. Paleozoic evolution of the Polar Urals: The Voikar basin with oceanic-type crust existed for at least 65 Ma. Bulletin of Moscow Society of Naturalists. Department Geological. 2014. No. 5. P. 56−70.

4. Sobolev I.D., Soboleva A.A., Udoratina O.V., Varlamov D.A., Hourigan J.K., Khubanov V.B., Buyantuev M.D., Soboleva D.A. Devonian island-arc magmatism of the Voikar zone of the Polar Urals. Geotectonics. 2018. No. 5. P. 39–74.

5. Schuth S., Gornyy V.I., Berndt J. et al. Early Proterozoic U-Pb zircon ages from Basement Gneiss at the Solovetsky Archipelago, White Sea, Russia. International Journal Geosciences. 2012. Vol. 3. No. 2. P. 289–296.

RECONSTRUCTION OF THE EXHUMATION HISTORY OF THE KONDYOR RIDGE BASED ON THE RESULTS OF U-Th-He DATING OF APATITE

Sokolova L.A.[1], Yakubovich O.V.[1,2], Podolskaya M.M.[3]

[1]Saint-Petersburg State University, Saint-Petersburg, Russia, sokolovalidia@index.ru
[2] The Institute of Precambrian Geology and Geochronology Russian Academy of Sciences (IPGG RAS), Saint-Petersburg, Russia
[3] Vernadsky Institute of Geochemistry and Analytical Chemistry of Russian Academy of Sciences, Moscow

Abstract. The Kondyor massif is the source of the unique placer deposit of platinum group minerals. Herein, we applied U-Th/He method to date apatite from alkaline metasomatites which are developed in the central part of the massif in order to determine its exhumation history. U-Th/He dating results of 8 apatite crystals revealed rapid (~ 30 m/Myr) erosion of the massif, which implies that the formation of the unique Pt placer deposit was preceded by extensive erosion of the Pt-bearing rocks.

Key words: thermochronology, apatite, Aldan shield, Kondyor massif

The alkaline-ultramafic massif Kondyor is located in the southeast of the Aldan shield and is known as a source of unique Kondyor-Uorgalan platinum placer deposit. Circular intrusion on the surface is represented by a symmetric bowl-shaped depression, about 8 km in diameter, surrounded by a mountain ridge. The massif formed due to the intrusion of the Kondyor and Aldan complexes into the Early Archean and Middle Riphean rocks about 120–130 Ma [1].

The U-Th/He method is based on the alpha-radioactive decay of ^{235}U, ^{238}U, ^{232}Th. U-Th/He age is calculated based on concentrations of U, Th, and He in the mineral. Thermal retention of He in apatite crystals is low, corresponding to a closure temperature of approximately 70°C [2]. Assuming a thermal gradient of 3°C per 100 m [3], this temperature corresponds to a depth of approximately 2500 m. Thus, U-Th/He data on apatite extracted from the bedrock of the Kondyor massif will provide information on the time of exhumation of the massif.

For U-Th/He dating large apatite grains were manually extracted from the rock fragments. Sample 43-Ya (stream Uzhniy) and 333 (drill hole) were derived from the alkaline metasomatites which are developed in the central part of the massif. Their chemical composition was studied using a scanning electron microscope HITACHI TM-3000 microanalyzer (Centre for Microscopy and Microanalysis, Research park of St.Petersburg State University) and FT-IR spectrometer BRUKER VERTEX-70 (Center of X-ray diffraction studies, Research park of St. Petersburg State University). The He concentration was measured on an MSU-G-01-M mass spectrometer at the Institute of Precambrian Geology and Geochronology Russian Academy of Sciences. Millimeter-sized grains, free from visible under the binocular microscope inclusions, were wrapped into Ta foil and placed into a mass spectrometer. The samples were heated in several steps to 1100°C which allows complete He release. Tantalum envelopes with degassed apatite grains were removed from the mass-spectrometer for U and Th measurement by the isotope dilution method. The decomposition of apatite was carried out in concentrated nitric acid at 130 °C for 24 hours. The concentrations of U and Th were measured using the HR ICP MS ELEMENT 2 at the Vernadsky Institute of Geochemistry and Analytical Chemistry of the

Russian Academy of Sciences. U-Th/He ages were calculated using Isoplot R software [4]. he reliability of the obtained data was confirmed by the parallel dating of Durango apatite, which is an international standard for apatite He dating.

In total, we have analyzed 8 grains of apatite, which is represented by its Sr-rich variety ($Ca_4Sr(PO_4)_3(OH)_2$). U-Th/He ages of 43-Ya apatite vary from 68 to 92 Ma, with a mean age of 79.2 Ma. Sample 333 gives a mean age of 82.8 Ma (AHe ages in the range from 60 to 104 Ma).

Apatite He ages exhibit an over-dispersion, which might reflect the complexity of the mineral structure or very slow erosions rates [5]. Etching of the polished fragments of the apatite grains in 5 M HNO3 acid for 20 seconds at 20 °C revealed the presence of numerous dislocation loops, which, likely, indicate that structural defects are responsible for the large dispersion of the He ages [6].

The average U-Th/He age is 80 Ma, which implies the apatite crystals were ~ 2500 meters deep at that time. Given that during Neogene and Quaternary time, the Kondyor massif exhibits the uplift of 600 m [7], in the interval from 80 Ma to 24 Ma mean exhumation rate was 33 m/Myr. This value differs from the modern average erosion rates (1–10 m/Myr) revealed for the cratonic shields by cosmogenic nuclides [8]. This implies that the formation of the unique Pt placer deposit was preceded by extensive erosion of the Pt-bearing rocks.

References:

1. Mochalov A.G., Golovkin S.A., Petrov S.V., Borozdin A.P., Yakibovich O.V., Safay A.A., Prikhodko V.S., Antonov A.A., Korneev S.I. 12 International Platinum Symposium Field trip 2 : PGM placer deposits and their sources in the ultramafic and alkaline rocks of the concentrically zoned Konyor massif, Far East, Russia. 2014. 58 p.
2. Reiners P.W., Carlson R.W., Renne P.R., Cooper K.M., Granger D.E., McLean N.M., Schoene B. Geochronology and thermochronology. 2018. 464 p.
3. Peyton S.L., Carrapa B. An Introduction to Low-temperature Thermochronologic Techniques, Methodology, and Applications. Application of structural methods to Rocky Mountain hydrocarbon exploration and development. 2013. P. 15–36.
4. Vermeesch P. IsoplotR: A free and open toolbox for geochronology. Geoscience Frontiers. 2018. Vol. 9. No. 5. P. 1479–1493.
5. Fitzgerald P.G., Baldwin S.L., Webb L.E., O'Sullivan P.B. Interpretation of (U-Th)/He single grain ages from slowly cooled crustal terranes: A case study from the Transantarctic Mountains of southern Victoria Land. Chemical Geology. 2006. Vol. 225. No. 1–2. P. 91–120.
6. McDannell K.T., Zeitler P.K., Janes D.G., Idleman B.D., Fayon A.K. Screening apatites for (U-Th)/He thermochronometry via continuous ramped heating: He age components and implications for age dispersion. Geochimica et Cosmochimica Acta. 2018. Vol. 223. P. 90–106.
7. Khoroshilova T.S., Mochalov A.G., Makhorkina T.I. Placer deposits "Konder" and "Chad" of the Ayano-Maisky district of the Khabarovsk Territory. Magadan, Moscow, 1993. 81 p. (In Russian)
8. Dunai T.J. Cosmogenic Nuclides: Principles, Concepts and Applications in the Earth Surface Sciences. 2010. 199 p.

A HOLOCENE CLIMATIC RECORD INDICATED BY GEOCHEMICAL INDICATORS AND GRANULOMETRY FROM BANNOE LAKE IN THE SOUTHERN URAL

Yusupova A.R., Nourgalieva N.G., Kuzina D.M.

Institute of Geology and Petroleum Technologies, Kazan Federal University, Kazan, Russia,
yusupovaanast095@gmail.com

Abstract. The work is devoted to the geochemical and granulometry study of the Bannoe lake sediments. The main aim of this investigation is to identify the events and trends of environmental and climate changes in the Late Quaternary. The present study of grain size and organic geochemistry of core sediments from Bannoe Lake provides paleoclimatological record of South Ural for the Holocene Period.

Key words: geochemical indicators, lacustrine sediments, particle size content, Holocene

The Bannoe Lake (53°35’48.13” N 58°37’47.28” E) is in the Southern Urals. The altitude of the lake is 438 m, the length is ~4.2 km, the width is ~1.9 km, and the basin area is 36.3 km^2 [1; 2; 3]. According to the radiocarbon dating the age of the lake is 12.5 thousand years [4]. For a detailed complex analysis, core No. 3 was selected according to the results of seismoacoustic studies [5]. The total core length is 508 cm. The sediment was sliced at 2 cm thick samples.

High resolution analyses of lake sediments retrieved from Bannoe Lake were conducted using a combination of variables including particle size content, total organic carbon (TOC), total nitrogen (TN), total inorganic carbon (TIC) and total sulfur (TS) contents, $\delta^{13}C$ value of organic matter ($\delta^{13}C_{org}$), and $\delta^{18}O$, $\delta^{13}C$ values of carbonate content ($\delta^{18}O_{carb}$ and $\delta^{13}C_{carb}$). The C/N ratio (TOC/TN) is regarded as an effective indicator of the origin of organic matter in sediments [6; 7]. Endogenous organics, rich in proteins and poor in cellulose, are characterized by C/N values from 4 to 10. Exogenous organics, poor in proteins and rich in cellulose (the remains of cell walls of higher (terrestrial) plants), are characterized by C/N values of more than 20 [8].

The result of particle size analysis is showing that the content of clay fraction in the sediment varies in the range (9.54-26.27) %, silt fraction are dominant at 56.39%-78.12%, sand - (2.76-26.71) % (Figure 1).

The TOC values changes from 1.56%-16.41%, the TN content ranged from 0.23%-2.23%. The TOC and TN indices increase up the section, which is explained by the increasing the biota activity and the organic matter accumulation. The TS values varied from 0.057% to 0.78%, which is typical for freshwater lakes [9]. The ratio C/N values vary between 5.98-17.79%; average value of C/N is 8.86 and indicates the dominance of endogenous biota. The greatest contribution of exogenous plants is noted at 408 cm (C/N=17.79) and 188 cm (C/N=13.00). The values of δC_{org} vary from -27.65 ‰ to -24.22 ‰, which in combination with data on the C/N indicator (C/N~9), makes it possible to verify the mixed origin of organic matter in the studied lake sediments. The $\delta^{18}O_{carb}$ ranges from -22.25‰ to -5.31‰, the $\delta^{13}C_{carb}$ varies from -18.4‰ to 2.39‰, and the TIC values vary from ~0.03% to 4.86%. An increase in the values of $\delta^{18}O_{carb}$ (a rapid increase in the dryness of the climate) and $\delta^{13}C_{carb}$ (an increase in biomass) recorded at depths of 308-298 cm and 198-178 cm, indicating a decrease in the lake level.

The periods of high and low humidity in the Southern Urals identified during the study are consistent with the Blytt–Sernander classification [10; 11; 12]. The results of geochemical and particle size investigations made it possible to reveal the features of climatic and other environmental changes for the Holocene Period of South Ural.

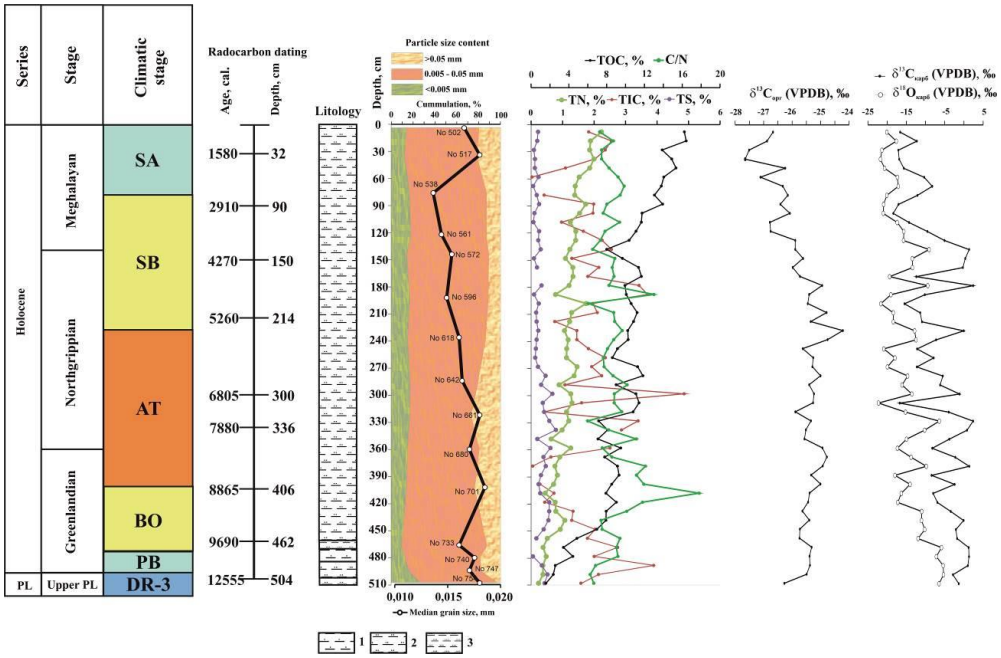

Figure 1 – Results of particle size and isotope analysis of Lake Bannoe sediments. Legend: 1 – clayey silt, 2 - silt, 3 – sandy silt

This study was funded by the Russian Foundation for Basic Research, project #20-35-90058. Part of the study was funded by grant of the President of the Russian Federation for state support of young Russian scientists - candidates of sciences № MK-4100.2021.1.5.

References:

1. Gareev A.M. Rivers and lakes of Bashkortostan. Ufa. Kitap. 2001. 259 p.
2. Gareev E.Z. Geological natural monuments of the Republic of Bashkortostan. Ufa. 2004.
3. Abdrakhmanov R.F. Popov V.G. Geochemistry and formation of underground waters of the Southern Urals. Ufa: Academy of Sciences of the Republic of Belarus, Gilem. Rev. ed. corresponding member RAS V.N. Puchkov. 2010. 420 p.
4. Yusupova A., Kuzina D., Batalin G., Gareev B., Nourgalieva N. (2020): First Geochemical Data on Lacustrine Sediments, Lake Bannoe (Bannoe), Southern Urals. In Proceedings 4th Kazan Golovkinsky Stratigraphic Meeting 2020 Sedimentary Earth Systems: Stratigraphy, Geochronology, Petroleum Resources. Kazan. P.292-297.
5. Krylov P.S., Nurgaliev D.K., Yasonov P.G., Dautov A.N., Golovtsov A.V., Sitdikov R.N., Krylova A.S. Seismoacoustic research of Lake Bannoe bottom sediments (South Ural, Russia). ARPN Journal of Engineering and Applied Sciences. 2020. Vol. 15. No. 1. P. 133–135.
6. Meyers P.A. Applications of organic geochemistry to paleolimnological reconstructions: A summary of examples from the Laurentian Great Lakes. Organic Geochemistry. 2003. Vol. 34. P. 261–289.
7. Routh J, Meyers P.A, Hjorth T, Baskaran M, Hallberg R. Sedimentary geochemical record of recent environmental changes around Lake Middle Marviken, Sweden. Journal Paleolimnology. 2007. Vol. 37. P. 529-545.
8. Krishnamurthy R.V, Bhattacharya S.K, Kusumgar S. Palaeoclimatic changes deduced from 13C/12C and C/N ratios of Karewa lake sediments, India. Nature. 1986. Vol. 323. P. 150-152.
9. Ding X., Li D., Zheng L., Bao H., Chen H., Kao S. Sulphur Geochemistry of a Lacustrine Record from Taiwan Reveals Enhanced Marine Aerosol Input during the Early Holocene. Scientific Reports. 2016. Vol. 6. Art. 38989
10. Blytt A.G. ForsØg til enTheori om Indvandingen af Norges Flora Nyt Mag. Naturvid. Christiana (Oslo). Vol. 21. P. 279-362.
11. Blytt A.G. Immigration of the Norwegian Flora. Cammermeyer. Oslo. Christiania. 89 p.
12. Sernander R. Studier öfver den Götländska vegetationens utvecklingshistora. Uppsala. Akademisk afhandling. 1984. 112 p.

Section REGIONAL GEOLOGY AND TECTONICS

DEFORMATION OF THE SOUTHEASTERN PART OF THE TATARKA-ISHIMBA SUTURE ZONE (YENISEI RIDGE): STRUCTURAL AND $^{40}Ar/^{39}Ar$ GEOCHRONOLOGICAL DATA

Bogdanov E.A.[1,2], Kadilnikov P.I.[1], Matushkin N.Yu.[1,2]

[1]A.A. Trofimuk Institute of Petroleum Geology and Geophysics SB RAS, Novosibirsk, Russia, bogdanovea@ipgg.sbras.ru
[2]Novosibirsk State University, Novosibirsk, Russia

Abstract. We present structural data for metaterrigenous rocks and metagranites from tectonic units of southeastern part of the Tatarka-Ishimba suture zone (Yenisei Ridge). Fold-thrust and strike-slip deformations were caused by the Central Angara – Siberian Craton oblique collision in the late Tonian Period. New $^{40}Ar/^{39}Ar$ geochronological data from metagranites shows a superposed tectonothermal event, which is likely associated with an early magmatic stage of the Tatarka active continental margin complex in the Cryogenian Period.

Key words: Tatarka-Ishimba suture zone; Yenisei Ridge; metaterrigenous rocks; metagranite; cataclasite

According to the current Yenisei Ridge tectonic model, the Tatarka-Ishimba suture zone was formed due to the Central Angara – Siberian Craton collision between 761 and 750 Ma, based on U-Pb data for zircons from syncollisional granites [1]. Deformation in the suture zone has been defined as sublatitudinal compression (geographic coordinates) as well as sinistral kinematics, which characterize the collision as oblique [2]. The Tatarka-Ishimba suture zone has a N-NW strike in the Transangarian (northern) part of the Yenisei Ridge, changing to a NE strike at the junction zone between the Central Angara and Angara-Kan terranes to the South. This report focuses on structural, mineralogical and $^{40}Ar/^{39}Ar$ geochronological study of rocks in two sites located in the eastern part of this junction zone – Ribnaya River site (10–20 km from its mouth) and Skorodumskiy Point site (left bank of Angara River, in front of Ribnoe village).

The first site (Ribnaya River) is represented by exposed metaterrigenous rocks extending to 25 km (overall length of studied outcrops is 2.5 km) assigned to the Mesoproterozoic Uderey Formation of the Sukhopit Group [3]. This structure is bounded to the West by the Tatarka fault of N–NE strike. In the East, it conjuncts with the tectonic sheets (2–4 km) of the Ribnaya ophiolites (MP_3–NP_1) by faults of NE orientation. The metaterrigenous rocks have an intense schistosity of N-NE orientation (dip direction 260°–310°, dip angle 55–85°) as well as overturned folding with the same orientation of axial planes, combined with reverse faults and thrusts forming the common tectonic sheet structure (sheet thickness is 4–6 km). The relict primary bedding of metasandstones and metasiltstones is oblique to schistosity within the inner parts of the sheets, and subparallel near fault and thrust zones. Isoclinal folds develop along the thrust extensions. Their hinges plunge steeply to NW (trend 320–325°, plunge 57–59°) and appear as indicators of superposed strike-slip deformation. The axial planes of these folds are subparallel to the crenulation cleavage (dip direction 204–241°, dip angle 35–87°) that is concordant with strike-slip kinematics.

The rocks of Skorodumskiy Point comprise two different tectonic units. The northwestern unit (length 300 m) consists of intensively schistose metaterrigenous rocks similar to those of the Ribnaya River site. The strike of the schistosity is NE (dip direction 300–345°, dip angle 44–75°). We identified granitic pegmatoid bodies within this unit (thickness 2–50 m) that are subparallel to the schistosity. They have tectonic contacts marked by cataclastic quartz-epidote-biotite-muscovite schists. The southeastern unit (length 500 m) is bordered by a subvertical fault (strike ~30°). It consists of cataclastic metagranites, overlapping quartz-feldspar veins (thickness up to 10 m) and underformed metabasite bodies (thickness 20–30 m). The foliation of the calaclasites dips to NW (dip direction 290–330°, dip angle 70° to subvertical). It appears as cataclastic flow highlighted by preferred mineral grains orientation of quartz and potassium feldspar. Potassium feldspar forms large grains (up to 7 mm). Oligoclase presents as smaller grains (2–3 mm) replaced by albite. Quartz is partly recrystallized, has subgrains and undulose extinction. Biotite is replaced by chlorite and muscovite. Cataclastic metagranites display a younger fracturing without explicit and regular orientation. The fractures are filled out by a fine-grained aggregate of quartz and muscovite (up to 0.05 mm), and overgrown by larger (up to 3 mm) grains of undeformed muscovite. Accessory minerals are zircon and apatite. The three bodies of metabasites (thickness 20–30 m) located within the southeastern unit are undeformed. They have a medium-grained texture and are composed of amphibole (Fe-hornblende, ferro-pargasite and ferro-edenite), albitized plagioclase and individual grains of potassium feldspar. Secondary minerals include chlorite and epidote. Ore minerals are presented by ilmenite, mangano-ilmenite, pseudobrookite, pyrite and chalcopyrite. Geochemical characteristics of these metabasites are similar to trachybasalts of the Yagodka pluton (Tatarka complex), which associate with granitoids. The isotopic age of the latter was determined as 711 Ma according to U-Pb data for zircons [4].

The $^{40}Ar/^{39}Ar$ age of muscovite from our metagranite sample from Skorodumskiy Point has been determined as 711±8 Ma (IGM SB RAS Analytical Center, analyst – A.V. Travin).

In conclusion, the southeastern part of the Tatarka-Ishimba suture zone has a fold-thrust pattern and a SE vergence of its tectonic sheets, which are composed of metaterrigenous rocks and ophiolites. Strike-slip deformations highlight sinistral kinematics in these sheets (with an amplitude up to 5 km), identified by superposition of cataclastic and mylonitic zones. Such kinematics are related to the slipping of the Central-Angara terrane along the Siberian Craton margin during their oblique collision. A subsequent, superposed tectonothermal event has occurred approximately 711 Ma according to $^{40}Ar/^{39}Ar$ age of muscovite from metagranites. It is synchronous with the early stage of magmatism of the Tatarka active continental margin complex [4, 5].

References:

1. Vernikovsky V.A., Vernikovskaya A.E., Kotov A.B., Sal'nikova E.B., Kovach V.P. Neoproterozoic accretionary and collisional events on the western margin of the Siberian craton: new geological and geochronological evidence from the Yenisey Ridge. Tectonophysics. 2003. Vol. 375. No. 1–4. P. 147–168.

2. Matushkin N.Yu. Geology and kinematics of Ishimba and Priyenisei fault of the Yenisei Ridge. PhD thesis. Novosibirsk. 2010. 207 p.

3. Kachevsky L.K., Kachevskaya G.I., Grabovskaya Zh.M. Geological Map of the Yenisei Ridge. Scale 1:500,000. 1998.

4. Romanova I.V., Vernikovskaya A.E., Vernikovsky V.A., Matushkin N.Yu., Larionov A.N. Neoproterozoic alkaline magmatism and associated igneous rocks in the western framing of the Siberian craton: Petrography, geochemistry, and geochronology. Russian Geology and Geophysics. 2012. Vol. 53. No. 11. P. 1176–1196.

5. Vernikovsky V.A., Vernikovskaya A.E., Salnikova E.B., Berezhnaya N.G., Larionov A.N., Kotov A.B., Kovach A.P., Vernikovskaya I.V., Matushkin N.Yu., Yasenev A.M. Late Riphean Alkaline Magmatism in the Western Framework of the Siberian Craton: A Result of Continental Rifting or Accretionary Events? Doklady Earth Sciences. 2008. Vol. 419. No. 2. P. 226–230.

PETROGRAPHY, U-Pb DETRITAL ZIRCON GEOCHRONOLOGY AND PROVENANCE OF THE ILIKTA FORMATION OF THE SIBERIAN CRATON (WESTERN BAIKAL AREA)

Efremova U.S., Donskaya T.V.

Institute of the Earth's crust, Irkutsk, Russia, ulianavolpe@gmail.com

Abstract. The petrographic and U-Pb detrital zircon geochronological studies of the sedimentary rocks of the Ilikta Formation of the Siberian Craton were carried out. The U-Pb ages are mostly Paleoproterozoic with a main peak of about 2.00 Ga, which is close to the age of the Kutima and Chuya granitoids as well as the Goloustnaya granite-gneisses and record the contribution of these rocks into the Ilikta Formation. The Ilikta rocks are unmetamorphosed or undergone green schist metamorphism. The Ilikta sediments were deposited in an intracontinental basin after the end of collisional events in the Akitkan orogenic belt and before the emplacement of the granitoids of the South Siberian post-collisional magmatic belt.

Key words: Ilikta Formation, petrography, detrital zircons, Paleoproterozoic, Siberian Craton

The Ilikta Formation is the upper part of the Paleoproterozoic Sarma Group, which belongs to the Akitkan orogenic belt of the Siberian Craton. The Ilikta Formation is exposed within the Baikal uplift. According to the published data, the Ilikta Formation is composed of schists and sandstones, as well as metavolcanics of intermediate and felsic composition [1]. These rocks overlie the metamorphosed rocks of the Paleoproterozoic Khargitui Formation and Kocherikovo granitoids [1]. The Ilikta Formation rocks are intruded by the 1.88–1.85 Ga granitoids of the South Siberian post-collisional magmatic belt [2] and mafic dykes with an age of 1750 Ma [3] and 720 Ma [4].

The lower part of the Ilikta Formation was detailed studied in two sections: one in the Cape Tyteri of Baikal Lake, and the other in near the Onguren village. The Ilikta Formation sandstones were collected for petrography and U-Pb zircon dating by laser ablation inductively coupled plasma mass spectrometry (LA-ICP-MS).

The section in the Cape Tyteri is composed of mainly unmetamorphosed sandstones. The studied sample 1018 from the Cape Tyteri is spotted sandstone with a psammitic structure. This sandstone is composed of quartz (30%), plagioclase (24%), K-feldspar (15%), chlorite (7%), and lithic fragments of mainly granitoids and rare cherts and altered dolerites (17% in total). Secondary processes were cataclase, chloritization, silicification, and carbonatization. The U-Pb zircon dating of sample 1018 was performed at the Department of Geosciences, National Taiwan University. In total, 59 detrital zircons were analyzed, of which 29 grains that provide concordant value were considered. Most of the ages are 1960–2060 Ma, with the main peak at 2003 Ma. Some zircon grains gave peaks at 2295 and 3049 Ma.

The section of the Ilikta Formation near the Onguren village is composed of metasandstone. These sedimentary rocks undergone green schist facies metamorphism related to the Early Paleozoic dynamometamorphic processes. The studied sample 2135 is foliated and mylonitized sandstone. It consists of quartz (30%), plagioclase (18%), sericite (20%), chlorite (12%), K-feldspar (10%), muscovite (5%), and lithic fragments of granite. Alteration processes were sericitization, chloritization, and enriched with iron hydroxides. U-Pb isotopic analysis of zircons of sample 2135 was carried out at the Institute of the Earth's Crust. For this sample, 113

detrital zircons were analyzed, and 73 grains gave concordant ages with the main peak at 1989 Ma. Other zircons form small peaks at 2275, 2347, 2461, 2565 and 2887 Ma.

The U-Pb detrital zircon geochronology of the Ilikta Formation of the Sarma Group of the Siberian Craton indicates that studied sandstones contain mainly Paleoproterozoic and rarer Archean zircons. The main peaks of 2003 and 1989 Ma are close to ages of the Kutima (2019±19 Ma [5]) and Chuya granitoids (2020±12 Ma [6]) as well as the Goloustnaya granite-gneisses (1985±15 Ma [7]) of the Baikal uplift of the Siberian Craton. Other Paleoproterozoic and Archean zircons are also typical of the magmatic and metamorphic rocks of the basement of the southern Siberian Craton [8]. The Ilikta sedimentary rocks are unmetamorphosed or undergone green schist facies metamorphism related to the Early Paleozoic dynamometamorphic processes. Therefore, we assume that the Ilikta Formation sediments were deposited in an intracontinental sedimentary basin after the end of collisional events in the Akitkan orogenic belt that took place in 1.98–1.95 Ga [7, 9]. As the Ilikta Formation is intruded by the 1.88–1.85 Ga post-collisional granitoids of the South Siberian post-collisional magmatic belt [2], the sedimentary rocks were deposited before the emplacement of these granitoids.

Funding: This work is supported by the Russian Science Foundation under grant 18-17-00101.

References:

1. State Geological Map of the Russian Federation. Scale 1: 1,000,000 (Third Generation). Angara–Yenisei Series. Sheet N-48. 2012.

2. Donskaya T.V., Gladkochub D.P. Post-collisional magmatism of 1.88–1.84 Ga in the southern Siberian Craton: An overview. Precambrian Research. 2021. Vol. 367. Art. 106447.

3. Gladkochub D.P., Pisarevsky S.A., Ernst R., Donskaya T.V., Söderlund U., Mazukabzov A.M., Hanes J. Large igneous province of about 1750 Ma in the Siberian Craton. Doklady Earth Sciences. 2010. Vol. 430. No. 2. P. 168–171.

4. Gladkochub D.P., Donskaya T.V., Mazukabzov A.M., Stanevich A.M., Sklyarov E.V., Ponomarchuk V.A. Signature of Precambrian extension events in the southern Siberia craton. Russian Geology and Geophysics. 2007. Vol. 48. No. 1. P. 22–41.

5. Donskaya T.V., Gladkochub D.P., Mazukabzov A.M., Presnyakov S.L., Bayanova T.B. Paleoproterozoic granitoids of the Chuya and Kutima complexes (southern Siberian craton): Age, petrogenesis, and geodynamic setting. Russian Geology and Geophysics. 2013. Vol 54. No. 3. P. 283–296.

6. Neymark L.A., Larin A.M., Nemchin A.A., Ovchinnikova G.V., Rytsk E.Yu. Anorogenic nature of magmatism in the Northern Baikal volcanic belt: Evidence from geochemical, geochronological (U-Pb), and isotopic (Pb, Nd) data. Petrology. 1998. Vol. 6. No. 2. P. 124–148.

7. Donskaya T.V., Gladkochub D.P., Mazukabzov A.M., Lepekhina E.N. Age and sources of the Paleoproterozoic premetamorphic granitoids of the Goloustnaya block of the Siberian craton: Geodynamic applications. Petrology. 2016. Vol. 24. No. 6. P. 543–561.

8. Rojas-Agramonte Y., Kröner A., Demoux A., Xia X., Wang W., Donskaya T., Liu D., Sun M. Detrital and xenocrystic zircon ages from Neoproterozoic to Palaeozoic arc terranes of Mongolia: Significance for the origin of crustal fragments in the Central Asian Orogenic Belt. Gondwana Research. 2011. Vol. 19. No 3. P. 751–763.

9. Savelyeva V.B., Danilova Yu.V., Shumilova T.G., Ivanov A.V., Danilov B.S., Bazarova E.P. Epigenetic graphitization in the basement of the Siberian craton as evidence of the migration of hydrocarbon-enriched fluids in the Paleoproterozoic. Doklady Earth Sciences. 2019. Vol 486. No. 1. P. 498–502.

COMPOSITION OF UST-BELSKY AND ALGAN TERRANES JURASSIC-CRETACEOUS TUFF-SANDSTONES (KORYAK HIGHLAND, NE RUSSIA)

Gushchina M.U., Moiseev A.V., Tuchkova M.I.

Geological Institute RAS, Moscow, Russia, 119017, dybree@yandex.ru

Abstract. The results of studies on the lithogeochemical features of the Jurassic–Cretaceous tuff-sandstones of the Ust-Belsky and Algan terranes are presented. These rock types formed under similar environment, but the areas of provenance were different, being associated with the volcanic structure of different ages. According to the results, they were formed due to the erosion of volcanic formations in the marine environment with a normal oxygen regime, near the coast. The source was associated with the Island arc on the west from Late Jurassic-Early Cretaceous rocks, and with an Andean-type margin on the northwest from Late Albian-Late Cretaceous rocks.

Key words: Koryak highland, tuff-sandstones, lithogeochemical analysis.

The Ust-Belsky and Algan terranes are located in the northeast of Russia and included the northwestern part of the Koryak-Kamchatka fold system, which was formed in the process of the successively amalgamation of different terranes to the continent. The Jurassic-Cretaceous age is important for the history of Northeastern Eurasia. The Uda-Murgal Island arc was developed along the border of the Asian continent and the Northwest Pacific in the Late Jurassic-Early Cretaceous time. The structural plan changed at the pre-Late Albian age. The Uda-Murgal Island arc ceased to exist, and the Okhotsk-Chukotka volcanic belt started to form. The region is a fold-thrust structure of two main fold belts of the Koryak-Kamchatka folded system, which are combined in this region. The West-Koryak fold belt represents by the Ust-Belsky terrane. The Anadyr-Koryak fold belt depicts by the Algan terrane. Both terranes include tuff-terrigenous deposits of the Jurassic-Cretaceous age.

This work presents the results of mineralogical and geochemical investigations of the Jurassic-Cretaceous tuff-sandstones of the Algan and Ust-Belsy terranes.

The Ust-Belsky terrane consists of several tectonic sheets. The Valanginian tuff-sandstones form the structures of the northwestern Udachninskaya and southeast Mavrinskaya sheets. The Late Albian tuff-sandstones are also present in the Udachninskaya sheet structures.

The Algan terrane comprises several tectono-stratigraphic complexes (TSC). All TSCs include volcanic-siliceous-terrigenous rocks of different ages. The Tithonian-Valanginian tuff-sandstones form the structures of the Algan TSC. Late Albian-Turonian tuff-sandstones shape the structures of the Perekatnaya TSC. The Coniacian-Campanian tuff-sandstones form the structures of the Lamut TSC.

According to the results of geochemical and mineralogical data, the tuff-sandstones form two different rock types in conformity with tectonic stages.

1) The Late Jurassic-Early Cretaceous tuff-sandstones contain less quarts ($Q_{7-39}F_{20-63}L_{24-71}$) and REE (61-141 ppm) and are characterized by low ratios of LREE to HREE (from 3.0 to 5.3). Mafic and intermediate volcanic lithic fragments are dominant. The mafic rock fragments are often represented by spilite lithoclasts. The Algan TSC tuff-sandstones contain clasts of cherts. The cement is commonly of pelitic grain-size and is replaced completely with a sericite–

chlorite–quartz aggregate. Tuff-sandstones of the Udachninskaya sheet contain a larger amount of cement (20%), than tuff sandstones of the Mavrinskaya sheet (5-7%) and Algan TSC (5-11%). All tuff sandstones mostly have poor sorting and rounding of the grains. But, the grains of the Udachninskaya sheet are larger and worse sorted than the grains of the Mavrinskaya sheet and Algan TSC. Comparison with REE, Fe/Mn and Ti/Mn concentrations also shows a moderate decline from the Udachninskaya sheet to Algan TSC. The pyroclastic material is represented by crystalloclasts and lithoclasts.

2) The Late Albian-Late Cretaceous tuff-sandstones contain more quarts ($Q_{5-19}F_{34-51}L_{36-56}$) and REE (86-270 ppm) which is characterized by higher ratios of LREE to HREE (3.9-8.6). Acidic and intermediate volcanic lithic fragments are dominant. Granitoid lithoclasts occur as quartz–feldspar intergrowth. Large fragments of intraclasts of siltstones and mudstones appear in the shape of weakly lithified rolls, sometimes elongated in one direction. All tuff sandstones mostly have poor sorting and rounding of the grains. The decreased amount of quartz and feldspar, increased lithoclast proportion and the grains coarsening occur from the southeast to the northwest in tuff-sandstones of the Perekatnaya TSC. The cement is sericite or clayey (7-12%). The pyroclastic material is represented by crystalloclasts, lithoclasts and vitroclasts.

According to [1] the concentration of K_2O, Na_2O and SiO_2 indicates that sedimentation of all tuff-sandstones was associated with the volcanic arc. Following Braccialli et al. [2] the concentration of Ni, V and Th points the occurrence of erosion products of mafic rocks in the composition of first type rocks, and more products of acidic rocks in our second type rocks. According to [3] the Fe/Mn (15-111) ratios show that deposits formed in shoal and shoal–coastal environment. Agreeing with [4] U/Th (0.3–0.6), Ni/Co (0.9–3.0) ratios specify oxidative near-bottom environment.

Thus, tuff-sandstones were formed due to the erosion of volcanic formations in moderately deep oxidative near-bottom marine environment by high-density flows, near the coast. The Late Jurassic-Early Cretaceous source was in the west of the region. Sedimentation occurred synchronously with volcanism of intermediate and basic composition, which was associated with the existence of the Uda-Murgal arc. Tuff-sandstones of the Ust-Belsky terrane were formed in different part of the forearc basin. Tuff-sandstones of the Algan terrane formed in the trench-slope basin. The Late Albian-Late Cretaceous source was in the northwest of the region. Sedimentation occurred synchronously with volcanism of intermediate and acidic composition, which was associated with the existence Okhotsk-Chukotka volcanic belt.

Funding: This work is supported by the Russian Science Foundation under grant 22-27-00665. The framework of State Contract no.0135-2019-078 supported basic funding for employees of the GIN RAS.

References:

1. Roser B.P., Korsch R.J. Determination of tectonic setting of sandstone-mudstone suites using SiO_2 content and K_2O/Na_2O ratio. The Journal of Geology. 1986. Vol. 94. No. 5. P. 635–650.

2. Braccialli L., Marroni M., Pandolfi L., Rocchi, S. Geochemistry and Petrography of Western Tethys Cretaceous Sedimentary Covers (Corsica and Northern Apennines): From Source Areas to Configuration of Margins. Geological Society of American Special Papers. 2007. Vol. 420. P. 73–93.

3. Reznikov A.N. The Fe-Mn coefficient as an indicator of the sedimentary environment. Izvestia vyssih ucebnyh zavedenij. Neft′ i gaz. 1961. Vol. 19. No. 1. P.19–22.

4. Jones B., Manning D.A.C. Comparison of geochemical indices used for the interpretation of palaeoredox conditions in ancient mudstones. Chemical Geology. 1994. Vol. 111. No. 1–4. P. 111–129.

STRUCTURES AND COMPOSITIONS OF THE RESIDUAL DUNITE-HARZBURGITE COMPLEX OF THE NORTH BALKHASH OPHIOLITE ZONE (CENTRAL KAZAKHSTAN): GEOCHEMICAL AFFINITY AND TECTONIC SETTING OF FORMATION

Milyukova A.G., Skoblenko A.V.

Geological Institute of the Russian Academy of Sciences, Moscow, Russia,
aleksandramilyukova@gmail.com

Abstract. In this article, the preliminary results of study of the ultramafites of the North Balkhash ophiolite zone (NBOZ) forming blocks in the serpentinite mélange are presented. The ultramafites of the NBOZ comprise mainly serpentinized harzburgites with minor dunites. The studied mantle peridotites are investigated regarding to geochemical and petrographical characteristics. According to all the data, these rocks are thought to have been referred to the forearc peridotites formed as a result of the high degrees of a partial melting.

Key words: ophiolites, the Central Asian Orogenic belt, residual peridotites

In the structure of the western segment of the Central Asian Orogenic Belt (CAOB) numerous fragments of the oceanic crust and upper mantle attributed to the different parts of the ophiolite suites of various tectonic affinities are developed. One of the most complete fragments of the ophiolitic suites in the west CAOB is known from the North Balkhash ophiolite zone (NBOZ),in the central part of the Junggar–Balkhash area [1]. The structurally lowest position of the NBOZ is referred to the serpentinite mélange, which contains varisized blocks of igneous, metamorphic and volcanic-sedimentary rocks. The largest blocks confined to the Itmurundy, Tesiktas, Arkharsu and East Arkharsu massifs are composed of spatially separated fragments of the restite (dunite-harzburgite) and layered (dunite-wehrlite-pyroxenite-gabbro-plagiogranite) complexes. Besides, there are some blocks of chromitites, plagiogranites, eclogites, and garnet blueschists in the mélange.

The ultramafites of the NBOZ comprise mainly serpentinized harzburgites with minor dunites made up by anhedral porphyroclasts of olivine, which are separated by aggregates of the smaller, optically strain-free, equant, recrystallized olivine grains. The harzburgites show high modal contents of orthopyroxene (~10–26 vol%) and low modal proportions of clinopyroxene (<3 vol%). The dunites are composed of olivine (~90 vol%) with minor spinel (1–2 vol%). The primary structures of the rocks are characterized by numerous features of deformation, and the secondary looped textures are associated with the ubiquitous serpentinization of the rocks. Magnetite is found at the center of the sieve textures or overgrown the chromium spinel grains and reflects the later stages of the hydration process, and the orthopyroxenes are replaced by bastite.

The olivine from the harzburgites and dunites is magnesian with no zoning preserved and shows high contents of forsterite in the range of 91–92. NiO contents in olivine of all the examined peridotites are in the range of 0.39–0.4 wt%, which is typical for the mantle-derived olivines. Orthopyroxene is mainly enstatite (En_{89-91}) with Mg# of 0.91–0.92, and displays low contents of Al_2O_3 (1.1–1.2 wt%), CaO (0.37–0.52 wt%), TiO_2 (0.0014–0.0079 wt%) and Cr_2O_3 (0.37–0.52 wt%). Clinopyroxene in all the harzburgites is diopside ($En_{2.4-2.5}Fs_{49-49.4}Wo_{49-49.4}$)

with Mg# ranged from 0.95 to 0.97. Chromium spinel forms small (< 0.5 mm) euhedral and anhedral dark-brown grains with Cr/(Cr + Al) ranging from 0.63 to 0.67. The spinel demonstrates very high contents of chromium and iron (48.2–51.5 wt% of Cr_2O_3 and 20.3–21.3 wt% of FeO_{tot}) and corresponds to chromite or alumochromite.

Due to the high LOI values (8.4–12.5 wt%) all major elements in the peridotites were normalized on a volatile-free basis to reduce the effect of dilution caused by serpentinization. The peridotites have high whole-rock contents of MgO (44.89–50.79 wt%), moderate contents of FeO_{tot} (7.78–8.88 wt%) with low contents of Al_2O_3 (0.37–0.98 wt%) and CaO (0.57–0.98 wt%), which is in agreement with the low modal contents of clinopyroxene. These features are like those known from the fore-arc peridotites of the subduction zones, which are residuals after high degrees of partial melting of the mantle rocks. The ultramafic rocks show relatively wide ranges of MgO/SiO_2 ratios (1.0–1.26) at low Al_2O_3/SiO_2 (< 0.02), reflected by the loss of MgO during serpentinization with the interaction between the rock and seawater. The ratios of FeO/SiO_2 (0.18–0.19), Cr_2O_3/SiO_2 (<0.01) and CaO/Al_2O_3 (0.85–1.54) are consistent with those calculated for the isochemically serpentinized mantle restite peridotites (FeO/SiO_2 = 0.170–0.202; Cr_2O_3/SiO_2 = 0.0065–0.0119; $CaO/Al_2O_3 \leq 2{,}0$) [2]. The peridotites have extremely low total REE content (ΣREE = 0.26–0.66 ppm) and are depleted in all the incompatible elements, LILEs (Rb = 0.09–4.1 ppm; Ba = 2.64–6.69 ppm; Cs = 0.01–0.35 ppm) and HFSE (Sc = 6.88–9.52 ppm; Zr = 0.7–2.73 ppm; Y < 0.08 ppm; Nb = 0.04–0.07 ppm; Th and U < 0,01 ppm). Except for the subtle LILE enrichment (e.g. Rb = 4.59*DMM), trace element distributions observed in the peridotites imply their origination from a depleted MORB mantle source (Ni = 2033–2327 ppm, Cr = 2050–2817 ppm and Co = 95–111 ppm).

Based on the low modal contents of clinopyroxene, high Cr# in Cr-spinel and Mg# in olivine along with the insignificant whole-rock concentrations of the incompatible elements, the investigated peridotites are considered to have been assigned to the residues of a depleted mantle after high degrees of melting of 18–22%. The residual origin for the studied peridotites is also indicated by an emplacement of the compositional points on the ‘Fo-in-olivine vs. Cr#-in-spinel’ diagram within the olivine–spinel mantle array (OSMA) [3]. Furthermore, the observed in the ultramafic rocks high chromium contents in spinel (Cr# > 60) with the high contents of forsterite in olivine (Fo_{91-92}) may indicate the suprasubduction origin of these rocks. In addition, the contents of Al_2O_3, Cr_2O_3 and magnesium numbers of the orthopyroxenes and clinopyroxenes from the harzburgites are comparable with those observed from the peridotites of the forearc oceanic basins formed in the suprasubduction environments [3]. The data are consistent with those obtained for the rocks from the structurally higher parts of the ophiolite suite referred to the Arkharsu massif, corresponding to the suprasubduction environment.

Funding: This work is supported by the Russian Science Foundation under grant 22-17-00069).

References:

1. Degtyarev K.E., Luchitskay M.V., Tretyakov A.A., Pilitsyna A.V., Yakubchuk A.S. Early Paleozoic suprasubduction complexes of the North Balkhash ophiolite zone (Central Kazakhstan): Geochronology, geochemistry and implications for tectonic evolution of the Junggar-Balkhash Ocean. Lithos. 2021. Vol. 380–381. Art. 105818.

2. Bazylev B.A. (1998): Petrochemical criteria for recognition of residual spinel peridotites among ultramafic rocks in different tectonic settings. 6-th Zonenshain Conference on Plate Tectonics & Europrobe workshop on Uralides. Moscow.

3. Arai S. Characterization of spinel peridotites by olivine-spinel compositional relationships: Review and interpretation. Chemical Geology. 1994. Vol. 113. No. 3–4. P. 191–204.

GEODYNAMIC SETTINGS OF THE RIPHEAN MAGMATISM IN THE SOUTHEASTERN PART OF THE ANABAR SHIELD

Novikov V.S.[1,2], *Savelev A.D.* [1,2]

[1]Russian Geological Research Institute (VSEGEI), Saint Petersburg, Russia,
snovikov50@icloud.com
[2]Saint Petersburg State University, Saint Petersburg, Russia

Abstract. An isotopic and geochemical study of the Upper Proterozoic mafic magmatic intrusions on the southeast Anabar Shield was undertaken. Based on the content of titanium oxide, three rock complexes were identified. It was established that these rocks belong to igneous complexes of intraplate and island-arc origin. The presence of subduction markers in the dikes of the southeastern part of the Anabar Shield may be caused by contamination of magma with the continental crust containing the subduction component.

Key words: Siberian Craton, Anabar Shield, dikes, geochemistry

One of the most difficult issues in the study of the Anabar Shield is the subdivision and correlation of numerous igneous complexes found within it. In the studied area, 6 mafic complexes have been identified in the interval of 1700–950 Ma [1], but not all of them have clear identification criteria. The lack of reliable isotope dating, as well as poor geochemical knowledge, does not allow one to reliably determine whether the bodies belong to a particular complex.

According to the content of TiO_2, the samples were divided into 3 groups: low- (< 1.7%), medium- (= 2.45%) and high-titanium (> 3%) (fig.1).

According to the similarity of geochemical data, the high-Ti group coincides with the rocks, whose age is 1380 Ma [1], the low-Ti group has an age of 1503 ± 5 by the U-Pb method according to baddeleyite [2]. A dike aged 1774 ± 6 was singled out as a separate group [3].

High-Ti group is isolated from the rest, it is located in the area of intraplate tholeiite basalts and have negative anomalies in Th, U and Sr (Figure 1). The host rocks for them are deposits of the Kotuykan Formation with an age of 1513–1690 Ma [3]. Therefore, dolerite bodies must be younger than 1500 Ma. Geochemically, they correspond to the Chieres dike with a U–Pb baddeleyite age of 1384 ± 2 Ma [1]. Thus, these bodies can be attributed to the Tokur complex, the formation of which accompanied the formation of the carbonate cover of the platform.

The diagrams also show one more point corresponding to a dike with an age of 1774 ± 6 Ma [3]. The distribution diagram of REE and trace elements for this dike is similar to the diagram for the first group, however, it has a Ta-Nb minimum. Dike complexes, whose age is about 1750 Ma [4], are branches of a giant radial dike swarm and are considered as a component of a large igneous province.

Thus, based on geochemical data, three complexes of basic composition intrusions are distinguished in the study area, the age of which is assumed to be 1780, 1500, and 1380 Ma. The formation of these complexes is associated with the activation of large igneous provinces and fixes divergent processes at different time intervals.

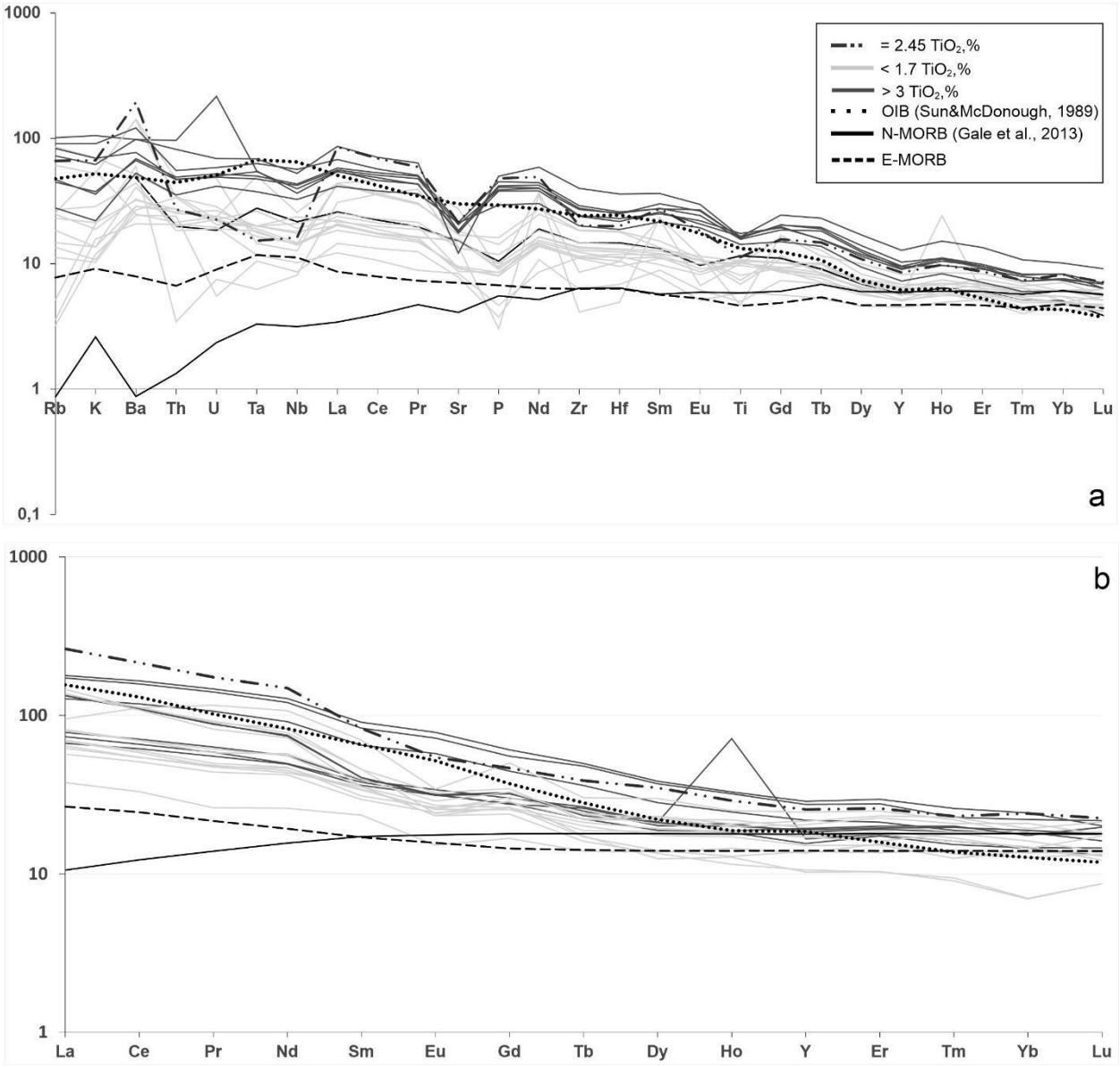

Figure 1 - Chondrite-normalized rare earth elements (REE) plot (a) and primitive mantle-normalized trace element diagram (b).

References:

1. State Geological Map of the Russian Federation. Scale 1:1,000,000. Sheet R-49 – Olenek. 2016.

2. Ernst R.E., Buchan K.L., Hamilton M.A., Okrugin A.V., Tomshin, M.D. Integrated paleomagnetism and U-Pb geochronology of mafic dikes of the Eastern Anabar Shield Region, Siberia: Implications for Mesoproterozoic paleolatitude of Siberia and comparison with Laurentia. Journal of Geology. 2000. Vol. 108. No. 4. P. 381–401.

3. Gladkochub D.P., Donskaya T.V., Ernst R., Mazukabzov A.M., Sklyarov E.V., Pisarevsky S.A., Wingate M., Suderlund U. Proterozoic basic magmatism of the Siberian Craton: Main stages and their geodynamic interpretation. Geotectonics. 2012. Vol. 46. No. 4. P. 273–284.

4. Gladkochub D.P., Donskaya T.V., Pisarevsky S.A., Ernst R.E., Soderlund U., Kotov A.B., Kovach V.P., Okrugin A.V. 1.79–1.75 Ga mafic magmatism of the Siberian craton and late Paleoproterozoic paleogeography. Precambrian Research. 2022. Vol. 370. Art. 106557.

PALEOMAGNETISM AND GEOCHRONOLOGY OF LAMPROITES TOMTOR'S DYKES (UDZHA RIVER, SIBERIAN PLATFORM)

Pasenko A.M. [1], Malyshev S.V.[2], Pazuhina A.A.[2]

[1]Schmidt Institute of Physics of the Earth, Russian Academy of Sciences, Moscow, Russia, a.m.pasenko@iperas.ru

[2]Institute of Earth Sciences, Saint Petersburg State University, Saint Petersburg, Russia

Abstract. Cryogenian was marked by spectacular low-latitude glaciation, which is based on paleomagnetic observations and glacial deposits found on every continent. In recent years, several critical articles have appeared in which the incorrectness of constructing paleomagnetic reconstructions is discussed, since several postulates of paleomagnetism are inapplicable to Cryogenian. Our new geochronological ($^{40}Ar/^{39}Ar$) and paleomagnetic studies suggested equatorial position of Siberia in early Cryogenian. However, new data make it possible to test not only the Snowball Earth hypothesis, but also consider another hypothesis for "low-latitude glaciations".

Key words: Paleomagnetism, Cryogenian, Siberia, Tomtor, $^{40}Ar/^{39}Ar$ dating

At present, the number of reliable paleomagnetic poles for the Neoproterozoic of the Siberian Platform is extremely small. At the same time, their sufficient number is a necessary condition for the development and testing of various geodynamic and paleogeographic reconstructions, which is especially important in developing models for the assembly and breakup of the Neoproterozoic supercontinent Rodinia.

On the territory of the Siberian Platform, Neoproterozoic rocks suitable for paleomagnetic studies are characterized by an extremely low distribution and low degree of exposure. Concurrently, studies of sedimentary rocks often face intractable problems of determining their age. Thus, even if the studied sedimentary rocks contain a stable paleomagnetic signal, the collected data are very difficult to interpret qualitatively. Under such conditions, it becomes critical to gather paleomagnetic poles from reliably dated igneous rocks. Therefore, at present, it is especially important to obtain high-quality paleomagnetic data specifically for igneous objects with a reliably determined age.

In this paper, we propose a new pole attained from dated lamproites of the first phase of emplacement of the Tomtor alkaline massif of the Udzha Uplift (age determined by the Ar-Ar method on phlogopite, 706.1 ± 8.8 Ma) [1, 2]. To obtain the discussed paleomagnetic pole, the authors selected a collection comprising 27 samples of four thin dikes and 41 samples of host rocks for the contact test. The host rocks are the red-colored rocks of the Mesoproterozoic Unguokhtakh Formation. In this outcrop, they are mainly represented by lapilli tuffs with inclusions of large (5–100 cm) fragments of carbonate and siliceous rocks, as well as spherical nodules (up to 10 cm) composed of finely bedded sandstone with carbonate cement.

Based on the results of magnetic cleanings with temperature and an alternating field, a high-temperature magnetization component was identified in all lamprophyre samples, from the directions of which the average direction of magnetization in the studied bodies was calculated, and, subsequently, the corresponding virtual geomagnetic pole for the Siberian Platform was calculated (Table 1).

The following arguments can be made in favor of the primacy of the direction of magnetization identified in the dikes of the Tomtor massif:

1. Grains of the main minerals-carriers of magnetization are predominantly in a pseudo-single-domain state, so they can carry a stable primary paleomagnetic signal.

2. In the studied samples, three different magnetic phases were revealed, which differ in the spectra of deblocking temperatures. All of them carry similar directions of magnetization, which gives us reason to believe that they could form almost simultaneously during melt crystallization and may carry a primary paleomagnetic signal.

3. A positive contact test indicates that the carbonatite dikes studied by us, together with the host rocks of the Unguokhtakh Formation, were not subjected to regional magnetization reversal.

For the time we are considering for the Siberian Platform, there is currently only one paleomagnetic pole, the pole obtained from siltstones of the Medvezhevka Formation of the Longdor Uplift of the Baikal-Patom folded region [3] (Table 1). Its age is estimated at ~720–710 Ma. The pole collected by us is in excellent agreement with this definition (after introducing a correction for the opening of the Vilyui rift [4]).

This coincidence is especially noteworthy, in light of the fact that these objects are located at a considerable distance from each other and belong to different tectonic blocks of the Siberian Platform. Thus, the proximity of the VGP for the carbonatites of the Tomtor massif (~705 Ma) to the paleomagnetic pole for the rocks of the Medvezhevka Formation (~720–710 Ma) of the Baikal-Patom region indicates the reliability of the presented paleomagnetic data and suggests that the paleomagnetic pole for the Siberian Platform at the time of 705–720 Ma was located in the central part of the Indian Ocean.

Table 1. Paleomagnetic poles for the rocks of the Tomtor massif of the Udzha Uplift and the Medvezhevka Formation of the Longdor Uplift of the Siberian Platform

Object	Age (Ma)	Plat(°)	Plong(°)	A95(°)	Source
Tomtor alkaline massif	706 ± 9	-20.7	88.6	3.4	this work
Medvezhevka Formation	720–710	-22.1	93.3	2.7	[3]

Funding: This work is supported by the Russian Science Foundation under grant №19-77-10048.

References:

1. Vladykin N.V., Kotov A.B., Borisenko A.S., Yarmolyuk V.V., Pokhilenko N. P., Sal'nikova E. B., Yakovleva S. Z. Age boundaries of formation of the Tomtor alkaline-ultramafic pluton: U-Pb and $^{40}Ar/^{39}Ar$ geochronological studies. Doklady Earth Sciences. 2014. Vol. 454. No. 1. P. 7–11.

2. Pasenko A., Ivanov A., Malyshev S., et al. (2021): Geochronological and paleomagnetic studies of small carbonatite intrusions of the Udzha uplift (Tomtor massif, northeast of the Siberian platform). in Conference Proceedings of Geodynamic EGU General Assembly, EGU21-12614, Vienna: Online Meeting.

3. Shatsillo A.V., Rud'ko D.V., Latysheva, I.V., et al. (2021). First paleomagnetic data on Neoproterosoic of the eastern slope of the Longdor uplift (Siberian Platform), in Conference Proceedings of Geodynamic Evolution of the Lithosphere of the Central-Asian Mobile Belt, (from Ocean to Continent). P. 391–394, Irkutsk: Institute of Earth's Crust SB RAS.

4. Pavlov V., Bachtadse V., Mikhailov V. New Middle Cambrian and Middle Ordovician palaeomagnetic data from Siberia: Llandelian magnetostratigraphy and relative rotation between the Aldan and Anabar–Angara blocks. Earth and Planetary Science Letters. 2008. Vol. 276. No. 3. P. 229–242.

KAZANIAN-STAGE CHROMSPINEL PLACERS IN THE SOUTHERN PRE-URALS, BASHKIRIA, RUSSIA

Rakhimov I.R.

Institute of Geology and Mineralogy, Ufa, Russia, rigel92@mail.ru

Abstract. Six minor alluvial placers and one relatively large coastal marine chromite placer were found in sandy sediments of the Kazanian Stage in the Southern Pre-Urals. All these placers are referred to as proximal chromite placers and have no analogues in the world. The bulk chemical composition of chromspinels from all placers is nearly the same and generally correlates with compositions of chromspinels from the Kraka ophiolite complex in the Southern Urals. The discovery of these placers allows introducing the new Southern Pre-Urals chromite-bearing region in the local raw material geology.

Key words: marine-coastal and alluvial chromite placers

Chromite placers are divided into three genetic types, i.e. eluvial-diluvial, alluvial and coastal marine [1]. The former occurs close to the removal source (area of the Great Dike in Zimbabwe, Camaguey in Cuba, Sarany in the Ural region), while the rest are at the distance of first kilometers to several tens of kilometers (on the Maharashtra bank in India, on the Oregon coast in the USA, on the north-eastern coast of the RSA, etc.) [2–4]. In the Ural region, chromite placers are known on the western (Sarany deposit) [5] and eastern (Alapay and Varshavka occurrences) slopes [6]. These placers are eluvial-diluvial and occur as boulder assemblages. No coastal marine placers are known in the Ural region, while alluvial placers are minor and have no commercial value, even potentially.

The Sabantuy placer was discovered first and studied most comprehensively [7]. The ore bed has the maximal and stable thickness (0.9–1.0 m) and the greatest area (≥16500 m^2, not less than 330 m long and 50 m wide). Minimal forecast resources (P_2 category) of chromite ores with the average Cr_2O_3 content of 11 wt.% and the average density of the ore of 3.2 g/cm^3 are estimated at 50160 t (15675 m^3). Layers of concentrated chromite-bearing sandstones called chromitolites are as thick as 1 to 130 mm. Chromitolites typically show a varied layering, i.e. horizontal, gently undulated, cross-undulated, cross-multidirectional and slanting and sinuous at places. Two former types prevail, but patterns of their distribution are still unclear. The chromite bed overlies fine-grained sandstones with subhorizontal and cross bedding that contain interlayers of gravel and pebbles in the upper part of the section. Most of chromspinel grains are octahedrons (regular or distorted). Sandstones enclosing the ore bed are typically well-sorted and mainly contain well-rounded debris. Sandstone grains are fragments of rocks (77–82%), quartz (9–12%), silicate (6–10%) and ore minerals (1%).

Other minor placers (Kolkhoznyi Prud, Verkhne-Yaushevo, Sukhoy Izyak, Bazilevo, Novomikhaylovka, Kiryushkino) are similar in lithology and insignificant thickness of the ore bed. They were discovered in gravel sandy quarries at the distance of 5 to 25 km from the Sabantuy placer. The areas of chromite placers vary from 200 to 1100 m^2. The ore beds with the thickness of from 1–3 to 30–40 cm were discovered in sandstone lens and flexuous cross-bedded layers among gravel-pebble units. Dip angles reached to 35°, average 17°.

The lithology of chromite-bearing sections is similar, but there is not a single identical section, which suggests local differences in the lithodynamic sedimentation environment. Most of the studied placers (excluding Sabantuy) show either unidirectional cross-bedding of chromite sediments, or subhorizontal bedding in thin rapidly pinching out lenses of sandstones. Sandy lenses are commonly wavy in the longitudinal section. Their debris are well-sorted and poorly rounded. These features are typical of alluvial deposits [8, 9]. Cross- and gently undulated, locally multidirectional slanting bedding was indicated in sandstones of the Sabantuy section. The debris is highly well-sorted and well-rounded. Such features are typical of coastal marine (possibly delta) sediments [8, 9].

Most studied grains (>70%) on the Al^{3+}–Cr^{3+}–Fe^{3+} diagram occupy fields of chromite and alumochromite, mainly reflecting variations of Cr and Al, and they are almost completely overlapped by compositional fields of chromspinels from the Kraka ophiolite massifs.

Chromite placers of the Southern Pre-Urals are unique, being placers of no proximal, but distal, though they are not complex. Distal placers are produced by rewashing of great masses of ore-bearing sediments. Thus, they contain various ore minerals characterized by particular stability in the hypergenesis area (ilmenite, zircon, rutile, magnetite, chromite, etc.). Chromite is the main mineral in the Southern Pre-Ural placers, while ilmenite and especially zircon are minor in them. Most the studied placers over the world, not only chromite-bearing, are young, while ancient mineral placers are studied far worse. Chromite placers of the Southern Pre-Urals show features of a proximal placer [10], but no primary source is found nearby (at least within a radius of 200 km), neither is any sign of its former presence. Probably it first find of such distal placers in the world. We presume that the potential of discovering new chromite placers in the study area is not constrained and all of them can be referred to the new Southern Pre-Ural chromite-bearing ore region.

Funding: This work is supported by the Council of the President of the Russian Federation, grant number MK-857.2021.1.5, and grant RB NOC-GMU-2021. The analytical studies were supported by State Contract of IG UFRC RAS (no. FMRS-2022-0012).

References:

1. Shilo N.A. Teaching on Placer Deposits. Vladivostok. Dalnauka. 2002. 576 p.

2. Griggs A.B. Chromite-bearing sands of the southern part of the coast of Oregon. Geological Survey Bulletin: 945-E. 1945. P. 113–150.

3. Pownceby M., Bourne P. Detrital chrome-spinel grains in heavy-mineral sand deposits from southeast Africa. Mineralogical Magazine. 2006. Vol. 70. P. 51–64.

4. Gujar A.R., Ambre N.V., Iyer, S.D., Mislankar P.G., Loveson, V.J. Placer chromite along south Maharashtra, central west coast of India. Current Science. 2010. Vol. 99. P. 492–499.

5. Abakumov I.V. Revaluation of alluvial deposits residual reserves of boulder chrome ores of the Saranovsky ore field. News of the Ural State Mining University. 2020. Vol. 58. No. 2. P. 74-82.

6. Avdonin V.V., Starostin V.I. Mineral geology: textbook for university students. Moscow. Publishing center Akademiya. 2010. 384 p.

7. Rakhimov I.R., Pushkarev E.V., Gottman I.A. Chromite Paleoplacer in the Permian Sediments at the East Edge of the East European Platform: Composition and Potential Sources. Minerals. 2021. Vol. 11. No. 7. P. 691.

8. Botvinkina L.N. Stratification of sedimentary rocks. Moscow. AS USSR Press. 1962. 542 p. (In Russian)

9. Reineck H.E., Singh I.B. Depositional Sedimentary Environments. New York, Berlin-Heidelberg. Springer-Verlag. 1973. 442 p.

10. Kukharenko A.L. Mineralogy of placers. Moscow. Gosgeoltekhizdat.1961. 318 p. (In Russian).

HOW WIDE WAS ~1000-950 MA MAFIC MAGMATIC EVENT: DATA FROM THE SIBERIAN AND NORTH CHINA CRATONS?

Savelev A.D., Khudoley A.K., Malyshev S.V., Pazukhina A. A.

Saint Petersburg State University, Saint Petersburg, Russia, aleksandr.d.savelev@gmail.com

Abstract. The study considers the distribution of the Meso-Neoproterozoic Sette-Daban complex (Siberia) and its relationship with mafic magmatism in the North China Craton. A comparison of geological, geochemical, paleomagnetic, and isotope data allows us to conclude that a single global event may exist.

Key words: Siberian Craton, North China Craton, Meso-Neoproterozoic, mafic magmatism, paleoreconstruction

During ca. 1000-900 Ma the Siberian Craton was a part of the Rodinia supercontinent. Mesoproterozoic–early Neoproterozoic mafic intrusions are widely distributed on the southeastern margin (in modern coordinates) of the Siberian Craton cutting Meso- and lower Neoproterozoic carbonate and clastic rocks [1]. The majority of the intrusions belong to the ca. 1005-975 Ma Sette-Daban magmatic event. However, sills from the west of the Allakh-Yun and Yudoma rivers yielded Sm-Nd ages of around 950 Ma overlapping within error with the 974 ± 7 Ma U-Pb baddeleyite age, and were likely related to the Sette-Daban event as well [2-4].

Close in age sedimentary rocks and mafic intrusions were also found in the North China Craton, where a set of sills yielded ca. 945 and 920 Ma U-Pb zircon SIMS ages [5]. These Neoproterozoic sills intruded the successions that contain correlative strata that are named Nanfen, Xinxing, and Liulaobei formations in Liaoning, Jiangsu, and Anhui provinces, respectively [5]. At the moment, there are several competing paleotectonic reconstructions of the position of Siberian and the North China cratons in the Meso-Neoproterozoic time [6, 7]. However, in many of those reconstructions, these cratons are quite close. Comparison of geochemical data on mafic intrusions from both cratons has established that they are similar both in composition and in the geodynamic settings. This indicates that intrusions from Siberia and North China may be parts of the same major mafic magmatic event, probably forming a LIP, which fragments are now recognized on several cratons.

Funding: This work is supported by the Russian Science Foundation under grant 19-31-27001.

References:

1. Savelev A.D., Malyshev S.V., Savatenkov V.M., Ignatov D.D., Kuzkina A.D. Meso-Neoproterozoic Mafic Sills along the South-Eastern Margin of the Siberian Craton, SE Yakutia: Petrogenesis, Tectonic and Geochemical Features. Minerals. 2020. Vol. 10. No. 9. Art. 805.

2. Rainbird R.H., Stern R.A., Khudoley A.K., Kropachev A.P., Heaman L.M., Sukhorukov V.I. U-Pb geochronology of Riphean sandstone and gabbro from southeast Siberia and its bearing on the Laurentia-Siberia connection. Earth and Planetary Science Letters. 1998. Vol. 164. No. 3–4. P. 409–420.

3. Pavlov V.E., Gallet Y., Petrov P.Y., Zhuravlev D.Z., Shatsillo A.V. The Ui Group and Late Riphean Sills in the Uchur-Maya Area: Isotope and Paleomagnetic Data and the Problem of the Rodinia Supercontinent. Geotectonics. 2002. Vol. 36. No. 4. P. 278–292.

4. Khudoley A.K., Kropachev A.P., Tkachenko V.I., Rublev A.G., Sergeev S.A., Matukov D.I., Lyahnitskaya O.Y. Mesoproterozoic to Neoproterozoic Evolution of the Siberian Craton and Adjacent Microcontinents: An Overview with Constraints for a Laurentian Connection. In Proterozoic Geology of Western North America and Siberia; Society for Sedimentary Geology: Tulsa, OK, USA. 2007. P. 209–226.

5. Zhao H., Zhang S., Ding J., Chang L., Ren Q., Li H., Yang T., Wu H. New geochronologic and paleomagnetic results from early Neoproterozoic mafic sills and late Mesoproterozoic to early Neoproterozoic successions in the eastern North China Craton, and implications for the reconstruction of Rodinia. GSA Bulletin. 2020. Vol. 132. No. 3–4. P. 739–766.

6. Li Z.X., Bogdanova S.V., Collins A.S., Davidson A., De Waele B., Ernst R.E., Fitzsimons I.C.W., Fuck R.A., Gladkochub D.P., Jacobs J., Karlstrom K.E., Lu S., Natapov L.M., Pease V., Pisarevsky S.A., Thrane K., Vernikovsky V. Assembly, configuration, and break-up history of Rodinia: A synthesis. Precambrian Research. 2008. Vol. 160, No. 1–2. P. 179–210.

7. Ding J., Zhang S., Evans D.A.D., Yang T., Li H., Wu H., Chen J. North China craton: The conjugate margin for northwestern Laurentia in Rodinia. Geology. 2021. Vol. 49. No. 7. P. 773–778.

EVOLUTION OF THE AUSTRALIAN-ANTARCTIC PART OF THE SOUTH EASTERN INDIAN RIDGE IN PALEOCENE – EOCENE

Sergeeva V.M., Leitchenkov G.L.

FSBI «VNIIOkeangeologia», Saint Petersburg, Russia, wanda@list.ru

Abstract. We consider the segment of South Indian Oceanic Ridge (SEIR) between 120˚ and 139˚ E. This segment lies between continental margins of Archean cratons – Gawler (Australia) and Mawson (Antarctica). In the east, this area is bounded by the George V transform fault, and in the west it includes the Australian−Antarctic Discordance (AAD) transform fault system. To identify the features of the formation of the SEIR, the early stage of spreading (83–40 Ma) combined with and shear tectonics in the eastern part of the paleocontinent of Australia-Antarctica are going to be considered.

Key words: South Eastern Indian Ridge, Australian−Antarctic Discordance, slab, spreading, Australia, Antarctica

The work discusses the features of the evolution of the South Indian Oceanic Ridge (SEIR) in the Paleocene–Eocene. The break-up of Australia and Antarctica occurred as a result of the propagation of spreading axes moving towards each other from the Indian and Pacific Oceans. The mode of the interaction (overlapping) of these spreading axes during 65–40 Ma determined the features of the break-up of the Australian-Antarctic craton Mawson-Gawler and the subsequent mode of the opening of the oceanic space of SEIR.

The main attention is given to the origin of the Australian-Antarctic Discordance which represent a segment of SEIR between 120˚ and 128˚ E. It is characterized by a rugged and chaotic morphology of the sea-floor [1] and by a series of closely spaced transform faults with a slight displacement of the spreading axes. The eastern part of the AAD is the most ancient, since the abnormally rough morphology of the sea-floor in this part has been observed since 21/24 chron (~ 50 Ma) [2]. The western structures of the oceanic crust of AAD are sufficiently younger. The Australian-Antarctic Discordance is underlain by the Australian-Antarctic Mantle Anomaly (AAMA) that is interpreted as a slab downwelling in a north-western direction under the basement of the AAD. The AAMA is about 1500 km across and 40-120 km deep [3].

There is a problem with the pre-rift disposition of Australia and Antarctica. The main feature of all models is the mismatch of the conjugate continent-ocean boundaries (COB), which is well observed because of the presence of a wide and elongated gap in the central part of the ancient paleocontinent, or in the overlap of continental margins in the western and eastern regions of Southern Australia and Antarctica [4–6].

The age of the palaeoreconstruction (40 Ma) corresponds to the junction of the Indian and Pacific axes of oceanic spreading with each other and to the final break-up of Australia-Antarctica within the Mawson-Gawler craton. This palaeoreconstruction (Figure 1) also reflects the position of Australia and Antarctica and the time by which the most ancient eastern structures of the AAD were started to form.

The age of 40 million years for reconstruction was chosen by us for several reasons. First, starting from the 18-o chron (40 Ma) the modern ocean spreading regime has been established in the SEIR [7, 8]. Second, the Indian and Pacific axes of spreading have been connected to each other for about 40 Ma. We can conclude, there were no younger tectonic events that could

significantly affect the ocean spreading in the SEIR. It also means that later significant stretching and deformation of the continental margins and of the conjugated COB are unlikely.

In the presented palaeoreconstruction (Figure 1), the gap between the conjugate COB of Australia and Antarctica has significant dimensions – about 1500 x 300 km, which is comparable to the size of AAMA under AAD – 1500 x 500 km [2]. In this work, we propose the model of formation of genetic relations between AAMA (causing the AAD structure) and the gap between conjugated COB of Australia and Antarctica 40 Ma.

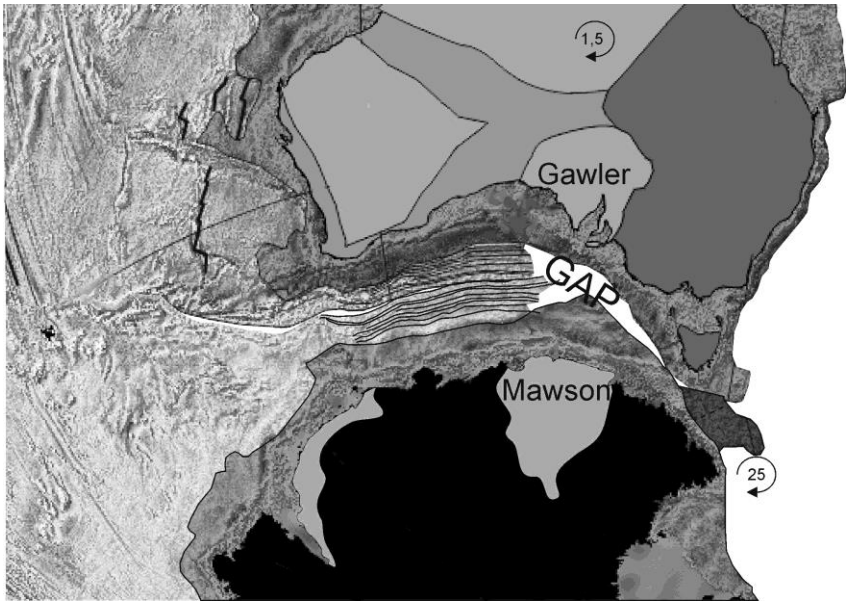

Figure 1 – Palaeoreconstruction of the pre-rifted disposition of Australia and Antarctica by 18-o Chron - 40 Ma (using data from [9])

Funding: This work is supported by the Russian Science Foundation under grant № 16-17-10139.

References:

1. Christie D.M., West B.P., Pyle D.G., Hanan B.G. Chaotic topography, mantle flow and mantle migration in the Australian–Antarctic discordance. Nature. 1998. Vol. 394. P. 637–644

2. Okino K., Matsuda K., Christie D.M., Nogi Y., Koizumi K. Development of oceanic detachment and asymmetric spreading at the Australian-Antarctic Discordance. Geochemistry, Geophysics, Geosystems. 2004. Vol. 5. No. 12. Q12012.

3. Ritzwoller M.H., Shapiro N.M., Leahy G.M. A resolved mantle anomaly as the cause of the Australian-Antarctic Discordance. Journal of Geophysical Research. 2003. Vol. 108. No. B12. 2559.

4. Powell C.M.A., Roots S., Veevers J. Pre-breakup continental extension in East Gondwanaland and the early opening of the eastern Indian Ocean. Tectonophysics. 1988. Vol. 155. No. 1–4. P. 261–283.

5. Royer J.Y., Sandwell D.T. Evolution of the eastern Indian Ocean since the Late Cretaceous: Constraints from Geosat altimetry. Journal of Geophysical Research. 1980. Vol. 94. No. B10. P. 13755–13782.

6. Williams S.E., Whittaker J.M., Muller R. D. (2012): Full-fit reconstructions of the southern Australian Margin and Antarctica – implications for correlating geology between Australia and Antarctica, in Eastern Australasian Basins Symposium IV, Crows Nest, NSW: Conference Action Pty Ltd.

7. Tikku A.A., Cande S.C. The oldest magnetic anomalies in the Australian–Antarctic Basin: Are they isochrons? Journal of Geophysical Research. 1999. Vol. 104. No. B1. P. 661–677.

8. Leitchenkov G.L., Guseva Yu.B., Gandyukhin V.V., Ivanov S.V., Safonova L.V. Structure of the Earth's crust and tectonic evolution history of the Southern Indian Ocean (Antarctica). Geotectonics. 2014. Vol. 48. No. 1. P. 5–23.

9. Sandwell D.T., Muller R.D., Smith W.H.F., Garcia E., Francis R. New global marine gravity model from CryoSat-2 and Jason-1 reveals buried tectonic structure. Science. 2014. Vol. 346. No. 6205. P. 65–67.

MICROSTRUCTURAL ANALYSIS OF A TECONIC FAULT (ON EXAMPLE OF THE PRIMORSKY FAULT OF THE BAIKAL RIFT ZONE)

Svecherevskiy A.D.[1], Ustinov S.A.[1,2], Ostapchuk A.A.[2], Petrov V.A.[1]

[1]Institute of Geology of Ore Deposits, Petrography, Mineralogy and Geochemistry of the Russian Academy of Sciences, Moscow, Russia, svecherevskiy@igem.ru
[2]M.A. Sadovsky Institute for Dynamics of Geosphere of the Russian Academy of Sciences, Moscow, Russia

Abstract. The results of the analysis of microfractures in 15 oriented rock samples collected across the core of the Primorsky Fault of the Baikal Rift Zone are presented. For the automatic detection and analysis of microfractures in images of oriented thin sections, a special technique for microstructural analysis (STMA) was proposed. Petrographic data were compared to the quantitative parameters of microfracture networks. The damage zone of the Primorsky Fault including three clusters characterized by different porosity, permeability and deformation type, was identified.

Keywords: microstructural analysis, microfracture mapping, Primorsky Fault, tectonite, Baikal Rift Zone.

Microstructural analysis in geology is mainly used to establish the spatial and temporal relationship between microfracture ensembles of different genetic types, as well as to reconstruct the stress–strain fields, which act within small volumes of mineral aggregates [1, 2]. The technique of traditional microstructural analysis is reduced to statistical measurements of the position of certain crystallographic or optical elements of grains of some minerals in the rock [3]. However, the main problem of the traditional microstructural analysis method is the technical complexity of its implementation, the lack of a computer-automated software, the need to obtain a large amount of data and the extremely ambiguous interpretation of the data.

Modern methods of microstructural analysis always rest on the determination of geometric parameters of all microstructures, for which its number can reach hundreds of thousands in a single oriented thin section. Obviously, without the use of any special technique of automatic detection, the solution to this problem is not only technically complex, but is also time-consuming. The research methodology is aimed at identifying the heterogeneity of the fault zone based on the analysis of the spatial distribution of microfracture parameters. For the automatic detection and digitalization of microfractures in images of oriented thin sections and automatized analysis of objects at the microscale, a special technique for microstructural analysis (STMA) was proposed.

Oriented rock samples were taken from outcrops across the strike of the Primorsky deep Fault of the Baikal Rift Zone (Irkutsk region, Russia) in the area of the Sarma river. The Primorsky Fault is the largest and best-documented neotectonic structure [4, 5] in the region. It belongs to the Obruchev fault system. The main thrust event occurred in the Paleozoic [6], but the compression structures became active again in later tectonic events. The age of the last activity remains poorly established and varies from Mesozoic to Miocene–Pliocene in different models [6, 7]. The setting of neotectonic regional stress changed from early orogenic shear strike-slip about 30 million years ago to late orogenic extension about 3 million years ago [8].

The main trace of the Primorsky Fault is geomorphically expressed as a ledge and is available for geological surveys over 200 km.

The selected and analyzed samples of rocks are represented by numerous varieties of predominantly metamorphic and igneous rocks, as well as their metasomatically altered varieties. Shales, gneissose granite, plagiogranites, amphibolites and gabbro, varied in mineral composition, were distinguished. The studied rock samples are classified as mylonites, blastomylonites, cataclasites, blastocataclasites and host rocks, which were not subjected to intensive deformations. Among other characteristics, the type of deformation was assessed, and metamorphic and metasomatic changes were characterized.

In the first stage of STMA, images of thin sections were mapped in a local rectangular coordinate system using QGIS. At the second stage, a directional filtering of the image was carried out. Four filtered images were produced by ENVI software related to the directions N-S, NE-SW, E-W and NW-SE. In the third stage, the automatic extraction of lineaments (microfractures) using PCI Geomatica was carried out.

The main quantitative parameters of the identified microfractures including number of objects (microfractures), cumulative length, length of each microfracture, mean aperture of each microfracture, length of each straight segment of each microfracture, strike azimuth of each straight segment of each microfracture, number of intersections of microstructures, studied area of thin section were calculated in QGIS. The spatial distribution of microfractures over the area of the thin section was analyzed by constructing density maps. Rose diagrams of microfractures were built according to the values of their spatial orientation and considering their lengths.

In this study, fluid transfer properties are used as indicators of structural features of rock samples and probable heterogeneity of the fault zone. Calculated porosity and permeability are in agreement with the results of petrographic analysis. It allows the identification of zones that characterize the heterogeneity of the fault. A preliminary scheme of heterogeneity of the Primorsky Fault was created. Three zones, which are characterized by different values of porosity and permeability, types of deformations and type of tectonites, were identified.

Funding: This work is supported by the Russian Science Foundation under grant 20-77-10087.

References:

1. Lespinasse M., Désindes L., Fratczak P., Petrov V. Microfissural mapping of natural cracks in rocks: Implications for fluid transfers quantification in the crust. Chemical Geology. 2005. Vol. 223. P. 170–178.

2. Duarte M.T., Liu H.Y., Kou S.Q., Lindqvist P.A., Miskovsky K. Microstructural modeling approach applied to rock material. Journal of Materials Engineering and Performance. 2005. Vol. 14. P. 104–111.

3. Lukin L.I.; Chernyshev V.F.; Kushnarev I.P. Microstructural Analysis. Moscow. Nauka. 1965. 124 p. (In Russian).

4. Cheremnykh A.V., Cheremnykh A.S., Bobrov A.A. Faults in the Baikal region: morphostructural and structure-genetic fea-tures (case study of the Buguldeika fault junction). Russian Geology and Geophysics. 2018. Vol. 59. No. 9. P. 1100–1108.

5. Cheremnykh A.V., Burzunova Yu.P., Dekabryov I.K. Hierarchic features of stress field in the Baikal region: Case study of the Buguldeika Fault Junction. Journal of Geodynamics. 2020. Vol. 141–142. Art. 101797.

6. Aleksandrov V.K. Thrusts in the Baikal Region. Novosibirsk. Nauka. 1990. 102 p. (In Russian).

7. Gladkochub D.P., Donskaya T.V., Wingate M.T.D., Poller U., Kr¨oner A., Fedorovsky V.S., Mazukabzov A.M., Todt W., Pisarevsky S.A. Petrology, geochronology, and tectonic implications of ca. 500 Ma metamorphic and igneous rocks along the northern margin of the Central-Asian Orogen (Olkhon terrane, Lake Baikal, Siberia). Journal of the Geological Society of London. 2008. Vol. 165. P. 235–246.

8. Delvaux D., Moyes R., Stapel G., Petit C., Levi K., Miroshnitchenko A., Ruzhich V., San'kov V. Paleostress reconstruction and geodynamics of the Baikal region, Central Asia. Part II: Cenozoic rifting. Tectonophysics. 1997. Vol. 282. P. 1–38.

LITHOGEOCHEMICAL CHARACTERISTICS AND GEODYNAMIC OF THE UPPER PALEOZOIC YAKSHA FORMATION (WESTERN TRANSBAIKALIA)

Tashlykov V.S

Dobretsov Geological Institute of the Siberian Branch of Russian Academy of Sciences, Ulan-Ude, Russia, foxjer@mail.ru

Abstract. The paper considers the petrographic and lithogeochemical features of the terrigenous rocks of the Yaksha Formation. Based on the data obtained, it was established that the rocks of the Yaksha Formation belong to the graywackes. Lithogeochemical and petrographic features indicate the presence of volcanogenic material in the source area. The lower member of the Yaksha Fromation was accumulated in the conditions of a relatively shallow shelf coast. The upper member of the Yaksha Formation is in deeper water conditions. The most probable geodynamic setting for the formation of terrigenous deposits of the Yaksha Formation was an active continental margin or island arc.

Key words: the Yaksha Formation, terrigenous rocks, sedimentation environments, lithogeochemical characteristics, Upper Paleozoic.

The Bagdarin Synform occupies the central and northern parts of the Vitim Plateau. Structurally, the synform is considered as a graben-syncline with a complex fold-cover structure formed at the end of the Early Hercynian stage [1, 2]. Precambrian metamorphic rocks and weakly metamorphosed sediments of the Upper Paleozoic ($D–C_{21}$) are widespread within its limits. Ideas about the age, volume and stratigraphic position of synform formations, the history of their sedimentation and geodynamic evolution, are still debatable. One of the least studied aspects is the material composition of sedimentary complexes. Identification of the environments of accumulation of the Upper Paleozoic terrigenous rocks of the Bagdarin synform will make a significant contribution to the reconstruction of the history of the formation of the West Transbaikal region and the development of geodynamic models of the evolution of the Central Asian and Mongolian-Okhotsk fold belts.

The Yaksha Formation (D_3jk), with a total thickness of 1300 m, is composed of terrigenous-carbonate rocks and is subdivided into the lower and upper members of the Yaksha Formation [1–3]. The lower member of the Yaksha Formation (460 m thick) is essentially carbonate, composed of silty limestones, siltstones, and shales. The upper member of the Yaksha Formation is essentially terrigenous (850 m thick) and is represented by the rhythmic intercalation of sandstones, argillaceous and carbonaceous shales, siltstones, siltstones, with limestone interbeds. Sandstones and siltstones contain quartz, plagioclase, magnetite, apatite, and epidote. The cement of terrigenous rocks is chlorite. The paleontological characteristics of the Yaksha Formation (corals, conodonts, algae, stromatoporoids, bryozoans, crinoids, chitinozoans, myospores) determine its stratigraphic position in the Upper Devonian within the Fransian and Famennian ages [1]. According to the petrographic and lithochemical characteristics, the terrigenous rocks of the Yaksha Formation correspond to graywackes. According to the hydrolyzate modulus ($HM = (Al_2O_3 + TiO_2 + Fe_2O_3 + FeO + MnO)/SiO_2$), terrigenous rocks are classified as siallites: from low-hydrolyzate hyposiallites (0.30–0.35) to high-hydrolyzate supersiallites (0.49–0.55). [4, 5] The type of siallites and siferlites can include volcanic-sedimentary and even volcanic rocks, for which the absolute content of MgO (>3%) is used for recognition. The values of the titanium modulus ($TM = TiO_2/Al_2O_3$) make it possible to classify

the rocks as normo-titanium (0.030–0.070) and super-titanium (0.071–0.100) siallites. According to Yudovich and Ketris [6], the super-titanium composition can be attributed to volcanomictic sediments and oceanic rocks, since the basic volcano- and pyroclastic admixture has a high titanium content. According to lithofacies and geochemical data, the lower member the Yaksha Formation accumulated under conditions of a relatively shallow shelf coast, with an insignificant input of terrigenous clastics, while the upper member of the Yaksha Formation accumulated in deeper water, neritic conditions of the open shelf margin [5]. Reconstruction of geodynamic settings allows us to conclude that terrigenous rocks are associated with an active continental margin or continental island arc [7]. This corresponds to the range of compositions of volcanic rocks of the Kuril–Kamchatka island arc.

The obtained data suggest that the Yaksha Formation includes sediments of predominantly greywacke composition. The lithogeochemical and petrographic features of this stratosubdivision testify to the presence of volcanogenic material in the source area. The most probable geodynamic setting for the formation of terrigenous deposits of the Yaksha Formation was an active continental margin or island arc.

References:

1. Minina O.R., Doronina N.A., Nekrasov G.E., Vetluzhskikh L.I., Lantseva V.S., Aristov V.A., Naugolnykh S.V., Kurylenko A.V., Khodyreva E.V. Early Hercynides of the Baikal-Vitim fold system (Western Transbaikalia). Geotectonics. 2016. Vol. 50. No. 3. P. 276–294.

2. Ruzhentsev S.V. Minina O.R., Nekrasov G.E., Aristov V.A., Golionko B.G., Doronina N.A., Lykhin D.A. Baikal-Vitim fold system: structure and geodynamic evolution. Geotectonics. 2012. Vol. 46. No. 2. P. 87–110.

3. Shelgachev K.M., Shatkovskaya L.V., Kurbatova E.I., Minina O.R., Khokhlov E.V. State geological map of the Russian Federation, scale 1:200,000. Sheet N-49-XVIII. 2011.

4. Pettijohn F.J. Sedimentary rocks (translated from English). Moscow. Nedra. 1981. 751 p.

5. Tashlykov V.S, Minina O.R, Lithogeochemical characteristics of the Upper Devonian Yaksha Formation (Western Transbaikalia), Vestnik of Geosciences. 2020. Vol. 5. No. 305. P. 17–23.

6. Yudovich Ya.E., Ketris M.P. Fundamentals of lithochemistry. St. Petersburg. Nauka. 2000. 479 p.

7. Bhatia M.R. Plate tectonics and geochemical composition of sandstones. The Journal of Geology. 1983. Vol. 91. No. 6. P. 611–627.

CONDITIONS AND FEATURES OF THE FORMATION OF METABASITE AND METATERRIGENOUS ROCKS OF THE TELETSK ZONE OF GORNY ALTAI

Zindobryi V.D.[1], *Buslov M.M.*[2]

[1]Saint Petersburg State University, Saint Petersburg, Russia, viktor_zindobryi@mail.ru
[2]V.S. Sobolev Institute of Geology and Mineralogy, Novosibirsk, Russia

Abstract. The paper presents the data of petrographic, geochemical and mineralogical studies of metabasite rocks of the Teletsk zone of Gorny Altai. It is shown that the material composition of metabasalts belongs to basalts oceanic, terrigenous schists - basaltic andesites and andesites of island arcs. Chemical analysis of amphiboles showed that it belongs to calcium and is zoned: crystal compositions vary from tremolites (in the centers) to hornblende and pargasites (on the periphery). The obtained set of data allows us to consider that the studied rocks are part of an accretionary wedge, in which oceanic basalts and turbidites, formed as a result of the destruction of rocks in the island arc.

Key words: amphibole, basalt, terrigenous schist, Gorny Altai, geochemistry

In this paper, we consider the features of the material composition of the metabasites and metaterrigenous rocks of the Teletsk shear zone, in the eastern part of the Gorny Altai and extending for over 300 km, from Lake Teletskoye in the north to the village of Aktash in the south.

In the structure of the eastern part of Gorny Altai, three large blocks are currently distinguished: Gorny Altai, West Sayan and Teletsk, separated from each other by the large North Sayan, Teletsk-Bashkaus, Shapshal and other smaller fault collision-shear zones [1–4].

As a result of the petrographic studies of rocks from the Teletsk zone, among the metamorphosed volcanic and terrigenous rocks, two types of rocks were distinguished according to the mineral composition and degree of metamorphism:

1. Metabasalts, represented by plagioclase and plagioclase-amphibole porphyrites and aphyric basalts, metamorphosed under greenschist facies conditions and retaining primary igneous structures.

Aphyric metabasalts, which do not have pronounced phenocrysts, contain crystals of amphibole, epidote, chlorite, plagioclase and quartz in their composition, and to a greater extent, compared to porphyrites, are transformed into greenschist facies of metamorphism.

2. Terrigenous schists are clearly banded and are represented by quartz, amphibole, chlorite; quartz, amphibole, epidote and quartz, amphibole, biotite schists, formed under epidote-amphibolite facies conditions.

Geochemically, terrigenous schists and metabasalts are represented by several types of protoliths. Most plots of rare-earth elements (REE) normalized to chondrite [5] for metabasalts with preserved igneous structures and terrigenous schists show slightly sloping REE distribution spectra slightly enriched in light REE (LREE) relative to heavy REE (HREE) – $(La/Yb)_N$ = 2.40 on average. On multielement diagrams, they also form slightly negative spectra with different degrees of Rb, Cs, Ba, Th, and K differentiation: weakly expressed in metabasalts and more distinct in metamorphic rocks. In addition, the metabasalts show a Ti-minimum, while the

metamorphic rocks show P-minimum. Such spectra are characteristic of oceanic basalts of the enriched mid-ocean ridge basalts (E-MORB) type.

In addition to mid-ocean ridge basalts, the Teletsk zone contains metamorphic rocks, the protolith of which was other types of oceanic basalts. One sample has distribution spectra of REE close to ocean island basalts (OIB) (metabasalt B-17-121) with $(La/Yb)_N$ = 7.42, and the second one is close to ocean plateau basalts (OPB) (metabasalt B-17-128) with $La/Yb)_N$ = 1.57. In the multielement diagram, metabasalt B-17-121 demonstrates clearly manifested K- and P-minimums, and the slope of the spectrum is generally strongly negative. It can be assumed that OIB served as the protolith for this sample. Metabasalt B-17-128 on the multielement diagram does not have clearly expressed anomalies and the spectrum slope in any direction, therefore, the OPB probably served as a protolith for it.

Terrigenous schists are rocks with negative distribution spectra of REE with high LREE/HREE ratios close to OIB – $(La/Yb)_N$ = 6.33 on average. They also have a strong negative Eu-anomaly, indicating plagioclase fractionation. On the multielement diagrams, the studied rocks demonstrate strong differentiation of Rb, Cs, Ba, Th, K, increased values of the LILE/HREE ratio, and distinct Nb-, Ta-, P-, and Ti-minimums. Based on these data, it can be assumed that these rocks formed as a result of destruction an calc-alkaline basaltic andesites and andesites of island arcs.

The study of amphiboles from these rocks showed that they are zonal and, according to the nomenclature [6], with Na_B values on average 0.1–0.2 belong to calcium amphiboles. The compositions of the central parts of the crystals according to the ratio (Na+K+Ca) and (Al+Fe) correspond to tremolites and low-alkaline magnesian hornblendes, and the periphery – to high-alkaline hornblendes and pargasites.

Based on this, it should be assumed that these rocks are part of the accretionary complex, which combines basalts of the oceanic crust and turbidites of the deep-sea trench as products of destruction of island arc.

References:

1. Buslov M.M., Sintubin M. Structural evolution of the Teletsk zone of the Altai-Sayan folded region. Geology and Geophysics. 1995. Vol. 36. No. 10. P. 91–98.

2. Smirnova L.V. Structural-kinematic and metamorphic evolution of the Teletsk-Bashkaus shear zone in the Teletsk region (Gorny Altai). Dissertation for the degree of candidate of geological and mineralogical sciences. 2002. 165 p.

3. Buslov M.M., Watanabe T., Smirnova L.V., Fujiwara I., Iwata K., de Grave I., Semakov N.N., Travin A.V., Kiryanova A.P., Kokh YES. The role of shifts in the Late Paleozoic-Early Mesozoic tectonics and geodynamics of the Altai-Sayan and East Kazakhstan folded regions. Geology and Geophysics. 2003. Vol. 44. No. 1–2. P. 49–75.

4. Dehandschutter B., Vysotsky E., Delvaux D., Klerkx J., Buslov M.M., Selesnev V.S., De Batist M. Structural evolution of the Teletsk graben (Russia Altai). Tectonophysics. 2002. No. 351. P. 139–167.

5. Sun S., McDonough W.F. Chemical and isotopic systematics of oceanic basalts: implications for mantle composition and processes. Geological Society of London, Special Publication. 1989. Vol. 42. P. 313–345.

6. Leake B.E., Woolley A.R., Arps C.E. S., Birch W.D., Gilbert M.C., Grice J.D., Hawthorne F.C., Kato A., Kisch H.J., Krivovichev V.G., Linthout K., Laird J., Mandarino J., Maresch W.V., Nickel E.H., Rock N.M.S., Schumacher J.C., Smith D.C., Stephenson N.C.N., Ungaretti L., Whittaker E.J.W., Youzhi G. Nomenclature of amphiboles: Report of the Subcommittee on Amphiboles of the International Mineralogical Association Commission on New Minerals and Mineral Names. Mineralogical Magazine. 1997. Vol. 61. P. 295–321.

Section PALEONTOLOGY AND STRATIGRAPHY

STATISTICAL METHODS IN PALEONTOLOGY: APPLICATOINS TO MORPHOLOGY AND BIODIVERSITY OF AN EARLIEST CRETACEOUS BELEMNITES OF NORTHERN SIBERIA

Efremenko V.D.[1,2]

[1]A.A. Trofimuk Institute of Petroleum Geology and Geophysics, Novosibirsk, Russia, efremenkovd@ipgg.sbras.ru
[2] Novosibirsk State University, Novosibirsk, Russia

Abstract. The possibility of synonymy of the belemnite species Boreioteuthis hauthali (Blüthgen, 1936) and B. freboldi (Blüthgen, 1936) was evaluated using cluster analysis. Using rarefaction and extrapolation (Hill numbers), the dynamics of belemnite species diversity in the Anabar region of northern Siberia in the Ryazanian and Valanginian was analyzed, independent on the number of observed individuals.

Key words: statistics, belemnites, Cretaceous, paleontology

Statistical methods have been previously applied to the Jurassic belemnites of the family Cylindroteuthididae [1]. For the Cretaceous cylindroteuthidids, they are applied for the first time. The application of statistical methods is mainly due to the possibility of solving those problems that cannot be solved by other methods or considerably simplify their solution.

One of the most important purposes of using of statistics in paleontology is to solve systematic problems on large samples. The task solved in context of this work is to consider the possible synonymy of the Early Cretaceous Boreal species Boreioteuthis hauthali (Blüthgen, 1936) and B. freboldi (Blüthgen, 1936). Various researchers either separate these species [2] or combine them under the name B. hauthali [3]. This is due to the great similarity of the rostrum morphology of these species. To solve the problem, measurements of rostra (in accordance with the adopted methodology [1]) studied from northern Siberia were loaded into the PAST program. The number of specimens considered was 53, and the parameter matrix contained the values of three relative parameters, PA%, LL%, and ll%. The table also included measurements from the literature [2,3]. To consider the differences, a similarity plot was constructed using the UPGMA algorithm, which is the most suitable according to the results of tests on known samples. As can be seen, there is neither a clear division of the sample into two groups on the graph, nor a separation of rostra identified as B. freboldi from B. hauthali (Fig. 1), and this is evidence in favor of the synonymy of these species. The graph shows the isolation of several rostra identified mainly as B. freboldi, but this rather indicates that they are a separate species, distinct from B. freboldi and B. hauthali. Of course, cluster analysis should not be determinative in systematic constructions. However, the data obtained allow us to work with large samples, finding regularities in them that are not detectable by standard methods.

The next aspect of the work is the study of biodiversity. In order to estimate the biodiversity by summarizing data from several sites, it is not sufficient to simply count the total number of species per stratigraphic unit (e.g., ammonite zone). This can lead to misleading data

due to the different number of observed individuals per unit. Stratigraphic units characterized by more fossil finds will show greater diversity. To avoid this problem, it is necessary to average the diversity in all units by the same number of finds. A sample-size-based extrapolation or rarefaction of Hill numbers was performed using an algorithm in the iNEXT Online program [4]. Fourteen finds were chosen as the average value to estimate the dynamics of species diversity of belemnites (generalized to an ammonite zone) in the Anabar region for the Ryazanian–Valanginian. As it turned out, the data obtained should be extrapolated for half of the ammonite zones (Ryazanian), and they should be rarefied for the rest half (Valanginian). The plot constructed using the iNEXT package shows differences from the standard diversity plot (simple summation of observed species). In particular, fluctuations in diversity are not detected for the Valanginian when using a unified standardization method. Despite fewer finds of belemnites in the Ryazanian, a greater species diversity is predicted, but with wide confidence intervals. Thus, the number of finds has a great influence on the apparent diversity and can lead to incorrect conclusions.

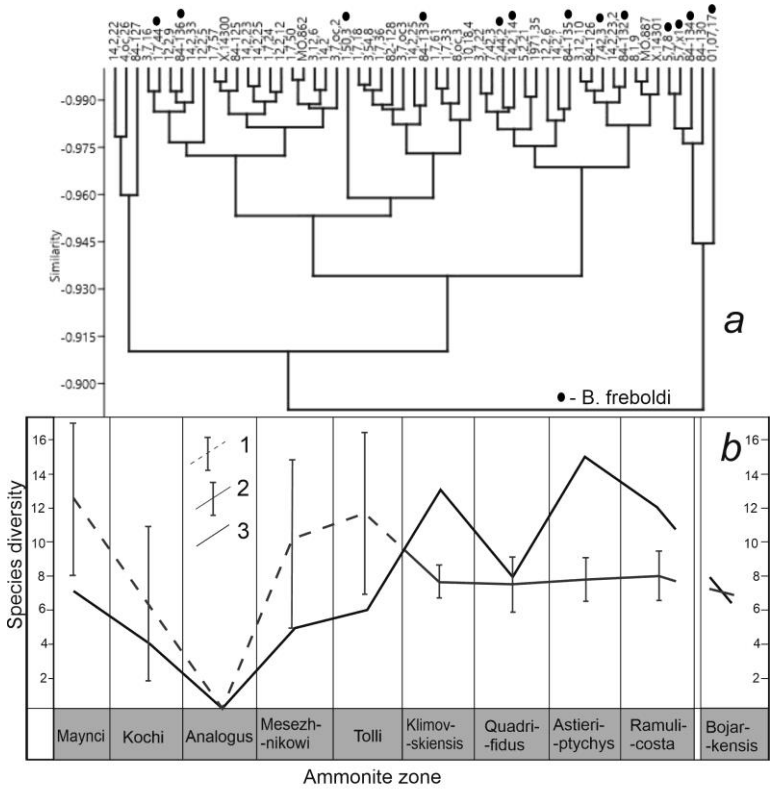

Figure 1 – The result of clustering of belemnite rostra assigned to the species Boreioteuthis freboldi (Blüthgen, 1936) and B. hauthali (Blüthgen, 1936) (a), and belemnite species diversity curves for the Ryazanian–Valanginian of Anabar region (b): 1–2 – sample-size-based extrapolation (1) and rarefaction (2) with confidence intervals; 3 – total number of observed species.

Funding: This work is supported by project FWZZ-2022-0004 and is a contribution to project IGCP 679.

References:

1. Dzyuba O.S. Belemnites (Cylindroteuthidae) and biostratigraphy of the Middle and Upper Jurassic of Siberia. Novosibirsk. GEO. 2004. 203 p.

2. Sachs V.N., Nalnjaeva T.I. Upper Jurassic and Lower Cretaceous belemnites of the northern USSR. The genera Pachyteuthis и Acroteuthis. Moscow-Leningrad: Nauka. 1966. 260 p.

3. Doyle P., Kelly S.R.A. The Jurassic and Cretaceous belemnites of Kong Karls Land, Svalbard. Oslo: Norsk Polarinstitutt. 1988. 77 p.

4. Hsieh T.C., Ma K.H., Chao A. iNEXT: an R package for interpolation and extrapolation of species diversity (Hill numbers). Methods in Ecology and Evolution. 2016. Vol. 7. P. 1451–1456.

MIDDLE JURASSIC PALEOPHYTOGEOGRAPHY OF SIBERIAN PALEOFLORAL REGION

Frolov A.O.

Institute of the Earth's crust SB RAS, Irkutsk, Russia, frolov88-21@yandex.ru

Abstract. In the Middle Jurassic the Siberian paleofloral region included the North Chinese and West Siberian provinces. Within the North Chinese province there were Fergana and Ordos subprovincies. The Ural, Predyenisey and Angara-Viluy subprovinces are distinguished within the West Siberian province. Axial groups of plants, which characterized by frequent occurrence in the geological record, wide geographical distribution, and pronounced endemism at the family, generic, and species levels, were used to distinguish subprovinces.

Key words: paleofloristic zoning, paleofloral subprovincies, species endemism level, migratory species.

In Eurasia in the Early and Middle Jurassic, there were two large paleofloral regions: Euro-Sinian and Siberian [1]. The Siberian region included the West Siberian and North Chinese provinces [2]. Axial groups of plants are used for detailed paleofloristic zoning. They are characterized by frequent occurrence in the geological record, wide geographical distribution, and pronounced endemism [3]. The ferns Coniopteris, Cladophlebis, representatives of orders Ginkgoales, Leptostrobales, and conifers conditionally ascribable to the family Pinaceae (Pityophyllum, Pityospermum, Schizolepis) are the axial groups in the Early and Middle Jurassic floras of the West Siberian province. In addition to the taxa listed above, the cycads (Ctenis, Nilssonia), bennettites (Anomozamites, Pterophyllum) and Voltziaceae conifers (Ferganiella, Lindleyocladus, Podozamites) are the axial groups for the even-aged floras of the North China Province [4]. Migratory species from the Euro-Sinian region take a special place in the Jurassic floras of Siberian region: ferns (Clatropteris, Phlebopteris, Todites), bennettites (Nilssoniopteris, Ptilophyllum, Otozamites) and conifers (Brachyphyllum , Pagiophyllum). When distinguishing subprovinces, the attention was paid to the migratory species and endemics presence in floras as part of axial groups.

The North Chinese province included the Fergana and Ordos subprovincies [4]. The Fergana subprovince unites the Middle Jurassic floras of the Fergana and Issyk-Kul depression, the Karatau and Angren ridges. These floras have a high level of species endemism as part of axial groups (43% of total species). Endemics are present among the Coniopteris, Cladophlebis, Ctenis, Nilssonia Anomozamites, Pterophyllum, Nilssoniopteris, Ginkgoites, Sphenobaiera, Eretmophyllum, Pseudotorellia, Czekanowskia, Phoenicopsis, Ferganiella, Podocarpophyllum genera. The Leptostrobales and Ginkgoales are characterized by the highest species endemism. And in the latter there is an endemic genus Nagrenia. The participation of migratory species from the Euro-Sinian region is relatively small (12% of total species). They are represented by ferns (Todites, Clatropteris, Gonatosorus, Marattiopsis, Osmundopsis), bennettites (Nilssoniopteris, Anomozamites, Pterophyllum, Williamsonia), Caytoniales (Sagenopteris) and Cheirolepidiaceae conifers (Pagiophyllum).

The Ordos subprovince includes the Middle Jurassic floras of Northern China (Qinghai, Gansu, Shaanxi, Shanxi, Hebei, Liaoning and Inner Mongolia). The species endemism level is

high in the flora (44% of total species). Endemics are present among the ferns (Coniopteris, Cladophlebis), cycads (Nilssonia), bennettites (Anomozamites, Pterophyllum, Wielandiella, Weltrichia), Ginkgoales (Ginkgoites, Sphenobaiera, Pseudotorellia, Yimaia, Vittifoliolum). A smaller number of endemics is observed among Leptostrobales. Migrants from the Euro-Sinian region make up 5% of the total number of species. They are represented by ferns (Marattia, Todites), bennettites (Nilssoniopteris) and conifers (Brachyphyllum).

The Ural, Predyenisey and Angara-Viluy subprovinces are distinguished within the West Siberian province [4]. The Ural subprovince unites the Middle Jurassic floras of the the Alakul depression, Turgai, Maikyuben, Karaganda and, probably, Pechora and Dzhungar Basins. The flora of subprovince contains endemics (26%) and migrants (28%) as a part of axial groups. The highest endemism level is observed in Cladophlebis ferns and Leptostrobales. Unlike the even-aged floras of the Predyenisei and Angara-Vilyui subprovinces, migratory species from the Euro-Sinian region and especially from the North China province of the Siberian region are very importance here. Migrants are dominated by ferns Coniopteris, Todites, Cladophlebis, to a lesser extent cycads (Nilssonia, Taeniopteris) and bennettites (Anomozamites).

The Predyenisei subprovince includes the floras of Western Siberia and Kuznetsk Basin. The species endemism level is 32%. The largest number of endemics is observed in the composition of the order Leptostrobales, and especially in the genus Phoenicopsis. The migratory species are large (20% of total species). However, the natives of the North China province of the Siberian region predominate over the species of the Euro-Sinian region. The ferns (Coniopteris, Cladophlebis) and cycads (Nilssonia) are most diverse among the migratory species.

The Angara-Vilyui subprovince in the Middle Jurassic unites the floras of the Kansk, Irkutsk, Ulugkhem, Lena and South Yakutia Basins. The endemics is observed in ferns (Coniopteris, Osmunda, Cladophlebis, Raphaelia), Gingoales (Baiera, Sphenobaiera, Ginkgoites, Leptotoma, Pseudotorellia, Eretmophyllum) and Leptostrobales (Czekanowskia, Phoenicopsis). Unlike the Middle Jurassic flora of the Predyenisei subprovince, in which the Leptostrobales endemic species prevail in the genus Phoenicopsis, a species endemism of the genus Czekanowskia is more developed in this flora. The migratory species in the flora of the Angara-Vilyui subprovince are not large (9% of total species), compared with other subprovinces of the West Siberian province. Probably the composition of thermophillous migratory species was affected by the northernmost location of the Angara-Vilyui subprovince. Migrants are represented by ferns (Phlebopteris, Coniopteris spectabilis, Cladophlebis), bennettites (Anomozamites) and conifers (Pagiophyllum).

References:

1. Vakhrameev V.A. Jurassic and Cretaceous Floras and Climates of the Earth. Cambridge. Cambridge University Press. 1991. 340 p.

2. Kiritchkova A.I., Kostina E.I., Bystritskaya L.I. Phytostratigraphy and Flora of the Jurassic of Western Siberia. St. Petersburg. Nedra. 2005. 378 p.

3. Ignatiev I.A. Princeples and methods of land palaeofloristic zonation in the Palaeozoic. In book: Biosphere–ecosustem–biota in the Earth history: paleobiogeographic aspects. To the centenary of Academician V.V. Menner. Moscow. Nauka. 2005. P. 113–132.

4. Frolov A.O., Mashchuk I.M. Jurassic flora and vegetation of the Irkutsk Coal Basin. Irkutsk. V.B. Sochava Institute of Geography SB RAS Publishers. 2018. 541 p.

ELEMENTAL CHEMOSTRATIGRAPHY AS A SEQUENCE STRATIGRAPHICAL TOOL (A CASE STUDY FROM THE NORTH-EASTERN ULYANOVSK-SARATOV TROUGH OF THE EASTERN RUSSIAN PLATFROM)

Mohammad N.[1,2], *Zorina S.O.*[1]

[1] Kazan Federal University, Institute of Geology and Petroleum Technologies, Kazan, Russia
nosheen.g.mohammad@gmail.com
[2] Damascus University, Damascus, Syria

Abstract. The element geochemical ratios can be exploited for high-frequency sequence stratigraphic division of the Mesozoic deposits of the Ulyanovsk-Saratov Trough. Based on the terrigenous input proxies (Al, K, and Ti), Si/Al, Ti/Al, Zr/Al, and Si/Zr ratios, sequence stratigraphy framework comprising transgressive-regressive cycles is constructed. The Sr/Ba, Ca/Mg, Fe/Mn, and Rb/Ca ratios were chosen as markers for facies alterations, physical and chemical conditions including water salinity and sediment transport distance. Chemostratigraphy, which may be applied to various fine-grained successions, is used to support its geological history (including sedimentation patterns and a local record of relative sea level).

Key words: sequence stratigraphy, high-frequency sequence, Chemostratigraphy

The study area is located on the eastern Russian Platform, which was covered by an epeiric sea during the Late Jurassic – Early Cretaceous and acted as a strait between northeastern Peri-Tethys and the Boreal-Arctic Sea. It is part of the 850-kilometer-long Ulyanovsk-Saratov Trough, which is filled with the Middle–Late Jurassic, Cretaceous, and Paleogene deposits [1]. The Tatar-Shatrashany borehole is located 3 km to the north-east of the Tatar Shatrashany village (Drozhzhanovsky district, the Republic of Tatarstan). The study section comprises the Upper Jurassic to the Lower Cretaceous succession of marine mudrocks interbedded by sandstones, marlstones, and black shales (Fig. 1).

Major and trace element geochemical analyses using inductively coupled plasma mass-spectrometry (ISP-MS) and X-Ray fluorescence analysis (XRF) were used to determine the sequence stratigraphy, sea-level curves, and geochemical features in the Upper Jurassic–Lower Cretaceous deposits of the north-eastern Ulyanovsk–Saratov Trough. In total, more than 100 samples were examined (Fig. 1).

Principal component analysis was utilized to direct relevant geochemical proxies and elements. Based on the terrigenous input proxies (Al, K, and Ti), the Si/Al ratio, the Ti/Al ratio, the Zr/Al ratio, and the Si/Zr ratio, a sequence stratigraphic framework consisting of transgressive-regressive cycles is created [2]. Where Maximum flooding surface (MFS) is defined as the point at which the terrigenous elements are at their lowest, the Si/Al ratio is greatest, and the Ti/Al and Zr/Al ratios are decreasing. This would signify a greater relative sea level since less terrigenous material is being deposited, as well as enhanced biogenic silica or lower clastic dilution.

The ratios Sr/Ba, Ca/Mg, Fe/Mn, and Rb/Ca were used as facies change markers in this study, these ratios might be utilized to determine physical and chemical factors like water salinity and sediment transport distance [3, 4]. The succession of sedimentary rocks may be separated into elemental ratios, each of which has a unique set of characteristics.

The geochemical elemental ratio data demonstrate that around the Maximum Flooding Surface (MFS), the ratios Rb/Ca and Fe/Mn are quite low, whereas the ratios Ca/Mg and Sr/Ba are generally high. While at the Sequence Boundary (SB), the Ca/Mg and Sr/Ba ratios are quite low, the Rb/Ca and Fe/Mn ratios are very high. These characteristics can be utilized to identify high-frequency sequence division. The main results that Five second order sequences and lots of those of the third-order were distinguished in the Mesozoic succession of the Ulyanovsk-Saratov Trough depending on the geochemical data which has also been proven by correlation with ammonite biostratigraphic zones [5, 6].

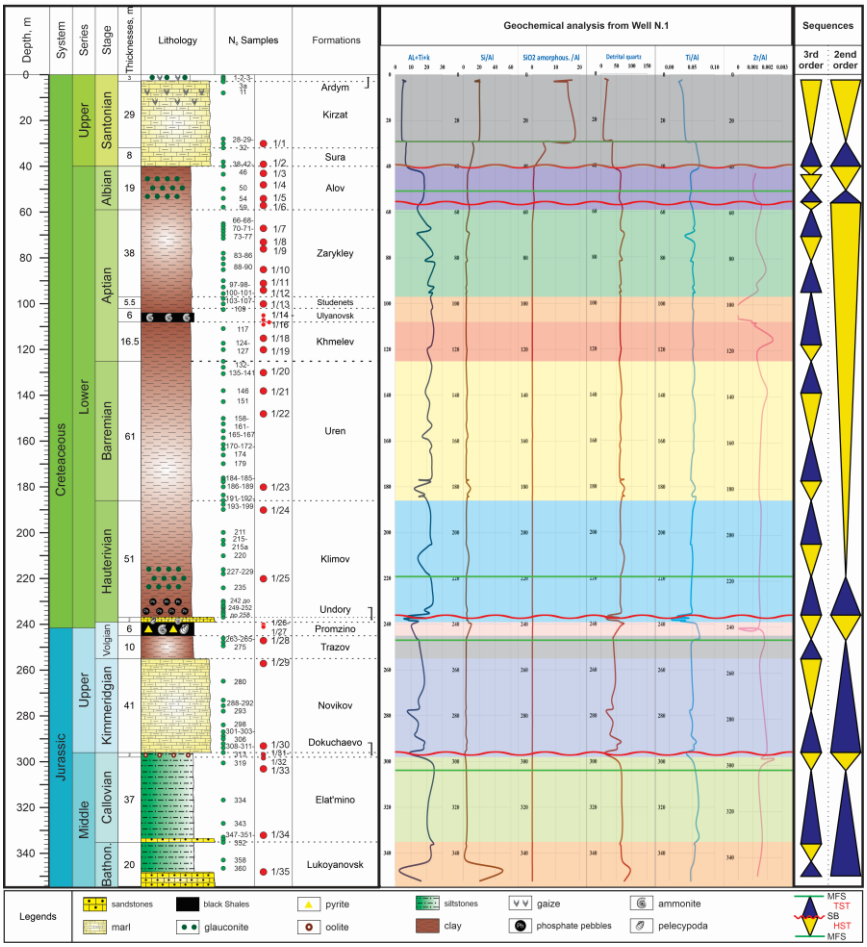

Figure 1 – Stratigraphic scheme of the Tatar-Shatrashany well with Geochemical analysis and sequences.

References:

1. Baraboshkin E. Y., Alekseev A. S., Kopaevich L. F. Cretaceous palaeogeography of the north-eastern Peri-Tethys. Palaeogeography, Palaeoclimatology, Palaeoecology. 2003. Vol. 196. No. 1–2. P. 177–208.
2. LaGrange M.T., Konhauser K.O., Catuneanu O., Harris B.S., Playter T.L., Gingras, M.K. Sequence stratigraphy in organic-rich marine mudstone successions using chemostratigraphic datasets. Earth-Science Reviews. 2020. Vol. 203. P. 103–137.
3. Deng H.W., Qian K. Sedimentary geochemistry and environmental analysis. Gansu science and technology press. Lanzhou. 1993. P. 18–31.
4. Liu X.M., Wang S.J., Sun C.X., Jia Y.H., Li, T.Y. Strontium as an essential indicator of paleosalinity. Acta Mineral. Sin. 200. Vol. 20. P. 91–96.
5. Zorina S.O. On Mesozoic Stratigraphy of the East European Platform: Formation, Sequence, Event and Chronostratigraphic Approach. 2005. 158p. (In Russian)
6. Zorina, S.O., Startseva, G. Biofacies of benthic foraminifers, paleobathymetry and sequence stratigraphy of the Middle Jurassic-Lower Cretaceous deposits of the eastern Russian Plate (Tatarsko-Shatrashanskaya well 1 area, Republic of Tatarstan). Lithosphere. 2010. Vol. 4. P. 81–93. (In Russian)

PALEOTEMPERATURES AND OXYGEN ISOTOPIC COMPOSITION OF THE MIDDLE VOLGIAN BLACK SHALES (ULYANOVSK-SARATOV TROUGH, EASTERN RUSSIAN PLATFORM)

Nikashin K.I., Zorina S.O.

Kazan federal university, Kazan, Russia, kostya97@inbox.ru

Abstract. The organic carbon-rich rocks of the Upper Jurassic Promzino Formation and their host rocks (Ulyanovsk-Saratov Trough, Eastern Russian Platform) have been studied, and oxygen isotope ratios in the skeletal remnants therein have been determined to evaluate the potentially hyperthermal conditions during the black shales accumulation. The presence of *Tasmanaceae* algae evidences the warm water conditions in the basin. Paleotemperatures in the region were not extremely high in the Late Jurassic (17 – 23 °C). Moreover, no abrupt temperature rise is detected. Nevertheless, the warm climate could have been one of the factors contributing to the enhanced burial of organic matter.

Key words: hyperthermal events, OAE, organic carbon-rich shales, paleotemperatures

In the Mesozoic, several hyperthermal events are known, which are episodes of a rapid increase in global temperature to extremely high values [1]. All of them are recorded in marine sections composed of black shale horizons. In the Eastern Russian Platform (North-Eastern Peri-Tethys), several Mesozoic black shale formations widely occur, one of those is the Middle Volgian Promzino Formation. Little attention has yet been paid to studying potentially hyperthermal conditions in the Late Jurassic and their manifestation in the sedimentary succession of the North-Eastern Peri-Tethys. The aim of our research is to find out whether the Promzino black shales were formed during the hyperthermal conditions or just during the greenhouse phase. To reconstruct the depositional environments of the organic carbon-rich rocks, we have studied their geochemical features, clay mineral composition, and the stable oxygen isotopes in the fossil shells. The study material includes 20 core samples from the Tatar-Shatrashany borehole (Republic of Tatarstan), rock samples, and shell material from the outcrops located near the village of Embulatovo (Republic of Tatarstan) and the Gorodishchi section (Ulyanovsk Region).

The Promzino Formation is composed of marls, calcareous mudrocks, and bituminous shales accumulated under alternating oxic and anoxic conditions [2]. The association of clay minerals in the rocks studied includes smectite and illite-smectite, which are probably products of weathering under the arid conditions. It should be noted that smectite and illite-smectite could also be products of the volcanic ash transformation, which have been reported from the Promzino Formation by many researchers [2; 3]. Probably, both formation mechanisms of these minerals were carried out. Thin sections analysis using fluorescence microscope revealed abundant algae *Tasmanaceae* [4], which could have been confined to warm water column [5].

To reconstruct paleotemperatures, the stable oxygen isotopes of biogenic carbonates (ammonites, foraminifers, and belemnites) were analyzed. Lack of significant diagenetic alterations of carbonates was preliminarily established. According to SEM images, primary shell microstructures are well preserved. The results of the elemental analysis demonstrate a low Mg/Ca ratio in the shell material, which is typical of pristine low-Mg calcite [6].

Based on first results of the $\delta^{18}O$ analysis, a paleotemperature curve was constructed (Fig. 1) using equations from [7, 8]. This curve shows quite a warm climate in the Late Jurassic in study region, with water column temperatures ranging from 17 to 23 °C. However, a positive temperature excursion during the deposition of black shales is observed neither in our curve nor in the Veiser's one constructed for the temperate belt of the Northern hemisphere [9]. Rather abrupt warming in almost 4 °C is traceable from [10] for the Russian Platform, but the maximum temperature obtained (20 °C) is much lower than that typical for the hyperthermal events.

Nevertheless, the warm climate, maintaining high productivity, was one of the factors contributing to the enhanced burial of the organic matter in the eastern Russian Platform.

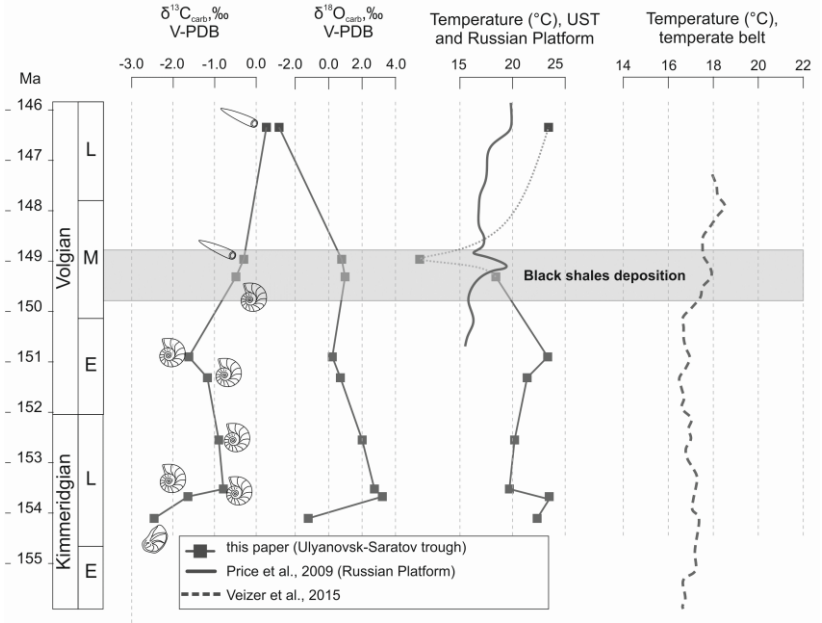

Figure 1 – Variations of $\delta^{18}O_{carb}$, $\delta^{13}C_{carb}$, and the temperature curve for the Upper Jurassic composed section of the Ulyanovsk-Saratov Trough

Funding: This article is a contribution to the IGCP 739 Project.

References:

1. Foster G.L., Hull P., Lunt D.J., Zachos J.C. Placing our current "hyperthermal" in context of rapid climate change in our geological past. Philosophical Transactions of the Royal Society A. 2018. Vol. 376. P. 1–11.

2. Nikashin K.I., Zorina S.O. Volcanogenic material in the Upper Jurassic-Lower Cretaceous deposits of the Eastern Russian Platform and its sources. Izvestiya Saratovskogo universiteta. Novaya seriya. Seriya: Nauki o Zemle. 2021. Vol. 21. No. 1. P. 49–57.

3. Rentgarten N.V., Kuznetsova K.I. Pyroclastic material in the Late Jurassic deposits of the Russian platform. Doklady Akademii nauk SSSR. 1967. Vol. 173. No. 6. P. 1422–1425.

4. Maksiuotova L.F. Benthic foraminifera and sedimentary conditions of the Upper Jurassic and Lower Cretaceous deposits of the eastern part of the Russian Platform: Master Thesis. Kazan Federal University, TU Bergakademie Freiberg. 2018. 37 p.

5. Parke M., den Hartog-Adams I. Three species of Halosphaera. Journal of the Marine Biological Assiociation of the United Kingdom. 1965. Vol. 45. No. 2. P. 537–557.

6. Brand U., Veizer J. Chemical diagenesis of a multicomponent carbonate system – 1: Trace elements. Journal of Sedimentary Research. 1980. Vol. 50. No. 4. P. 1219–1236.

7. Anderson T.F., Arthur M.A. Stable isotopes of oxygen and carbon and their application to sedimentologic and paleoenvironmental problems. Stable isotopes in sedimentary geology. SEPM Short Course 10. 1983. P. 1–51.

8. Grossman E.L., Ku T.L. Oxygen and carbon isotope fractionation in biogenic aragonite: temperature effect. Chemical geology. 1986. Vol. 59. P. 59–74.

9. Veizer J., Prokoph A. Temperatures and oxygen isotopic composition of Phanerozoic oceans. Earth-Science Reviews. 2015. Vol. 146. P. 92–104.

10. Price G.D., Rogov M.A. An isotopic appraisal of the Late Jurassic greenhouse phase in the Russian Platform. Palaeogeography, Palaeoclimatology, Palaeoecology. 2009. Vol. 273. P. 41–49.

DEPOSITIONAL ENVIRONMENTS OF THE UPPER DEVONIAN DEPOSITS OF THE EASTERN RUSSIAN PLATFORM

Tahhan F.[1,2], *Zorina S.O.*[1,2]

[1] Kazan Federal University, Kazan, Russia, fatmeh.m.tahhan@gmail.com
[2] Institute of Geology and Petroleum Technologies, Kazan, Russia

Abstract. This study aims to reconstruct sedimentary environments of carbonate rocks of the Upper Devonian Frasnian Deposits on the Eastern European Platform. The work includes petrographic analysis, facies and microfacies analysis, determination of the qualitative and quantitative composition of microfauna (bioclasts) in the samples, photographing, constructing a scheme and profile characterizing the facies inhering of the studied territory and the selected well, XRD analysis, and Rock-Eval pyrolysis. The typical deposits, facies zones, and sedimentation conditions in the presented territory are investigated.

Key words: Republic of Tatarstan, carbonate rocks, facies, petroleum resource potential, depositional environments.

The study area is situated in the Russian Federation, in the Republic of Tatarstan, on the Eastern European Platform. The studied wells are located in the Volga-Kama region, 800 km east of Moscow.

The Upper Devonian carbonate layers in this region have high-productivity reservoirs with the potential to find additional hydrocarbon resources.

The studies were carried out in Kazan Federal University, Institute of Geology and Petroleum Technologies. Eighteen cores of carbonate rocks are sampled from six wells (23006, 220, 1192, 33, 34, 840) from Almetyevck, Sarmanovo, Leningorsk and Mendeleevck deposits. The samples were recovered from depths of 1662.2–1976 m and covered the Mendymain Formation, Domanikovian and Kynovian Formation. Facies and microfacies analyses were carried out using Flugel's technique [1], which included rock description and facies characterization (facies zone and standard microfacies type). Petrographic analysis is based on the quantitative ratio of carbonate grains and micrite matter, then the size of the bioclasts and their basic composition are taken into account. X-ray diffraction is used to identify the mineral compositions of rocks. Rock-Eval pyrolysis is used to determine the oil-generating potential of rocks [2, 3].

The petrographic analysis showed that the rock types include limestones, sandy limestones, and mudstones which belong to different facies. The identification of sufficiently large and poorly rounded, unsorted quartz fragments in some samples of carbonate rocks testify to the formation of rocks under deep-water conditions and their possible formation by turbidite flow [4].

Four Wilson`s zones are identified for study rocks [5]: deep basin zone, open sea shelf, shelf zone with free water exchange, and shelf zone with limited water exchange, these indicate sharply changing conditions during the accumulation of the Frasnian deposits (Fig 1).

According to Rock-Eval pyrolysis, it was found that kerogen types of the studied samples are dominated by Types II and III depending on the values of hydrogen index (HI) which ranging between 365 - 513 mg\g.

The studied samples contain high values of S2 (petroleum yield) and Total organic carbon (TOC), with values ranging from 13.18-41.03 and 3.61-8%, respectively. Thus, these samples have very good to excellent source rock potential.

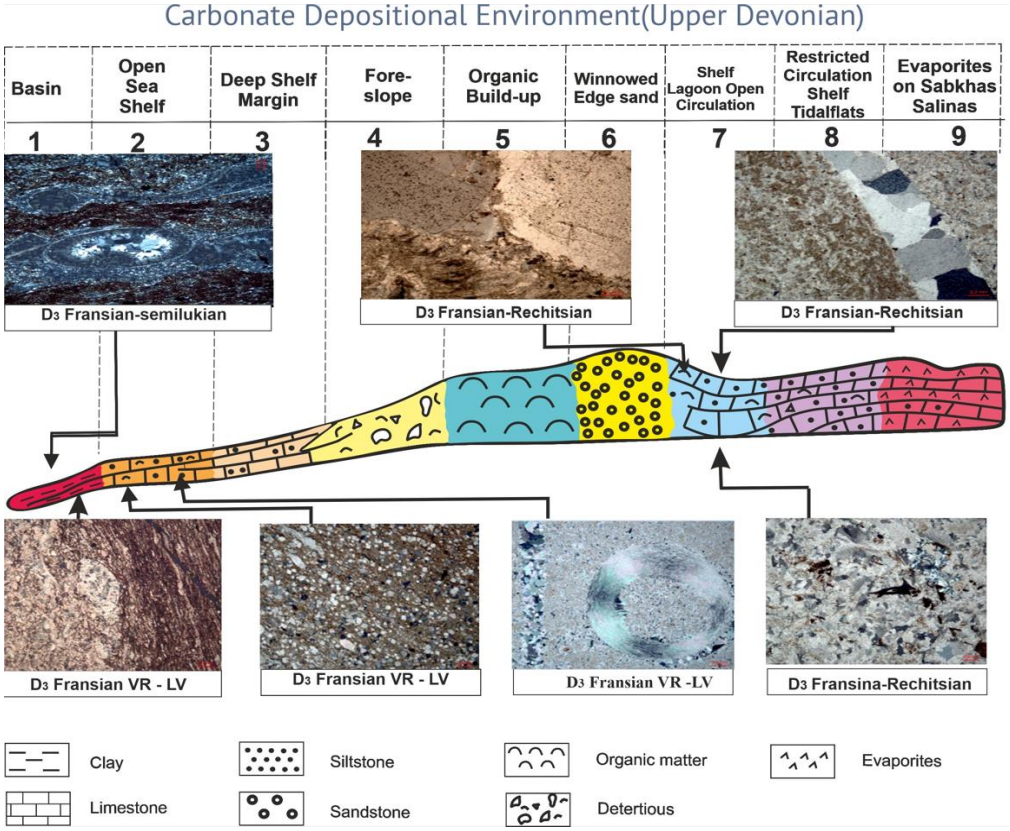

Figure 1 – Carbonate depositional environments (Upper Devonian). Standard Facies Zones.

Funding: This work was supported by the Ministry of Science and Higher Education of the Russian Federation under agreement No. 075-15-2020-931 within the framework of the development program for a world-class Research Center "Efficient development of the global liquid hydrocarbon reserves".

References:

1. Flügel E. New Perspectives in Microfacies, in Microfacies of Carbonate Rocks. Berlin, Heidelberg. Springer. 2010. 1006 p.

2. Al-Areeq N.M., Al-Badani M.A., Salman A.H., Albaroot M.A. Petroleum source rocks characterization and hydrocarbon generation of the Upper Jurassic succession in Jabal Ayban field, Sabatayn Basin, Yemen. Egyptian. 2018. Vol. 27. No. 4. P. 835–851.

3. Atta-Peters D., Achaegakwo C. A., Garrey P. Palynofacies organic geochemical analyses and hydrocarbon potential of the Takoradi 11-1 Well, Saltpond Basin, Ghana. Petroleum and Coal. 2015. Vol. 57. No. 5. P. 478–499.

4. Scholle P. A., Ulmer-scholle D. S. A Color Guide to the Petrography of Carbonate Rocks. Tulsa, Oklahoma, U.S.A. American Association of Petroleum Geologists. 2003. 470 p.

5. Wilson J.L. Carbonate Facies in Geologic History. New York. Springer. 1975. 471 p.

HISTORY OF VEGETATION CHANGE IN THE SENTSA RIVER VALLEY IN THE HOLOCENE

Volchatova E.V. [1], *Bezrukova E.V.* [1-3], *Kulagina N.V.* [1-2]

[1]Institute of Geochemistry, A.P. Vinogradov SB RAS, Irkutsk, Russia. volchatova@igc.irk.ru
[2]Institute of the Earth's Crust SB RAS, Irkutsk, Russia.
[3]Irkutsk Scientific Center SB RAS, Irkutsk, Russia.

Abstract. As it knowns, water systems are influenced by various factors, primarily natural ones: climate change, development of soils and vegetation of the surrounding landscape, and biotic interactions [1–4]. Registration of such changes and their development in time helps to understand the formation of the modern picture of the world and predict its changes in the future. To understand larger processes, one should start with single objects. The Sentsy river valley is located on the Okinsky plateau, in the Eastern Sayan mountain system, Republic of Buryatia. The Sentsa River is one of the major tributaries of the Oka River and it is formed by the confluence of the Dunda-Gol and Khoyto-Gol rivers.

Key words: spore-pollen analysis, palynology, stratigraphy, vegetation, climate.

Based on the spore-pollen analysis, as well as the time dates obtained using radiocarbon dating and stratigraphic presentation of the set of results, we reconstructed the composition of vegetation and the climatic conditions of its formation in the Sentsa River valley over the last 4700 years.

Based on the obtained data, using cluster analysis, two major stages in the development of vegetation over time were identified, one of which includes two subzones.

During the formation of deposits in the time interval 4720 years ago - older than 1070 years ago in the valley of the Senza River, woody vegetation dominated, which was prevail by spruce-cedar forests with the participation of larch and, rarely, fir. The high abundance of spruce pollen, whose pollen distribution radius is not large, suggests that the valley spruce forests grew much closer to the studied section than later.

The composition of the reconstructed vegetation of this stage suggests the existence of a moderately cold and humid climate, which was not favorable for the occurrence of intense fires.

During the formation of the spectra of the subzone about 1000 years ago - 800 years ago forests continued to predominate in the composition of the vegetation of the Sentsa River valley, but the proportion of spruce in them significantly decreased. Single pollen grains of fir in the SPS of this subzone suggest its disappearance from the river valley. Simultaneous expansion of herbaceous-shrub vegetation from birches, willows, sphagnum-sedge associations suggests the development of a swamping process in the river valley, which could be an important reason for the death of valley spruce and fir forests, which cannot tolerate stagnant moisture. It is assumed that swamping was caused by the recent activation of volcanic activity on the Oka Plateau [5, 6]. This led to the establishment of a stagnant hydrological regime in the lower part of the Sentsa valley and led to intensive swamping of its bottom [7]. The latest stage of volcanic activity on the Okinsky Plateau ultimately led to a significant degradation of spruce forests in the Sentsa River valley.

According to the estimated age, the youngest stage in the development of the natural environment in the Sentsa River valley began about 800 years ago, that is, after the completion

of the active phase of volcanism on the Oka Plateau [8]. After a break in the area of the studied section, larch taiga prevailed with a small proportion of spruce along the river valley. Grass-sedge groups dominated on the swamp/marshy meadow.

In the last few decades, the SPS composition shows a wide development of cereal communities in the Sentza River valley, most likely due to a change in the moisture regime. This is evidenced by the high abundance of spores of fungi of the genus Tilletia found in these spectra, the species of which parasitize on species of the grass family.

The larch taiga with a slight admixture of birch and spruce currently growing in most of the Sentsa River valley proves the accuracy of the analysis and confirms the data obtained. As well as in the SPS of the upper core samples, larch forests dominate in the landscape of the present time, and in the lower reaches of the river one can also find park-type cedar mixed-grass forests. The undergrowth consists of thickets of Altai honeysuckle (Lonicera altaica) and golden rhododendron (Rhododendron aureum), and the common lingonberry (Vacciniumvitis-idaea) dominates in the shrub layer.

On the flat areas of the valley and on the slopes of the southern exposure, kobresia-cereal steppe groups are widespread. Meadow and meadow-marsh complexes are often occur.

Funding: The research was carried out with partial support of the RFBR grants No. 19-05-00328, RFBR-Royal Society of London No. 21-55-10001.

References:

1. Michelutti N., Wolfe A.P., Briner J.P., Miller G.H. Climatically controlled chemical and biological development in Arctic lakes. Geophys Res. 2007. Vol. 112. G03002.

2. Moore P.D., Webb J.A., Collinson M.E. Pollen analysis. Second edition. Blackwell Scientific Publications. 1991. 216 p.

3. Baulch D. L., Bowman C. T., Cobos C. J., Cox R. A., Just Th., Kerr J. A., Pilling M. J., Stocker D., Troe J., Tsang W., Walker R. W., Warnatz J. Evaluated Kinetic Data for Combustion Modeling. Supplement II 2005 by the U.S. Secretary of Commerce on behalf of the United State. Journal of Physical and Chemical Reference Data. 2005. Vol. 34. No. 3. P. 757-1397.

4. Reuss N., Leavitt P. R., Hall R. I., Bigler C., Hammarlund D.. Development and application of sedimentary pigments for assessing effects of climatic and environmental changes on subarctic lakes in northern Sweden. Paleolimnology. 2010. Vol. 43. P. 149–169.

5. Ivanov A.V., Arzhannikov S.G., Demonterova E.I., Arzhannikova A.V., Orlova L.A. Jom-Bolok Holocene volcanic field in the East Sayan Mts., Siberia, Russia: structure, style of eruptions, magma compositions, and radiocarbon dating. Bulletin of Volcanology. 2011. Vol. 73. P. 1279–1294.

6. Arzhannikov S. G., Ivanov A. V., Arzhannikova A. V., Demonterova E. I., Orlova L. A., Pigati D. Stages of formation of the Zhombolok lava field (Eastern Sayan). Geodynamic evolution of the lithosphere of the Central Asian mobile belt. Irkutsk: Publishing House of the Institute of the Earth's Crust SB RAS. 2013. P. 22–24.

7. Shchetnikov A.A., Bezrukova E.V., Filinov I.A., Ivanov E.V., Kerber E.V. Lacustrine morpholithogenesis in the Valley of Volcanoes (Eastern Sayan). Geography and natural resources. 2016. No. 3, P. 37–48.

8. Shchetnikov A.A., Bezrukova E.V., Krivonogov S.K. Late Glacial to Holocene volcanism of Jom-Bolok Valley (East Sayan Mountains, Siberia) recorded by microtephra layers of the Lake Kaskadnoe-1 sediments. Journal of Asian Earth sciences. 2019. Vol. 173. P. 291-303

Section GEOMORPHOLOGY AND QUATERNARY GEOLOGY

INFLUENCE OF CLIMATIC CONDITIONS ON THE DISTRIBUTION OF THE AEOLIAN RELIEF (NORTH WESTERN SIBERIA)

Malikova E.L.

V.S. Sobolev Institute of Geology and Mineralogy, Novosibirsk, Russia, malikovael@igm.nsc.ru

Abstract. An analysis of climatic factors in the north of Western Siberia in the Nadym Ob region showed that the active advancement of dunes here occurs in summer. On sandy massifs, eolian landforms are concentrated in the southeastern parts of the swells, where the sand moves under the influence of northern and northwestern winds. It has been established that the highest intensity of deflation was observed in the 70s and 90s. XX century. At present, deflation has decreased to the lowest values for the entire time of observations.

Key words: eolian landforms, climatic conditions, dunes, north of Western Siberia, sand massifs.

Sandy deserts are found on almost all continents, with the exception of Antarctica [1]. Much attention of scientists from all over the world has always been riveted to sand deposits, their shape and how their spatial extent changes, since about 25% of the Earth's desert area is covered with sand [2], and this poses a huge potential threat to the development of global infrastructure and agriculture. economy. Dunes are one of the most common aeolian landforms and play an important role in understanding the evolution of the aeolian environment. Sand dunes are formed and changed under the influence of many external factors and, accordingly, come in different forms, including dunes, linear, domed, etc. [3].

For this study, the Nadymsky district was taken. It is located in the subzone of the northern taiga of the West Siberian Plain. Traces of eolian activity are observed here almost everywhere. The studied sandy massif is located 30 km from the city of Nadym, this sandy massif is extended from west to east for 1 km, from north to south for 2 km, up to 12 m high [4, 5].

The direction and strength of the wind are the main factors in the formation of dunes. The spatial distribution of dunes within the bulge is in good agreement with the directions and strength of the prevailing winds. The most active advancement of the dune occurs in summer; therefore, almost all eolian forms are concentrated in the southeastern part of the blow, where the sand moves under the influence of northern and northwestern winds. Despite the fact that the winds of the southern rhumb are close in strength and intensity to the northern winds, the main part of these winds falls on the cold season. For this reason, in the winter season, the dunes remain almost immobile. Frozen and snow-covered sand is not subject to winding, and therefore, accumulative landforms are practically not observed in the northern parts of the territory [6].

The modern period of dune formation began after 1500 AD. [7]. Since that time, aridization and the strength of northern winds have intensified, which caused the dune to grow, which continues to the present. Strengthening of northern winds is confirmed by the location of the highest dunes in the southeastern part of the blow.

To assess the deflationary potential of the region, the climate factor (C) proposed by E.M. Lyubtsova [8], calculated by the formula:

$$C = 102v3/(H/T + 10)2,$$

where C is the climate factor; v is the average annual wind speed, m/s; H is the annual amount of precipitation; T is the average annual temperature. For the calculations, meteorological observation data from the Nadym airport weather station from 1955 to 2020 were used. [9, 10].

An assessment of the deflationary potential through the climate factor (C) showed that the highest intensity of deflation was observed in the 1970s and 1990s. XX century, when the climate factor reached C=2.78. At present, it has decreased to the minimum values for the entire observation period (C=0.001). What does it say about the cyclical climate fluctuations. During the observation period in this territory, deflation was moderate and strong, but in the last decade there has been a tendency to reduce deflation. This is probably due to the increase in temperature and precipitation (Fig. 1) in the study area in recent years [6].

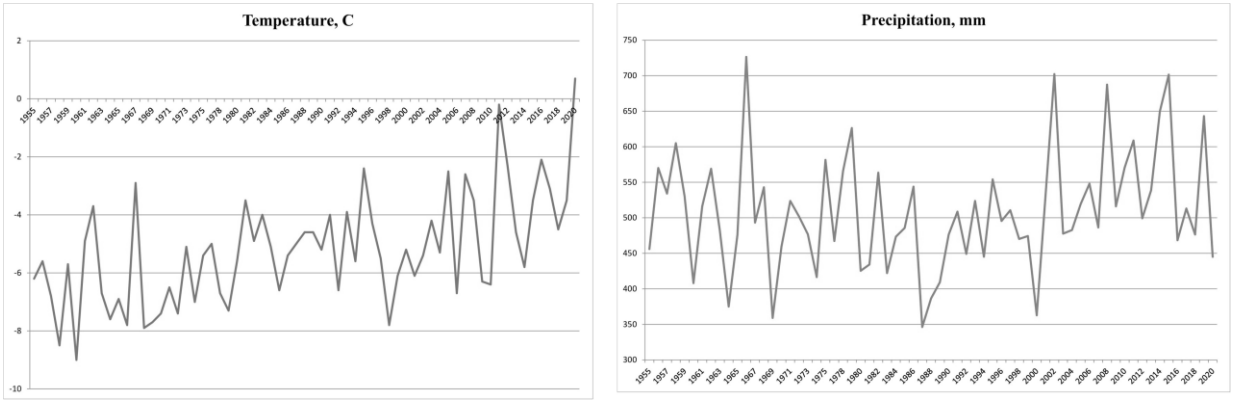

Figure 1 - Graphs of changes in the average annual temperature (left) and precipitation (right) in the area of Nadym

Funding: The work was carried out within the framework of the state assignment of the IGM SB RAS

References:

1. Zheng Z., Du S., Taubenböck H., Zhang X. Remote sensing techniques in the investigation of aeolian sand dunes: A review of recent advances. Remote Sensing of Environment. 2022. Vol. 271. P. 1-23.

2. Ali E., Xu W., Ding X. Improved optical image matching time series inversion approach for monitoring dune migration in North Sinai Sand Sea: algorithm procedure, application, and validation. ISPRS Journal of Photogrammetry and Remote Sensing. 2020. Vol. 164. P. 106-124.

3. Breed C.S., Grow T. Morphology and distribution of dunes in sand seas observed by remote sensing. A Study of Global Sand Seas: United States Geological Survey Professional Paper. 1979. P. 253-302.

4. Nikulina E.L. Late Holocene aeolian forms of the relief in the Nadym ob Area. IX Siberian Conference of Young Scientists of Earth Sciences. 2018. P. 420-422.

5. Malikova E.L. On aeolian landforms on the example of the Nadym Ob region. Scientific notes of the Crimean Federal University named after V.I. Vernadsky. Geography. Geology. 2020. Vol. 6. No. 3. P. 321-334. (In Russian

6. Malikova E. (2021): Aeolian forms of the relief of the Nadym Ob area and factors of their formation. In Proceedings of INQUA SEQS 2021 Conference, Wrocław, Poland. University of Wrocław & Polish Geological Society. P. 58–59.

7. Zykina V. S., Zykin V. S., Vol'vah A. O., Ovchinnikov I. Ju., Sizov O. S., Soromotin A. V. Stroenie, kriogennye obrazovanija i uslovija formirovanija verhnechetvertichnyh otlozhenij Nadymskogo Priob'ja // Kriosfera Zemli. 2017. Vol. XXI. No. 6. P. 14–25

8. Bazhenova O.I., Lyubtsova E.M., Ryzhov Yu.V., Makarov S.A. Spatio-temporal analysis of the dynamics of erosion processes in the south of Eastern Siberia. Novosibirsk. Nauka. 1997. 208 p.

9. Sizov O.S. Geoecological aspects of modern aeolian processes in the northern taiga subzone of Western Siberia. Novosibirsk. Geo. 2015. 124 p.

10. Weather archive www.gismeteo.ru

Section GEOECOLOGY, HYDROGEOLOGY, ENGINEERING GEOLOGY AND ENVIRONMENTAL MANAGEMENT

CHANGES IN THE FORMS OF DISSOLVED ORGANIC MATTER AND IRON UNDER IRRADIATION IN NATURAL BOREAL WATERS

Aleshina A.R

Lomonosov Moscow State University, Moscow, Russia, lis.aleshina@yandex.ru

Abstract. Experiments on sunlight irradiation of several river and marsh waters of the boreal zone resulted in the transformation of dissolved organic matter, its degradation to low molecular weight compounds up to mineralization and simultaneous coagulation of compounds >0.22 μm. As a result of redox cycle of Fe and organic matter transformations, the formation of Fe(III) hydroxides occurred. The resulting hydroxides can form organic-mineral compounds >0.22 μm, with which other metals can potentially co-precipitate.

Key words: dissolved organic carbon, irradiation, Fe, natural waters, photochemical oxidation

The sunlight-induced oxidation is the main agent of dissolved organic matter (DOM) transformation in natural waters as molecules of DOM are very photoreactive [1]. Iron is also involved in a dynamic redox cycle in boreal organic-rich natural waters under sunlight [2]. To study the effect of sunlight on the forms of DOM and iron, experiments on irradiation of natural water samples were conducted in the Republic of Karelia. Water samples were taken from different water bodies of Yaroslavl (sample №1), Vologda (№2, 3), Vladimir regions (№7) and Republic of Karelia (№4, 5, 6). All samples were filtered through a sterilized 0.22 μm filter to assure the absence of microbial cells [3]. Filtered fluids were transferred into four Petri dishes (about 35 ml of sample in each), covered with transparent film for light access and placed under the sun for 10 days.

Before and after experiments the pH, the concentration of dissolved organic carbon (DOC), humic substances (HS) and Fe in filtrates <0.22 μm and <1 kDa of water samples were measured. The pH of water samples was measured by a Hanna HI 9025 pH meter, the concentration of DOC – by a liquid element analyzer (LiquiTOC trace, Elementar, Germany), the content of dissolved Fe – on a ContrAA 300 atomic absorption spectrophotometer (Analytik Jena Company). The concentration of HS in the samples was determined by their reaction binding to Toluidine Blue [4].

The content of HS in filtrates <0.22 μm after irradiation in samples №2 and 6 decreased by 5 and 14%, respectively. In samples №3 and 7 this value reached 62 and 92%. In other samples the content of HS as a result of irradiation was even below the detection limit of 5 mg/L.

After irradiation, the DOC content decreased in all <0.22 μm filtrates, and the higher the initial DOC content, the greater the relative decrease. Thus, in sample №1 the DOC content decreased by only 4%, and in sample №7 - by 73%. The proportion of DOC in the low molecular weight (LMW, <1 kDa) fraction generally increased in all samples after irradiation: from 20-70% (before) to 80-98% (after irradiation). At the same time, some of the DOC coagulated into compounds >0.22 μm and was removed from the solution during refiltration.

Table 1. Sample descriptions and initial contents of DOC and HS (mg/L) and Fe_{total} (µg/L) in filtrates <0.22 µm

Sample №	Sample description	DOC, mg/L	HS, mg/L	Fe, µg/L
1	swamp near the village Vepreva Pustyn'	21.9	6.0	58
2	Koy River	20.1	13.6	170
3	Kovzha River	13.4	23.9	238
4	the brook near Lemb Lake	19.6	6.3	384
5	Lundozhma River	28.6	15.3	774
6	Western bog on the shore of Tsipringa Lake	50.8	22.7	13270
7	headwaters of the Senga River	61.0	36.7	4197

The total dissolved Fe concentration in the <0.22 mm fraction decreased by 3-96% during 10 days of the experiment. The smallest changes occurred in samples №3 and 5 - there most of the Fe remained in the form of 1 kDa to 0.22 µm compounds. In samples №1, 2, 4, and 6 more than 80% of the dissolved (<0.22 µm) Fe passed into the >0.22 µm fraction, reaching a maximum (96% of the initial content) in sample №6, where the highest concentration of Fe was in the initial sample. In sample №7, half of the Fe was in the >0.22 µm fraction, and the other half was almost entirely in the <1 kDa fraction.

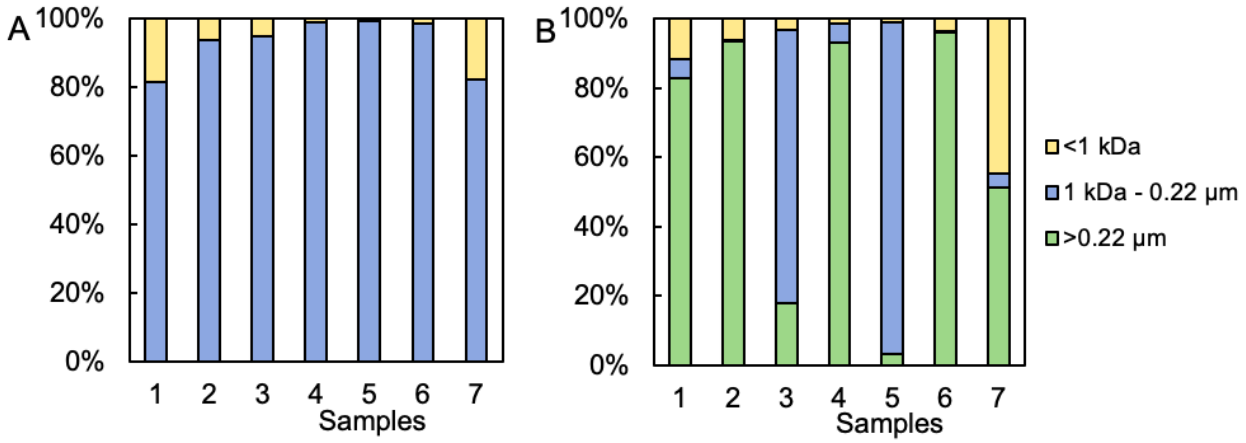

Figure 1 – Distribution of Fe_{total} forms in the studied samples before (A) and after (B) irradiation by fractions <1 kDa, 1 kDa - 0.22 µm, and >0.22 µm.

During sunlight irradiation, Fe became involved in redox cycle and release from stable complexes with organic substances. By the ligand-to-metal charge transfer the photochemical reduction of Fe(III) to Fe(II) occur and the latter release from the complexes with further oxidation to Fe(III) and hydrolysis followed by polymerization [5]. Thus, sunlight irradiation of boreal waters can lead to the formation and deposition of large organo-mineral colloids.

Funding: This work is supported by the Russian Foundation for Basic Research under grant 20-35-90017.

References:

1. Xue S., Wang C., Zhang Z., Song Y., Liu Q. Photodegradation of dissolved organic matter in ice under solar irradiation. Chemosphere. 2016. Vol. 144. P. 816-826.

2. Garg S., Jiang C., Miller C.J., Rose A.L., Waite T.D. Iron redox transformations in continuously photolyzed acidic solutions containing natural organic matter: kinetic and mechanistic insights. Environmental Science & Technology. 2013. Vol. 47. No. 16. P. 9190-9197.

3. Kitidis V. CDOM Dynamics and Photoammonification in the Marine Environment. Ph.D. Thesis, University of Newcastle. 2002. 182 p.

4. Sheng G.-P., Zhang M.-L., Yu H.-Q. A rapid quantitative method for humic substances determination in natural waters. Analytica Chimica Acta. 2007. Vol. 592. No. 16. P. 162-167.

5. Drozdova O.Yu., Aleshina A.R., Tikhonov V.V., Lapitskiy S.A., Pokrovsky O.S. Coagulation of organo-mineral colloids and formation of low molecular weight organic and metal complexes in boreal humic river water under UV-irradiation. Chemosphere. 2020. Vol. 250. P. 1-10.

HYDROCHEMICAL RESEARCHES OF SEASONAL SNOW AND WATER QUALITY OF RIVERS IN THE ZERAVSHAN VALLEY

Kurbonov N.B.[1,2], Normakhmedova Z.O.[2], Mitusov A.V.[3], Normatov I.Sh.[2]

[1]Institute of Water Problems, Hydropower and Ecology, National Academy of Sciences of Tajikistan, Dushanbe, Tajikistan, knomvarb.0502@gmail.com
[2]Department of Meteorology and Climatology, Tajik National University, Dushanbe, Tajikistan,
[3]Kazakh-German University, Almaty, Kazakhstan

Abstract. In this thesis provides data on the chemical composition of seasonal snow in the upper reaches of the Zerafshan River and the quality of the water of the Zerafshan River from the formation zone to the very lower reaches, to the border with Uzbekistan. It has been shown, using modern methods of analysis, that the concentration of heavy metals in the composition of water, starting from the place where wastewater is discharged into the river to the very lower reaches, does not exceed the maximum allowable concentration.

Key words: hydrochemical research, seasonal snow, water quality, glaciers.

Water relations between the countries of Central Asia during the USSR were regulated according to the scheme “Integrated use and protection of water resources in the Amu-Darya and Syr-Darya river basins” [1-2]. The main goal of this scheme was to establish the real volume of water available for use in the Amu-Darya and Syr-Darya river basins, as well as to distribute the region’s water resources between the republics taking into account the interests of all water users. It should be noted that the scheme “Integrated use and protection of water resources in the Amu-Darya and Syr-Darya river basins” did not include a number of important water aspects, namely, the environmental and sanitary conditions of the river and large canals. This was because the named scheme was aimed at providing water to agricultural lands used for growing strategic raw materials - raw cotton. This led to new serious environmental problems.

After the adoption by Tajikistan of a number of government programs for the development of hydropower resources of the water arteries of the Zerafshan River basin, the Republic of Uzbekistan raises water quality problems in a new. These problems are mainly associated with the pollution of the river by the wastewater of the Anzob mining and processing enterprise in the Zerafshan valley [1-2].

In order to establish the degree of influence of the Anzob mining and processing plant on changing the chemical composition of the water of the Zerafshan river during 2012-2016, water samples were taken at points located, respectively, before and after the wastewater storage facility of the plant, with a frequency of three times a month [3-5].

It was found that the excess concentration of heavy metals in the waters of the Zerafshan River and its tributaries.

Along with monitoring the chemical composition of the waters of the Zerafshan River on its average course and in the lower reaches, the availability of information on the composition and transportation of various chemical elements and compounds from the river formation zone itself is of considerable interest, i.e. on the glaciers of the Zerafshan river basin. After all, it is known that glaciers are accumulators for atmospheric aerosols, fine dispersed chemical elements and compounds. In order to have information on the chemical composition of the water runoff formed from glaciers in the formation zone, a set of physicochemical analyzes of seasonal snow was carried out on the glaciers Zerafshan, Rossinch, Dekhavz and Turo of the Zerafshan river basin and the waters of the Zerafshan river tributaries formed from these glaciers. It was found that the presence of anions SO_4^{2-}, NO_3^-, Cl^- and cations Ca^{2+}, Mg^{2+} predominates on the glaciers studied by us [3-5]. The results are interpreted within the framework of the concept of a stratospheric aerosol layer consisting of tiny drops of sulfuric acid, which were formulated in the

early 60^{-s} of the last century and based on the transfer of microparticles and components by long-range airflows [6-8].

Funding: The work was carried out within the framework of the Research work of the Laboratory of Water Quality and Ecology of the Institute of Water Problems, Hydropower and Ecology of the National Academy of Sciences of Tajikistan and in cooperation with the Department of Meteorology and Climatology of the Tajik National University and the Kazakh-German University.

References:

1. Normatov I., Olsson O., Groll M., Kurbonov N. (2013): Monitoring and analyses of impact of the industrial complexes on water quality of the Central Asian Transboundary Rivers. In Sustainable development of Asian countries, water resources and biodiversity under climate change. Barnaul. P.166-173.
2. Kurbonov N., Groll M., Normatov I., Opp C., Stulina G. (2016): Status Qua and Future Conflicts in Transboundary River Catchments Water Resources in the Zeravshan River Basin (Tajikistan-Uzbekistan). In Proceedings of the 8th International Siberian Early Career GeoScientists Conference. P. 348.Novosibirsk.
3. Kurbonov N.B., Normatov I.Sh. (2018): Hydrochemistry and studies of the isotopic composition of the Zeravshan River and its tributaries. In Proceedings of the XXIX Youth Scientific School-Conference "Actual Problems of Geology, Geophysics and Geoecology", dedicated to the memory of Corresponding Member of the Academy of Sciences of the USSR K.O. Kratz and Academician of the Russian Academy of Sciences F.P. Mitrofanov. Petrozavodsk: Russia. P.271-274. (In Russian)
4. Kurbonov N.B., Mitusov A.V., Kobuliev Z.V., Frumin G.T. (2020): Dynamics of changes in the chemical composition of the water of Iskanderkul Lake and its tributaries. In Proceedings of the XXXI Youth Scientific School-Conference "Actual Problems of Geology, Geophysics and Geoecology", dedicated to the memory of Corresponding Member of the Academy of Sciences of the USSR K.O. Kratz. St. Petersburg. P. 141-148. (In Russian)
5. Normakhmedova Z.O., Mitusov A.V., Kurbonov N.B. Water quality of the Iskanderkul Lake and its tributaries. Central Asian Journal of Water Research. 2020. No. 6(2). P.38-47 (In Russian).
6. Julia N. Chizhova, Nadine A. Budantseva, Yurij K. Vasil'chuk. Heavy metals in the Polar Ural and Caucasus Glaciers. Arctic and Antarctic. 2017. No.1. P. 35-50 (In Russian)
7. Toderich K.N., Tsukatani T., Mardonov B.K., Gus Gintzburger, Zemtsova O.Y., Tsukervanik E.S., Shuyskaya E.V. Water Quality, Cropping and Small Ruminants: A Challenge for the Future Agriculture in Dry Areas of Uzbekistan. Kyoto Institute of Economic Research. 2002. Art. 553. P. 10.
8. Traufetter F., Oerter H., Fischer H., et al. Spatio-temporal variability in volcanic sulphate deposition over the past in snow pits and firn cores from Amundsenisen, Antarctica. Journal of Glaciology. 2004. Vol.50. No. 168. P. 137-146.

CONDITIONS FOR THE FORMATION OF LAKES PESCHANOE AND NIZHNEE (BARABA LOWLAND)

Malov G.I., Strakhovenko V.D, Ovdina E.A.

V.S. Sobolev Institute of Geology and Mineralogy, Novosibirsk, Russia, malovgi@igm.nsc.ru

Abstract. The mineral and chemical composition of samples for two small lakes (Peschanoe and Nizhnee) of the Baraba lowland was studied. When studying the structure and composition of sapropel deposits in lakes, certain types and classes of sapropel were identified. It was revealed that the composition of sapropel deposits of lakes is formed by a combination of local factors (species composition of biota, soil-forming substrate, presence/absence of an anthropogenic factor) and regional (climate, topography of the catchment area).

Key words: sapropel, small lakes, Baraba lowland, Novosibirsk region.

Lakes Peschanoe and Nizhnee are located in the forest-steppe landscape zone on the territory of the Baraba lowland in the south of Western Siberia. The important regional factor of lake formation and sapropel formation in this region include a sharply continental climate with long winters, hollow-crest relief, sinusoidal fluctuations in atmospheric precipitation and, as a result, surface water levels [1]. The studied lakes are located 10 km from each other. Both lake basins were formed in a suffosion-subsidence manner in a depression between hill [2]. According to the geographical position, the lakes are intrazonal, in terms of area they are small (SPeschanoe = 126 ha, SNizhnee = 64 ha), according to the thermal classification they belong to lakes with changing temperature stratification, they are drainless and shallow (average depth of Lake Peschanoe - 1 ,67m, Lake Nizhnee - 1.25m), they are fresh and eutrophic reservoirs.

Detailed studies of lake systems in the course of fieldwork on a grid of sampling (1 point per 12 ha) and sensing (1 point per 1.6 ha) made it possible to establish the features of the morphometric, hydrological, chemical composition of bottom silts, etc. Bottom sediments were sampled using a cylindrical sampler with a vacuum lock from a catamaran. Analytical studies were carried out at the Analytical Center for multi-elemental and isotope research SB RAS, Novosibirsk: AA, ICP-MS, X-ray diffraction, gamma spectrometry, SEM studies. Statistical processing of research materials was carried out using the Statistica software package.

In Lake Peschanoe, three stages of the formation of a sapropel deposit (Fig. 1) are distinguished, matching the time of sedimentation with the established (according to literary sources) cycles of fluctuations in the level of lakes in Western Siberia, coinciding with cycles of high and low activity in the summer or winter period of precipitation [1]. In the first and third stages calcium organomineral sapropel is formed (Table 1). The main source of the substance of the mineral part of the sapropel deposit during these periods is authigenic mineral formation - low-magnesian calcite, in the formation of which the biogeochemical processes of lakes play a decisive role [3]. In the second stage, siliceous mineralized sapropel accumulates, which sharply prevails in the northeastern part of the lake. There are no authigenic minerals in the composition of the mineral fraction; quartz and oligoclase sharply predominate. A river flows from the northeast side of the lake, which, at high water levels, flows into the lake, which entails an increased supply of terrigenous particles of quartz-feldspar composition (soil-forming substrate - loam). Thus, in the formation of the sapropel deposit of Lake Peschanoe, the decisive role in the

formation in sapropel is played by local factors - the species composition of the biota, hydrochemical features, and the presence of a river.

Sapropel deposit of Lake Nizhnee has an organic-mineral siliceous composition, which changes slightly with a decrease in the organic part towards the bottom of the section, which is explained by the mineralization of organic matter with time. The absence of significant changes in the chemical composition of the sapropel deposit in different cycles of fluctuations in the level of lakes in Western Siberia is associated with an increase in the area of the lake water surface by combining with lakes surrounding it, for which local factors (species composition of biota, soil-forming substrate, the presence / absence of an anthropogenic factor) seem to be identical, which requires further study.

It was revealed that the composition of sapropel deposits of lakes is formed by a combination of local factors (species composition of biota, soil-forming substrate, presence/absence of an anthropogenic factor) and regional (climate, topography of the catchment area).

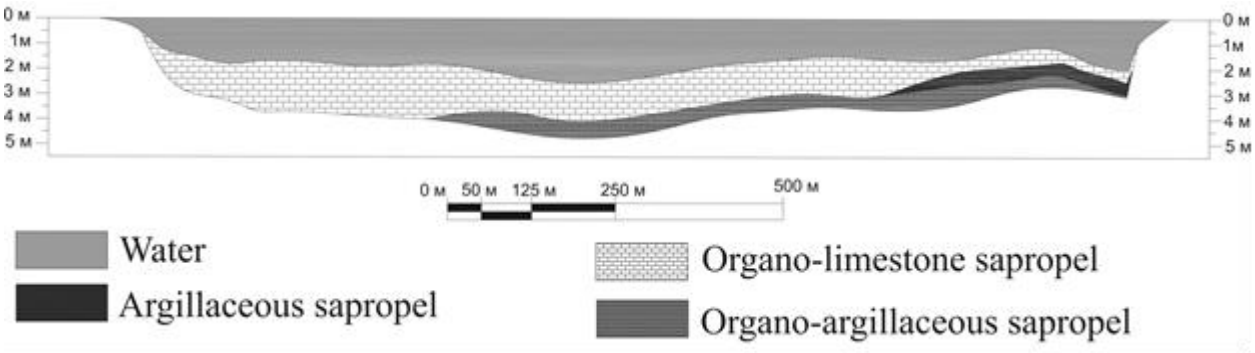

Figure 1 – The structure of the sapropel deposits of Peschanoe lake

Table 1. Types and classes of sapropel in the studied lakes

	Lake Peschanoe			**Lake Nizhnee**
Sapropel type	Organic-mineral	Mineralized	Organic-mineral	Organic-mineral
Sapropel class	Ca	Si	Ca	Si
Ash content, %	43	78	46	41

Funding: The work was carried out within the framework of the state task of the IGM SB RAS with the financial support of the Ministry of Science and Higher Education of the Russian Federation.

References:

1. Shnitnikov A. V. Intra-secular fluctuations in the level of steppe lakes in Western Siberia and Northern Kazakhstan and their dependence on climate. Proceedings of the Laboratory of Lake Science of the Academy of Sciences of the USSR. 1950. Vol. 1. 129 p.

2. Strakhovenko V.D., Ovdina E.A., Malov G.I., Yermolaeva N.I., Zarubina E.Y., Taran O.P., Boltenkov V.V. Genesis of organomineral deposits in lakes of the central part of the Baraba Lowland (south of West Siberia). Russian Geology and Geophysics. 2019. Vol. 60. No. 9. P. 978–989.

3. Ovdina E.A., Strakhovenko V.D., Solotchina E.P. Authigenic carbonates in the water-biota-bottom sediments' system of small lakes (south of Western Siberia). Minerals. 2020. Vol.10. No. 6. Art. 552.

GLAUCONITE-UREA NANOCOMPOSITES AS POLYFUNCTIONAL AND ENVIRONMENT-FRIENDLY FERTILIZERS

Maximov P.N.[1], Rudmin M.A.[12], Dauletova A.B.[1]

[1] Division for Geology, Tomsk Polytechnic University, Tomsk, Russia, rudminma@tpu.ru
[2] Laboratory of Sedimentology and Paleobiosphere Evolution, University of Tyumen, Tyumen, Russia

Abstract. This investigation includes the design of controlled-release nanocomposites based on a mixture of glauconite and nitrogen nutrients operating mechanical activation. Nitrogen occurs as intercalations in the exchangeable site (interlayer space remain) of the glauconite unit structure, absorbed part within micro-flakes or adsorbed part on the surface of mineral particles. The nanocomposites are to be classified as polyfunctional controlled-release fertilizers. Further, the simultaneous release of potassium makes the composite a complex release fertilizer.

Key words: glauconite, urea, polyfunctional nanocomposites, eco-friendly fertilizers, controlled-release fertilizers.

Controlled-release fertilizers (CRF) are vital to the development of eco-friendly agriculture [1]. Many researchers assessed the fertilizer potential of various substances and materials, such as clay minerals [2,3], chemical products and hydrogels, or complex composites. Compared to synthetic chemical substances, phyllosilicates are inexpensive and readily obtainable. Smectite (montmorillonite), vermiculite, kaolinite and to a lesser extent palygorskite and chrysotile are studied as slow-release or controlled-release fertilizers [4]. Recently, the potassium-iron rich clay mineral glauconite was also tested for CRF [3,5]. The encapsulated complex fertilizers are prepared by selecting an inhibitor and adding a nutrient within it through intercalation. Glauconite has superb sorption and ion-exchange properties, with a relatively high (from ~4 % to 8 %) K_2O content. Glauconite is finely ground in planetary mills for the preparation of nanocomposite CRF [3,5].

The study intends to develop polyfunctional "green" controlled-release fertilizer by activating glauconite-urea composites and assessing the relations between glauconite and nitrogen. We investigate a) nitrogen types in the nanocomposites formed after mechanical activation of glauconite and urea, b) the degree of intercalation and adsorbed nitrogen, and c) the effect of CRF on plant growth. Mixtures of glauconite (G) and urea (N) were prepared with a ratio of 1:1. The preparation was conducted independently in the planetary mill for 3, 8, or 14 min to obtain three nanocomposites, named G1N1-pm3, G1N1-pm8, G1N1-pm14.

This study concentrates on the release rates of nitrogen and potassium from the prepared composites based on the intercalation between urea and glauconite. Three different interrelationships between glauconite and urea are as follows: urea is intercalated into the interlayer space of glauconite; it is absorbed into the micropore space between glauconite micro-flakes; and adsorbed in the form of films incorporating micro-aggregates.

The mechanical activation of the glauconite and urea mixture was used to formulate the nanocomposite controlled-release fertilizers. The intercalation between urea and glauconite increases marginally from 21.2 to 23.1%, with the growth of activation tome. The nitrogen skin on glauconite flakes and plate thickens with time. The shift of first XRD-reflection to lower

angles for the longer duration milling (Fig. 1) and the absence of a weight loss in thermogravimetric curves at the temperature of the solvating water removal indicates the enhanced intercalation of urea into the interlayer space of mineral. The NH_2 FTIR-peak at 1155 1/cm increases with milling time, suggesting the greater adsorbtion of nitrogen on glauconite flakes. The NH_2 stretching at 3346-3500 1/cm becomes more frequent with the activation, confirming a higher degree of nitrogen intercalation, and minor shifts of NH_2 and NH peaks evidence the gradual character of this process.

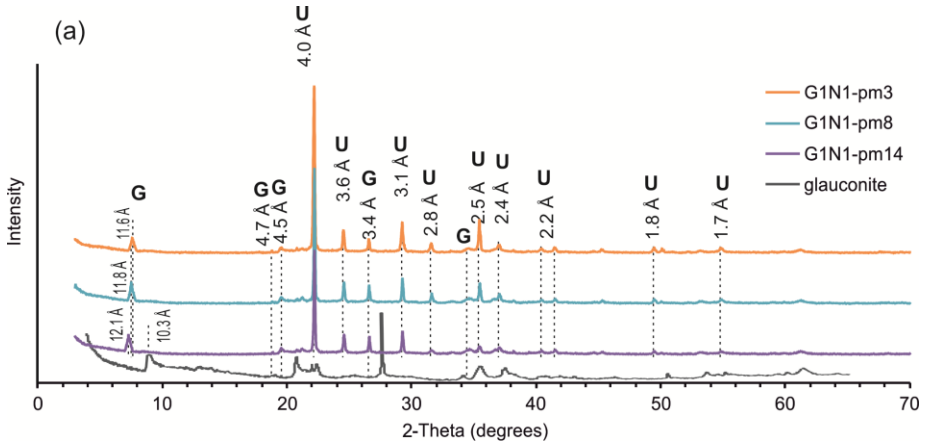

Figure 1 – XRD patterns of the composites for different grinding times. Note the shift of glauconite peaks in the composites.

Nitrogen releases from the nanocomposites in three stages during the course of the experiment. At the first stage, the external coating of the composite releases nitrogen in the first few days the absorbed nitrogen leaches at the second stage, after twenty-one days, and finally, the intercalated portion releases nutrients. Besides, the composites release the potassium in the leached solution, initially at a faster rate, slowing down after seven days. The application of the nanocomposites improves the seeding and growth of plant (*Avéna satíva*). The nanocomposites and traditional urea are equally effective fertilizer for crop production (dry weight and plant height). Therefore, nanocomposites based on glauconite and urea mixture provide an alternative to traditional urea. Further, because of the slow release of nutrients, it is an environment-friendly option. Besides, glauconite-urea composites are complex polyfunctional fertilizer that releases multiple nutrients simultaneously.

Funding: This work is supported by the President of the Russian Federation to support young Russian scientists (project number MK-1825.2022.1.5).

References:

1. Trenkel M.E. Slow- and Controlled-Release and Stabilized Fertilizers: An Option for Enhancing Nutrient Use Efficiency in Agriculture. Paris. International Fertilizer Industry Association (IFA). 2010. 163 p.

2. Pereira E.I., da Cruz C.C.T., Solomon A., Le, A., Cavigelli M.A., Ribeiro C. Novel Slow-Release Nanocomposite Nitrogen Fertilizers: The Impact of Polymers on Nanocomposite Properties and Function. Industrial & Engineering Chemistry Research. 2015. Vol. 54. P. 3717–3725.

3. Rudmin M., Banerjee S., Yakich T., Tabakaev R., Ibraeva K., Buyakov A., Soktoev B., Ruban A. Formulation of a slow-release fertilizer by mechanical activation of smectite/glauconite and urea mixtures. Applied Clay Science. 2020. Vol. 196. P. 1–10.

4. Rashidzadeh A., Olad A. Slow-released NPK fertilizer encapsulated by NaAlg-g-poly(AA-co-AAm)/MMT superabsorbent nanocomposite. Carbohydrate Polymers. 2014. Vol. 114. P. 269–278.

5. Rudmin M., Abdullayev E., Ruban A., Buyakov A., Soktoev B. Mechanochemical Preparation of Slow Release Fertilizer Based on Glauconite–Urea Complexes. Minerals. 2019. Vol. 9. P. 1–10.

AUTHIGENIC MINERALIZATION IN EXOGENETIC CONDITION ON EXAMPLE OF TAILINGS AND MINE SYSTEMS

Myagkaya I.N.

V.S. Sobolev Institute of Geology and Mineralogy, Novosibirsk, Russia,
i_myagkaya@igm.nsc.ru

Abstract. It were showed the autigenic minerals formation in the surface environment of the sulfide ore wastes distribution halos on the example of two objects (Novo-Ursk and Aktash deposits) that are part of the Altai-Sayan mercury province. The excess of mercury-bearing minerals (sulfides and selenides; the presence of triple and quadruple chalcohalides is assumed) as identified autigenic phases combines these objects. They occur as complex, fine and ultrafine aggregations and accretions of themselves, which makes a difficult to identify of their true compositions.

Key words: sulfide ore wastes, dispersion halo, secondary minerals, environment.

Recently, there has been an increasing interest in the knowledge of the species and speciation of elements in the environmental components. The studies of mineral species of elements (potentially toxic, noble) are actual, providing ecological and geochemical information about possible ways of migration and accumulation of elements. Often the secondary minerals occur as thin, ultrafine and complex phases in an inhomogeneous environment (soils, suspended/particulate matter, bottom sediments etc.). The research of these minerals is painstaking and can be technically complicated due to the characteristics of the substance and the forming phases themselves. However, the works are increasing their scale and relevance [1, 2].

The study was carried out using SEM (MIRA 3 LMU, *Tescan*, Czech Republic) on the example of natural organic matter (NOM) from the dispersion halo of the sulfide tailings of the Novo-Ursk deposit (Kemerovo region) [2] and in the particulate matter of snow cover from the dispersion halo of the Aktash deposit (Gorny Altai) [3]. Both objects are located in the western part of the Altai-Sayan mercury province (Kuznetsk-Altai mercury belt).

Wide range of secondary minerals was found in the NOM of the Novo-Ursk deposit dispersion halo, such as: sulfates (gypsum, jarosite, barite, anglesite); Fe(III) hydroxides; secondary aluminosilicates; sulfides (framboidal pyrite, zinc sulfides (sphalerite group), mercury sulfides (metacinnabarite is assumed)); mercury selenides (timannite); silver iodides (iodargyrite) and Au^0. Hg sulfides form ultrafine complex aggregations with different amounts of elements impurities (Fe, Zn, Cu, Ag, As, Se, I, P, Cl) that are in different relationships with each other. The presence of Zn and Cu impurities in mercury-bearing phases is associated with the formation of Hg and Zn sulfides accretions; the presence of Ag and I is associated with small amounts of their own minerals. Iodargyrite (AgI) was found in one of the NOM sample.

A significant amount of the primary minerals characterized for studied area was found (quartz, aluminosilicates, carbonates, phosphates (including REE)), technogenic particles (spherules of different composition, etc.) in the particulate matter of snow cover from the dispersion halo of the Aktash deposit. Secondary minerals are mainly mercury-bearing phases that form ultrafine aggregations with a size that isn't more than 20 μm; they consist of a set of separate individuals with a size of 100 nm to 1 μm (note that on both study objects). The size of

these phases makes a difficult to identify of their true compositions. However, it is known that in oxidation zones it is possible to form halide (triple (general formula $Hg_3(S,Se)_2Hal_2$) and quadruple (general formula AgHgS(Hal), where Hal = I, Br, Cl) chalcohalides) and oxy-halide mercury compounds. They form polymorphic varieties and element's impurities (Se, S, Ag, Br, I, Cl) may present in their composition [4]. These autigenic minerals are also called "seasonal" and form and disappear under the influence of climatic and atmospheric condition variations [5]. Thereby they phases are a source of elements in the environmental components. Comparison of the autigenic minerals compositions for the studied objects with the compositions of known phases [6] suggests the presence of several varieties of mercury-bearing phases forming ultrafine accretions: sulfides; selenides; compounds similar in composition to sulfo-selenium salts (triple and quadruple chalcohalides). So, mercury minerals (sulfides and selenides; triple and quadruple chalcohalides) dominate among the autigenic minerals, which occur as complex, fine, thin accretions with each other for both objects.

The author's great thanks to colleagues: PhD M.A. Gustaytis and PhD E.V. Lazareva, V.I. Malov and B.Yu. Saryg-ool.

Funding: The works were partly performed on a government assignment to the V.S. Sobolev Institute of Geology and Mineralogy, at the Analytical Center for Multi-Elemental and Isotope Research IGM SB RAS (Novosibirsk, Russia). The composition Hg-minerals was specified with the RSF support (No. 18-77-10056).

References:

1. Smieja-Król B., Pawlyta M., Gałka M. Ultrafine multi-metal (Zn, Cd, Pb) sulfide aggregates formation in periodically water-logged organic soil. Science of the Total Environment. 2022. Vol. 820. Art. 153308.

2. Myagkaya I.N., Lazareva E.V., Zhmodik S.M., Zaikovskii V.I. Interaction of natural organic matter with acid mine drainage: Authigenic mineralization (case study of Ursk sulfide tailings, Kemerovo region, Russia). Journal of Geochemical Exploration. 2020. Vol. 211. Art. 106456.

3. Gustaytis M.A., Myagkaya I.N. Distribution of mercury in the hair of residents of Aktash (Republic of Altai). Soils and environment. 2022. Vol. 5. No. 1. Art. e165. (In Russian).

4. Magarill S.A., Borisov S.V., Pervukhina N.V. et al. (2008): Features of the structure formation of rare mercury minerals and the role of crystal chemical analysis in studying the migration of heavy metals in natural and man-made environments. Biodiversity, ecology problems of the Altai Mountains and adjacent regions: present, past, future: Proceedings of the International Conference. Gorno-Altaysk: RIO GAGU. (In Russian).

5. Obolensky A.A., Ozerova N.A., Vasiliev V.I. Natural sources of mercury in Siberia. Chemistry in the interests of sustainable development. 1995. No. 3. P. 11-22. (In Russian).

6. Electronic mineralogical directory https://webmineral.com

GEOCHEMISTRY AND MINERALOGY OF SMALL LAKES BOTTOM SEDIMENTS IN THE SUBTAIGA ZONE, SOUTH OF WESTERN SIBERIA

Ovdina E.A.[1], *Strakhovenko V.D.*[1,2], *Malov G.I.*[1], *Malov V.I.* [1,2]

[1]V.S. Sobolev Institute of Geology and Mineralogy, Novosibirsk, Russia, ovdina@igm.nsc.ru
[2]Novosibirsk State University, Pirogova str., 1 Novosibirsk, Russia

Abstract. The work is devoted to the study of the bottom sediments' composition of three small lakes systems located in the same landscape zone. Differences in geochemical and mineral composition between lake systems have been established. In the mineral composition, the differences can be traced in the authigenic component - calcite-dolomite carbonates are found in the bottom sediments of the Kyshtovskaya lake system, which are not found in the lakes of other systems. The presence of carbonates is associated with the development of carbonatophilic biota in the lakes of the Kyshtovskaya system.

Key words: small lake, lacustrine bottom sediment, South of Western Siberia, calcite-dolomite carbonates

The research area is the south of the Vasyugan plain, a subtaiga landscape zone. The objects of research are small lakes. The paper considers three lake systems. In the northeastern part of the subtaiga zone, there are the Krasnoyarovskaya (5 lakes) and Samuskaya (3 lakes) lake systems. In the southwestern part, there is the Kyshtovskaya system (7 lakes).

The aim is to compare data on the geochemical and mineral composition of lacustrine bottom sediments in the subtaiga zone, south of the Vasyugan plain.

The materials of field and analytical work 2016-2019 were used. Sampling was carried out from a catamaran with a cylindrical sampler with a vacuum shutter. The core of bottom sediments was tested in layers with a step of 5 cm, to a depth of 50 to 250 cm. Physical and chemical variables of water were recorded *in situ* (pH, Eh, TDS). Analytical studies of the lake components were conducted in the Analytical Center for multi-elemental and isotope research SB RAS, Novosibirsk and at the Analytical Center of the Federal State Budgetary Educational Institution "NGPU", Novosibirsk. Methods of atomic absorption spectrometry, X-ray diffractometry, ion chromatography, scanning electron microscopy, X-ray spectral fluorescence analysis were used.

According to the main ions content, the water of the Krasnoyarovskaya lake system is sulfate-bicarbonate magnesium-sodium, ultra-fresh (0.01 g/L), pH 5.0-6.0. The water of the Samuskaya system is sulfate-bicarbonate sodium-calcium, ultra-fresh (0.02-0.03 g/L), pH 6.3-6.8. The water of the Kyshtovskaya system is bicarbonate magnesium-calcium, fresh (0.2 g/L), pH 7.9-8.8.

The lacustrine bottom sediments in the south of Western Siberia are organomineral silts (sapropels) and mineral silts, differing in the ratio of organic and mineral components (ash content) and chemical composition. The peculiarities of genesis and diverse composition determine the diversity of classifications and typological characteristics of sapropels. Depending on the ash content, sapropels are divided into types: organic (up to 30%); organic-mineral (30-50%); mineral-organic (50-70%), mineralized (70-85%). Bottom sediments with ash content >85% belong to mineral silts [1; 2].

Comparison of the elements average concentrations in the lakes bottom sediments with the composition of the upper continental crust [3] showed almost complete convergence of the

distribution graphs for the Krasnoyarovskaya and Samuskaya systems. High concentrations of Ca, Mn and Sr were observed in the lakes of the Kyshtovskaya system (Figure 1). Depletion of carbonatophilic elements in the bottom sediments of the Krasnoyarovskaya and Samuskaya systems is associated with the almost complete absence of carbonates in them against the background of the terrigenous component represented by quartz, feldspar, mica, as well as the biogenic component represented by diatoms (SiO_{2bio}). The bottom sediments of the lakes of these systems belong to the silicon class. Calcite-dolomite carbonates and aragonite are formed in the lakes of the Kyshtovskaya system on the geochemical barriers of drifting biota-water, water-submerged biota and water-bottom sediments [4]. The main authigenic minerals are low-magnesian calcite, calcite and aragonite. The lakes of the Kyshtovskaya system belong to the calcium class. The main difference is observed in the dominant primary producers – for the calcium class these are cyanobacterial colonies, reeds, and charales; for silicon class - diatoms, reeds, stratiotes, etc.

According to the results of this study, it is shown that lakes with different types and classes of sapropel deposits are located within the same landscape zone. The unique composition of small lakes in the south of Western Siberia is ensured by the predominance of local factors over global ones, the main of which is biota.

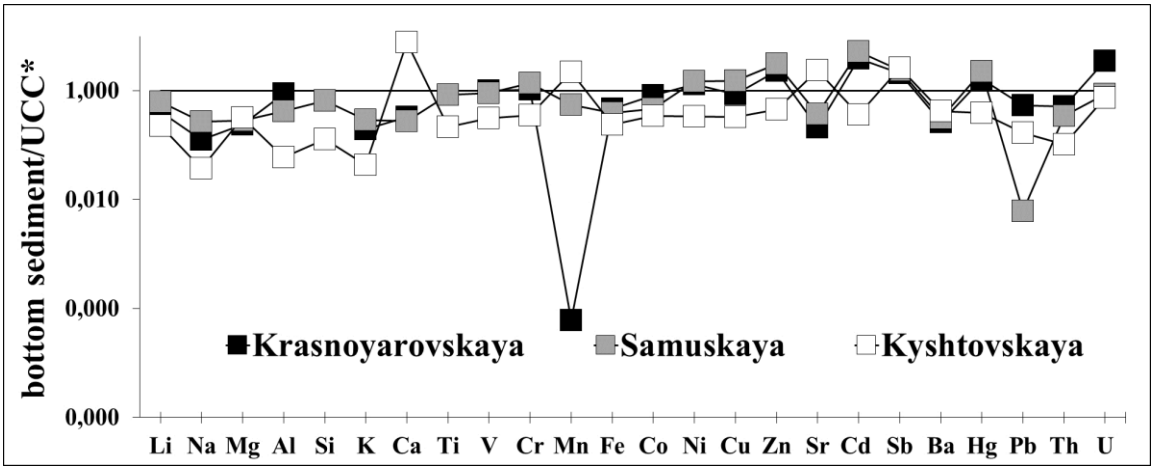

Figure 1 – The multi-element spectrum of the average values of the studied elements for lake systems bottom sediments normalized to the values of the upper continental crust* concentrations according to [3].

Funding: Work is done on state assignment of IGM SB RAS with the financial support of the Ministry of Science and Higher Education of the Russian Federation.

References:

1. Korde N.V. Biostratigraphy and typology of Russian sapropels. Moscow: Publishing House of the USSR Academy of Sciences. 1969. 219 p. (In Russian)
2. Strakhovenko V.D., Ovdina E.A., Malov G.I., Yermolaeva N.I., Zarubina E.Y., Taran O.P., Boltenkov V.V. Genesis of organomineral deposits in lakes of the central part of the Baraba Lowland (south of West Siberia). Russian Geology and Geophysics. 2019. Vol. 60. No. 9. P. 978–989
3. Wedepohl K.H. The composition of the continental crust. Geochimica et Cosmochimica Acta. 1995. Vol. 59. No. 7. P. 1217-1232
4. Ovdina E.A., Strakhovenko V.D., Solotchina E.P. Authigenic carbonates in the water-biota-bottom sediments' system of small lakes (south of Western Siberia). Minerals. 2020. Vol. 10. No. 6. Art.552.

METHOD FOR DETERMINING THE PARTICLE SIZE COMPOSITION OF BOTTOM SEDIMENTS IN THE SUBMICRON SIZE RANGE

Revunova A.V.

Institute of Limnology RAS – Saint Petersburg Federal Research Center RAS, St. Petersburg, Russia, reina_abc@mail.ru

Abstract. The paper proposes several ways to improve sample preparation for a better analysis of particle size distribution by pipetting method. Improvements are proposed based on work with a homogenized sample in 7-fold repetition and control under a microscope. A membrane filtration method is also described for studying the granulometric composition in a smaller range (0.2-1 μm). This is relevant for modern industrial development and environmental monitoring requirements, because particles of this size have the highest surface activity due to the huge total surface density.

Key words: particle size composition, Stokes' law, membrane filtration, pipetting method, bottom sediments.

Instructions for determining the particle size composition of clay soils are given in GOST 12536-2014 [1] and are almost verbatim duplicated in the book "Instructions for hydrometeorological stations and posts" [2]. The so-called pipette method for determining particle size composition is presented in these documents. It is based on Stokes' law, which describes the motion of a small particle in a liquid. Its essence is to take a sample containing particles smaller than a certain diameter after a certain settling time in a liter cylinder. The assumptions that must be taken into account when applying this method have repeatedly described in scientific articles [3, 4]. Other methods, also described in GOST [1] have much lower accuracy (areometric) or require specific equipment (fractional). Further, the pipette method is suitable for accounting for particles with a diameter of up to 0. 001 mm (1 μm). Meanwhile, the modern development of science and industry requires the determination of particle size distribution in much smaller sizes.

In this paper, several improvements are proposed for enhancing the preparation of clay soil samples, as well as a method for determining the granulometric composition by the direct method of membrane filtration (developed by the scientific group of the Institute of Limnology RAS - SPB FRC RAS [5]). The need to improve sample preparation was revealed precisely when filtering a sample from the upper 5 cm of a suspension taken from a liter cylinder after 21 hours and 7 minutes of settling at a constant temperature in the laboratory (22.5 °C) and with a sample with a specific gravity of 2.6 g/cm [1]. Despite settling for the specified time, particles suspended in the top 5 cm of the suspension clog the pores of filters with a diameter of 1 and even 2 micrometers (Fig. 1).

All proposed improvements are based on experiments comparing 7 samples prepared according to GOST [1] and 7 prepared with changes. In addition to the statistical (indirect) method of control, a direct method is used - observation under a binocular with a 1000x magnification. The list is started with «0» number, because filters are not directly related to sample preparation but play a crucial role in the analysis. So, the improvements are:

0. Use of plastic membrane filters instead of pulp and paper.

1. Stop using a rubber pestle
2. Replacing sodium pyrophosphate with 30% hydrogen peroxide
3. Removal of chitin particles by centrifugation
4. Addition of sodium pyrophosphate just before filtration
5. Vibration during filtration.

With the simultaneous use of all the proposed methods, filters with a pore diameter of 1 μm are not clogged with larger particles, and it becomes possible to take into account particles with a size of 0.2-0.8 μm.

Figure 1 – Problem: clogged filter pores with a pore diameter of 1 μm.

Funding: the work was carried out as part of government assignment of the Institute of Limnology, RAS No. 0154-2019-0003.

References:

1. GOST 12536-2014 Soils. Methods of laboratory granulometric (grain-size) and microaggregate distribution. 2015. 24 p.

2. Instructions for hydrometeorological stations and posts: Vol. 2. Part 2. Hydrological observations at posts. Leningrad. Gidrometeoizdat. 1975. 263 p.

3. Blokhin A. N., Kulizhsky S. P. Evaluation of the application of the laser diffractometry method in determining the granulometric composition of soils. Bulletin of Tomsk State University. Biology. 2009. No. 1(5). P. 37-43.

4. Zdobin D. Yu., Semenova L.K. On the granulometric analysis of clay soils: laser and classical methods. Geoecology. Engineering geology, hydrogeology, geocryology. 2011. No. 6. P. 560-567.

5. Pozdnyakov Sh.R., Ivanova E.V., Revunova A.V., Shmakova V.Yu., Ryzhkevich T.I. On the issue of assessing the granulometric composition of sediments of the submicron range. Regional ecology. 2019. No. 3(57). P. 45-54.

FORMATION OF TIMBER DRIFTING AND LOGJAMS ON THE DEBRIS FLOW OF SAKHALIN ISLAND

Rybalchenko S. V.

Special Research Bureau for Automation of Marine Researchers, Far East Branch of RAS, Yuzhno-Sakhalinsk, Russia, rybalchenko_sv@mail.ru

Abstract. The paper considers the regional features of the phenomena of timber drifting and logjams on the debris flow rivers of Sakhalin Island, the factors formation of timber drifting are studied, the mechanisms of the occurrence of logjams are established. Regional climatic and geological features lead to the formation of a significant amount of entrained and suspended river sediments during floods on most watercourses, which causes its high transporting and abrasive ability and affects channel deformations, the involvement and movement of timber drifting, the formation of logjams.

Key words: debris flow, timber drifting, logjams, slope exogenous processes, riverbank erosion.

Due to the geographical features of the region and the history of the development of the territory, most settlements, transport infrastructure and economic activities on the territory of Sakhalin Island are located near the mouth of mountain rivers. The road transport network stretches along the coastal strip and crosses a large number of watercourses. These circumstances cause a high threat of timber drifting and logjams for residential areas and the transport network of Sakhalin Island, as well as the relevance of the study of such phenomena.

Since 2008, the author has conducted long-term field studies of the formation of timber drifting and logjams on the debris flow of Sakhalin island the framework of scientific works and scientific and technical support of engineering surveys in terms of dangerous exogenous processes. In the course of these works, observations were made on the emergence and development of timber drifting and logjams, as well as debris flow processes. The author analyzed the arrays of experimental data on this issue obtained by domestic and foreign researchers, as well as in the framework of his own experiments [1]. A comparative analysis of the phenomena of timber drifting and logjams on debris flow rivers in other regions, including within the boundaries of the cryolithozone on the territory of Kamchatka, the Magadan region and the Stanovoe Highlands, has been carried out.

The purpose of the study is to study the regional features of the phenomena of timber drifting and logjams on the debris flow of Sakhalin island in order to develop further practical recommendations for their prevention. To study the regional features of the phenomena of timber drifting and logjams on the Sakhalin Island watercourses, it is necessary to study the factors of the formation of timber drifting, to establish the mechanism of the occurrence of logjams, to determine the regional features of the phenomena of timber drifting and logjams.

On the territory of Sakhalin Island, timber drifting and logjams are ubiquitous. Logjams are especially characteristic for small streams of the mountain-taiga type. The catchments of watercourses are represented by V-shaped valleys with steep sides and a significant longitudinal slope of the riverbed, which ensures a minimum time of reaching and the formation of maximum expenses, these circumstances lead to rapid rises of water during floods. Rain floods formed in small watercourses of Sakhalin Island (both debris flow and non-debris flow) are characterized by high turbidity values [2]. Significant slopes and easily eroded rocks composing the sides and bottoms of the riverbed, combined with a high intensity of precipitation, lead to a strong

saturation of streams with a solid fraction. As a result, the density of flood flows often approaches the density of sediment flows. At the same time, their eroding and abrasive ability increases sharply, which significantly affects channel deformations, the involvement and movement of timber and the formation of logjams. High-density flows have an increased transporting capacity relative to the logs, since they increase the pulling force of the flow acting on the midsection of the root system of log, and also increase the buoyancy of log, due to an increase in the pushing Archimedean force.

In contrast to full-flowing rivers, the main source of logs for small Sakhalin watercourses is not channel processes associated with erosion and abrasion of the banks, but slope exogenous processes actively occurring in the sides of the catchment basin (debris flows, landslides, erosion, etc.) due to the geological features of the region. among which it is worth highlighting high soaking, porosity, low physical-mechanical characteristics and low resistance to weathering of rocks, which causes their active involvement in various exogenous processes. The climate of the island is humid monsoon with annual precipitation amounts exceeding 2000 mm in mountainous areas [3]. All this causes a high activity of aquatic and water-gravity exogenous geological processes (debris flows, landslides, erosion, etc.), contributing to the entry of a large number of large plant residues into the river. Also, a significant contribution to the volume of logs entering the channel is made by extensive wind tunnels formed during numerous cyclones with wind modulation in V-shaped valleys and near-ridge zones. In the future, wildwoods is transferred by slope exogenous processes and temporary watercourses to the talweg of the catchment basin.

According to the results of the work, the regional features of the formation of logjams include the geological structure of catchment basins composed of easily eroded soils, and the rock composition of floodplain forests, mainly represented by birch, willow and alder with a developed crown, which contributes to the formation of logjams in scaffolding spaces, culverts and in places of a cramped or meandering channel. When the core of the logjams is formed from floating logs and the flow is redistributed along the flow arms, there is an active deposition of entrained and suspended sediments in the bottom parts due to a decrease in the flow velocity, resulting in the formation of stable ground-wood logjams that spring up the channel. This mechanism of logjams formation is typical for all debris flow rivers in Russia.

Funding: The presented results were obtained with the financial support of the state task FWWW-2022-0005

References:

1. Kazakov N.A., Bobrova D.A., Kazakova E.N., Rybalchenko S.V. Investigation of the dynamics of debris flows on an experimental stand. Hydrosphere. Dangerous processes and phenomena. 2019. Vol. 1. No. 4. P. 491-503

2. Kazakov N.A., Zhukova Z.I. Conditions for the formation of debris flow floods in small watercourses. Natural disasters and natural disasters in the Far Eastern region. 1990. Vol. 2. P. 394-400.

3. Kazakov N.A., Gensiorovsky Yu.V. The effect of the vertical gradient of precipitation on the characteristics of hydrological, avalanche and debris flow processes in the lowlands. Geoecology. Engineering geology. Hydrogeology. Geocryology. 2007. No. 4. P. 342-347

STUDY OF VERTICAL DISTRIBUTION OF TRACE METALS IN BOTTOM SEDIMENTS OF SHALLOW COVES OF PETER THE GREAT BAY

Ryumina A.A., Tishchenko P.Ya., Shkirnikova E.M., Goryachev V.A.

V.I. Il`ichev Pacific Oceanological Institute, Vladivostok, Russia, ryumina.aa@poi.dvo.ru

Abstract. In the period from 2018-2022, geochemical studies of the bottom sediments cores of the Voevoda, the Novgorodskaya and the Uglovoy coves were carried out, which included measurements of the trace metals and organic carbon concentrations along the core depth with an interval of 10 cm. Also the granulometric composition of cores and the sedimentation rate were studied; the work was based on the measurement of the content of technogenic radionuclide ^{137}Cs. A linear relationship between the concentration of zinc, lead, copper and nickel with organic carbon was found in Voevoda cove.

Key words: trace metals, organic carbon, granulometry, sedimentation rate.

The work purpose is to study the vertical distribution of metals (Pb, Zn, Ni, Cu, Mn, Cr, Co) and organic carbon in the bottom sediments of three shallow coves of Peter the Great Bay. The Voevoda cove and the Novgorodskaya cove have significant areas covered with sea grass *Zostera Marina L.* (further in the text ZM). There aren't sea grasses in Uglovoy cove practically. The cores of dark gray, almost black, color with a characteristic smell of hydrogen sulfide were raised for the Voevoda and the Novgorodskaya coves. The Uglovoy cove sediments are gray, extremely fine and homogeneous.

The methods by which the selected samples were analyzed are described below. Granulometric analysis was performed on the Analysette 22 NanoTec laser particle analyzer (Fritsch, Germany). The ^{137}Cs content in bottom sediment samples was measured using a gamma spectrometer with a GEM150 ultrapure germanium detector (crystal diameter 88.5 mm, height 99.8 mm), with a DSPEC jr 2.0 digital multichannel analyzer (ORTEC, USA). Organic carbon in the solid phase of precipitation was measured using a TOC-VPN analyzer with a prefix for burning solid samples SSM-5000A (Shimadzu, Japan). The metal content in the samples was determined by flame atomic absorption spectrometry on the AA-3600 apparatus (Shimadzu, Japan).

Granulometric analysis of the surface, middle and lower horizons of studied bays cores showed that the psammite fraction present in all samples from the Voevoda cove (from 1.39% to 17.1%) and in the surface layer of the Novgorodskaya cove (3.64%). Siltstones predominate for the Voevoda cove. Also the siltstone fraction prevails in the surface layer (73.98%) in the Novgorodskaya cove samples, but the pelite fraction content increases with core depth increasing. In the Uglovoy cove samples the pelitic fraction prevails (from 54.83% to 73.04%).

The sedimentation rate in bottom sediment samples was estimated from measurements of the activity of the technogenic radionuclide ^{137}Cs by core depth (the maximum ^{137}Cs activity corresponds to the time of the most intensive nuclear weapons tests, 1963) [1]. The sedimentation rate for the Voevoda cove is 8 mm/year, 7 mm/ year for the Novgorodskaya cove and 3 mm/year for Uglovoy cove. Previously, the sedimentation rate in the northern part of the Amurskiy Bay was determined using the ^{210}Pb radioisotope and corresponded to 7.2 mm/year [2] and 3.6 – 5.2 mm/year [3]. Earlier obtained results are in good agreement with our estimates.

Based on sedimentation rate information, it is possible to draw conclusions about the age of the studied bottom sediments. The age of the lower layer of the Novgorodskaya cove is 120 years, 90 years is for the Voevoda cove and 296 years is for the Uglovoy cove.

The organic carbon content is high in bottom sediments covered with meadows of ZM. The content of organic carbon decreases within the upper 40 cm of bottom sediments free of ZM and then it does not change with depth for all the studied basins. A sharper decrease of the organic carbon is observed in the upper horizons for sediments covered with ZM, which is apparently due to a more active apparent degradation of organic matter in the upper layer of precipitation.

The concentrations of copper and zinc in the Voevoda cove are significantly higher in the core taken in the thickets of ZM. The decrease in their concentration with depth, in our opinion, is due to the use of organic matter by detritophages in food. As a result of this process in the upper part of the bottom sediments, heavy metals pass from the bottom sediments into the organisms of detritophages and accumulate in them.

Lead is distributed randomly along the vertical profile. For nickel, cobalt, and chromium, small fluctuations in concentrations are noticeable. The highest concentrations of manganese were found in Novgorodskaya cove. The high content of manganese may be due not only to allochthonous runoff, but also to the fact that it is a typomorphic element [4].

For the samples taken in Voevoda cove, a linear relationship between the concentration of metals and the content of organic carbon was found. This correlation can be explained by the physiological features of ZM. The polysaccharide zosterol is synthesized in its leaves. This substance is a natural ligand with respect to heavy metals [5]. When grass dies off, organocomplexes enrich bottom sediments with trace elements and organic carbon.

Funding: This work is supported by the Russian Foundation for Basic Research 20-05-00381-a and the program of fundamental scientific research, topic 0211-2021-0014.

References:

1. Tsabaris C., Kapsimalis V., Eleftheriou G., Laubenstein M., Kaberi H., Plastino W. Determination of ^{137}Cs activities in surface sediments and derived sediment accumulation rates in Thessaloniki Gulf, Greece. Environmental Earth Sciences. 2012. Vol. 67. No. 3. P. 833-843.

2. Anikiev V.V., Dudarev O.V., Kasatkina A.P., Kolesov G.M. Influence of terrigenous and biogenic factors on the formation of sedimentation flows of chemical elements in the coastal zone of the Sea of Japan. Geochemistry. 1996. No. 1. P. 59-72.

3. Astakhov A.S., Kalugin I.A., Aksenov K.I., Darin A.V. Geochemical indicators of paleotayfuns in shelf deposits. Geochemistry. 2015. No. 4. P. 387-392.

4. Ocean Chemistry. Volume 2. Geochemistry of bottom sediments. Under the general editorship of Volkov I.I. Moscow. Nauka. 1979. 536 p.

5. Khozhaenko E.V., Khotimchenko R.Y., Kovalev V.V., Khotimchenko M.Y., Podkorytova E.A. Metal Binding Activity of Pectin Isolated from Seagrass Zostera marina and its derivatives. Marine Pharmacology. 2015. Vol. 41. No. 6. P. 485-489.

EVALUATION OF METHODS FOR CALCULATING THE INTENSITY AND VOLUME OF SNOW TRANSFER ACCORDING TO ACTUAL DATA ON THE EXAMPLE OF YUZHNO-SAKHALINSK

Sergeev M.S.

Special Research Bureau for Automation of Marine Researches, Yuzhno-Sakhalinsk, Russia, sergeevkorsakov@yandex.ru

Abstract. This paper analyzes the works of various researchers available at the time of writing on the topic of methods for calculating the intensity and volume of snow-drift. The main methods of counting are revealed. According to them, the values were calculated and compared with the actual data obtained from field observations. The features of calculations using different methods are established, the most suitable calculation scheme is selected. According to our results, a method for calculating the volume of snow transfer was determined that most accurately coincides with empirical data.

Keywords: low-level snow drifting, snow-drift transport, Sakhalin

In this paper, the process of transferring previously fallen snow by wind is considered. This process is called a low-level blizzard, as well as a snow-drift transport. The damage from low-level blizzards is the formation of snow drifts on roads and railways most often. Horizontal visibility may also deteriorate. Such phenomena often cause automobile and railway accidents. So, on March 12, 2022, in the area of the study, a low-level blizzards caused two car accidents and the closure of an entire section of road.

Thus, the assessment of the volume (q) of snow-drift transport is an urgent and at the same time the most difficult task, the solution of which will avoid both economic damage and human casualties. To solve this problem, it is necessary to analyze the methods for calculating snow transfer volumes based on actual data. For this purpose, full-scale observations of snow transfer were carried out in the vicinity of Yuzhno-Sakhalinsk on the territory of agricultural fields at their junction with the highway.

The analysis of the results of calculating snow-drift transport volumes was carried out using semi-empirical formulas (Table 1) from the works [1-3]. Rectangular drifting snow gauge with a hole area of 10 cm^2 and a volume of 1000 cm^3 were used for measurements (Figure 1). The location of the drifting snow gauges is on the surface of the snow mass, the direction of the first drifting snow gauge is strictly in the wind, the second at an angle of 45 degrees. Wind speed measurements were carried out at altitudes of 0.1-2 and 2 meters.

The results of calculations using three formulas (Table 1), showed significant differences both among themselves and between the actual data.

A comparison of the actual data with the calculated data showed that the closest values are shown by the formula of the Canadian scientist Pomeroy. Probably, such a difference in the calculated values is due to the use of empirical coefficients. So, for each specific locality, it is necessary to add additional parameters related only to a specific territory to the existing dependency. This approach means that in order to assess snow transfer, preliminary studies are required to determine the desired coefficient for each individual site.

Table 1 – Comparison of snow-drift transport volumes by formulas with actual values

Data	[2] $q = \frac{V^{4,2}}{704077}$	[1] $q = 0,034(V-3)^3$	[3] $q = 0,0215V^3$	Our measurements
28/02	33,6	18,6	54	35
	gramm / 600 sec / 1000 sm^2			
12/03	39,6	20,4	34,32	40
	gramm / 120 sec / 1000 sm^2			
20/03	20	7,6	33	19
	gramm / 600 sec / 1000 sm^2			

Figure 1 – Drifting snow gauges during the study 28.02.2022

*Funding: The presented results were obtained with the financial support of the state task for the implementation of the topic №FWWW-*2022-0005.

Reference:

1. Byalobgenski G.V., Dyunin A.K. Winter maintenance of highways. 2nd edition. Transport Publ. 1983. 197 p.
2. Tabler R.D., Pomeroy J.W. Drifting snow. Cold Regions Hydrology. 1990. P. 95-145.
3. Mihael V.M., Rudneva A.V. Zoning of the territory of the USSR for the transfer of snow. Questions of applied climatology. 1967. P. 79-91.

FEATURES OF INTEGRATED PROCESSING AND UTILIZATION OF MINING WASTES AS A SECONDARY RESOURCE (ON THE EXAMPLE OF PHOSPHOGYPSUM)

Suchkov D.V., Litvinova T.E., Shaykina K.D.

Saint Petersburg Mining University, Saint Petersburg, Russia, s205055@stud.spmi.ru

Abstract. The study is devoted to an actual issue of integrated processing and utilization of large-tonnage mining wastes (on the example of phosphogypsum). Based on the literature and patent reviews, it has been established that the joint utilization of the waste and CO_2-containing industrial gases will make it possible to obtain a number of commercial products: Ca^{2+} carbonate (phosphochalk); NH_4^+, Na^+ or K^+ sulfate and REEs concentrate. At the same time, an important task is to control the particle size of the pulp of finely dispersed phosphochalk.

Key words: industrial gases, phosphochalk, phosphogypsum, REEs, waste utilization.

Utilization of large-tonnage industrial waste is one of the most urgent environmental problems in Russia and in the world, since the maintenance of disposal facilities is associated with the land withdrawal and concomitant pollution of the environment. In particular, a large-tonnage wastes of phosphogypsum (PG) are formed in the production of extractive phosphoric acid at the stage of phosphorus extraction from mineral raw materials. It contains about 80% $CaSO_4 \cdot nH_2O$ ('hemihydrate' when 'n = 0.5' or 'dehydrate' when 'n = 2'). The global annual PG yield is more than 150 million tons, including 14 million tons in Russia. According to the UN, no more than 4% of waste is recycled in the world [1].

PG has a significant difference from natural gypsum-containing raw materials. It is a certain amount of undesirable impurities, such as heavy elements oxides. On the one hand, this limits the possible application of PG. On the other hand, its use without prior extraction of valuable chemicals leads to the loss of the latter [2].

In the North-West Federal District of Russia (NWFD) there are 3 large PG-stacks with a mass of already placed PG up to 150 million tons. In the conditions of an excessively humid climatic zone of the North-West of the Russian Federation, complete isolation of the stacks is impossible. The issue of disposal of such large-tonnage technogenic wastes as PG, in conjunction with the need for environmental monitoring of existing facilities, is one of the most important environmental problems of the NWFD and Russia in a whole [1].

The study is solving the topical **issue** of useful utilization of large-tonnage wastes of the mineral resource complex. The **aim** is to develop a technical solution for the effective use of the study **object** – technogenic raw material (phosphogypsum) – as a secondary resource. The **subject** of the study is the possibility of using wastes for the obtaining of marketable products. The **scientific novelty** of the research lies in the establishment of physical and chemical laws that underlie the process of carbonate conversion of PG during its processing into phosphochalk ($CaCO_3$). Special attention is also paid to the issue of the fineness of the obtained $CaCO_3$ (the existing technical solutions do not focus on this problem).

The **practical significance**: recommendations have been developed for the complex PG utilization to obtain a number of valuable products: ammonium, sodium or potassium sulfate (depending on the conversion conditions), phosphochalk and a concentrate of REEs. The

proposed solution also implies the possibility of associated utilization of industrial flue gases containing carbon dioxide CO_2, which is used in the process of carbonate conversion.

As a solution to the problem of complex waste utilization, it is proposed to produce $CaCO_3$ (phosphochalk) from PG by the gas-liquid method (saturation of the PG suspension with CO_2), and the source of CO_2 can be industrial gases generated during the production of mineral fertilizers. Thus, the development of the proposed topic of scientific research can be considered promising and relevant for the mineral resource complex.

PG conversion is supposed to be carried out using M_2CO_3 solutions, where M^+ are NH_4^+, Na^+, or K^+ ions (hereinafter). Gas-to-liquid shifting (using CO_2) can be done by pre-carbonizing the MOH solution to produce M_2CO_3 or directly carbonizing the PG slurry. Depending on the additional treatment, the solution after separation of the $CaCO_3$ precipitate may contain rare earth elements that are promising for isolation at an additional stage of the process [3, 4].

The resulting phosphochalk, being a product of hydrochemical synthesis, has an increased chemical activity. It can replace natural limestone in the production of alumina, chemicals and cement. $CaCO_3$ is in great demand in metallurgy [3]. As part of the analysis of the potential sales market in the conditions of the NWFD, it was established that phosphochalk may be in demand by the Cherepovets Metallurgical Plant. When organizing PG processing at Apatit JSC (also located in Cherepovets), logistics costs are minimized, which increases the competitiveness of products.

The main disadvantage of the existing technological solutions for the processing of PG for phosphochalk is the fineness of the resulting $CaCO_3$ crystals (2-6 μm) [3]. This leads to a significant decrease in filtering properties. Difficulties with separating the product from the solution increase wear on equipment that requires more frequent maintenance. Therefore, within the framework of the study, special attention is paid to the issue of obtaining products with desired properties, namely, the regulation of the particle size of the pulp of finely dispersed phosphochalk.

On the basis of the performed literature and patent analysis, the method of hydrochemical processing of PG for phosphochalk was chosen as the most promising direction that allows achieving complex waste utilization. Further experimental and theoretical studies are aimed at finding and choosing reaction parameters that will allow one to control the particle size of phosphochalk upwards without loss of PG utilization efficiency. The introduction of these technical solutions will lead to a more rational use of the country's mineral resource base and increase the efficiency of its reproduction, as well as reduce the environmental pollution.

Funding: This research was carried out in the accredited Center for the Collective Use of the St. Petersburg Mining University and supported by the grant of the Government of St. Petersburg.

References:

1. Meshcheryakov Yu.G., Fedorov S.V. Industrial processing of phosphogypsum. St. Petersburg. Stroyizdat St. Petersburg. 2007. 104 p.

2. Bashlykova T.V., Valkov A.V., Petrov V.I. Extraction of rare earth elements from phosphogypsum and gold mining waste. Nonferrous metals. 2012. Vol. 3. P. 40-42.

3. Altiner M. Effect of Alkaline Types on the Production of Calcium Carbonate Particles from Gypsum Waste for Fixation of CO_2 by Mineral Carbonation. International Journal of Coal Preparation and Utilization. 2018. P. 113-131.

4. Ennaciri Y., Mouahid F.E., Bendriss A., et al. (2013): Conversion of phosphogypsum to potassium sulfate and calcium carbonate in aqueous solution. In: MATEC Web of Conferences, Vol. 5, REMCES XII – XIIe Rencontre Marocaine sur la Chimie de l'État Solide, Marocco.

MICROPLASTICS IN WATER AND SEDIMENTS OF LAKE LADOGA AND THE GULF OF FINLAND

Tikhonova D.A., Ivanova E.V.

[1]Institute of Limnology of the Russian Academy of Sciences, St. Petersburg Federal Research Center of the Russian Academy of Sciences, Saint Petersburg, Russia, tdasha94@mail.ru

Abstract. Concentrations of microplastics and their characteristics were studied in water and sediments of Lake Ladoga and the Gulf of Finland. Microplastic particles were analyzed using microscopy and spectroscopy methods to assess their shape, size, color, and chemical composition. The results showed that the Gulf of Finland was more contaminated with microplastics than Lake Ladoga. The study of the vertical distribution of microplastics in Lake Ladoga is still ongoing, preliminary results showed that microplastic particles were present in all water layers.

Keywords: microplastics, Lake Ladoga, the Gulf of Finland

Plastic is one of the most popular and widely used artificial materials. Plastic objects eventually degrade into smaller particles called microplastics. Nowadays, microplastics are present in all environmental matrices. Moreover, it is impossible to withdraw microplastics from the environment, where these particles can be potentially hazardous for ecosystems. Studying microplastics in water bodies provides better understanding of distribution and behavior of these particles.

We conducted the studies of microplastics in water and sediments of Lake Ladoga and its tributaries and the Gulf of Finland. These water bodies are strategic to Saint Petersburg and Leningrad Region. Lake Ladoga drains into the Gulf of Finland via the Neva River. The Gulf of Finland is a terminal drainage basin collecting many pollutants, including microplastics, from municipal wastewater and the Neva runoff. The study of microplastics in the Gulf of Finland showed relatively high concentrations of these particles in the coastal area [1].

The water of Lake Ladoga was sampled using a special filtration device that can be used from a research vessel, a boat or ice. This device accurately determines the water volume and allows sampling from different depths of the water column with a pump [2]. Water samples from various depths provide better understanding of the vertical distribution of microplastics and their behavior in the water column. Preliminary results showed that microplastic particles were present throughout all depths of the water column of Lake Ladoga, however the highest concentrations were found in the surface layer as in other studies [3, 4]. Plastic particles gradually foul up with biofilm consisting of microorganisms and humic substances and then sink to the bottom, where these particles accumulate in sediments.

Sediment samples were taken using the Ekman grab. Sediment treatment included density separation with $ZnCl_2$ solution (1.7 g/cm^3) for extracting microplastics from mineral substance. The Fenton's reagent was used to dissolve organic matter impeding visual identification of microplastics [5]. After all treatment steps, samples were analyzed using an optical microscope Euler Professor 770T to assess size and color of microplastic particles. Additionally, a lipophilic stain Nile Red was used together with a fluorescence microscope Micmed-2 (LOMO) to facilitate the process of distinguishing between plastic particles and biological matter, for

example, algae or chitin fragments. The chemical composition of particles was studied using a Raman spectrometer Horiba Jobin-Yvon LabRam HR800 (the Resource Center Geomodel, St. Petersburg State University). Blank samples with distilled water treated the same way as the real samples were used to control the external contamination.

Concentrations of microplastics in sediments are significantly higher than in water, as sediments are the deposit environment for microplastic particles, reflecting the long-term pollution processes. Concentrations of microplastics both in water and sediments were several times higher in the Gulf of Finland than in Lake Ladoga. The majority of found particles were less than 1 mm in size. Microplastics were mostly presented by fibers, however occasionally there were also fragments, films, and pellets (fig. 1). Among the plastic fibers there were polyethylene terephthalate, polyethylene, polycarbonate, and nylon particles.

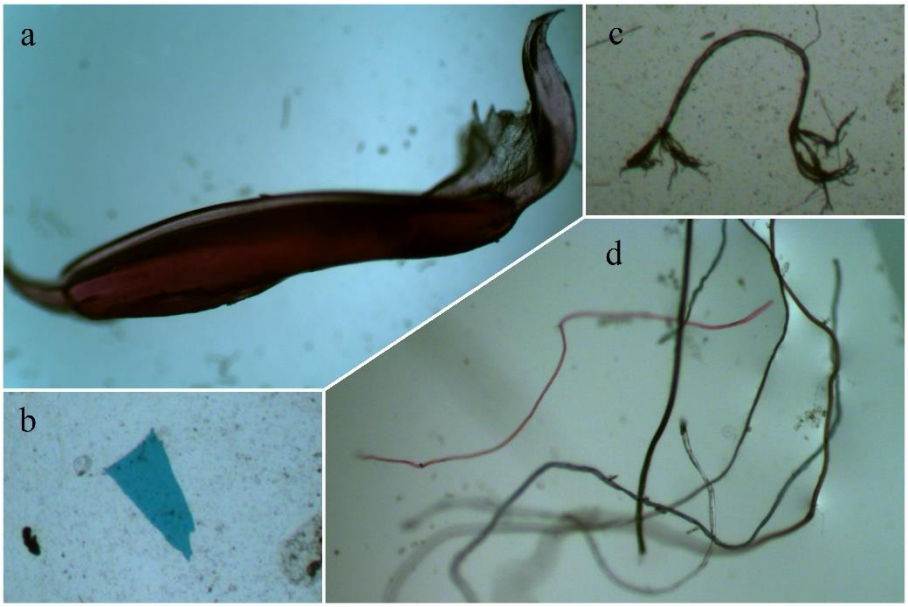

Figure 1 – Microplastic particles in water and sediments of Lake Ladoga (a, b – fragments, c, d – fibers).

Funding: This study was carried out under Governmental Order to Institute of Limnology of the Russian Academy of Sciences, St. Petersburg Federal Research Center of the Russian Academy of Sciences (subject no. 0154–2019-0003 "Development of integrated methods for studying and evaluating the characteristics of solid particles at nanoscale size in water bodies with different levels of anthropogenic impact").

References:

1. Pozdnyakov Sh.R., Ivanova E.V., Guzeva A.V., Shalunova E.P., Martinson K.D., Tikhonova D.A. Studying the concentration of microplastic particles in water, bottom sediments and subsoils in the coastal area of the Neva Bay, the Gulf of Finland. Water Resources. 2020. Vol. 47. No. 4. P. 599-607.

2. Pozdnyakov Sh.R., Karetnikov S.G., Ivanova E.V., Tikhonova D.A., Lapenkov A.E., Guzeva A.V. Experience of using a filtration device for studying vertical distribution of microplastics in water column. Russian Journal Of Applied Ecology. 2021. Vol. 4. No. 28. P. 41-45. (In Russian)

3. Reisser J., Slat B., Noble K., du Plessis K., Epp M., Proietti M., de Sonneville J., Becker T., Pattiaratchi C. The vertical distribution of buoyant plastics at sea: an observational study in the North Atlantic Gyre. Biogeosciences. 2015. Vol. 12. P. 1249-1256.

4. Song Y.K., Hong S.H., Eo S., Jang M., Han G.M., Isobe A., Shim W.J. Horizontal and vertical distribution of microplastics in Korean coastal waters. Environmental Science and Technology. 2018. Vol. 52. No 21. P. 12188-12197.

5. Ivanova E.V., Pozdnyakov Sh.R. Tikhonova D.A. Analysis of microplastic concentrations in water and bottom sediments as a new aspect of ecological monitoring. IOP Conference Series Earth and Environmental Science. 2021. Vol. 834. No. 1. Art. 012057.

DISSOLVED ORGANIC MATTER IN CO_2-RICH MINERAL WATERS OF TRANSBAIKALIA

Ukraintsev A.V.

Dobretsov Geological Institute of Siberian Branch of Russian Academy of Sciences,
Ulan-Ude, Russia, ukraintsev87@bk.ru

Abstract. The article presents the results of dissolved organic matter (DOM) study in several CO_2-rich mineral waters of Transbaikalia. The qualitative composition of DOM has been established. Relatively high contents of alkanes were found in all samples. It is probably due to the fact that their solubility increases under the influence of the fluid of carbon dioxide. According to OEP (odd-even predominance) index calculations, the composition of hydrocarbons is mainly formed without the participation of biogenic factors.

Key words: CO_2-rich mineral waters, dissolved organic matter (DOM), carbon dioxide fluid

It is considered that CO_2-rich mineral springs are located mainly in tectonically active regions on continental margins undergoing collisional processes characterized by active modern volcanic activity [1]. But also in the central parts of the continents there are areas where a flow of carbon dioxide takes place and mineral waters are formed. One of these areas is located in the northeastern part of Eurasia on the territory of Transbaikalia. It was studied the composition of DOM in the waters of four fields of cold CO_2-rich mineral waters: Kuka, Molokovka, Darasun and Shivanda.

The composition of DOM was determined using a technique based on concentration by solid-phase extraction [2] with gas chromatography-mass spectrometric finish (Agilent 7000B GC/MS). The extraction was performed using a portable unit immediately after sampling. This made it possible to record exactly DOM composition that is present directly at the outlets of mineral water springs.

The qualitative composition of DOM is diverse, it includes alkanes, alcohols, acids, ethers and aromatic compounds. Normal alkanes and isoalkanes are found in CO_2-rich mineral waters. Normal alkanes have molecular lengths from C14 to C18. We found the alcohols with one, two and three hydroxyl groups, with carbon chain lengths C17 and C18; carboxylic acids are with carbon chain lengths exceeding 16. In total, 156 organic compounds were identified, which we combined into 9 groups (Table 1).

Relatively high contents of alkanes, both normal and branched, were found in all samples. The increased content of alkanes in CO_2-rich mineral waters is probably due to the fact that their solubility increases under the influence of carbon dioxide, which is in a supercritical state.

Significant contents of alcohols of various structures and dicarboxylic acids were established. All samples contain aromatics and phthalates. Esters are mainly represented by di-(2-ethylhexyl) ester of adipic acid; the origin of this compound in samples has not yet been explained. In all samples, there is a small percentage (from 1.7 to 3.9) of compounds for which it was not possible to determine even their belonging to any class.

The largest percentage of saturated hydrocarbons is observed in the waters of the Darasun field. According to our observations, a distinctive feature of these waters is their high gas

saturation. Carbon dioxide comes in large quantities from the depth and that creates conditions for the accumulation of alkanes of various structures in the waters of Darasun.

Table 1. Composition of hydrocarbons found in CO_2-rich mineral waters, %

	n-alkanes	Isoalkanes	Sum of alkanes	Alcohols	Isoalcohols	Sum of alcohols	Dicarboxylic acids	Aromatic compounds	Ethers and esters	Unspecified substances
Kuka	2.51	10.84	13.35	8.1	0.11	8.21	0.68	3.91	68.6	1.89
Molokovka	4.32	14.44	18.76	11.7	0.22	11.92	0.68	5.82	55.98	3.04
Darasun	5.01	19.75	24.76	6.55	0.48	7.03	0.7	2.29	58.96	3.86
Shivanda	5.51	16.54	22.05	16.91	0.62	17.53	2.38	4.43	46.59	1.7

The predominant source of organic matter can be indicated by the OEP (odd-even predominance) index calculated by formula (1) [2].

$$OEP_i = \left(\frac{C_i + 6C_{i+2} + C_{i+4}}{4C_{i+1} + 4C_{i+3}}\right)^{(-1)^{i+1}} \quad (1)$$

OEP index values closed to 1.0 indicate the abiogenic origin of hydrocarbons; in turn, values that differ from 1.0 up or down indicate the dominant biogenic source of organic matter [3]. Our data allowed to calculate the OEP index for hydrocarbons of the studied waters by five homologues, starting with C14. Odd-even predominance index values for hydrocarbons in Molokovka (OEP_{14} = 1.05), Shivanda (OEP_{14} = 1.02) and Darasun (OEP_{14} = 1.06) waters deviate from 1.0 by no more than 0.06. This suggests that organic matter is deeply transformed, the composition of hydrocarbons was formed without the participation of biogenic factors. The composition of DOM in the Kuka field water is characterized by an OEP index equal to 1.52. Apparently, the formation of hydrocarbons in these waters is influenced by factors of biogenic nature. This assumption is supported by the data in Table 1, in Kuka water there is the lowest among the studied waters percentage of alkanes, both normal and branched.

The results obtained show that the presence of hydrocarbons in waters is mainly determined by the peculiarities of the geological and hydrogeological structure of the areas where mineral springs come out, and the influence of supercritical carbon dioxide fluid plays a decisive role in the formation of DOM composition.

Funding: Work was done as part of the state assignment of the Geological Institute of the SB RAS, project AAAA-A21-121011890033-1 «Geoecological risks and extreme natural phenomena in Siberia and Russian Far East».

References:

1. Barnes I., Irvin W.P., White D.E. Global distribution of carbon dioxide discharges and major zones of seismicity. Water Resources Investigation WRI. Geological Survey (U.S.). Washington, DC. Vol. 78. No. 39. 1978. 12 p.

2. Ukraintsev A.V., Plyusnin A.M. (2019): Application of solid-phase extraction method for the analysis of dissolved organic substances composition in CO_2-rich mineral waters. In Proceedings of the V All-Russian Baikal Youth Scientific Conference on Geology and Geophysics. P. 90-92 (In Russian).

3. Scalan E.S., Smith J.E. An improved measure of the odd-to-even predominance in the normal alcanes of sediment extracts and petroleum. Geochimica et Cosmochimica Acta. 1970. Vol. 34. No. 5. P. 611-620.

4. Poturay V.A., Kompanichenko V.N. Composition and distribution of saturated hydrocarbons in the thermal waters and vapor–water mixture of the Mutnovskii Geothermal Field and Uzon Caldera, Kamchatka. Geochemistry International. 2019. Vol. 57. No. 1. P. 74-82.

THE FLOW CHARACTERISTIC OF THE CAMBRIAN BLUE CLAYS IN SCOPE OF HAZARDOUS WASTE DISPOSAL

Vilkina M.V.[1,2], *Nikulenkov A.A.*[1,2], *Rumynin V.G.*[1,2]

[1]St.Petersburg Division, Sergeev Institute of Environmental Geoscience, Russian Academy of Sciences, St. Petersburg, Russia, wilkina.mari@hgepro.ru
[2]Saint Petersburg State University, St. Petersburg, Russia

Abstract. Along with the advances that technological progress has brought to daily life, it has also presented dilemma of waste disposal. The preset research investigates hydrogeological settings of the block structured Cambrian Blue Clays at Krasnyi Bor site in scope of safe hazardous waste disposal. The study combines both theoretical and field data obtained from the articles and visual analysis of the open-pit mine, laboratory head permeability tests, and in-situ Lugeon tests. The investigation proved the Cambrian Blue Clays to act as an aquitard and an aquifer depending on the lithostatic load. To describe the mechanism of the fracture aperture further investigations might be in need.

Key words: hazardous waste disposal, block-fractured clays, Lugeon tests, clays fracture aperture

By the middle of the 20th century, a number of the countries, including the USSR were grappling with the issue of the hazardous waste disposal [1]. In Russia long-term storage of containments was chosen as a prior method of disposal. In this regard, the waste storage location must meet a number of criteria, including logistical accessibility and the presence of an impermeable layer. According to the geological survey results, such a site was discovered to the south of Saint Petersburg, where the Cambrian blue clays appear at the surface.

During of 45 years of operation of the landfill 70 soil excavations were made. Now they store up to 1.7 million tons of highly toxic waste. Industrial waste is disposed in both solid and liquid form.

Cambrian blue clays have a block-fractured structure, which calls their aquitard properties into question. These properties are mostly noticeable in the upper part of the geological cross-section as this particular part has been exposed to the weather changes and the glacier action. The total thickness of the clays at the investigation site reaches 90 m. The regional groundwater flow is directed north to the Neva River. Along with the groundwater flow the solute containments are washed out of the landfill.

In 2014 it was decided to liquidate Krasnyi Bor landfill. The main goal was to prevent the spread of contamination from soil excavations into the environment. First, it was decided to recycle the liquid content of the excavations; and then to cover the landfill with impermeable geomembrane. The construction of a cutoff wall along the polygon perimeter is planned to prevent the spread of highly toxic content into groundwater. For maximum efficiency the cutoff wall should be installed to the depth of impermeable layers. As a result, the flow parameters of the Cambrian blue clays play an important role in ensuring environmental safety.

To date, there are two principal approaches to consider the properties of block-fractured clays. Proponents of the first approach consider clays as an unsuitable medium for waste disposal. A number of research [2, 3] conclude that the clay massif enhances the water flows

through the fractures supporting this idea by the presence of iron hydroxide on the block walls, the negative impact of microbial contamination of rocks, and high values of the hydraulic conductivity. The second group of the researchers accept the concept of the block-fractured clays, yet assume the fractures to be in a closed state as they are subjected to the lithostatic pressure. This statement is also supported by the swelling properties of clays and the formation of a film upon contact with industrial chemical waste.

The purpose of the present study was to investigate the flow parameters of the Cambrian blue clays at the site of Krasnyi Bor landfill. Different laboratory and field methods were used for отмечать this.

The laboratory methods included determining of clay permeability by falling head permeability tests in the oedometer based on Terzaghi theory, as well as the constant head permeability method. The values obtained from both methods show a good correlation between each other and vary from 8.00E-08 to 6.3E-06 m/day. These values do not exceed the maximum allowable hydraulic conductivity for landfill basement of 8.64E-06 m/day (1E-10 m/sec) set by Russian Federation regulation. Though laboratory methods show first-order accuracy, they do not account for a problem of the representative elementary volume REV. For this reason, the field methods were used as well.

The visual analysis of the closely located open-pit mine proved the clays to have a block-fractured structure. The size of the blocks separated by fractures has a strong tendency to grow with depth. Thus, the blocks' size at the upper bench ranges from 5 to 10 cm, while the size of the blocks at the lower bench reaches up to several meters. When the cores are raised to the ground, there are no visible signs of an open state of fracture in the core samples taken from the landfill's boreholes. The core samples are splatted apart by an orthogonal fracture network after a few hours or days. This occurs as a result of moisture loss and the removal of lithostatic pressure.

To investigate the hydraulic conductivity of the Cambrian blue clays the in-site Lugeon tests were performed. The Lugeon tests technique implies water injection into isolated by packer borehole interval. The pressure of the water injection is gradually increased and then gradually decreased. The Moye solution [4] enables the interpretation of injection tests as well as the quantification of clay permeability. Water injection pressure equal to 4 lithostatic pressure causes fractures to open, resulting in hydraulic conductivity values of 5E-01 m/day.

During the research following results were obtained: the behavior of the block-fractured Cambrian blue clays depends on the conditions they are located at (1); under the influence of the lithostatic pressure the hydraulic conductivity approximately equals n·E-07 estimated by laboratory methods (2); when the clays are exposed to the day surface the hydraulic conductivity may reach up to 0.5 m/day estimated by Lugeon tests. The double nature of the Cambrian blue clays should be taken into consideration when constructing hazardous waste landfill.

Funding: This work is supported in scope of Federal Targeted Program "Ecology" in Russia.

References:

1. Arnould M. Discontinuity networks in mudstones: a geological approach. Implications for radioactive wastes isolation in deep geological formation in Belgium, France, Switzerland. Bulletin of Engineering Geology and the Environment. 2006. Vol. 65. P. 413–422.

2. Tavenas F., Jean P., Leblond P., Leroueil S. The permeability of natural soft clays. Part II: permeability characteristics. Canadian Geotechnical Journal. 1983. Vol. 20. No. 4. P. 645–660.

3. Zeng L. L., Hong Z. S., Cai Y. Q., Han J. Change of hydraulic conductivity during compression of undisturbed and remolded clays. Applied Clay Science. 2011. Vol. 51. No. 1–2. P. 86–93.

4. Moye D.G. Diamond drilling for foundation exploration. Civil Engineering Transactions, Institution of Engineers of Australia. 1967. Vol. 9. No. 1. P. 95–100.

Section NEW INFORMATION AND GEO-INFORMATION TECHNOLOGIES IN GEOLOGY

SUPERVISED CLASSIFICATION OF PERIGLACIAL LANDFORMS IN THE LENA DELTA SECOND TERRACE BY USING MACHINE LEARNING ALGORITM

Kartoziia A.A.[1,2,3], *Chupina D.A.*[1], *Glushkova N.V.*[1]

[1]V.S. Sobolev Institute of Geology and Mineralogy, Novosibirsk, Russia,
andrei.kartoziia@igm.nsc.ru
[2]A.A. Trofimuk Institute of Petroleum Geology and Geophysics, Novosibirsk, Russia
[3]Novosibirsk State University, Novosibirsk, Russia

Abstract: Monitoring of Arctic landscape changes under the influence of global warming become an important goal for nowadays geosciences. New methods of machine learning have achieved impressive results in landscape's recognition accuracy. We have analyzed Sentinel imagery (31/07/2020) and obtained index map images in Google Earth Engine. We assessed spatial distribution of identified land classes, which concern to different steps of thermokarst activity. Our work have showed possibility of using random forest method for mapping periglacial landforms.

Key words: the Lena delta, Arga Island, supervised classification, random forrest, Google earth engine

Monitoring of Arctic landscape changes under the influence of global warming become an important goal for nowadays geosciences. Classification methods of remote sensing data allow recognizing and estimating landscape changes. Now, new methods of machine learning have achieved impressive results in landscape's recognition accuracy. In particular, the random forest method is described like as one of the best method of machine learning [1]. The cloud platforms for remote sensing data geoinformation works allow analyzing big volumes of data with very big velocity and in on-line regime.

The main aim of this work is to assess intensity of thermokarst process for a second terrace of the Lena Delta. To achieve this aim, we set ourselves the task of mapping various types of landforms, which are associated with active thermokarst processes.

The Lena River Delta is the largest Arctic river delta in the world. We have studied the second terrace of the delta (Arga Island), which is located in the western part of the delta and occupies it's one third. This terrace has a height of 20–30 m a.s.l. and is built of fluvial massive fine-grained deposits without silt, clay, or organic matter. The deposition of these sediments mainly occurred in the marine isotope stage (MIS) 3 Interstadial and continued in the MIS 2 glacial period. It's surface consist of a number of landforms such as thermokarst hollows, valleys and undegradated flat uplands.

We have analyzed Sentinel imagery (31/07/2020) and obtained index map images in Google Earth Engine [2]. Firstly, we visually identify typical objects and landforms of Arga Island's surface. These are thermokarst hollows, valleys, undegradated flat uplands, slope's surfaces, as well as sands and water bodies. All of these have specific pixel values due to

different vegetation or water presence. In its turn, vegetation is an indicator of various successions, which are developing according to landscape transformations.

Then, we have created 100 training polygons for all identified five landscape classes. After it, we created a number of index map images. We used NDVI, NDWI, EVI and tasseled cap indexes. We have trained a classifier by using training polygons and inputting Sentinel imagery and index map images. After described technical steps we have classified key-site Arga Island's surface. Finally, we have assessed spatial distribution of identified land classes, which concern to different steps of thermokarst activity.

Thus, our work have showed possibility of using random forest method for mapping periglacial landforms. This method might be used for landscape changes monitoring and for detection of hazards, which concern to permafrost degradation.

Funding: This work is done on the state assignment of V.S. Sobolev Institute of Geology and Mineralogy, Siberian Branch of the Russian Academy of Sciences.

References:

1. Pirotti F., Sunar F., Piragnolo M. Benchmark of machine learning methods for classification of a Sentinel-2 image The International Archives of the Photogrammetry, Remote Sensing and Spatial Information Sciences. 2016. Vol.+ XLI-B7. P. 335–340.

2. Gorelick N., Hancher M., Dixon M., Ilyushchenko S., Thau D., Moore R. Google Earth Engine: Planetary-scale geospatial analysis for everyone. Remote Sensing of Environment. 2017. Vol. 202. P. 18–27.

USING OF GIS TECHNOLOGIES FOR A STRUCTURAL PREDICTIVE DEPOSIT SEARCH MODEL DEVELOPMENT ON THE EXAMPLE OF SOUTHEASTERN TRANSBAIKALIA

Lapaev D.S, Ustinov S.A., Ishmuhametova V.T., Nafigin I.O., Petrov V.A.

Institute of Geology of Ore Deposits, Petrography, Mineralogy and Geochemistry of the Russian Academy of Sciences, Moscow, Russia, lapaev@igem.ru, ustinov@igem.ru

Abstract. On the example of the territory of southeastern Transbaikalia, using GIS technologies, a complex structural predictive model of mineral deposits was created. To achieve the goal, an extensive set of available information on the object of study was used and lineament analysis was applied. Based on the interpretation of the results of lineament analysis, a scheme of neotectonic stresses was created. The spatial distribution of the supposed ore-controlling structures was estimated based on the creation of schemes of object distribution densities, analysis and interpretation of rose diagrams.

Key words: GIS technologies, predictive search model, lineament analysis, south-eastern Transbaikalia

The structural and material reasons for the spatial combination of different types of multimetal mineralization in the same ore-containing structures requires practical solutions to numerous issues of the genesis of ores, deposits, their lateral and vertical zonality, the possibility of forming extended ore-bearing columns. This fact, considering a large shortage of easily discovered deposits, increases the chances of detecting hidden mineralization in the structures of ore areas. In order to solve these tasks, it is extremely relevant to develop and implement new predictive prospecting models based on structural features that are the most stable for all predictive taxa and, in particular, for local ore-controlling structures.

Fault zones are universal structural units used in predictive constructions within the hierarchical system of taxa accepted in ore geology. Starting from the mineragenic zone and ending with the ore body, discontinuous faults from the deep fault to local fracture zones are distinguished as constituent elements of search objects corresponding to the scale of work. This allows to consider discontinuous structures as one of the determining factors of mineralization control, mainly of hydrothermal genesis. The hypothesis of the spatial-genetic connection of hydrothermal ore bodies and faults is considered as the most promising for solving problems of forecasting deposits. It is based on the idea of the presence of vertical permeable structures (channels) through which fluids moved from the magma chamber to ore-neutralizing structures in the surface layers of the cover [1].

Identification of ore-controlling and ore-containing structures among the general ensemble of discontinuous fractures of a particular territory is possible through a detailed study of the developed deposits that play the role of reference objects for the studied area.

Southeastern Transbaikalia is a region characterized by an extremely complex geological structure, the development of rich and, most importantly, diverse endogenous mineralization. It is known that all the numerous models explaining the patterns of spatial placement and the peculiarities of the formation of endogenous mineralization of the studied area are based on the ideas about the development of its tectonic structures. Metallogeny of the area is mainly

associated with the processes of Mesozoic tectonic-magmatic activation – uranium-molybdenum (Streltsovka group), polymetallic and fluorite deposits have been explored or exploited. Numerous hydrothermal manifestations of gold, silver, barium, lithium, arsenic and tin are known. Taking into account the prospects for the discovery of new deposits, in order to compile a geological justification and set the tasks of evaluation and exploration work, it becomes necessary to identify the features of the tectonic structure of the area under consideration, conduct geodynamic reconstructions, assess the stress state of rock massifs and the kinematics of movements in the zones of major faults.

At the first stage of the work, a lineament analysis, the purpose of which is to identify diagnostic signs (lineaments) on the studied area [2] was carried out. This analysis is one of the most effective remote methods for studying the framework of discontinuous fractures and the deep structure of territories.

The lineament analysis of the territory was carried out using a special technique based on the construction and analysis of detailed digital elevation models (DEM), proposed and tested on real geological objects by employees of the Geoinformatics Laboratory of IGEM RAS [3]. In the process of lineament analysis, the decoding of lineaments (presumably faults) was carried out, followed by the identification of smaller rectilinear relief elements near them, which may correspond to feathering breaks in the fault zone. These results made it possible to implement the structural-geomorphological method of L.A. Sim [4,5] and construct a tectonic scheme of neotectonic stresses.

With the help of a specialized software module, a diagram of the densities of structural elements for known and established fault zones is constructed. When applying the tectonic scheme to the resulting density scheme of all linear structural elements, it is possible to identify areas characterized by maximum structural permeability, taking into account the kinematics of fault zones.

It is assumed that the areas characterized by the highest density of lines, as well as those formed in the presence of additional stretching conditions, are promising for setting up search operations.

Funding: This work is supported by IGEM RAS in the frames of the Program of the Ministry of Science and Higher Education of Russian Federation.

References:

1. Serebryakov E.V., Gladkov A.S., Gromova I.A. Structural predictive prospecting model of the indigenous diamond deposits of the Nakyn kimberlite field (Yakut diamond province). The Scientific Heritage. 2020. Vol. 55. No. 3. P. 36-50. (In Russian)

2. Katz Ya.G., Poletaev A.I., Rumyantseva E.F. Fundamentals of lineament tectonics. Moscow. Nedra. 1986. 144 p. (In Russian)

3. Ustinov S.A., Petrov V.A. The use of detailed digital relief models for structural and lineament analysis (on the example of the Urtuisk granite massif, SE Transbaikalia). Geoinformatics. 2016. No. 2. P. 51-60. (In Russian)

4. Sim L.A. The study of tectonic stresses by geological indicators (methods, results, recommendations). Izvestiia VUZov. geol. and razv. 1991. No. 10. P. 3-22. (In Russian)

5. Rebetsky Yu.L., Sim L.A., Marinin A.V. From Slickensides to Tectonic Stresses. Methods and Algorithms; Moscow. GEOS Publishing House. 2017. 234 p. (In Russian).

Section GEOPHYSICAL RESEARCH METHODS

AMBIENT NOISE CORRELATION REVEALS TEMPORAL CHANGES OF SEISMIC VELOCITIES BELOW BEZYMIANNY VOLCANO PRIOR TO AN EXPLOSIVE ERUPTION

Berezhnev Y.M.[1,2], Belovezhets N.N.[1,2], Shapiro N.M.[3,4], Koulakov I.Y.[1,2]

[1]Novosibirsk State University, Novosibirsk, Russia, y.berezhnev@g.nsu.ru
[2]A.A. Trofimuk Institute of Petroleum Geology and Geophysics, Novosibirsk, Russia
[3]Schmidt Institute of Physics of the Earth, Moscow, Russia
[4] Centre National de la Recherche Scientifique, Université Grenoble Alpes, Grenoble, France

Abstract. Strong explosive eruption of Bezymianny volcano (Klychevskoy volcano group) occurred on 21 December of 2017, which preparation phases were recorded by a local seismic network. Seismic noise correlation revealed temporal seismic velocity changes beneath the volcano preceding the event. Observed velocity responses was consistent with modeled effect of strain redistribution of magma migration.

Key words: seismic noise, volcano monitoring, ambient noise, velocity changes estimation

Bezymyanny volcano is an active explosive stratovolcano with andesitic-dacitic composition, part of Klychevskoy volcano group. Currently Bezymianny produces extrusive-explosion eruptions about one-two times per year [1]. One of the strongest recent eruptions of Bezymianny occurred on 20th of December 2017 [2], which preparation phases and itself was recorded by local seismic network. In the present study we used data from the network, implemented a method of seismic noise cross-correlation to reveal temporal changes of seismic velocities beneath the volcano. After that we verified it using modeling of strain in the medium below the edifice.

We used continuous data of the five broadband seismic stations and analyzed it in the period from 1 August 2017 to 1 January 2018 that spanned the eruption and its all preparative phases. To extract the Green's function, we applied the following procedures to the vertical component of seismograms [3]. First, seismic signal was demeaned, detrended and prefiltered in frequency range of 0.1 to 1.2 Hz. Then we removed instrumental responses and resampled signals from 100 Hz to 10 Hz. Next we normalized signals in time and frequency domain using one-bit normalization and spectral whitening in ranges of periods 1-3 s, 2-4 s, 3-6 s and 3-8 s. Finally, we computed the cross-correlation function (CCF) of preprocessed signals for all pairs of stations and all periods. To estimate temporal velocity changes we applied Bayesian least-square inversion [4] of multiple window cross-spectrum analysis measurements [5]. Evaluated relative velocity changes for each pair of station was averaged in each passband to extract precursors of the eruption.

To evaluate the effect of strain redistribution due to magma migration prior to the eruption, we used a model of a spherical pressure source [6] and estimated average strains and velocity changes [7] in the observation area in depth. Next we used sensitivity kernels of the fundamental mode of the Rayleigh surface wave based on the tomographic model of Bezymianny volcano before the eruption [8] to evaluate the observed temporal velocity changes. So, velocity changes

response prior the eruption obtained from strain model is consistent with averaged measurements prior such strong eruption.

Funding: This work is supported by the Russian Science Foundation under grant 22-27-00374.

References:

1. Ozerov A. Y., Ariskin A. A., Kyle P., Bogoyavlenskaya G. E., Karpenko S. F. A petrological–geochemical model for genetic relationships between basaltic and andesitic magmatism of Klyuchevskoi and Bezymiannyi volcanoes, Kamchatka. Petrology. 1997. Vol. 5. P. 550–569.

2. Girina O. A., Loupian E. A., Melnikov D. V., Manevich A. G., Sorokin A. A., Kramareva L. S., Uvarov I. A., Kashnitskiy A. V. Bezymianny volcano eruption on December 20, 2017. Modern problems of remote sensing of the Earth from Space. 2018. Vol. 15. No. 3. P. 88–99.

3. Bensen G. D., Ritzwoller M. H., Barmin M. P., Levshin A. L., Lin F., Moschetti M. P., Shapiro N. M., Yang Y. Processing seismic ambient noise data to obtain reliable broad-band surface wave dispersion measurements. Geophysical Journal International. 2007. Vol. 169. No. 3. P. 1239–1260.

4. Brenguier F., Campillo M., Takeda T., Aoki Y., Shapiro N.M., Briand X., Emoto K, Miyake H. Mapping pressurized volcanic fluids from induced crustal seismic velocity drops. Science. 2014. Vol. 345. P. 80–82.

5. Clarke D., Zaccarelli L., Shapiro N. M., Brenguier F. Assessment of resolution and accuracy of the Moving Window Cross Spectral technique for monitoring crustal temporal variations using ambient seismic noise. Geophysical Journal International. 2011. Vol. 186. No. 2. P. 867–882.

6. McTigue D. F. Elastic stress and deformation near a finite spherical magma body: Resolution of the point source paradox. Journal of Geophysical Research. 1987. Vol. 92. P. 12931 - 12940.

7. Hotovec-Ellis A. J., Gomberg J., Vidale J. E., Creager K. C. A continuous record of intereruption velocity change at Mount St. Helens from coda wave interferometry. Journal of Geophysical Research: Solid Earth. 2014. Vol. 119. No. 3. P. 2199–2214.

8. Koulakov I., Plechov P., Mania R., Walter T. R., Smirnov S. Z., Abkadyrov I., Jakovlev A., Davydova V., Senyukov S., Bushenkova N., Novgorodova A., Stupina T., Droznina S. Y. Anatomy of the Bezymianny volcano merely before an explosive eruption on 20.12.2017. Scientific Reports. 2021. Vol. 11. No.1. Art. 1758.

ASSESSMENT OF DECLINATION AND INCLINATION OF THE VECTOR OF REMANENT MAGNETIZATION ACCORDING TO HISTORICAL DATA AT STUDY OF ARCHAEOLOGICAL OBJECTS IN THE BAIKAL REGION

Dudinskaya E.V., Absalyamova D.F.

Irkutsk National Research Technical University, Irkutsk, Russia, lenchik.nyash@gmail.com

Abstract. The possibility of obtaining prior information on values of declination and inclination of a vector of remanent magnetization by analogy method based on results of an archaeomagnetic research in Britain is considered. The assessment of parameters is carried out based on the correlation of the normal magnetic field for the IGRF model for the quatercentenary temporary row.

Key words: inversion, magnetic survey, ironmaking furnaces, magnetic susceptibility, remanent magnetization

The possibility of obtaining a priori information in the study of the remains of ancient ironmaking furnaces according to magnetic survey data is considered. The results of measurements of the magnetic susceptibility of samples were used, the declination and inclination of the remanent magnetization vector were determined by analogy with the results of archaeomagnetic studies in Britain based on the correlation of the normal magnetic field for the IGRF model during last 400 years.

The method of magnetic exploration makes it possible to detect and study the distribution of magnetic inhomogeneities in rocks according to the features of the geomagnetic field's structure.

For the inversion of magnetic survey data with the determination of the parameters of inductive and remanent magnetization [1], it is important to have priori estimates of the ranges of magnetic susceptibility, which determines the inductive component, as well as the declination and inclination of the vector of residual magnetization.

To work out the elements of the magnetic field inversion technology, the results of magnetic surveys performed on the remains of ancient ironmaking furnaces known in various parts of the world can be used [2, 3, 4]. These objects are characterized by the presence of metallurgical products with a high content of ferromagnetic materials, which determines their significant magnetic susceptibility and thermoremanent magnetization acquired during the production process.

The remains of metallurgical furnaces are usually well localized, which allows to obtain realistic estimates of geometric parameters using data from previous archaeological studies. So, ancient metallurgists of the Olkhon region 2000 years ago used forges cut in cut in the indigenous sandy-loamy rocks. The inner cavity of the furnace, 170-190 cm deep, had a triangular shape and transverse dimensions of about 1 m. In 2021 a UAV magnetic survey was carried out at the Burun-Khal II facility using the SibGIS UAS complex [4].

Relatively large fragments of the furnace coating and caked slag may have significant remanent magnetization, the parameters of which are still unknown for such archaeological sites of the Western Baikal region. Therefore, to determine the estimates of the declination and inclination of the remanent magnetization vector, we used the analogy method with the

involvement of relevant UK information on the remains of iron-making furnaces in Cornwall [4] and archaeomagnetic calibration curves [4, 5].

Figure 1 – Forges cut down in the indigenous sandy-loamy rocks.

To establish a connection between the elements of the normal magnetic field in Britain and the Western Baikal region, the IGRF magnetic field model embedded in the NOAA Magnetic Field Calculators [6] was used. It made it possible to determine the declination and inclination values for two points "London" and "Irkutsk" in the time interval from 1590 to 2021.

The high absolute values of the linear correlation coefficients for declination and inclination allow us to make the conclusion about possible deviations of the directions of the vectors of remanent magnetization formed at the turn of AD in the means of iron-making production from the direction of the vector of the modern magnetic field. In the case of undisturbed occurrence of remnants of furnaces and products of iron-making production, the deviation in declination may be ± (5 ÷ 10) °, and in inclination ± (10 ÷ 15) °.

References:

1. Davydenko A.Y. (2020): Magnetic field inversion based on an elastic network and vector scanning to assess the magnetic susceptibility and residual magnetization of three-dimensional objects. In the collection: Questions of theory and practice of geological interpretation of geophysical fields. Materials of the 47th session of the International Scientific Seminar of D. G. Uspensky - V. N. Strakhov. P. 105-110. Voronezh.

2. Davydenko S.Y., Tereshkin S.A., Davydenko A.Y., Snopkov S.V., Parshin A.V., Davydenko Y.A. The use of UAVs and ground-based geophysical methods in the study of the ancient metallurgical complex at the BarunKhal II site (Western Baikal region). Geoarchaeology and archaeological Mineralogy. 2021. Vol. 8. P. 35-40.

3. Kharinsky A.V., Kozhevnikov N.O., Snopkov S.V. (2012): Metallurgical centers of the western coast of Lake Baikal in the 1st millennium AD. In Materials of the II International Congress of medieval archeology of the Eurasian steppes Barnaul, History and culture of medieval peoples of the steppe Eurasia. Publishing house Alt. University.

4. Smekalova T., Bruce B. Magnetic Directions of Furnaces in Wales. 1999.

5. Batt C. M. The British archaeomagnetic calibration curve: an objective treatment. Vol. 39. No. 1. 1997. P. 153-168.

6. Magnetic Field Calculators https://www.ngdc.noaa.gov/geomag/calculators/magcalc.shtml?#igrfwmm

CRUSTAL THICKNESS IN CENTRAL KAMCHATKA INFERRED FROM RECEIVER FUNCTION TECHNIQUE

Ivanov A.D.[1,2], Jakovlev A.V.[1,2], Koulakov I. Yu.[1,2]

[1]A.A. Trofimuk Institute of Petroleum Geology and Geophysics, Novosibirsk, Russia,
[2]Novosibirsk State University, Novosibirsk, Russia, a.ivanov19@g.nsu.ru

Abstract. The P-receiver function technique was applied to one year data of 55 seismic stations in the Central zone of Kamchatka. Crustal thickness and the average crustal V_p/V_s ratio under each station are determined using grid search technique H-k stacking. The crustal thickness varies from 25 to 40 km. The average crustal V_p/V_s ratio in the upper crust ranges from 1.6 to 1.9. The obtained results consist with the other researcher's studies.

Key words: Central Kamchatka; crustal thickness; receiver function technique

Kamchatka peninsula located in the transition zone between the continental and the oceanic plates. Therefore, tectonic structure is very complex here. Information about the deep structure of the Earth's crust and mantle beneath Central Kamchatka is of great importance for understanding the mechanism of formation of volcanic structures in this region and for creating geodynamic models.

The method of receiver function is one of the main methods for determining of the crustal thickness. The basics of the method were developed and presented in an article by L.P. Vinnik [1] in 1977. The receiver function method is used to determine the geometry of seismic boundaries in the crust and upper mantle. It is based on the analysis of the difference in the arrival times of direct and converted phases of seismic waves from distant seismic events. The first step of this method is rotation of the seismogram from geographical coordinate system (ZNE) to the ray coordinate system (LQT), the second step is deconvolution the radial component of the seismogram by the vertical component, and the third step is stacking. Here we use the method to transform time differences into seismic boundaries depth is grid search by Zhu and Kanamori [2].

From the continuous seismograms recorded from July 2019 to June 2020 by temporary and permanent networks consisting of 23 and 32 seismic stations respectively (fig.1), we selected more than 150 records corresponding to teleseismic events. These events were used for the receiver function analysis with use of grid search method (H-k staking) proposed by Zhu and Kanamori [2]. As a results, the depth of the Moho and V_p/V_s ratio beneath stations have been determined. Obtained results show that the crustal thickness varies from 25 to 40 km, the V_p/V_s ratio in the upper crust ranges from 1.6 to 1.9. Results consist with the previous studies [3,4,5].

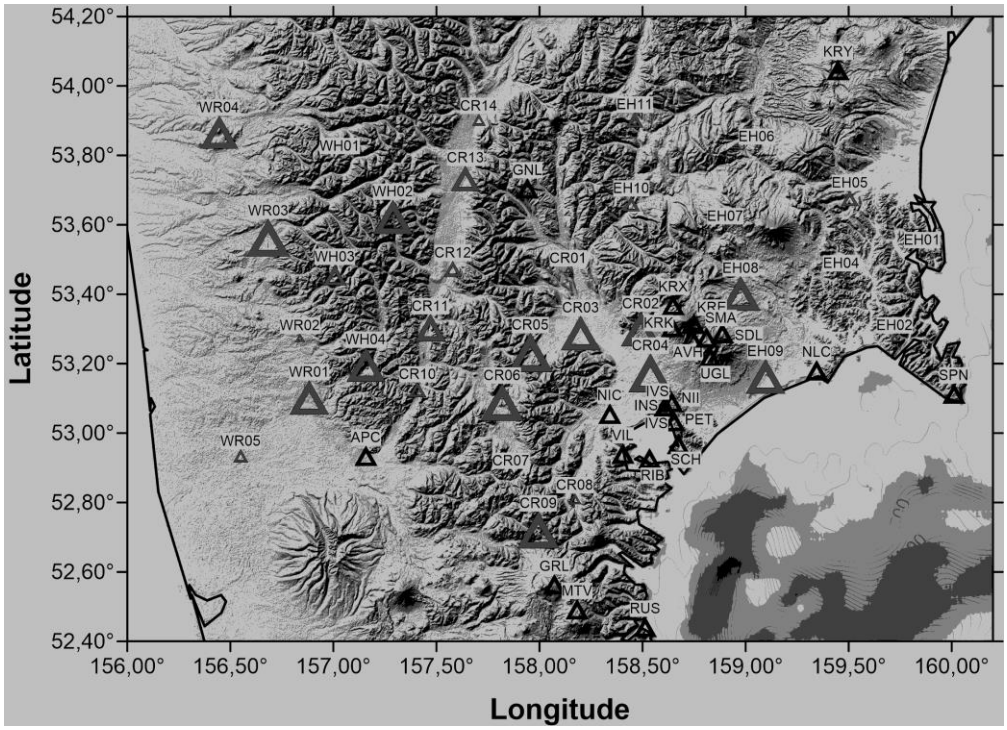

Figure 1 –Seismic stations location. The size of triangles proportional to the amount of data used for receiver function analysis.

Funding: This work is supported by the Russian Science Foundation under grant № 20-17-00075

References:

1. Vinnik L.P. Detection of waves converted from P to SV in the mantle Physics of the Earth and planetary interiors. 1977. Vol. 15. No. 1. P. 39–45.

2. Zhu L., Kanamori H. Moho depth variation in southern California from teleseismic receiver functions Journal of Geophysical Research: Solid Earth. 2000. Vol. 105. No. B2. P. 2969–2980.

3. Nikulin A. et al. Evidence for two upper mantle sources driving volcanism in Central Kamchatka Earth and Planetary Science Letters. 2012. Vol. 321–322. P. 14–19.

4. Levin V. et al. Crust and upper mantle of Kamchatka from teleseismic receiver functions Tectonophysics. 2002. Vol. 358. No. 1–4. P. 233–265.

5. Nurmukhamedov A.G., Nedyadko V.V., Rakitov V.A., Lipatyev M.S. Lithosphere boundaries in Kamchatka based on the earthquake converted-wave method (ECWM). Vestnik KRAESC. Seriya: Nauki o Zemle. Earth Sciences. 2016. Vol. 29. No. 1. P. 35–52. (In Russian)

CRUSTAL STRUCTURE OF THE BAIKAL RIFT ZONE BASED ON LOCAL SEISMIC TOMOGRAPHY

Komzeleva V.P.[12], Medved I.V[13], Koulakov I.Yu[12], Buslov M.M.[3], Seredkina A.I.[4]

[1]A.A. Trofimuk Institute of Petroleum Geology and Geophysics, SB RAS, Novosibirsk, Russia
[2] Novosibirsk State University, Novosibirsk, Russia, v.komzeleva@g.nsu.ru
[3]V.S. Sobolev Institute of Geology and Mineralogy, SB RAS, Novosibirsk, Russia
[4]N.V. Pushkov Institute of Terrestrial Magnetism, Ionosphere and Radio Wave Propagation of RAS, Moscow, Troitsk, Russia

Abstract. This study presents models of seismic tomography under the Baikal Rift Zone (BRZ), obtained from the latest seismological data recorded in the period from 1994 to 2016. 3D models of the deep structure of the BRZ were built to a depth of 60 km using the local seismic tomography algorithm. All models were subjected to thorough verification and synthetic modeling. The received interpretations of the features of the deep structure of the BRZ are discussed on the basis of modern ideas about the geological structure of the region and its geodynamics.

Key words: Baikal Rift zone; seismic tomography; geodynamics.

The Baikal Rift Zone (BRZ) is one of the largest neotectonic rift systems in the world, located in the junction zone of the Siberian Platform and the northern part of the Central Asian Fold Belt (Amur Plate). After the publication of [1], the geomorphology of mountain systems and the neotectonic structure of Central Asia began to be considered as the result of intercontinental deformations associated with the distant impact of tectonic stress from the Indo-Eurasian collision. Later it was established [2–6] that the presence of such large “hard” Precambrian blocks in the structure of the Central Asian fold belt as the Tarim, Central Tien Shan (Issyk-Kul), Tuva-Mongolian and others contributed to the transfer of tectonic voltage over long distances up to several thousand kilometers from the Indian to Siberian continents. It is believed that this process was also facilitated by numerous plumes, above which heated areas of the lithosphere could be subjected to deformations and shear displacements to a greater extent. Displacement vectors derived from GPS results [7, 8] describe well the formation of BRZ due to plate movement due to the Indo-Eurasian collision.

One of the main geophysical methods for studying the deep structure is seismic tomography, various approaches of which can reveal the features of the region. Thanks to the method of seismic tomography, it is possible to obtain sufficiently detailed three-dimensional images of the deep seismic structure, which makes it possible to trace the mechanisms of the geodynamic development of the region. The ever-evolving methods of analyzing and inverting seismic data, along with other geophysical and geological data, can help researchers move from assumptions caused by gaps in deep structure to more definitive conclusions when solving geodynamic problems.

The tomographic inversion was performed using the LOTOS (Local Tomography Software) nonlinear algorithm, which provides simultaneous inversion of P and S velocity structures and source coordinates. The theoretical principles and technical details of the algorithm are described in detail in [9].

According to the data obtained, some features of the structure of the upper part of the earth's crust in the region were revealed:

1) The Siberian craton in the Baikal region is manifested as a high-velocity anomaly, which characterizes it as a dense monolithic block;

2) In the area of the Irkutsk reservoir-Slyudyanka within the Siberian craton, an isometric high-velocity anomaly is observed, reaching a depth of ~30 km. It is assumed that the anomaly may be related to the local occurrence of Triassic sills of the Siberian trap province.

3) The Baikal rift zone is characterized by an anomaly of low velocities, the lower boundary of which can be traced to a depth of 35-50 km, which corresponds to modern ideas about the depth of the Moho boundary, for example, [10]. In addition, a thinning of the low-velocity anomaly can be traced under Lake Baikal, which may also be evidence of crustal thinning.

4) A large low-velocity anomaly is observed under the western part of the study region in the Eastern Sayan Mountains, which is apparently due to the presence of a Cenozoic plume that heats up the crust and thereby causes a slowdown in seismic velocities in the crust.

The novelty of this study lies in the work with new unique data, with the help of which results with a sufficiently high level of resolution were obtained. Based on the obtained results of seismic tomography, the question of the influence of the structural and material characteristics of the crystalline basement of Baikal on the formation of its structure as a result of the influence of regional compression from the Indo-Eurasian collision is considered.

This work is supported by the Russian Foundation for Basic Research under grant 19-35-60002 and partially by the Russian Science Foundation under grant 20-17-00075.

References:

1. Molnar P., Tapponnier P. Cenozoic Tectonics of Asia: Effects of a Continental Collision: Features of recent continental tectonics in Asia can be interpreted as results of the India-Eurasia collision. Science. 1975. Vol. 189. No. 4201. P. 419-426.

2. Buslov M.M., Kokh D.A., De Grave J. Mesozoic-Cenozoic tectonics and geodynamics of Altai, Tien Shan, and Northern Kazakhstan, from apatite fission-track data. Russian Geology and Geophysics. 2008. Vol. 49. No. 9. P. 648-654.

3. De Grave J., Buslov M.M. Distant effects of India–Eurasia convergence and Mesozoic intracontinental deformation in Central Asia: Constraints from apatite fission-track thermochronology. Journal of Asian Earth Sciences. 2007. Vol. 29. No. 2-3. P. 188-204.

4. Dobretsov N.L., Buslov M.M., Delvaux D., Berzin N.A., Ermikov V.D. Meso-and Cenozoic tectonics of the Central Asian mountain belt: effects of lithospheric plate interaction and mantle plumes. International Geology Review. 1996. Vol. 38. No. 5. P. 430-466.

5. Dobretsov N.L., Buslov M.M., De Grave, J., & Sklyarov E.V. Interplay of magmatism, sedimentation, and collision processes in the Siberian craton and the flanking orogens. Russian Geology and Geophysics. 2013. Vol. 54. No. 10. P. 1135-1149.

6. Dobretsov N.L., Buslov M.M., Vasilevsky A.N. Geodynamic complexes and structures of Transbaikalia: Record in gravity data. Russian Geology and Geophysics. 2019. Vol. 60. No. 3. P. 254-266.

7. Flesch L.M., Haines A.J., Holt W.E. Dynamics of the India-Eurasia collision zone. Journal of Geophysical Research: Solid Earth. 2001. Vol. 106. No. B8. P. 16435-16460.

8. Calais E., Vergnolle M., San'Kov V., Lukhnev A., Miroshnitchenko A., Amarjargal S., & Déverchère J. GPS measurements of crustal deformation in the Baikal-Mongolia area (1994–2002): Implications for current kinematics of Asia. Journal of Geophysical Research: Solid Earth. 2003. Vol. 108. No. B10.

9. Koulakov I. LOTOS code for local earthquake tomographic inversion: Benchmarks for testing tomographic algorithms. Bulletin of the Seismological Society of America. 2009. Vol. 99. No. 1. P. 194-214.

10. Zorin Y.A., Turutanov E.K., Mordvinova V.V., Kozhevnikov V.M., Yanovskaya T.B., Treussov A.V. The Baikal rift zone: the effect of mantle plumes on older structure. Tectonophysics. 2003. Vol. 371. No. 1-4. P. 153-173.

SEISMOACOUSTIC STUDIES OF LAKE SHIRA (REPUBLIC OF KHAKASSIA)

Krylov P.S., Nurgaliev D.K., Yasonov P.G.

Kazan (Volga region) Federal University, Institute of geology and petroleum technologies, Kazan, Russia, PSKrylov@kpfu.ru

Abstract. The work is devoted to preliminary high-resolution seismoacoustic investigations of Lake Shira. Lake sediments constitute natural archives of past environmental conditions and climatic change occurring in continental areas. Understanding the structure of bottom sediments makes it possible to reasonably select core sampling points. Further study of such cores makes it possible to obtain the most reliable results of paleoclimate changes.

Key words: lake, sediments, seismoacoustic

Many modern lakes are located in key geographic locations whose bottom sediments archived detailed records of changes in climate, landscapes, the evolution of lakes, and their ecosystems [1]. A comprehensive study of lakes bottom sediments of different depths and hydrological regimes located in different landscape and climatic zones provides a basis for paleoclimatic reconstructions of different periods. Comparison of data for different objects will allow in the future to identify trends in climate change in study region. However, the completeness of research on these issues is extremely uneven. This is due to both the large size of the study region and the laboriousness of such works. At the same time, by the joint efforts of researchers, the ‘blank spots’ are gradually eliminated [2].

In 2020, Lake Shira (Republic of Khakassia) was studied using a seismic acoustic method in order to identify the structure of the occurrence of bottom sediments. Continuous seismic profiling was applied based on the principle of central beam, which enables remote investigation of the lake bottom structure owing to the recording of acoustic waves reflected from the lake bottom. On this basis, it is possible to establish borders between sediment layers of different physical properties. The seismoacoustic profiling was carried out using specialized complex, designed and manufactured on the base of Kazan Federal University [3]. The complex includes: a source of elastic waves, a receiver, a seismic station, a laptop, a GPS-receiver, an inflatable boat, an electric motor, and power supply elements. The complex enables us to get seismic acoustic sections with vertical resolution at least 15 cm; depth study of various types of lake sediments at least 10 m; geodetic positioning system within several meters. It also provides the digital recording of information. As a source of elastic waves an inductive oscillator "boomer" was used. A storage battery was used as a source of electric power. The GPS receiver was used to coordinate profiles and boat location.

The seismoacoustic section shows that the maximum depth in studied area reached 22,5 m, the maximum apparent thickness of bottom sediments was about 8 m (recalculation of the time scale into depth scale according to the speed of sound propagation in water - 1500 m/s) (Figure 1). It is possible to distinguish 3 facies of bottom sediments. The upper unit (about 3 m) is characterized by a layered structure. Below, the unit (about 2m) is characterized by a chaotic type of record, probably represented of glacial deposits. Below unit 3 (about 3m) is also layered in places with a chaotic record. Below, there is an acoustic foundation where the acoustic energy

has not penetrated. Although in some places vertically inclined reflections are observed, probably from bedrock.

The right part of the section is characterized by the presence of gas in bottom sediments. This indicates a lot of facts - negative form of relief, characteristic of the pockmarks, attenuation of acoustic energy, noise on the section. This is not an equipment mistake since there is a similar picture on other seismacoustic sections. The issue of the hypsometric level of the lake bottom with a difference of 1 meter remains debatable.

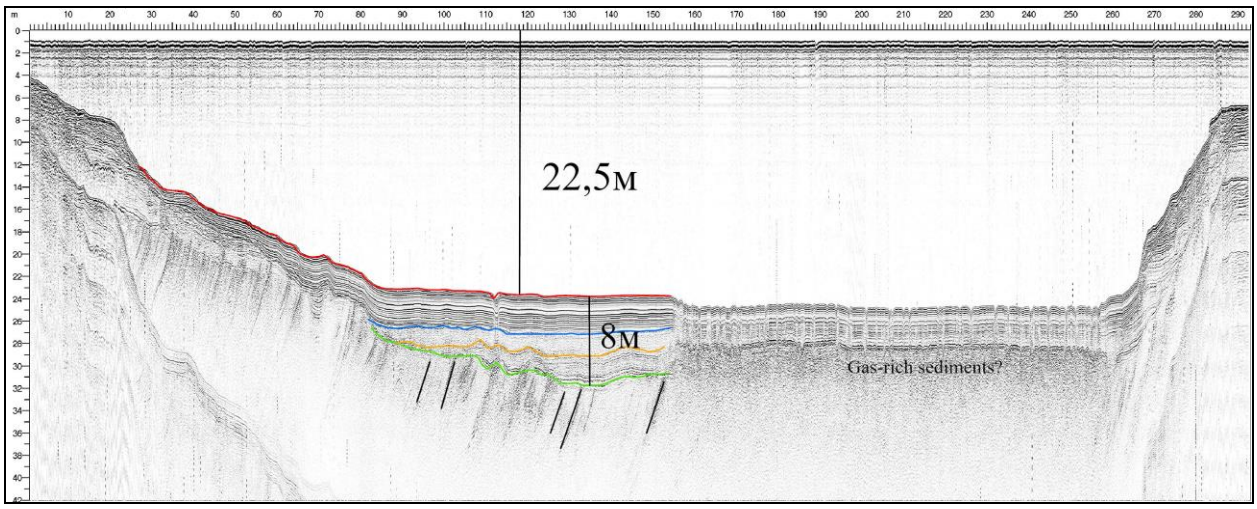

Figure 1 – Seismoacoustic section of lake Shira.

Preliminary seismoacoustic data made it possible to study in detail the structure of the occurrence of bottom sediments. These data may be useful for further core sampling for a detailed reconstruction of the paleoclimate.

Funding: This work is supported by the Russian Science Foundation under grant 22-47-08001.

References:

1. Subetto D.A, Fedotov A.P. Paleolake records as sedimentary proxies of climate changes of Northern Eurasia in the past. Limnology and Freshwater Biology 2020. Vol. 4. P. 439-439.
2. Ptitsyn A.B., Chu G., Dar'in A.V., Zamana L.V., Kalugin I.A., Reshetova S.A. The rate of sedimentation in Lake Arakhlei (Central Transbaikalia), from radiogeochemical and palynological data. Geology and Geophysics. 2014. Vol. 55. No. 3. P. 473-480.
3. Krylov P.S., Nourgaliev D.K., Yasonov P.G. Seismic investigations of Lake Chebarkul in the process of searching Chelyabinsk meteorite. ARPN Journal of Engineering and Applied Sciences. 2015. Vol. 10. No.2. P. 744-746.

THE FEATURES OF LITHOSPHERE STRUCTURES IN VARIOUS COLLISION ZONES OF EURASIA BASED ON SEISMIC TOMOGRAPHY STUDIES

Medved I.V.

V.S. Sobolev Institute of Geology and Mineralogy, Novosibirsk, Russia, zabelirina@yandex.ru
A.A. Trofimuk Institute of Petroleum Geology and Geophysics, Novosibirsk, Russia

Abstract: In this study, 3D models of crustal inhomogeneities down to ~ 60-150 km were constructed under the collision zones of the Caucasus, Eastern Anatolia, NW Himalayas and Tien Shan using the method of local seismic tomography. The different characteristic feature of crustal structure was found. Comparison of seismic tomography models of different collision zones can be the key to better understanding the processes in the crust and lithosphere.

Key words: collision zones, seismic tomography, geodynamics, crustal structure

There are a large number of different collision zones on Earth, formed in different geodynamic settings as a result of the collision of continental plates of different shapes and sizes. Researchers often use one or a combination of methods to study one region. In this study, we propose to compare the models of P and S anomalies of several regions. In this study, vertical sections were built under the collision zones of the Caucasus, Eastern Anatolia, NW Himalayas and Tien Shan using the method of local seismic tomography. 3D models of crustal inhomogeneities down to ~ 60-150 km were constructed using the LOTOS algorithm [1].

The main characteristic feature of all crustal models of collisional zones is a clear differentiation of the velocity anomalies of the orogen, formed due to shortening, and the continental plates, participating in the collision. Thus, the Arabian, East European, Indian, Tarim plates are associated with high velocity anomalies, and mountain structures, for example, the Greater and Lesser Caucasus, the Himalayas, are characterized by low velocities.

Volcanism is another geological feature that shows up well in seismic tomographic models. Young volcanism (up to ~ 2.5Ma) characterized by low-velocity anomalies in the models, while the older one characterized by high-velocity anomalies. Thus, the volcanic area of Kazbegi province including a group of Quaternary volcanoes (455-30 Ka) in Great Caucasus match to the locations of low-velocities in the P- and S-seismic models. But the Eastern Anatolia younger magmatism (6–4 Ma) occurred in the south around Lake Van, stands out as high velocity anomalies.

It is known that there is the lithospheric window under Tien Shan and Anatolia which is filled with overheated asthenospheric material that reaches the bottom of the crust, thereby weakening and heating the lower crust. It is most likely that the upper crustal high-velocity anomaly corresponds to the strong upper crust which is compacted by solidified material from Neogene-Quaternary volcanism, while the low-velocity anomaly is associated with the weak heated lower crust.

Thus, comparison of seismic tomography models of different collision zones can be the key to better understanding the processes in the crust and lithosphere.

Funding: The reported study was funded by Russian Foundation for Basic Research, project number 19-35-60002.

References:

1. Koulakov I. LOTOS code for local earthquake tomographic inversion: Benchmarks for testing tomographic algorithms. Bulletin of the Seismological Society of America. 2009. Vol. 99. P. 194–214.

SEISMOSTRATIGRAPHY AND SEDIMENTATION ENVIRONMENT IN THE WESTERN COOPERATION SEA

Minina V.V.[1], Ksenofontov I.V.[2]

[1]FSBI "VNIIOkeangeologia", St. Petersburg, Russia, valyakubova@yandex.ru
[2]SV "Polar Marine Geosurvey Expedition", Lomonosov, Russia

Abstract. The new high-resolution seismic data allowed revisiting the seismostratigraphy of the Cooperation sea basin and calculate the isochrones of the acoustic basement and the thickness of sedimentary cover and synglacial sediments. The maximum depth of the acoustic basement of 8-9 s is found along the foot of the continental slope. The thickness of the synglacial sediments is maximal at the eastern part of the study area, near the Prydz Bay. Underwater channels, their levees and sediment waves are characteristic for the area of study. The westward-flowing bottom currents off MacRobertson Land have reworked the channel levees into the mounded drifts.

Key words: Cooperation Sea, seismostratigraphy, sedimentation

The large sedimentary basin of the Cooperation Sea was formed as the result of rifting and the breakup of East Gondwana (separation of India and Antarctica) [1]. The most recent seismostratigraphic model for the Cooperation Sea basin is based on the seismic data from both Russian and foreign surveys in the Indian Ocean sector of the Antarctica. The model describes 9 regional reflectors (with ages in Ma): CS1 – 125-120, CS1a – 120-110, CS2 – 100-90, CS3 – 43-42, CS4 - 34, CS5 - 24, CS5a - 21, CS6 – 14-12 и CS7 – 5-3 Ma, of which the CS4 reflector is the most significant, as it indicates the onset of the large-scale glaciation of the Antarctica [2]. The basin off Enderby Land contains a large regional sediment lens within the CS2-CS4 sequence just before the upper continental rise, which is thought to be a plastered drift [1, 3].

The Cooperation Sea is considered to be one of the few areas of deep water formation: saline waters sink down and eventually form new westward flowing Antarctic Bottom waters [4]. The Antarctic coastal current is similarly oriented westward [4]. The combined action of the turbidity flows and bottom current results in several channel levees reworked into the mounded drifts, Wild and Darnley drifts being the biggest of them [5].

Numerous surveys were conducted in the Cooperation Sea by Russia, Australia, Germany and Japan, resulting in seismic datasets, covering most of the area, available at the Antarctic Seismic Data Library System [6]. The 66th Russian Antarctic Expedition (RAE), which took place in 2021 onboard RV "Akademic Karpinsky", has collected new high-resolution seismic data for the western part of the Cooperation Sea, allowing revisiting the seismostratigraphic model of the region.

The seismic data were interpreted with the help of Kingdom Software. The regional reflectors were correlated according to the intersections with the 62th RAE and other Russian and foreign seismic profiles. Horizons were picked and later exported in the Surfer. With the Kriging interpolation method, grids were created for the isochrones of the acoustic basement, sedimentary cover thickness and synglacial sediments thickness.

The maximum depth (in two-way travel time) of the acoustic basement was identified at the foot of the continental slope, reaching 8-9 s. Acoustic basement becomes shallower in the seaward direction. This correlates nicely with the thickness of the sedimentary cover (in isochrones): the maximum thickness is found at the foot of the continental slope – 4-5 s,

primarily in the eastern part of the area of study. The CS4 reflector is nicely tracked across the region. CS1 and CS2 reflectors gradually thin out in the seaward direction.

A regional sediment lens – clinoform – is clearly identified in the new seismic data, primarily in the S and SW parts, although it can be tracked further to the east then was previously described by [3].

The thickness of the synglacial sediments (CS4-sediment surface) is maximal at the eastern part of the study area, near the Prydz Bay. This is linked to the increased sediment input from the Amery ice shelf into the Bay. The thickness of the synglacial sediments decreases from east to west, as well as near the foot of the continental slope, where the sediments were deposited on top of the clinoform.

Underwater channels and their levees are well developed within the synglacial sediments, complicating the correlation of regional reflectors. The formation of sediment waves on top of channel levees suggests their turbidity flow origin, although it is still unclear what role could have westward flowing bottom currents played on their formation.

References:

1. Leitchenkov G.L., Guseva Yu.B., Gandykhin V.V., Ivanov S.V., Safonova L.V. Structure of the Earth's crust and tectonic evolution history of the Southern Indian Ocean (Antarctica). Geotectonics. 2014. Vol. 48. P. 5-23.

2. Leitchenkov G.L., Guseva Yu.B., Gandykhin V.V., Ivanov S.V. Crustal structure, tectonic evolution and seismic stratigraphy of the southern Indian Ocean. St. Petersburg. FSBI "VNIIOkeangeologia", SV "PMGE". 2015. 199 p.

3. Kuvaas B., Kristoffersen Y., Guseva J., Leitchenkov G., Gandjukhin V., Lovas O., Sand M., Brekke H. Interplay of turbidite and contourite deposition along the Cosmonaut Sea/Enderby Land margin, East Antarctica. Marine Geology. 2005. Vol. 217. P. 143-159.

4. Ohshima K.I., Fukamachi Y., Williams G.D., Nihashi S., Roquet F., Kitade Y., Tamura T., Hirano D., Herraiz-Borreguero L., Field I., Hindell M., Aoki S., Wakatsuchi M. Antarctic Bottom Water production by intense sea-ice formation in the Cape Darnley polynya. Nature Geoscience. 2013. Vol. 6. P. 235–240.

5. Nielsen R., Uenzelmann-Neben G. On the paleo foorprint of Cape Darnley Bottom Water off MacRobertson Land Shelf, East Antarctica. Marine Geology. 2022. Vol. 445. (In Press)

6. The Antarctic Seismic Data Library System (SDLS) https://sdls.ogs.trieste.it/

PROCESSING, ANALYSIS AND INVERSION OF AMT DATA ON THE BASELINE PROFILE DURING GEOLOGICAL SURVEY WORK (ALTAI AREA, KIVDINSKY SITE)

Panteev I. A.

Saint Petersburg State University, Saint Petersburg, igor.panteev22@gmail.com

Abstract. The accuracy and detail of the magnetotellurics study results depend on the correct choice of methods for processing, analyzing and inversing data in general [1]. The purpose of the work is to master the main stages of the deskwork of the AMT method, as well as to compile the correct geological model for the Kivdinsky site reference profile. The following objectives have been achieved: selection of the optimal data processing algorithm for obtaining high-quality sounding curves, analysis of the obtained data, selection of the inversion algorithm, inversion, obtaining the final model, preliminary geological interpretation of the results.

Key words: audio-magneto telluric sounding, processing, analysis, inversion, AMT data

The article results from the ground-based geophysical work performed as part of the support of geological survey work on sheet N-45-XXVII of the State Geological Map of the Russian Federation [2]. The fieldwork was carried out by the AMT method with Phoenix Geophysics equipment (Canada) on a 20 km long reference profile with a step between points of 200 m. To master the main stages of the deskwork, 6 control points were processed, recording on which was carried out for 12 hours.

AMT data processing was carried out using the MT-Corrector software (designed by LLC "Nord-West"). The software allowed us to resolve the following tasks: “out-of-tolerance” values initial rejection, formulation of splines, as well as to deploy the amplitude-phase correction (APC). The latter made it possible to increase the accuracy of the sensing curves for areas with low intensity of the natural electromagnetic field, restoring the amplitude curve by phase.

The data analysis performed in the MTS_Prof software (LLC "Nord-West") showed that the subsoil array has a two-dimensional structure, excluding the northern part of the profile (up to picket 4000) and the central part (8500-14000), where the environment is complicated by three-dimensional inhomogeneities. It was also found that the stretching of geoelectrical structures does not significantly deviate from the direction of the cross profile, which is acceptable for 2D inversion. Pseudo-sections of apparent resistance were drafted, where the influence of the shift effect was observed at some certain points, his indicates the presence of small near-surface inhomogeneities. It was possible to eliminate its influence manually by pseudo-sections of the impedance phase, which are less sensitive to the influence of this effect [3].

Data inversion was performed based on data on the dimension of the subsoil array and the strike of geoelectric structures. One-dimensional inversion was performed in the MT_ProfInv program (LLC "Nord-West"), a TM mod was used for the inversion. The resulting geoelectric section acted as the first approximation for two-dimensional inversion in the MT2DTools program (designed by LLC "Nord-West"). The deployed inversion algorithm was formulated by R. Maki [4, 5].

Initial geological input data, description of the subsoil array block structure and a large number of discontinuous violations were taken into account in order to choose the value for the regularization parameter (τ), This allowed us to discard some models with a high degree of smoothness and a large value of τ. Various minimization options were also applied: minimizing the gradient and Lapalasian of the model parameters.

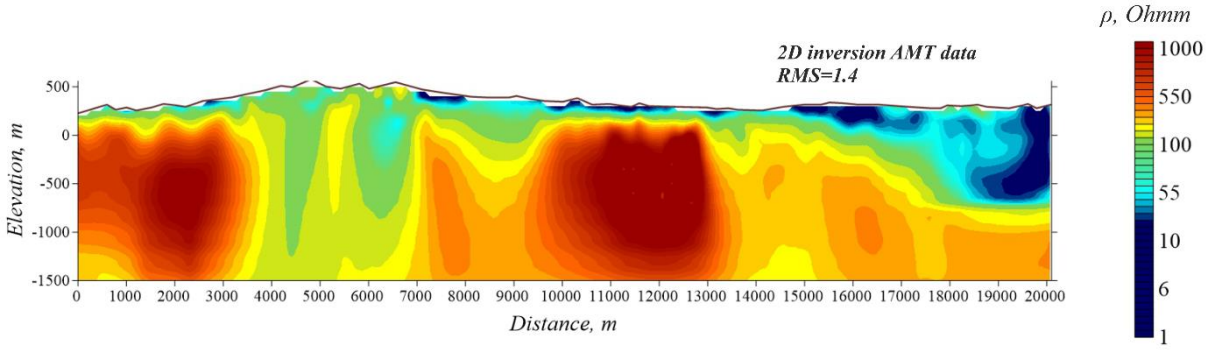

Figure 1 - Geoelectric section obtained by 2D inversion algorithm

Thus, the most correct version of the geo-electrical section was obtained using two-dimensional inversion of data with minimization of the Laplacian, involvement of Tipper data and a regularization parameter equal to 10 (Fig.1), which was used for geological interpretation.

The main conclusions that can be drawn based on the work done: at the processing stage, the APC is an effective tool; the analysis stage made it possible to determine the dimension of the medium and the stretching of geoelectrical structures, and, if necessary, to perform a reversal of the impedance tensor in accordance with the direction of inhomogeneities; for the most complete consideration of all available information, a bimodal inversion of data was carried out with the involvement of tipper data; the high quality of the field data made it possible to set sufficiently low values of the regularization parameter and obtain a well-structured model.

References:

1. Pushkarev P.Yu. (2017): Interpretation of low-frequency electromagnetic soundings of inhomogeneous medium in relation to solving geological problems. Proceedings of the All-Russian conference with international participation “Deep structure and geodynamics of Lake Ladoga region”. Petrozavodsk, KarRC RAS, p. 163-171. **(**In Russian)

2. State geological map of the USSR. Scale 1: 200,000. Sheet N-45-XXVII. 1964.

3. Berdichevsky M.N., Dmitriev V.I. Models and methods of magnetotellurics. Berlin. Springer. 2008. 563 p.

4. Mackie R.L., Rodi W. Nonlinear conjugate gradients algorithm for 2-D magnetotelluric inversion. Geophysics. 2001. Vol. 66. No. 1. P. 174-187.

5. Program for two-dimensional interpretation of magnetotelluric sounding data ZONDMT2D http://zond-geo.com/english/zond-software/electromagnetic-sounding/zondmt2d/.

COMPARATIVE CHARACTERISTICS OF PERIODIC EARTHQUAKES DURING ERUPTIONS OF KARYMSKY AND KIZIMEN VOLCANOES (RUSSIA, KAMCHATKA PENINSULA)

Shakirova A. A.

Kamchatka Branch of the Geophysical Survey of Russian Academy of Sciences, Piipa, 9, Petropavlovsk-Kamchatsky 683006, Russia

Abstract. Periodic earthquakes sometimes are recorded during volcanic eruptions. According to waveforms, earthquakes are grouped into multiplets. The characteristics of multiplets and records of volcanic earthquakes provide important information about the mechanism of their origin. Periodic signals were recorded during the eruptions of the Kizimen in 2010-2013 and Karymsky volcano in 2019 (Russia, Kamchatka Peninsula). For earthquakes during the Kizimen eruption, it was concluded that periodic earthquakes are caused by the movement of a powerful lava flow front along the slope of the volcano. For Karymsky, it was an acceleration of the rise of magma and an increase in gas pressure in the volcanic channel.

Key words: Kizimen, Karymsky, drumbeats, earthquake, eruption.

Volcanic eruptions on the Kamchatka peninsula occur every year. Some volcanoes are characterized by a certain periodicity of eruptions (Klyuchevskoy and Bezymyanny), some erupt constantly (Karymsky). There are also volcanoes whose eruptions are supported by seismic data for the first time (Kizimen).

The eruptions of the Karymsky and Kizimen volcanoes, which are characterized by different behavior, are considered. Karymsky is characterized by explosive activity and outpouring of low-viscosity lava flows. Kizimen is characterized by squeezing out viscous lava flow, summit extrusion, and moderate explosions. Nevertheless, during the eruption of these two volcanoes, periodic signals were recorded, which at first glance could have a similar mechanism of their generation.

When studying the eruption of the Kizimen volcano (2010-2013), it was found that quasi-periodic earthquakes belong to earthquakes of the “drumbeats” regime (Fig. 1b) [1]. This term was applied firstly to the eruption of Mount St. Helens in 2004 [2] when the regime was associated with the squeezing out of the blocks of the extrusive dome and the occurrence of friction between the extrusion and the walls of the channel. For quasi-periodic earthquakes of the “drumbeats” recorded on Kizimen, it was found that the movement of a viscous lava flow along the slope of the volcano for almost two years generated them. The more powerful the front of the lava flow, the rarer and stronger earthquakes were recorded. In the practice of world studies, such a phenomenon was registered for the first time. The waveforms of the earthquakes were classified as long-period and hybrid, 19 earthquake multiplets were identified based on this. Hybrid earthquakes occurred when brittle destruction of lava blocks occurred in the frontal part, which reached the highest viscosity (compared to the beginning of the eruption) due to prolonged cooling and degassing of the lava flow. The duration of the multiplets ranged from several days to five months and coincided with the time periods of the movement of two "tongues" of the lava flow.

In 2019, during the Karymsky eruption, earthquakes were also recorded with periodicity (Fig. 1a). These earthquakes preceded the explosions and ceased to be recorded after the explosion [3]. The waveforms of earthquakes belonged to long-period ones, and in February 2019, 8 multiplets were identified. The mechanism of generation of periodic earthquakes on the Karymsky volcano in February 2019 is associated with an increase in the rate of ascent of magmatic material along the volcanic channel. The accelerating rise of the magma caused an increasing gas pressure in the channel. The cessation of generation of long-period earthquakes after the explosion indicates a complete release of pressure in the volcanic edifice. The decreasing times periods between earthquakes are caused by a change in the rate of increase in gas pressure. The duration of earthquake registration from the first explosion to the eighth was reduced, which means that over time the channel became more cleared, and the path for the gas to escape was freer [3].

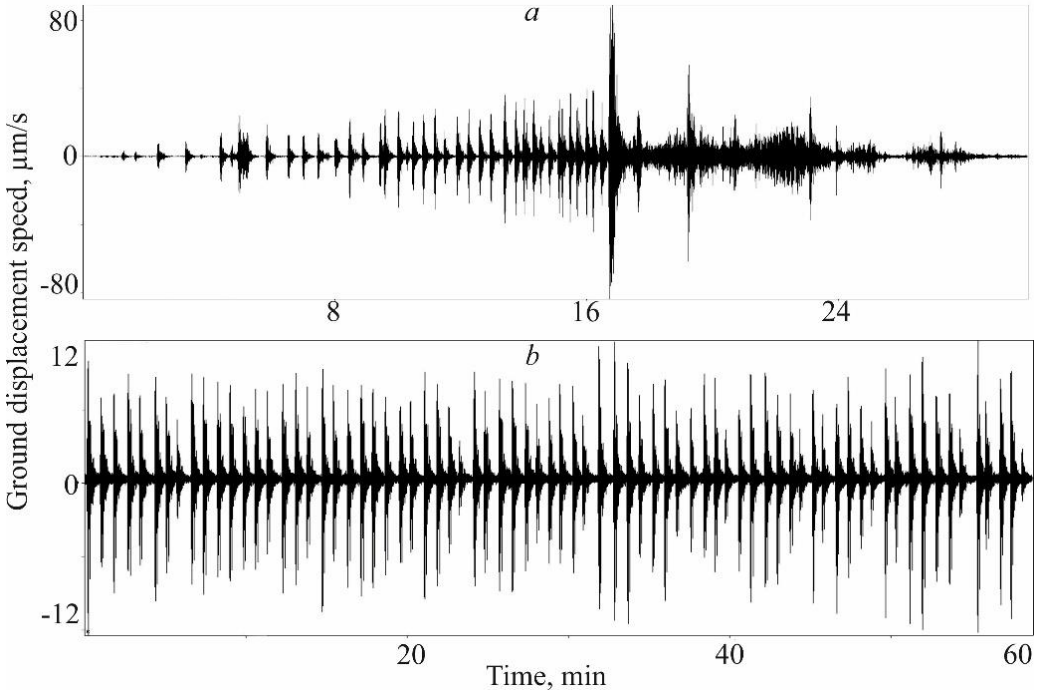

Figure 1 – Periodic earthquakes recorded during the eruption of Karymsky in 2019 (a) and Kizimen in 2011 (b).

Funding: The work was supported by the Ministry of Science and Higher Education of the Russian Federation (within the framework of state task № 075-01471-22). The data used in the work were obtained with large-scale research facilities «Seismic infrasound array for monitoring Arctic cryolitozone and continuous seismic monitoring of the Russian Federation, neighboring territories and the world».

References:

1. Firstov P.P., Shakirova A.A. Seismicity observed during the precursory process and the actual eruption of Kizimen Volcano, Kamchatka in 2009–2013. Journal of Volcanology and Seismology. 2014. Vol. 8. P.203–217.

2. Iverson M.R., Dzurisin D., Gardner C.A. et al. Dynamics of seismogenetic volcanic extrusion at Mount St Helens in 2004-2005. Nature. 2006. V. 444. P. 439-443.

3. Shakirova A.A. Seismic effects ahead of Karymsky volcano (Kamchatka) explosions in February 2019. Bulletin KRAUNTS. Earth Sciences. 2022. No. 1. P. 12-23 (In Russian).

ASSESSMENT OF ELECTRICAL RESISTIVITY VARIATIONS IN THE GORNY ALTAI REGION FAULT ZONE USING ERT MONITORING

Shaparenko I.O.

Institute of petroleum geology and geophysics, Novosibirsk, Russia,
shaparenkoio@ipgg.sbras.ru

Abstract. Dangerous geodynamic processes are often associated with tectonic movements along seismogenic faults. Regular observations by geoelectrical methods in fault zones indicate that when deformation processes are activated, it is in these zones that the most significant changes in the electrical conductivity of all horizons of the section, including near-surface deposits, are observed. Electrical resistivity tomography method is useful to be used in monitoring of the near surface because of its high detail, advanced measurement and interpretation technologies. The geoelectric characteristics of the fault structure in the territory of the Uimon depression of the Gorny Altai are determined.

Key words: Electrical resistivity tomography, fault zone, monitoring, Gorny Altai.

Dangerous geodynamic processes (earthquakes, landslides, etc.) are often associated with tectonic movements along seismogenic faults. Increased seismic activity affects the economic activity of the population, construction, road network, etc., so the study of fault structures is an urgent task. In addition, mineral deposits are associated with fault structures. Electrical resistivity tomography (ERT) method is successfully used in world practice in studies in seismically active regions [1,2].

The ERT method is based on the differentiation of rocks by electrical resistivity, combining the principles of sounding and profiling. We used the Skala48 multielectrode electrical exploration station, developed in the laboratory of electromagnetic fields at the IPGG SB RAS.

The Uimon depression is one of the largest depressions in this region, but it is the least studied. From the north, it is confined by the Terektinsky Range, which is separated from the deposits of the depression by the zone of the South-Terektinsky Fault, which strikes northwest. A characteristic feature of the structure of this zone is a series of tectonic scarps. ERT measurements near the Margala settlement are carried out annually on the last tectonic benches at the boundary with the deposits of the basin, considering the terrain, starting from 2011. A vertical block with reduced resistivity values is identified, which is attributed to the fault structure (Fig. 1). The decrease in resistivity is most likely associated with increased fracturing and watering of rocks. It is assumed that the scarp was developed in the neogene variegated clays deformed due to the thrusting of the Terektinsky Range onto the Uimon depression.

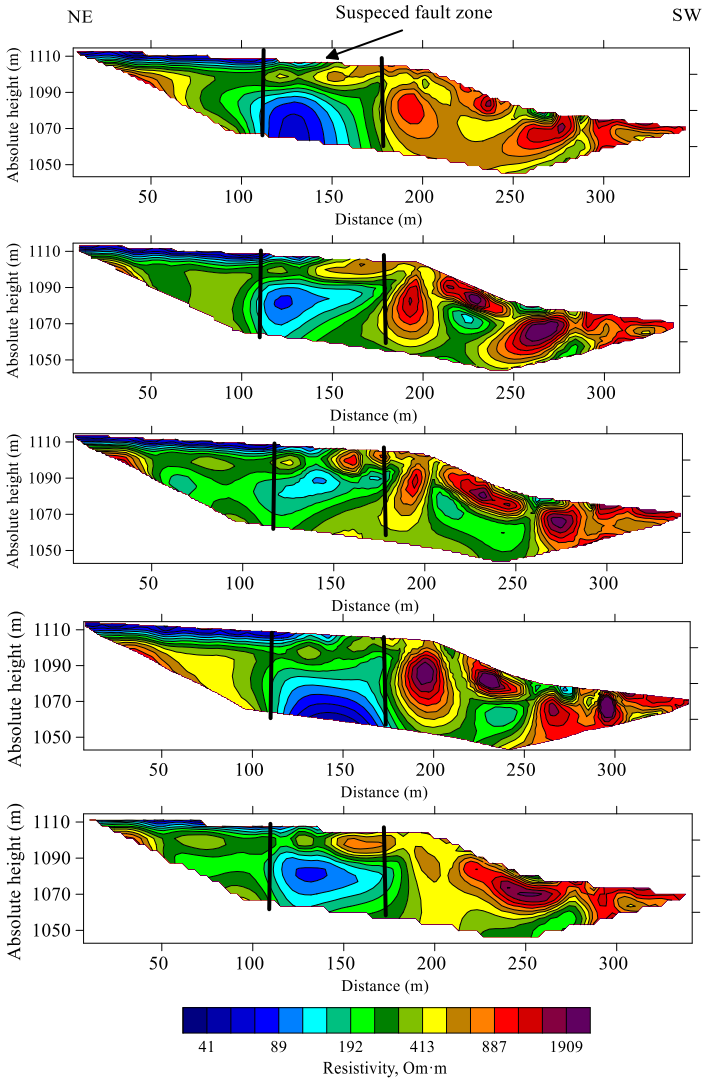

Figure 1 – geoelectrical sections in the same profile for 2011, 2017, 2019, 2020 & 2021 years. Made by author.

To sum up, ERT monitoring has many challenges but it could show some dependence of UES on seismicity. Different degrees of resistivity variations over the years of monitoring have been determined. In the future, I will try to make a correlation between resistivity and seismicity.

Funding: This work is supported by IPGG basic project № FWZZ-2022-0025.

References:

1. Barnes H., Hinojosa J. R., Spinelli G. A., Mozley P. S., Koning D., Sproule T. G., Wilson J. L. Detecting fault zone characteristics and paleovalley incision using electrical resistivity: Loma Blanca Fault, New Mexico. Geophysics. 2021. Vol. 86. No. 3. P. 209-221.

2. Turova I., Deev E., Pozdnyakova N., Entin A., Nevedrova N., Shaparenko I., Bricheva S., Korzhenkov A., Kurbanov R., Panin A. Surface-rupturing paleoearthquakes in the Kurai fault zone (Gorny Altai, Russia): trenching and geophysical evidence. Journal of Asian Earth Sciences. No. 197. Art. 104399.

THE EXPERIENCE OF USING THE GEORADOLOCATION METHOD TO DETERMINE THE LAYERS OF SNOW WITH THE HELP OF GPR "OKO-2"

Sidorenko A.I., Bobrova D.A.

Special Research Bureau for Automation of Marine Researches FEB RAS, Yuzhno-Sakhalinsk, Russia, a.sidorenko@skbsami.ru

Abstract. The paper describes an experiment to determine the layers of snow by the method of georadolocation using the GPR "OKO-2". The electrical properties of ice and snow differ depending on its characteristics, so there is a possibility of indicating snow layers by georadiolocation. The layers of snow thickness determined on the radarogram differ in structure, humidity and temperature. This would allow using this method to identify snow layers involved in the formation of avalanches. This method can also be used to determine the thickness of the snow cover in the study area.

Keywords: snow cover, snow layer, GPR, avalanches.

In recent years, geophysical non-destructive georadar methods have been developed for carrying out snow and ice measurements, including for determining avalanche-prone layers of snow thickness in avalanche collections. The snow pit work in the avalanche separation zone requires good physical preparation, experience, skills on the slope, special equipment and poses a risk to the life and health of a specialist, then such a method would make it possible to exclude a person from being in an avalanche zone. The use of georadar would make it possible to estimate the volume of accumulated snow and the expected volume of avalanches, to predict the depth and thickness of the avalanche layer without a person being in the danger zone.

The Sakhalin Region is one of the most avalanche-prone regions of Russia. The damage from avalanches consists in the annual blockages of roads and railways, damage and destruction of buildings and structures, ingress and death of people in avalanches. At least 70% of the region's territory, more than 60 settlements and more than 400 km of roads and railways are avalanche-prone.

The georadar method is based on the phenomenon of reflection of electromagnetic waves from the interfaces of surfaces on which the electrical properties change. The main parameter of the medium is its dielectric constant. For snow, depending on its type, the dielectric constant is ὲ=1.2÷3.33. For the experiment on determining the thickness of the snow cover and detecting the layers of the snow thickness, the GPR "OKO-2" was used. The georadar consists of two blocks: a control block and an antenna block. Antenna units have different frequencies (from 35 to 2400 MHz), depending on which the depth of investigation and resolution change.

In the experiment, measurements of the snow thickness in natural occurrence were made. Previously, stratigraphic work was carried out: snow layers were identified, their thickness, density, temperature at the layer boundary, texture and structure, including a description of the shape and size of crystals, were determined. To describe the structure of the layers, the morphogenetic classification created by E.G. Kolomyts was used, which makes it possible to predict the change in the snow mass. Thus, the characteristics of the layers of the snow mass were obtained, which differ in several ways at once.

After carrying out stratigraphic work in the same area, measurements were carried out using a georadar. Additionally, we used metal markers, which were installed at the boundary of the layers. When correlating the marker, the radarogram and the stratigraphic column of the snow mass, we found that the visually determined boundaries of the snow layers on the radarogram coincide with the boundaries of the snow layers obtained during stratigraphic work in the snow pit. As a result, the layers of the snow mass having the same texture and structure have the same wave propagation speed and, most likely, the dielectric constant. In this case, the layers differ in density.

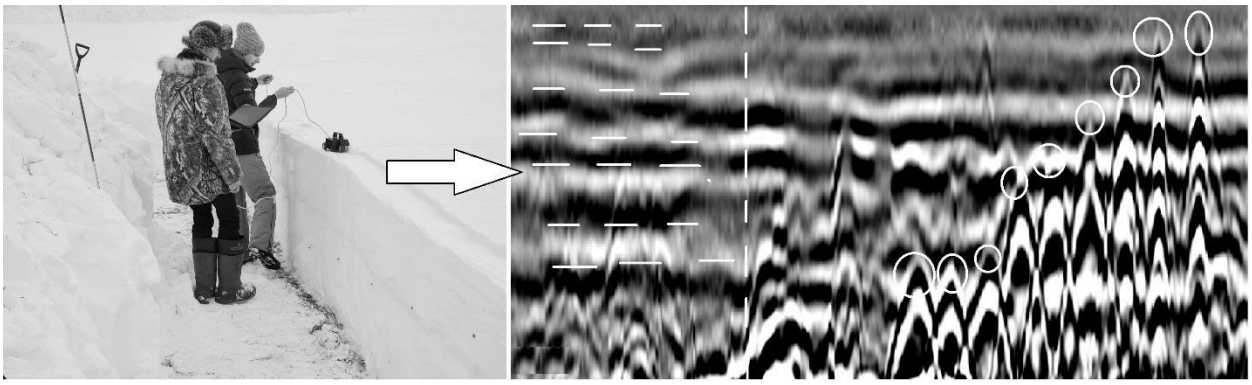

Moving the GPR **Layers of snow** **Layers of snow and markers**

Figure 1 – Using GPR to determine the layers of snow

Funding: The presented results were obtained with the financial support of the state task FWWW-2022-0005

Reference:

1. Ragulina G.A., Melvol'd H., Rusin I.N., Saloranta T.M. Georadar study of snow cover on the Hardangervidda mountain plateau, Norway, in 2008-2011. Bulletin of St. Petersburg State University. 2013. Vol. 7. No. 2. P. 108-118.

2. Vasilevich I.I., Chernov R.A. On the assessment of snow reserves in riverbed cuts by the method of georadiolocation on the territory of the Arctic region. Problems of the Arctic and Antarctica. 2018. Vol. 64. No. 1. P. 5-15.

3. Popov S.V., Eberlein L. Experience of using GPR to study the structure of the snow-firn strata and the soil of East Antarctica. Ice and snow. 2014. No. 4. P. 95-106.

4. Nikolaev M.R. Features of the application of the georadiolocation method in the study of snow cover. Collection of reports of the international scientific conference in memory of the outstanding Russian scientist Yuri Borisovich Vinogradov. 2020. P. 129-134.

5. Radio engineering device of subsurface sounding (georadar) "OKO-3", technical description, operating instructions. Moscow: "Logic Systems" LLC. 2008. 42 p.

6. Rodzin V.I., Semenov G.V. Fundamentals of environmental monitoring. Taganrog. TRTI. 1988. 260 p.

7. Kolomyts E.G. Snow structure and landscape indication. Moscow. Nauka. 1976. 205 p.

COMPARISON OF RESISTIVITY LOGGING TOOLS' CAPABILITIES AS APPLIED TO GEOSTEERING PROBLEMS

Temirbulatov O.P.[1], *Mikhaylov I.V.* [1, 2]

[1]Novosibirsk State University, Novosibirsk, Russia, o.temirbulatov@g.nsu.ru
[2]Trofimuk Institute of Petroleum Geology and Geophysics, Novosibirsk, Russia

Abstract. This work is devoted to revealing the capabilities of various logging tools: high-frequency electromagnetic, lateral sounding and that with toroidal coils in application to the topical problems of geosteering. Signals of the mentioned three borehole methods were modeled in the Oklahoma geoelectric benchmark model. The modeling of the signals was carried out in the Siberian Supercomputer Center SB RAS, using a numerical 3D finite-difference algorithm. Descriptions of the resulting signals in vertical, deviated and horizontal boreholes, as well as the results of the signals' comparison are provided.

Key words: geosteering, resistivity logging, numerical modeling, electrophysical characteristics, deviated and horizontal wells.

Nowadays geosteering is widely used to adjust the location of a well during drilling in order to increase penetration through the most productive part of oil-and-gas-bearing beds. Also, the development of numerical methods for modeling signals of borehole resistivity logging instruments contributed to the success of geosteering. This allowed finding out what signals geological environments would cause, and then apply data obtained during a drilling process in order to steer a borehole trajectory.

For numerical 3D finite-difference modeling of signals of high-frequency electromagnetic logging probes (VIKIZ), lateral sounding (BKZ), and that with toroidal coils (ZET) [1], the Oklahoma geoelectric benchmark model was chosen (Fig. 1) [2]. Signals are modeled in a well with inclinations from 0˚ to 90˚ and with drilling mud resistivity from 0.01 to 1 ohm·m. The results of modeling these signals allow us to justify the application of these three resistivity logging methods to geosteering problems.

For a detailed comparison of the capabilities of the mentioned probes in detecting the geoelectrical boundaries being approached, an interval of depth from 16 to 25 m was chosen in the area comprising thick conductive and resistive reservoir beds.

In the course of the comparative analysis, it was found that in a vertical well, the BKZ signals indicate the more conductive formation immediately when crossing the boundary (20.3 m). At the same time local maxima appear. The more resistive layer (22.4-27.9 m) is noted at a distance of no more than 0.1 m, while local minima are manifested. With a well inclination of 40˚, the conductive formations are noted when crossing the formation boundary (20.3 m), while approaching the more resistive formations is observed at a distance of up to 0.3 m. The resistive layer is evidenced when crossing the boundary at 22.4 m. In addition, there are no local extrema at 90˚ inclination.

The VIKIZ signals mark the approach to the more conductive formation (20.3-22.4 m) at a distance of no more than 0.75 m at zero well inclination. The approach to the resistive layer (22.4-27.9 m) is noted at a shorter distance of up to 0.2 m. With a well inclination of 40˚, the conductive layer can be noted at a distance of no more than 0.7 m. The more resistive layer

begins to affect the signal at a distance not exceeding 0.3 m. The conductive layer is observed only when passing through the geoelectrical boundary at 20.3 m, and the resistive one can be observed at a distance of no more than 0.5 m in horizontal wells. Moreover, with an inclination of 90˚, local maxima of the resistivity log appear in the boundary areas near the conductive beds.

The conductive formation 20.3-22.4 m starts to affect the signals of the tool with toroidal coils (ZET) at a distance of 1 m before crossing the boundary 20.3 m in a vertical well. In contrast, the more resistive formation (22.4-27.9 m) can affect the tool's signals at a distance of up to 1.2 m from the boundary. At an inclination of 40˚, the conductive layer 20.3-22.4 m is noted on ZET's signals at a distance of up to 1.6 m from the boundary. At the same time, the resistive bed starts to influence on the signal at a distance of 1 m. In a horizontal well, the conductive layer starts to affect the signal at a short distance – no more than 0.2 m from the geoelectrical boundary. The approach to the resistive formation is noted at a distance of 1 m. At the signals' frequency of 50 kHz, the boundaries can be detected at a maximum distance. The adjacent boundary is identified at relatively smaller distances at higher frequencies of the signals.

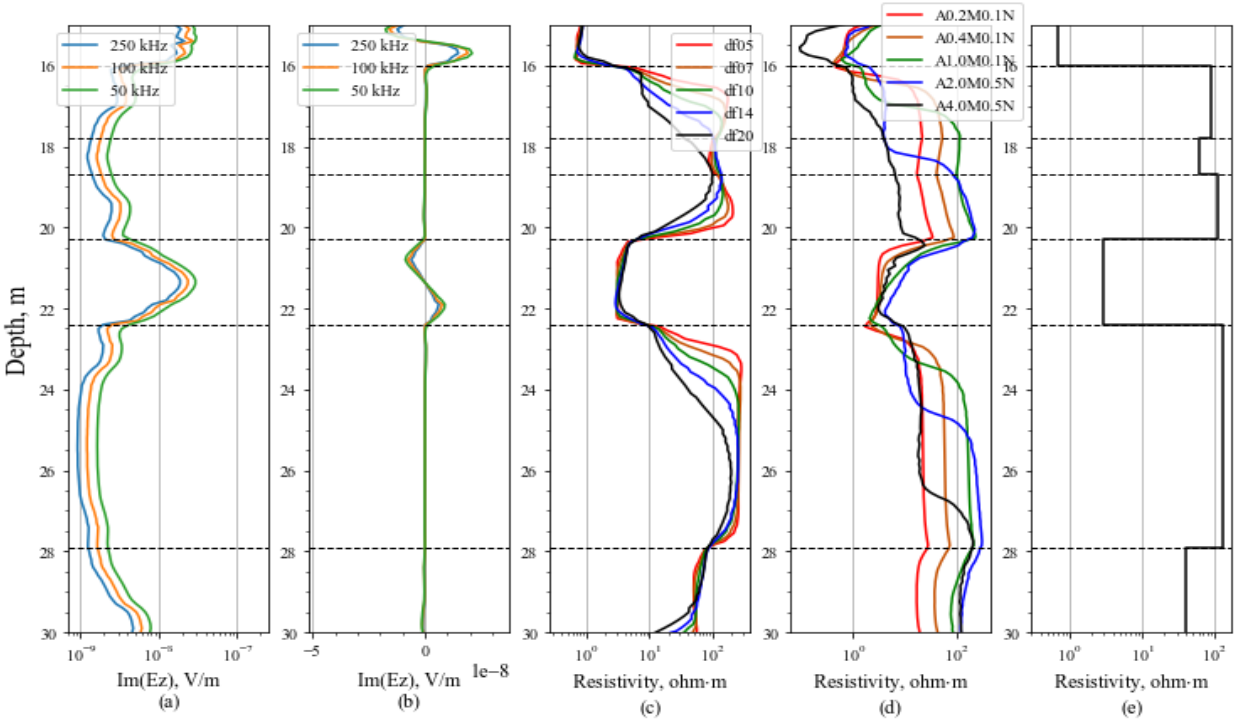

Figure 1 – Signals of ZET in summary (a) and differential (b) modes, VIKIZ (c) and BKZ (d) modeled in Oklahoma benchmark geoelectric model (e). Well deviation is 0 degrees.

To sum up, in non-horizontal wells the tool with toroidal coils helps to identify an approach to the boundary of a resistive formation at a greater distance in comparison with the BKZ and VIKIZ tools. Concerning VIKIZ's signals, an approach to a conductive formation can be evidenced at a greater spacing. In horizontal wells, VIKIZ's signals mark an approach to a resistive bed at the biggest distance, while the BKZ tool enables detecting a conductive formation at a distance of up to 1 m.

References:

1. Mikhaylov I.V., Surodina I.V., Temirbulatov O.P. Signals of electromagnetic tool with toroidal coils in deviated wells (following numerical simulation results). Russian Journal of Geophysical Technologies. 2021. No. 3. P. 18-27 (In Russian).

2. Agbash I.A., Sobolev A.Y. (2015): Geoelectric models for testing well-logging data processing algorithms. In Interexpo Geo-Siberia-2015. Novosibirsk. Russia. (In Russian)

APPROBATION OF THE METHOD OF ELECTROMAGNETIC PROFILING IN THE STUDY OF ARCHAEOLOGICAL SITES IN THE BAIKAL REGION

Trofimov I.V., Tereshkin S.A., Snopkov S.V.

Irkutsk National Research Technical University, Irkutsk, Russia, itrofimov@geo.istu.edu

Abstract. The upper part of the section is a part of the geological space in which objects of historical heritage are located. The study of the structure of the upper part of the section makes it possible to identify and study archaeological sites. In order to identify anomalies associated with anthropogenic soil disturbances, it is necessary to evaluate the possibilities of geophysical methods of solving archaeological problems. That goal was pursued by conducting experimental methodological work by the method of electromagnetic profiling with Nemfis equipment. The work was carried out on two sites with different geological sections and different archaeological objects.

Key words: archaeology, electromagnetic profiling with Nemfis, Barun-Khal II, Glazovsky burial ground.

Object No. 1. The park of the Paris Commune (PPC) is located in Irkutsk. It has the shape of an almost regular rectangle, bounded on the north by Botkin Street, on the west by 2nd Zheleznodorozhnaya Street, on the south by Mayakovsky Street, on the east by Sportivnij Lane.

Electromagnetic profiling was carried out in order to identify graves sites on the territory of the burial ground.

Object No. 2. Barun-Khal II is one of the significant monuments of ancient metallurgy near the village of Shara-Togot. The monument was opened in 1997 as a result of archaeological work led by Professor of INRTU A.V. Kharinsky. The purpose of electromagnetic profiling was to identify foothill pits, trenches and other construction sites of the metallurgical center. [1]

Excavation works of the monument of Barun-Khal II revealed that the metallurgical center is a foothill pit with a diameter of up to 2 m and a depth of up to 1.5 m, around which funnel-shaped furnaces were located, connected to the pit by means of a tuyere. The dimensions of the upper opening of the furnace are approximately 0.7 x 1 m [2]

The methodology of the work. Experimental methodological work in the PPC was carried out on two areas. The first had a grid measuring 14x24 meters, and at the second 11x13 meters.

Works on area No. 2 was carried out with a grid of 7x50 meters. In addition, in an attempt to confirm the results of Nemfis, a survey was carried out using the MMPos 1 magnetometer

All measurements were performed in 1 m increments.

Results. According to the results of experimental methodological measurements in the PPC, the following results were obtained (Figure a, b). On the maps of electrical resistance, local anomalies of increased resistance are highlighted. They are corresponded to the places of violation of the normal occurrence of soils, and are interpreted as pits of ancient burials.

The highlighted area in Figure (b,c) corresponds to the presumed continuation of the uncovered section of metallurgical production and is reflected both on the map with the results of Nemfis and on the map with the results of magnetic survey.

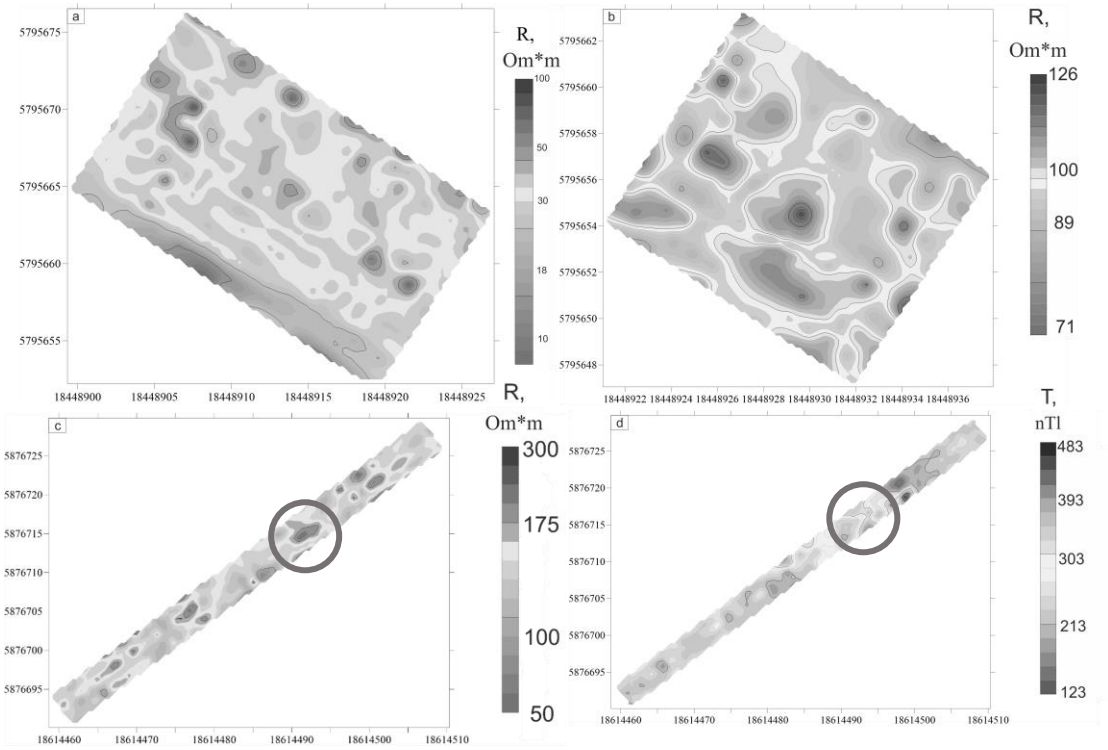

Figure 1 – Received cards, after data processing (PPC – a (area №1/40 kHz), b (area №2/40 kHz) / Barun-Hal II – c (62,5 kHz), d)

Conclusions

1. Electromagnetic profiling is a method that can be used in a complex of geophysical studies in the study of archaeological sites. Nemfis equipment mainly allows you to study the uppermost part of the geological section, in which the vast majority of archaeological sites are located.

2. As a result of processing the measurements, a number of local anomalies were identified, presumably of anthropogenic nature. Some of the electrical resistance anomalies correspond to magnetic induction anomalies.

3. During the experimental work, the features of the operation of Nemfis equipment were identified, which must be taken into account in order to achieve measurement accuracy.

References:

1. Kozhevnikov N.O., Kozhevnikov O.K., Nikiforov S.P., Snopkov S.V., Kharinsky A.V. (2000): The ancient center of iron metallurgy in the Barun-Khal valley. In Collection of scientific papers "Baikal Siberia in antiquity". No. 2, part 2. 66-100 p. Irkutsk. Publishing house of IGPU.

2. Davydenko S. Y., Davydenko Y. A., Davydenko A. Y., et al. (2021): Geophysical methods in the study of the ancient metallurgical complex in the western Baikal region (Section Barun-Khal II). Russia, in 17th Conference and Exhibition Engineering and Mining Geophysics, Gelendzhik.

POTENTIAL FIELDS STUDY IN THE KELBES-ZOLOTOKITAT ORE CLUSTER

Zaplavnova A.A. [1,2], *Esin E.I.*[1,2]. *Olenchenko V.V.*[1,2]

[1]A.A. Trofimuk Institute of Petroleum Geology and Geophysics, Novosibirsk, Russia,
ZaplavnovaAA@ipgg.sbras.ru
[2]Novosibirsk State University, Novosibirsk, Russia

Abstract. In the Kelbes-Zolotokitat region, gold placers are widespread. At the same time, the field of golden ore deep structure, clusters and fields are studied poorly. Magnetic and gravitational fields gradient analysis made it possible to identify areas promising for gold mineralization. The studies were carried out for maps fragments of airborne magnetic and gravimetric surveys at a scale of 1:500000. Based on the results, brief recommendations were given for further research using ground-based geophysical methods.

Key words: potential geophysical field, ore gold, F- approximation

Kelbes-Zolotokitaty ore belt is one of the oldest gold placer clusters in the Kuznetsk Alatau. It is located in the Barzas-Kelbes-Zolotoy Kitat interfluve. In the transitional geomorphological zone to the West Siberian Lowland [1].

On the territory of the Kelbes-Zolotokitat region, valley gold placers are widely distributed and studied. Presumably, the predominant ore gold source for these placers is gold-quartz mineralization confined to the Kamzhelinsky series. Mineralization is represented by vein and vein-disseminated zones (hydrothermally altered rocks). It appears in crushing and shearing areas [1].

In addition, it stands to mention that within the Kuznetsk Alatau, gold deposits of various formation types and different ages are widespread. Ore zones are characterized by a focal location type. They are associated with the Kuznetsk-Altai deep fault with feathering and transverse faults and also with the Sukhovsky horst, composed of the Kamzhelinsky series (R3–Є1) [1;2]. However, ore gold deposits were poorly studied in the Kelbes-Zolotokitat territory. Therefore, this region was chosen as the object of our research.

Geophysical studies of the ore gold deposits in the Kuznetski Alatau began in 1935 and included a magnetometric survey performed under the direction of N. I. Zakharenko. In the Kelbes-Zolotokitat region, the deep structure of gold ore regions, clusters and fields has been poorly studied. Also, the regional distribution of ore gold patterns and their reflection in geophysical fields have not been analyzed either [2]. The complexity of geophysical studies mostly arises from the sub-vertical geological boundaries and local objects typical for this area. During providing surveys in such conditions, a special role is played by the task of separating fields from the various geological structures, objects and regional effects. Therefore, an important part of the study of the Kelbes-Zolotokitat ore belt is the analysis of regional magnetic and gravitational fields.

The anomalous magnetic and gravitational fields transformants calculation was constructed using the linear integral representations of the F-approximation technique, described in detail by I. A. Kerimov [3]. The State Geological Map fragments, scale 1:500000, sheet N-45-III of airborne magnetometry and airborne gravimetry [4] were used in the calculations. The distance to the representability surface of the Fourier integral was 500 and 1000 meters from the measurement surface. The root-mean-square approximation errors do not exceed 1 nT and 0.01

mGal for magnetic and gravitational fields, respectively, which is comparable to initial measurement accuracy. Field gradient values at the measurement height were obtained from the calculated data.

Results of the studies showed the predominant linear type of magnetic and gravity anomalies, with a north-north-west strike according to geological structures. Also, in the eastern part, there is a sharp change in the magnetic field structure caused by the Olginsky granite massif. A comprehensive analysis of gravity and magnetic fields in the Kelbes-Zolotokitat region made it possible to identify areas associated with fault zones, dike complexes, and zones of hydrothermally altered rocks.

Potential field gradient analysis, with geological a priori data, gives a possibility to identify prospective areas for more detailed studies. Particular interest is the watershed section of the Konyukhta and Sololneshny rivers. Along with the dike complex (diabase and gabbrodiabase in the enclosing carbonaceous-siliceous-argillaceous shales of the Kamzhelinsky series), there is an extended negative magnetic anomaly, presumably associated with hydrothermal rocks alteration. In the explanatory note to the State Geological Map at a scale of 1:200000 [4], a gold areola is mentioned in this area according to schlich sampling data. Also, on the right bank of the Edinis River, small gold concentrations are observed in silicified rocks. These assumptions are in good agreement with the obtained geophysical information.

Thus, as an interpretation result of the airborne magnetic and gravity data at a scale of 1:500000, areas promising for ore gold deposits were identified. The watershed of the Konyukhta and Sololneshny rivers is noted as being of interest for further research. To clarify the location of ore-controlling structures, it is planned to conduct large-scale geophysical studies using ground-based electrical and magnetic methods.

Funding: This work is supported by the Russian Science Foundation under grant FWZZ-2022-0024

References:

1. Kolpakov V.V., Nesterenko G.V., Nevolko P.A., Zhmodik S.M. Mineralogical and geochemical characteristics and probable primary sources of native gold placers in the Kelbes-Zolotokitatsky region (northern part of the Kuznetsk Alatau). Geospherical Research. 2021. No. 3. P. 42–55.

2. Dolgal A.S., Khristenko L.A. Results and prospects of geophysical research in the search for ore gold on the eastern slope of the Kuznetsk Alatau. Bulletin of KRAUNC. Series: Earth Sciences. 2008. Vol. 12. No. 2. P. 57–69.

3. Kerimov I.A. F-approximation method for solving problems of gravimetry and magnetometry. Moscow. Fizmatlit. 2011. 263 p.

4. Kurtigeshev V.S., Bychkov A.I., Shatilova G.A., etc. State Geological Map of the Russian Federation, scale 1: 200 000. Second edition. Kuzbass series. Sheet N-45-III (Kemerovo). Explanatory note. Moscow. MB VSEGEI. 2013. 159 p.

Scientific publication

X International Siberian Early Career GeoScientists Conference: Proceedings of the Conference

13-17 June 2022, Novosibirsk

Technical Editors: E.A. Ovdina,
M.O. Shapovalova

Layout: A.G. Azhbakov
Cover: A.G. Azhbakov

Подписано в печать 23.05.2022 г.
Формат 60 х 84/8. Уч.-изд. л. 28,5. Усл. печ. л. 26,5.
Тираж 26 экз. Заказ № 107
Издательско-полиграфический центр НГУ
630090, Новосибирск, ул. Пирогова, 2.

MINERALOGY
2022

Sobolev Institute of Geology and Mineralogy Siberian Branch of the Russian Academy of Sciences (IGM SB RAS)

Trofimuk Institute of Petroleum Geology and Geophysics Siberian Branch of the Russian Academy of Sciences (IPGG SB RAS)

Novosibirsk State University (NSU)

Joint Stock Company "Siberian Anthracite"

Joint Stock Company «Almazy Anabara»

Data East, LLC

Public Joint Stock Company Gazprom Neft

Laboratory of ore-forming systems IGM SB RAS

SGA Siberian Student Chapter

ISBN 978-5-4437-1337-3